Prediction of Transgenic Tobacco Plant Processing Properties by Ultra Scale Down and Physical Property Measurement for Monoclonal Antibody Production

A thesis submitted for the degree of

Doctor of Philosophy

in

Biochemical Engineering

by

Sally Yasseen Hassan (MEng)

The Advanced Centre for Biochemical Engineering

Department of Biochemical Engineering

University College London

Project in collaboration with St. George's University of London and University of Birmingham

September 2008

The author confirms that the work presented in this thesis is the author's own. Where information has been derived from other sources, the author confirms that this has been indicated in the thesis.

ProQuest LLC
789 East Eisenhower Parkway
P.O. Box 1346
Ann Arbor, MI 48106-1346

Abstract

There are numerous potential advantages of producing significant quantities of a monoclonal antibody (MAb) via transgenic tobacco plants over other heterologous production systems, thus paving the way for new prophylactic and therapeutic applications within global human and animal health. However, current information on the key processing factors for large scale production of antibodies from transgenic plants is limited.

This thesis presents the issues involved in the production of monoclonal antibodies in transgenic tobacco plants with a specific focus on initial extraction and aids the design and characterisation of an optimal small-scale extraction process using ultrascale down and micromanipulation techniques based on large-scale principals, in addition to offering different harvesting and extraction strategies dependent upon the specific target subcellular or tissue compartment.

One of the preliminary objectives of this project was to examine methods for the initial extraction of recombinant IgG1 antibodies from the leaf tissue of transgenic tobacco. Three different transgenic plant lines were investigated with the intention of establishing the parameters for optimal extraction of MAbs that reside in the apoplasm (IgG), endoplasmic reticulum (IgG-HDEL), or are bound to the plasma membrane (mIgG). For each transgenic line, seven techniques for physical extraction were evaluated. For IgG that is secreted and accumulated in the apoplasm, dry freeze-thaw (the freezing of leaf discs at -20°C followed by room temperature thawing before buffer addition) was an appropriate technique for extraction of a high yield and a low release of native plant proteins from leaves in comparison to the other techniques investigated. In addition to lowering the downstream purification burden, the large-scale equipment involved in this step is likely to have a lower operating cost than a mechanical, energy-intensive grinding device. IgG-HDEL-expressing transgenic plants demonstrated an increase in IgG-HDEL yield with technique severity, demonstrating that harsher techniques such as dry-freeze-thaw followed by grinding were optimal. Conversely, the membrane-bound IgG required the leaf tissue to be ground in buffer that included a non-ionic detergent (Triton X-100), the optimal

concentration of which was 0.1% (v/v). Grinding samples on ice or at room temperature was found to have no effect on IgG yield for all three MAbs. This indication of plant-derived IgG stability at room temperature is an obvious cost benefit at industrial scale. For all forms of the IgG, there was a wide variety of usable pHs (pH 5 to 7) with the exception of very low pHs (pH 3 and 4). Overall, an important finding of this study was that determining factors of optimal antibody extraction from plants had a direct influence on the initial choice of expression strategy, and thus it was essential to be addressed from the outset. In addition, a principally important consideration was the use of small scale techniques that were applicable to large scale purification.

Another important factor of recombinant protein production in transgenic plants that is often overlooked is the initial bioprocesing step of harvesting. The major harvesting factors that need to be addressed are when to harvest, which part of the plant to harvest and how to harvest. Here some of these factors for the production of a secreted IgG and an intracellularly retained form of this IgG in transgenic tobacco were addressed. Data analysis resulted in an interesting observation of plant wound response and its consequences for time-response IgG levels. The same monoclonal antibody (MAb), (Guy's 13 that acts against *Streptococcus mutans*, the main agent of tooth decay in the mouth) targeted to two different subcellular compartments, showed varying IgG response levels after wounding. In addition, there was a significantly different type of wound response and the subsequent IgG levels for young and old plants expressing the secreted form of IgG with a negative effect (IgG reduction) on young growing plants and a positive effect (IgG boost) in older plants. Additionally, for secreted IgG expressing plants, IgG strongly depended on plant age with the highest amount of IgG being found in young leaves of old plants and or young plants, but with a marked reduction in older tissue that was most likely due to senescence. In contrast, intracellularly retained IgG that accumulated in the endoplasmic reticulum was not significantly affected by mechanical wounding and its frequency or by overall senescence.

In addition to transgenic tobacco leaves, tobacco roots were investigated as a potential source of the MAb. It was found that despite the focus of current related literature on recombinant protein recovery being from the leaves of whole transgenic tobacco plants, roots offer a promising alternative.

Moreover, despite the fact that the default pathway of IgG is secretion and thus, can be secreted into the medium within a hydroponic system for example, the secretion rate is slow and there is likely to be a large medium requirement. A substitute for this is mechanical root breakage in order to generate higher antibody yields. A novel approach is described here with the capability of determining the force magnitude for breaking single plant roots. Roots were taken from transgenic tobacco plants, expressing a secreted monoclonal antibody. They were divided into four key developmental stages. A novel micromanipulation technique was used to pull to breakage, single tobacco roots in buffer in order to determine their breaking force. A characteristic uniform step-wise increase in the force up to a peak force for breakage was observed. The mean breaking force and mean work done were 101mN and 97μJ per root respectively. However, there was a significant increase in breaking force from the youngest white roots to the oldest, dark red-brown roots. We speculate that this was due to increasing lignin deposition with root stage of development (shown by phloroglucinol staining). No significant differences between fresh root mass, original root length, or mean root diameter for any of the root categories were found, displaying their uniformity, which would be beneficial for bioprocessing. In addition, no significant difference in antibody yield from the different root categories was found. These data demonstrated that it is possible to characterise the force requirements for root breakage and should assist in the optimisation of recombinant protein extraction from these roots.

Following on from this, the determination of the minimum energy required for monoclonal antibody (MAb) extraction from transgenic tobacco roots is desirable, in order to optimise product yield. Mechanical breakage of transgenic tobacco roots (expressing a MAb) in a scalable laboratory scale mechanically stirred shear device was assessed. The resulting experimental data together with a mathematical model was used to estimate root tensile strength and this was compared with the mean tensile strength of such roots as previously determined by a micromanipulation technique where the scale corresponds to a single 1cm root section. Breakage of multiple roots (~100) in a small-scale mechanically stirred scalable shear device was investigated. Size distributions of the roots when passed through the breakage device at a rotational speed of $75s^{-1}$ were obtained as a function of time. It is

probable that root fragmentation in such a mechanically stirred shear device is due to root-impeller collisions. Assuming this mode of breakage, a relationship between the equilibrium mean length of the root debris and the critical physical parameters affecting it was established using a theory of failure based on a maximum strain energy criterion. Data on the stable size of the root debris agreed well with the model based on the maximum energy criterion. The data further suggest that root breakage within this device was approximately a first-order process. The model suggested that knowledge of root tensile strength was important since it directly determined the minimum energy required to break the transgenic roots. A macroscopic estimation of the relative root tensile strength by using experimental data within the suggested model gave an estimated tensile strength of 2200 $\pm$ 600 kPa (average $\pm$ SEM) which agreed well with the tensile strength measured by micromanipulation 2400 $\pm$ 200 kPa. Thus, measurement of root tensile strength by micromanipulation appeared to be a valid means of finding the minimum energy required for modelling breakage in a macroscopic mechanical shear device.

Acknowledgements

I would sincerely like to thank Dr. Eli Keshavarz-Moore (Department of Biochemical Engineering, University College London) for her invaluable guidance and personal support throughout the project (and look forward to working with her during the next few years). My sincere gratitude also goes to Prof. Julian Ma (Department of Cellular and Molecular Medicine, St. George's University London) for his invaluable advice, support and enthusiasm, and Prof. Colin Thomas (Department of Chemical Engineering, University of Birmingham) for his technical guidance and support. I am escpecially grateful to Dr. Craig van Dolleweerd (St. George's University London) for his academic input.

I am also grateful to Dr. Pascal Drake and Dr.Matthew Paul (St. George's University London), Dr. Wei Liu and Dr. ChangXiang Wang (University of Birmingham), and Dr.Daniel Bracewell and Dr. Sunil Chhatre (University College London) for academic advice. I extend my gratitude for technical support to Fotis Ioakeimidis and Thais Guerra (St.George's, University of London), Vinita Vishwanarayan, Alan Craig, Martin Town and Dr. Naveraj Gill (University College London), and to Lesley Tomkins (Centre for Electron Microscopy, University of Birmingham). I would also like to thank Prof. Nigel Titchener-Hooker (University College London) for recommending me for this particular PhD project. There are numerous people who have generously offered their help and support within all three universities that I had the privilege to work in during my PhD, and so if I have unintentionally missed anyone out, please forgive me. This project was funded by the EPSRC, University College London, University of Birmingham, and St.George's, University of London to whom I am very grateful.

Finally, I would like to thank all my friends who have helped me along this journey. My sincerest gratitude goes to the family that I am truly blessed to have. My sister (friend and collegue), Inass has been with me throughout the whole of my university education including post-graduate studies. My mother and father, through their bountiful encouragement and steadfast belief, have been the cornerstone in my education, and to whom I owe every success. This thesis is dedicated to my beloved grandmother, Nafeesa Zain El-Deen, who will forever be in my memories.

Contents

List of Figures

List of Tables

Nomenclature and Abbreviations

MAb = monoclonal antibody

IgG = Immunoglobulin

IgG (secreted form) = IgG that is targeted to and accumulates in the apoplasm

mIgG = membrane-bound IgG

IgG-HDEL = HDEL-tagged IgG that is intracellularly retained in the endoplasmic reticulum

P = power requirement (Nms^{-1})

F = applied force (N)

R = length of the arm (of the air bearing) pressing against the force sensor (m)

ω = angular velocity ($rads^{-1}$)

N = stirrer speed (s^{-1})

n_d = actual number of root debris (-)

n_{ni} = imaginary impact marks on a blade of the impeller after 30 secs (-)

R_i = impeller impact rate (s^{-1})

R^p= particle impact rate(s^{-1})

E_{max} = maximum impact energy for a particle (Nm)

η = collision efficiency (-)

n_{blade} = number of blades of the impeller (-)

n_r = number of times that a single root is broken (-)

$n_{r\text{-}i}$ = number of roots that collide with the impeller during that time period (-)

n_t = number of "imaginary" marks on the blade of the impeller (-)

f_c = frequency with which fluid elements are pumped through the impeller region (s^{-1})

Fl = impeller flow number (-)

τ_i = stress due to impeller blade root impact (Nm^{-2})

L = mean main root length (m)

number of roots subject to breakage (-)

F_b = peak force for breakage (N)

A_o = original root cross-sectional area (m^2)

d_o = original mean root diameter (m)

n_t = number of imaginary impact marks on a blade of the impeller at time t (-)

n_{30} = number of imaginary impact marks on a blade of the impeller at 30s.

t = agitation time (s)

S = eddy-hyphae contact frequency (s^{-1})

q_{frag} = specific (root or hyphal) fragmentation rate (s^{-1})

σ_{pseudo} = pseudo tensile strength (Nm^{-2})

Q_{frag} = fragmentation rate (s^{-1})

Chapter 1-Introduction

1.1. OVERALL RESEARCH AIMS

The overall aim of this thesis was to investigate techniques and strategies for the extraction of recombinant monoclonal antibodies (MAbs) from transgenic tobacco plants. Two parts of the plant were considered for extraction, the leaves which are the most commonly considered biomass, and the roots. The extraction of monoclonal antibodies that were targeted to three different subcellular compartments in transgenic plant leaves was investigated. These were IgG expressed in the apoplasm (i.e. secreted form), a membrane-bound IgG (mIgG) and IgG-HDEL that was intracellularly retained in the endoplasmic reticulum. An ultra-scale down technique was used to predict energy requirements for root breakage in a mechanically stirred shear device with the physical properties of the roots characterised by a novel micromanipulation technique. As the majority of available literature on the production of recombinant proteins from transgenic tobacco concentrate on the process steps subsequent to extraction such as those involved in purification, a key focus of this thesis was on the initial step of extraction. Extraction is arguably the most important part of downstream processing (for reasons that will be discussed later in Section 1.13), and this research assists in potentially increasing the feasibility of the commercial production of monoclonal antibodies using transgenic tobacco.

The system used in this study was tobacco (*Nicotiana tabacum*), expressing a monoclonal antibody, Guy's 13, that acts against *Streptococcus mutans*, the main causative agent of tooth decay in the mouth (Ma *et al.*, 1994).

1.2. THESIS LAYOUT

The layout of the thesis consists of Chapter 1 which addresses the overall aim of this research, followed by a literature review, and then the specific aims of the project. Chapter 2 then describes the materials and methods used in this research. Chapter 3 describes the regeneration and characterisation of IgG-HDEL transgenic plants. IgG (secreted form) and mIgG (membrane-bound) were already available as stably transformed plants in soil. Chapter 4 describes an investigation of the physical and chemical parameters important for the extraction and recovery of monoclonal antibodies targeted to the three different subcellular compartments in the leaves. Chapter 5 then examines harvesting strategies for two different forms of the monoclonal antibody.

Chapters 6, 7 and 8 are based on the alternative strategy of extracting the antibodies expressed in the roots of these plants. Chapter 6 characterises the mechanical properties of the roots by micromanipulation, and Chapter 8 relates the findings in Chapter 6 to the behaviour of roots in an ultra-scale down mechanical shear device used for extraction by combining experimental data with a theoretical mathematical model (described in Chapter 7). The penultimate chapter (9) consists of recommendations for harvesting and the downstream process based on the chosen targeting strategies and extraction findings from preceding chapters. The final chapter (10) details the overall conclusions from the thesis and subsequent recommendations for future work.

1.3. ANTIBODY STRUCTURE AND FUNCTION

An antibody is an immunoglobulin that is able to specifically combine with the antigen that was responsible for its production in a susceptible mammal. They are generated in the body as a response to the invasion of foreign molecules. These immunoglobulins exist as a single or multiple copies of a Y-shaped unit, formed from four polypeptide chains, including two identical copies of a heavy chain and two identical copies of a light chain (Ramos-Vara, 2005).

There are five classes of antibodies, namely: IgG, IgM, IgA, IgD and IgE, based on the number of Y-shaped units and the type of heavy chain. Heavy chains of IgG, IgM, IgA, IgD, and IgE, are referred to as γ, μ, α, δ, and ε, respectively. Antibody light chains are classified as either kappa (κ) or lambda (λ), according to small polypeptide structural differences. The heavy chain, however, determines the antibody subclass. Antibody subclasses vary in the number of disulfide bonds and the length of the hinge region (Male, 2004). IgG is the most commonly used antibody in immunochemical procedures since it is the major immunoglobulin (Ig) released in serum (Male, 2004).

Figure 1.1 illustrates the structure of IgG molecules that are typically tetrameric proteins consisting of two heavy chains and two light chains stabilised by both intra- and inter-chain disulphide bridges and carbohydrate moieties. The typical Y shape of IgG consists of the two variable, antigen specific F(ab) arms, which are vital for binding with antigen, and the constant Fc "tail" which binds to Fc receptors of immune cells and facilitates the manipulation of the antibody during most immunochemical procedures. The number of F(ab) regions on the antibody, indicate its subclass, and determines the valency of the antibody (i.e. the number of F(ab) parts with which the antibody can bind to its antigen) (Male, 2004).

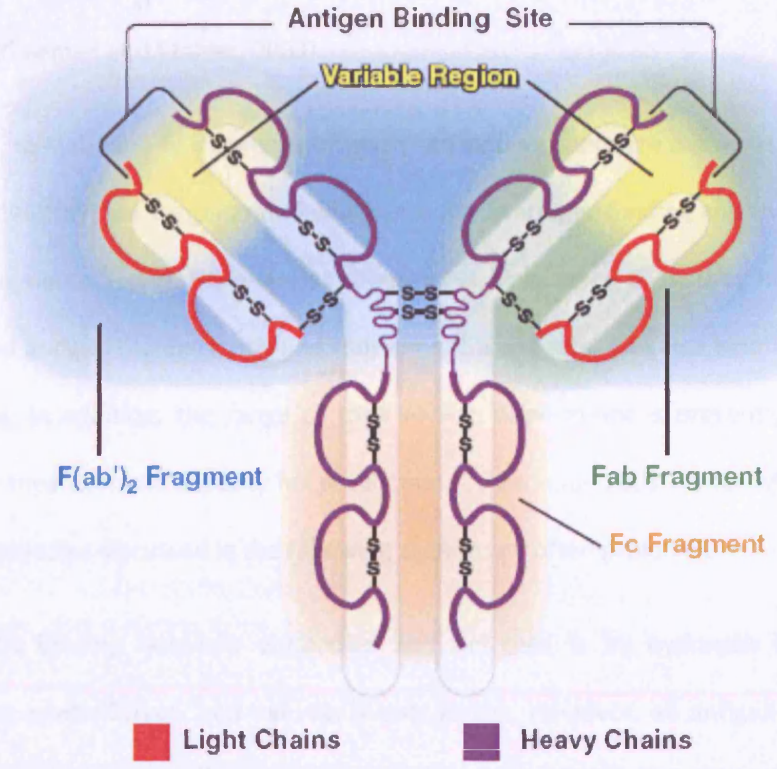

Figure 2.1: Antibody structure (Adapted from http://www.millipore.com/immunodetection/id3/antibodiestutorial)

Direct-conjugated antibodies are often labelled with an enzyme or fluorophore in the Fc region. The Fc region anchors the antibody to the plate in Enzyme-linked ImmunoSorbent assay (ELISA) procedures and can also be detected by secondary antibodies during immunoprecipitation, immunoblots and immunohistochemistry. The three regions of the Y-shaped antibody can be cleaved into two F(ab) and one Fc fragments by the proteolytic digestion with papain, or alternatively proteolytic digestion with pepsin can divide the Y-shaped immunoglobulin into two sections: one $F(ab')_2$ and one Fc at the hinge region (Male, 2004). The F(ab) fragment alone is sometimes useful, as it lacks the Fc region and hence does not precipitate the antigen nor is it bound by immune cells *in vivo*. In addition, their smaller size and lack of crosslinking (due to loss of the Fc region) means that Fab fragments are often radiolabelled for use in functional studies. Fab fragments are often preferred to whole antibodies as they are smaller in size

and therefore have higher diffusion rates, quicker clearance from circulation, and reduced immunogenicity (Coleman and Mahler, 2003).

In addition, to F(ab) and Fc fragments of whole antibodies, there are a diverse range of engineered molecular derivatives that can be generated which also retain antigen binding and specificity. An example is single-chain fragments, (scFv). However, although scFvs have many uses, they have drawbacks since they can only bind antigen monovalently and thus cannot aggregate, and also bind less avidly than their parent antibodies. In addition, the range of their *in vivo* applications is presently quite narrow, and limited mainly by their cost and capacity for production (Drake *et al.* 2003). Thus whole antibodies such as monoclonal antibodies discussed in the following section are often preferred.

The specific binding between antibodies and antigens is by hydrogen bonds, hydrophobic interactions, electrostatic forces, and van der Waals forces. However, all antigen-antibody binding is reversible (Sadik and Wallace, 1993).

These antibody properties have lead to many successful uses in passive immunisation, i.e. the administration of preformed antibodies. Antibodies used can be polyclonal (a mixture of immunoglobulin molecules secreted against a specific antigen, each recognising a different epitope) or monoclonal (discussed in the following section) and are derived from animal antibodies (serum, milk or egg), human antibodies (serum or milk), or monoclonal antibodies.

The many advantages of antibodies have meant that they are the single largest group of biotechnology-derived molecules in clinical trials with 20% of all biopharmaceuticals in clinical development being antibody products (Larrick *et al.* 2001). There are approximately 1000 therapeutic recombinant antibodies in development and 200 in clinical trials (Larrick *et al.*2001).

1.4. MONOCLONAL ANTIBODIES

A number of monoclonal antibodies have received regulatory approval and have been commercialised including Rituxan (non-Hodgkins lymphoma), Herceptin (breast cancer) or Zenapax (kidney transplant rejection) with many more in the pipeline (Shukla *et al.*, 2007). There are reported to be 18 approved monoclonal antibodies for therapeutic use (Reichert *et al.*, 2005). Consequently, monoclonal antibodies constitute one of the most important classes of biotherapeutics in development and production (Flatman *et al.*, 2007), a trend that is likely to continue in the foreseeable future. Pavlou and Belsey (2005) projected that the market would grow by 20.9% per year to reach $16.7 billion in 2008.

Monoclonal antibodies (MAbs) are a homogeneous population of antibodies that can be raised by fusion of B lymphocytes with immortal cell cultures to produce hybridomas. These hybridomas then produce multiple copies of the same MAb. This phenomenon has led to the wide use of antibodies in diagnosis, the management and treatment of infectious diseases and cancer, and is one of the most important entities in the current pipeline of new biologic compounds (Fischer and Emans, 2000). However, despite most commercial antibodies being MAbs, polyclonal antibodies are more effective in some cases, since, they consist of many different antibodies that have been raised against a range of epitopes on each antigen on a foreign molecule (Newcombe and Newcombe, 2007).

In spite of this, advantages of monoclonal antibodies include their specificity, rendering them to be ideal as the primary antibody in an assay, or for antigen detection in tissue, and will often result in significantly less background staining than polyclonal antibodies. In addition, in comparison to polyclonal antibodies, the homogeneity of monoclonal antibodies is very high, leading to more reproducible results between experiments. Moreover, the high specificity of monoclonal antibodies (MAbs) confers high efficiency of binding to antigen within a mixture of similar molecules, explaining their use in affinity purification.

Further advantages of monoclonal antibodies in *vivo* include bestowing immediate protection, highly effective targeting of specific epitopes, and the ability of circumventing the immune system in

order to reduce individual variation in protective efficacy. In addition, MAbs are effective in immunodeficient patients and generate a successful systemic and mucosal response. Many pathogens penetrate or function at mucosal surfaces, making passive immunisation for disease prevention essential. Thus, similarly to active immunization, passive mucosal immunization, involving the oral, intranasal, or intrauterine administration of antibody can be used for prevention or treatment of viral and bacterial infections (Wycoff *et al.*, 2004). At mucosal surfaces, the main antibody isotype present is the secretory IgA (SIgA) molecule.

SIgA has some advantages over IgG for mucosal passive immunization, such as its avidity effect as a result of it having four antigen binding sites, and it is also less susceptible to degradation by proteolytic enzymes in the gastrointestinal tract than IgG or monomeric IgA (Wycoff *et al.*, 2004). In addition, SIgA is able to block the non-specific binding of some bacterial pathogens to host epithelial cells, and IgA-antigen complexes inhibit the complement cascade and the ensuing inflammatory response (Wycoff *et al.*, 2004).

However, regardless of the monoclonal antibody type used, it is probable that a few milligrams per kg per day for a certain susceptible period would be necessary for effective mucosal passive immunization, and even larger quantities may be required to clear an existing infection. This therefore necessitates an efficient and economical production system (Wycoff *et al.*, 2004).

1.5. HOST PRODUCTION SYSTEMS FOR MONOCLONAL ANTIBODIES

To date monoclonal antibodies (MAbs) have been expressed mainly in mammalian cell culture, in myeloma lines and in Chinese Hamster Ovary (CHO) cells (James *et al.*, 2005, Wurm 2004). However, hybridomas may be low yielding or genetically unstable. Instead, MAb genes can be cloned from the hybridoma and expressed as recombinant antibody in another expression system.

Consequently, mammalian systems are currently the workhorse of monoclonal antibody (MAb) production. The majority of monoclonal antibodies that have been approved for therapeutic use (15) are made by recombinant DNA technology, and the remaining three are murine antibodies produced in

hybridomas (Birch and Racher, 2006). The recombinant antibodies are made in mammalian cell expression systems using Chinese hamster ovary (CHO) or murine lymphoid cell lines (e.g., NS0, Sp2/0-Ag14) (Birch and Racher, 2006). These systems are able to perform glycosylation and to process the recombinant protein similarly to the native host. However, mammalian cell culture is expensive and not sufficiently scalable for many potential applications. For example, it is thought that there may well be applications, such as topical passive immunisation (Ma *et al.*, 1998) or HIV microbicides (Shattock *et al.*, 2004) for which existing production systems cannot provide sufficient capacity. However, the capacity issues involved in MAb production by mammalian systems is becoming less of an issue with the evolving improvement in MAb yields in mammalian hosts. In the last 15 years, productivity of cell cultures has improved 100 fold (Birch and Racher, 2006) and modern cell culture processes have achieved antibody concentrations that exceed 5 g/L (Winder, 2005). Improvements in mammalian cell culture titres have been a result of developments in expression technology and in process optimisation, particularly for fed-batch fermentations. Products now reach clinical trials in shorter time spans for proof-of-principle testing. In this stage of process development, cell line creation is often the bottleneck (Birch and Racher 2006). However, for mammalian cell processes, it is also necessary to consider the risks of viruses. These are typically removed at the end of the purification train by at least two virus removal/inactivation steps often based on filtration, low pH treatment and sometimes, even the use of solvent/detergent (Birch and Racher 2006).

Another expression system being explored is *Escherichia coli*. Although *E.coli* is essentially the workhorse of the biotechnology industry, it is historically not well suited for expressing eukaryotic genes, especially if the protein product must be glycosylated and terminally processed. In addition, the recombinant protein can be toxic to bacteria, form inclusion bodies or be degraded by proteases. Despite this, *E.coli* has been found to be an excellent host system for the expression of monoclonal antibody fragments such as scFv and Fab. CIMZIA™ is an example of a pegylated Fab' fragment made in *E.coli* and is in phase III trials (Reichert *et al.*, 2005). In fact, progress has been made in the expression of full MAbs in *E.coli*. Simmons *et al.* (2002) were able to successfully express full-length IgG in the periplasm of *E.coli*.

This group found that an *E.coli*-derived anti-tissue factor IgG1 possessed all the properties of an aglycosylated antibody, such as efficient binding to antigen and neonatal receptor (Simmons *et al.*, 2002). However, the reported fermentation titres for this sub-optimal process was 130-150mg/L, significantly lower than that from optimised mammalian cell culture, but there is room for improvement in this category.

An alternative host system, yeast has been found to be capable of expressing both full-length immunoglobulin and Fab, however, the expression of IgG has been low and the expressed IgG could not mediate complement, (Ritter *et al.* 1995). Alternatively, transgenic animals, involving the expression of antibody in mammalian milk gland, have been shown to have a low efficiency of transformation. Nonetheless, production of functional IgG has been reported in goats (Ritter *et al.* 1995).

All the current inefficiencies in the use of these host systems dictate the need for an efficient system capable of producing large quantities of high quality monoclonal antibody at a low cost to meet market demand.

1.6. WORLD PRODUCTION CAPACITY

As the availability and demand for pharmaceutical MAbs increases and new applications that exploit MAbs are developed, highly scalable production systems will become increasingly important. Current total site capacity for antibody manufacturing using mammalian cell culture is estimated as being 20,000-200,000L, as a result of the increasing drive for low cost antibody production from high dosage requirements and an expanding market potential (Farid, 2007). Existing benchmark investment costs for antibody manufacturing facilities are \$660-\$1580/ft^2 (\$7130-\$17,000/m^2) and \$1765-\$4220/L (Farid, 2007). In another study, it was estimated that the cost to produce 1kg of antibody per year was approximately one million US dollars and the current capacity available for production did not exceed 1000kg per year (Gormord *et al.*, 2004). Key economic drivers for antibody manufacture were identified as being upstream titre and overall yield at the end of the process chain (upstream plus purification).

Farid (2007) highlighted that pressures of cost reduction was the main driving factor for future trends including alternative host technology (transgenic plants, animals, or *E.coli* and yeasts), disposables, and downstream technology improvements.

1.7. PRODUCTION OF RECOMBINANT MONOCLONAL ANTIBODIES IN TRANSGENIC PLANTS

1.7.1. PLANT EXPRESSION HOST SYSTEMS

The first plant-derived technical proteins have already reached the market (Hood *et al.*, 1997; Witcher *et al.*, 1998) and have proven to be economically competitive against established market sectors (Kusnadi *et al.*, 1998; Evangelista *et al.*, 1998). Some plant-derived biopharmaceutical proteins, such as antibodies, vaccines, human blood products, hormones and growth regulators have also reached the late stages of commercial development (Fischer and Emans, 2000; Giddings, 2001). In 1999, the global market for these plants was estimated to be $3 billion with trend that was expected to increase to $25 billion by 2010 (Persidis, 1999). Many consider there to be a great potential for producing high value products in transgenic plants.

Several plant species have already been genetically modified to improve various agronomic traits and output traits including their use as "biological factories". Biologically active antibodies have been successfully been produced in the leaves of tobacco and alfalfa, in tubers or seeds such as potato, corn, rapeseed, safflower, soybean, wheat and rice (Gormord *et al.*, 2004). The legumes, alfalfa and soybean produce lower mounts of leaf biomass compared to tobacco, but have the advantage of using atmospheric nitrogen through nitrogen fixation, thereby reducing the need for chemical inputs like fertilisers to optimise growth (Twyman *et al.*, 2003). Alfalfa is particularly useful because it has a large dry biomass yield per hectare and can be harvested up to nine times a year. Both of these legumes have been used to produce recombinant antibodies (Zeitlin *et al.*, 1998, Khoudi *et al.*, 1999). Alfalfa is being used to

produce an increasing number of products, by the Canadian company Medicago Inc. (http://www.medicago.com/).

The expression of recombinant antibodies in seeds allow long term storage at ambient temperatures, while expression in fruit or other vegetables, such as tomatoes (McGarvey *et al.*, 1995), potatoes (Chong *et al.*, 2000), and lettuce (Kapusta *et al.*, 1999), allow the possibility of direct or oral administration. At present, maize is the main production crop for recombinant proteins (Ma *et al.*, 2003). Food crops, however, may be more difficult to be accepted by regulatory authorities due to fear of the transgenic crop entering into the untargeted food chain (Ma *et al.*, 2003).

To compare some of these crops, Kusnadi *et al.* (1997) estimated the cost of producing a recombinant protein by assuming an accumulation of 10% (w/w) of the total crop protein, and on the basis of the commodity price of the crop, and the weight fraction of the total protein in the crop. It was found that potato cost almost 6x more in terms of ($/kg recombinant protein) than the majority of crops, and peanuts cost almost 3x more. The majority of crops in this study included corn, canola and sunflower which were similar in its estimated cost per unit mass recombinant protein. Soybeans and alfalfa leaves were slightly lower in this estimate of production costs. The leafy crops therefore had the lowest costs associated with extraction and processing. This indicates that the existence of a large scale production infrastructure and a high protein yield combined with low production costs make leafy crops a commercially viable host for large scale monoclonal antibody production. (Tobacco was not included in this study).

1.7.2. GENETIC MODIFICATION OF THE HOST CROP

The generation of transgenic plants expressing recombinant proteins encompasses the preparation of expression constructs, transformation, regeneration and the production and screening of several generations of plants. The screening phase is essential to guarantee transgene and expression stability and the biochemical activity of the protein, in addition to the lack of any adverse phenotypic changes in the host plant (Twyman *et al.*, 2003).

The two general methods used to transform plant lines for molecular farming are *Agrobacterium*-mediated transformation and particle bombardment (Ma *et al.*, 2003). *Agrobacterium*-mediated transformation is achieved using the natural gene-transfer mechanism of *Agrobacterium tumefaciens*. Alternatively, transplastomic plants can be generated by introducing DNA into the chloroplast genome by particle bombardment (Daniell *et al.*, 2002). The advantages of chloroplast transformation include high transgene copy numbers, accumulation of the recombinant protein within the chloroplast limiting toxicity, and the absence of functional chloroplast DNA in the pollen of most crops providing natural transgene containment.

Chloroplast transgenic systems offer both high yields and biosafety benefits with respect to transgene containment, due to maternal inheritance. However, the use of this system as a general approach in molecular farming is limited as chloroplasts are unable to carry out many post-translational modifications, including glycosylation (Daniell *et al.*, 2002). In addition, biosafety concerns have been brought to light by the recent evidence of *in vitro* horizontal gene transfer from chloroplasts of transplastomic plants to bacteria (Kay *et al.*, 2002). As particle bombardment shows less genotype dependence, this method of transformation can also be applied to cereals such as rice, wheat, maize, as well as soybeans and other legumes (Christou, 1996). These transformation methods generally lead to the introduction of superfluous DNA sequences into the nuclear genome. During transformation, the human gene is incorporated into the genome of a plant virus, with which the plant is infected. The virus can then spread throughout the plant, producing the recombinant protein along with its native proteins.

There has been a recent move towards transient expression of plant systems, rather than transformation. Transient expression by agro-infiltration in tobacco leaves can be used to produce significant amounts of protein in short periods of time (Kapila *et al.*, 1997), for example milligrams of recombinant antibodies are produced in just a number of days to weeks, in this way (Vaquero *et al.*, 2002). Equally, virus-infected plants have also been used to transiently express antibodies (Verch *et al.*, 1998). Plant virus vectors (based on the tobacco mosaic virus, TMV) are used to transiently but rapidly express genes of interest in non-transgenic plants, such as tobacco. TMV and related vectors move quickly throughout the entire plant, causing protein synthesis and accumulation in most tissues. Overall upstream production times are thus reduced from a typical length of 2 years for normal transgenic plant systems to a period of weeks to months. This technology was commercialised by Large Scale Biology (now known as Kentucky BioProcessing). Disadvantages of transient expression however, are that agro-infiltration has a low scale-up capacity, and viral vectors provide additional biosafety concerns in terms of containment. Alternatively, transient expression systems can simply be used to evaluate expression constructs and product quality before committing to the expense of transgenic plants (Fischer *et al.*, 1999).

1.7.3. CURRENT EXPRESSION LEVELS AND TARGET ACCUMULATION

In plant production systems, yields in excess of 1% of the total soluble protein are routine (Ma *et al.*, 2003). This is a result of about 25 years of placing considerable effort on the optimisation of recombinant protein expression levels including MAbs in transgenic plants. Among the strategies that have been investigated, there is the use of plant codon optimised genes (Mason *et al.*, 1992), and the use of different promoter genes (Kay *et al.*, 1987; Padidam *et al.*, 2003), silencing suppressors (Anandalakshmi *et al.*, 1998; Plasterk *et al.*, 2000), or different targeting strategies for the accumulation of the recombinant protein (Conrad and Fiedler 1998). Recombinant protein yields in transgenic plants can be optimised by expression-construct design, or by amplifying transcription and translation rates (Twyman *et al.*, 2003). For dicotyledonous species, such as tobacco, the strong and constitutive

cauliflower mosaic virus 35S (CaMV 35S) promoter is often used to promote transgene expression (Tyagi, 2001). The CaMV 35S promoter however, has a lower activity in cereals, and so the themaizeubiquitin-1 (ubi-1) promoter is favoured (Christensen and Quail, 1996). Transcription rate in cereals is also enhanced by the inclusion of an intron (Vain *et al.*, 1996). However, in contrast to the optimisation of expression, relatively less work has been carried out on the optimisation of downstream processing for recombinant proteins from plant tissues.

1.7.4. PROTEIN FOLDING AND ASSEMBLY AND GLYCOSYLATION

Protein folding and assembly is largely regulated by enzymes and molecular chaperones. Chaperones have a quality control function that allow them to associate with malfolded proteins or proteins that have not assembled with their partner chains. Chaperones also influence the folding of proteins and often hold proteins in a partially folded state until they are ready to be folded or associated with their partner chains. These associations are time-dependent. One of the first discovered chaperones was Binding Protein (BiP). Antibody assembly in B cells of mammals requires BiP to stabilise nascent polypeptide chains (followed by other chaperones). In the final stages of assembly, kappa chain stabilises the heavy chain.

Plants have been found to assemble antibody efficiently (Ma *et al.*, 1994). It is known that plant BIP has 69% homology with mammalian BiP (Nuttall *et al.*, 2002), and it is possible that plant BiP is involved in the assembly of the recombinant IgG in plants. Being eukaryotic, plants are also able to carry out various posttranslational modifications. Glycosylation of proteins occurs as the protein passes through the secretory pathway. Synthesis of N-linked glycans in mammals, insects and plants begins in the ER and produces identical glycan structures in this compartment (Mannose-9 core) (Cabanes-Macheteau *et al.*, 1999). Following the ER, the glycoproteins are transported to the Golgi apparatus, where the glycan chains are trimmed and modified. The extent and type of modification depends on the organism.

Plant glycosylation patterns differ from the mammalian pattern in that they possess fucose with a different linkage, as well as xylose, and also lack the galactose and terminal sialic acid (Cabanes-Macheteau *et al.*, 1999). Cabanes-Macheteau *et al.*, (1999) compared the glycan structures present on a murine IgG1k MAb (Guy's 13) with those on the recombinant plant-expressed form. It was found that Guy's 13, had two potential N-glycosylation sites. One potential glycosylation site was the constant region of the heavy chain (as in most antibodies) and the second potential site for glycosylation was an N-glycosylation consensus sequence in the Fab part of the IgG1 molecule.

It was found that for plant-derived Guy's 13, both N-glycosylation sites situated on the heavy chain of the antibody were N-glycosylated as in murine-derived Guy's13. However, the plant-derived antibody had a larger number of glycoforms than its mammalian-derived counterpart. In addition, 60% of the oligosaccharides N-linked to the plantibody had $\beta(1, 2)$-xylose and $\alpha(1, 3)$-fucose residues attached to the $Man_3GlcNAc_2$ core (Cabanes-Macheteau *et al.*, 1999).

It has been suggested that the differences between plant and human glycosylation patterns may present potential problems in producing effective pharmaceutical proteins from transgenic plants. This may be manifested by the alteration of the half-life or the tissue-specific targeting of the recombinant glycoprotein, or if plant-derived glycoproteins are used in human therapy, there is a concern that immune responses may be directed against the plant glycans on these recombinant proteins.

Contrary to this, however, Cabanes-Macheteau *et al.*, (1999) reported that differences in glycosylation were not a limitation to the use of plantibody Guy's 13 for topical passive immunisation. Further studies are necessary, however to address concerns about the potential use of plant-derived antibodies in systemic immunisation. Like Cabanes-Macheteau *et al.*, (1999), most research has focused on determining whether any anti-plant glycan responses are induced in immunised animals. Chargelegue *et al.*, (2000) were also unable to detect any anti-glycan responses in mice for the murine Guy's 13 MAb with plant-specific glycans, produced in transgenic tobacco. Similarly, for topical application of a plant-derived secretory antibody (SIgA/G) applied to tooth surface, there was no anti-glycan response (Ma *et*

al., 1990). Nonetheless, further research is being done in this area. For example, Bardor *et al.*, (2003) looked at the immune responses to plant glycoproteins, rather than the previous papers described that had looked to see whether any immune response was generated against the glycans present on self proteins. Bardor *et al.*, (2003) demostarted immunoreactivity in mammals to two typical plant glyco-epitopes, core α(1,3)-fucose and core xylose.

Strategies have also been employed to 'humanise' the glycan structures of recombinant glycoproteins such as the use of purified human β(1,4)-galactosyltransferase and sialyltransferase enzymes to modify plant-derived recombinant proteins in *vitro* (Blixt *et al.*, 2002), and the expression of human β(1,4)-galactosyltransferase in transgenic plants to produce recombinant antibodies with galactose-extended glycans (Bakker *et al.*, 2001). In the latter case, 30% of the antibody was galactosylated, in similar proportions to hybridoma cells. However, in *vivo* sialylation is expected to be more difficult to accomplish since plants do not have the precursors and metabolic capability to make this carbohydrate group (Twyman *et al.*, 2003).

1.7.5. ADVANTAGES OF TRANSGENIC PLANTS OVER OTHER EXPRESSION SYSTEMS FOR MONOCLONAL ANTIBODY PRODUCTION

Transgenic plants have successfully been used for the production of full-length IgG antibody (Hiatt *et al.*, 1989), multimeric secretory antibody (Ma *et al.*, 1995) and a wide range of functional antibody fragments including single-domain antibody (Benvenuto *et al.*, 1991), single-chain Fv molecules (Owen *et al.*, 1992), Fab and F(ab')2 (De Neve *et al.*, 1993). One of the most successful examples is the expression of complex full-length immunoglobulins that are accumulated in transgenic tobacco to levels of up to 8% (v/v) of the total soluble protein (Ma *et al.*, 1994). Although, it is known that there are slight differences in glycosylation patterns of plant-derived antibodies to those produced in humans that may pose a risk for systemic immunisation, these may not be a disadvantage for passive immunization, as discussed in the Section 1.7.4.

Transgenic plants offer numerous advantages over traditional host systems for MAb production, including the ease and potential of scale-up at the upstream level of processing, with the possibility of the scale of agriculture, the ability of plant cells to correctly fold, assemble and process complex proteins, and low preliminary costs (plants instead of steel bioreactors, bearing in mind the cost of steel is rising, and the lack of a need for skilled personnel to run the bioreactors), (Drake *et al.*, 2003). The estimated cost of producing recombinant proteins in plants is at 2-10% of the cost of microbial fermentation systems and at 0.1% of the cost of mammalian cell cultures (Giddings, 2001; Twyman *et al.*, 2003). This is dependent on the product yield and the market value of the product. Whilst conventional fermentation systems have limited capacity according to its initial volumetric size, the scale of plant-based production systems can be modulated rapidly. A field of transgenic plants can be scaled-up more than 1000-fold in a single generation (Schillberg *et al.*, 2002). Therefore, simply by increasing or decreasing the amount of cultivated land, production can be scaled up or down rapidly according to market demands.

Other advantages include the low risk of endotoxins or viruses, prions and oncogenic DNA in comparison to other host systems such as bacteria and mammalian respectively, and the avoidance of ethical issues associated with use of transgenic animals (Drake *et al.*, 2003). The main disadvantage of transgenic plants is the current lack of a robust regulatory framework for this newer production host (Hood *et al.*, 2002), but this is making progress (Spök *et al.*, 2008). A review by Hood *et al.*, (2002), reported that challenges of production of MAbs in transgenic plants include manufacturing capacity, glycosylation (discussed in Section 1.7.4), overall production cost, timelines, and production issues specific to plants (Hood *et al.*, 2002). The timescale for production of transgenic plants is long and is therefore currently a challenge in the field. The testing phase to ensure transgene and expression stability and the biochemical activity of the product, as well as the absence of adverse phenotypic changes in the host plant is approximately 2 years (Twyman *et al.* 2003).However, recent trends in the plant biotechnology field have been a move to transient expression systems, as discussed in Section 1.7.2 above, to shorten production times. In comparison, microbial and animal cell expression systems can produce the first batches of recombinant protein at shorter timescales. Plant cell-suspension cultures

also have a shorter testing time period than transgenic plants and have also been used for molecular farming especially where high containment is an advantage (Fischer *et al.*, 1999).

The main argument for production of recombinant proteins in plants is that current global protein production facilities are limited. On the other hand, production of vaccines at agricultural scale is limited only by the amount of land available. For example, 250 acres of greenhouse space could provide enough hepatitis B virus vaccine for South East Asia every year (Ma *et al.*, 2005).

1.7.6. REGULATORY CONSIDERATIONS AND BIOSAFETY

Biosafety concerns include the potential exposure of herbivores to pharmaceutical products expressed in the transgenic plants, and leaching of the recombinant proteins into the environment (Twyman *et al.*, 2003). Similarly, another biosafety concern is horizontal gene transfer or the potential for transgene spread by pollen, or dispersal of seed (Sparrow *et al.*, 2007). A further issue is the toxicity and allergenicity of the recombinant proteins.

There have been some efforts to tackle these concerns. For example, regulated promoters can be used in preference to constitutive promoters for biosafety. Although constitutive promoters enable high-level accumulation of recombinant proteins in seeds, the proteins are also expressed in other parts of the plant, such as the leaves, pollen and roots. In some cases, this could have an adverse effect on the growth and development of vegetative plant parts, and might expose herbivores, pollinating insects and microbes in the rhizosphere to the effects of the recombinant protein. Limited protein accumulation to only seeds would lower these risks (Stoger *et al.*, 2002). Alternatively, inducible promoters can be used to restrict recombinant protein expression to the time of harvest. This has been achieved with recombinant glucocerebrosidase expressed in tobacco (Cramer *et al.*, 1999). To mitigate the risk of transgene spread by pollen dispersal, physical and genetic barriers can be used. For example, temporal isolation can be used to genetically isolate crops by sowing different crops at different times so that flowering occurs at different times, thus preventing the possibility of cross pollination (Sparrow *et al.*, 2007). Alternatively, to

prevent the possibility of pollination, the flowers can be physically removed. (It should be noted however, as discussed in Section 1.8, that this will increase the amount of alkaloids in tobacco leaf tissue, thereby increasing the purification burden.

1.7.7. THE PLANT BIOPHARMING INDUSTRY

At the moment, public acceptance of biotechnology-derived foods is particularly low in Europe. However, biotechnology-derived drugs are more likely to be accepted by the public, especially with the enforcement of strict regulatory measures (Twyman *et al.*, 2003). The commercial take-off for the plant biopharming industry is relatively recent. However, in spite of this, the industry has demonstrated growth and has attracted a significant investment. According to Twyman *et al.*, (2003), there were about 100 small biopharming companies, each concentrating on the development of a few products in 2003. A list of current leaders in the biopharming industry, each of which many products in the pipeline is shown in Table 1.1.

Company	Base	Main Crop	Main product developments	Business news	Reference
Prodigene, Inc.	USA	Corn	Recombinant proteins such as trypsin. High-value industrial enzymes, and human and animal vaccines, such as an edible human vaccine for hepatitis B are also in the pipeline.	Launched the first large scale-up manufacturing of recombinant trypsin from transgenic plants. In 2002, Prodigene became under scrutiny of the FDA after it was discovered that their transgenic corn was contaminating non-transgenic corn crop, but is still in business.	http://www.prodigene.com/
Kentucky BioProcessing, Llc.	USA	Tobacco	Recombinant proteins such as Aprotinin. Parvovirus Vaccine for animals and HPV vaccine for humans are in development.	Formerly known as Large Scale Biology (LSB). Kentucy Bioprocessing (KBP) bought Large Scale Biology's assets in 2004, after LSB was approaching bankruptcy. Now, KBP has acquired an extensive intellectual property portfolio that involves the expression, extraction and purification of proteins in a plant based system.	http://www.kbpllc.com/
SemBioSys Genetics, Inc.	Canada	Safflower	Insulin and other protein-based pharmaceuticals for metabolic and cardiovascular diseases.	Currently has a positive forecast in the marketplace.	http://www.sembiosys.com/
Meristem Therapeutics, Llc.	Europe	Tobacco, Corn	Plant-derived human gastric lipase; IgA for cancer tumours.	There is collaboration with between Meristem Therapeutics and Solvay Pharmaceuticals (http://www.solvay.com) for the development of plant-derived human gastric lipase (currently in phase II clinical trials).	http://www.meristem-therapeutics. com
Planet Biotechnology, Inc.	USA	Tobacco	CaroRxTM, a recombinant antibody used for the prevention of dental caries; RhinoRx™ for Colds due to Rhinovirus; DoxoRx™ for Drug-induced Alopecia	Has a Protected-SIgA™ Technology. CaroRxTM is currently in phase II clinical trials.	http://www.planetbiotechnology.com

Table 1.1: Companies using transgenic plants to make biotechnology derived drugs

1.8. *NICOTIANA TABACUM*

1.8.1. ADVANTAGES OF TRANSGENIC TOBACCO

Tobacco is now well-established as a successful crop system for molecular farming and is consequently one of the strongest candidates for the commercial production of recombinant proteins (Schillberg *et al.*, 2002; Stoger *et al.*, 2002). It has been shown that transgenic tobacco is capable of expressing many recombinant proteins to very high levels. One of the most successful examples is the expression of complex full-length immunoglobulins that are expressed in transgenic tobacco to levels of up to 8% of total soluble protein (Ma *et al.*, 1998). Large scale purification of monoclonal antibodies from transgenic tobacco plants in particular offers many advantages over the commonly used host production systems. In addition to those discussed above (Section 1.7.5), tobacco in particular is agronomically well established, it provides a large amount of biomass (more than 100,000 kg per hectare for close-cropped tobacco, (Ma *et al.*, (2003)), provides prolific seed production, and is a non-food crop, meaning that there is no risk of transgenic material entering the food chain, (Sparrow *et al.*, 2007). In addition the technology for gene transfer and expression in tobacco is now mature. Hence, tobacco is emerging as a strong contender out of the many plant production systems being considered.One of the more recent and potentially more promising developments involving tobacco is an alternative non-transgenic technology that has been described to produce MAbs in these plants (Gleba *et al.*, 2007).

The main disadvantage of using tobacco as opposed to other plant systems for example dry cereal crops such as corn or maize is the need to process fresh wet tissue and the presence of toxic alkaloids and phenolics (that can cause protein structural modifications) in its leaves that are essential to be removed, thus making downstream processing more complicated. In addition, the moist environment of the leaves may mean that the protein product is more susceptible to proteolytic degradation. Although many tobacco cultivars produce high levels of toxic alkaloids, there are low-alkaloid varieties that can be used for the production of pharmaceutical proteins. Aside from immediate processing of harvested tobacco leaves, it may be possible to freeze or dry the leaves for transport, provided this does not negatively affect the recombinant protein. In contrast, the dry desiccated environment of seeds enables antibodies

to be stably stored within the seeds for a minimum of 3 years (Stoger *et al.*, 2002). However, as seeds are a food crop, there is a concern that there would be the potential for genes to spread into crops that are grown for food purposes and the possibility of inadvertent contamination during seed collection and storage.

As mentioned above, agricultural practices in the traditional tobacco industry are currently well-established. However, in a biopharmaceutical production setting, in order to meet containment requirements, it is likely that tobacco plants will not be allowed to flower, thus preventing cross-pollination or gene-flow. This will probably be achieved either by harvesting leaf tissue before plants are mature enough to flower or cutting flower tops as soon as they form. Thus, gene flow can be minimized. Tobacco has the disadvantage that its biomass must be processed immediately after harvest (Kostandini *et al.*, 2006).

Kostandini *et al.*, (2006) claimed that transgenic tobacco will have a significant impact on the production practices of the relatively small number of contracted growers. Contrary to traditional tobacco, manual methods of harvesting (such as cutting, spiking or spearing) is not likely to be suitable for transgenic tobacco which, are more likely to require mechanical harvesting and immediate transportation to processing facilities. Examples of mechanical harvesting equipment include cutting machines, spearing machines, cutting-notching devices and machines, and the mechanical leaf harvester.

1.8.2. TRANSGENIC TOBACCO LEAVES OR ROOTS

It has also been established that recombinant protein in transgenic tobacco are expressed also in parts of the plant other than leaves, and there has been evidence of rhizosecretion from the roots (Borisjuk, 1999; Drake *et al.*, 2003), so that there are many potential strategies for harvesting from tobacco plants. However, thus far, monoclonal antibody extraction from tobacco plants has primarily been from fresh leaf tissue.

Studies considering the modular growth of *Nicotiana tabacum* plants found that 50% of the plant's fresh weight is located in the leaves, with the other 50% allocated to the root and shoot axis (Walter and Schurr, 1999). But, as the plant size increases, the proportion of the shoot axis rises at the expense of the root. (These relations were found to be identical for plants grown at different growth rates due to different nutrient supply). Hence, tobacco leaves represent the majority of the total plant's biomass for large plants and thus would appear to be the obvious tissue choice for extraction. On the other hand, the extraction and recovery of the MAb from tobacco roots may also be a viable option, provided that the roots are found to have similar levels of expression to the leaves. Furthermore, roots also contain a lower level of toxic phenolics and alkaloids, for example, *Nicotiana tabacum* leaves possess 3X as much nicotine as roots of the same plant (Dawson *et al.*, 1959). Also, as transgenic plant production is being considered using hydroponic culture, it is relevant to consider harvesting from root material. This would potentially simplify downstream processing for removal of these major contaminants. On the other hand tobacco leaves are easier to handle that roots that could be prone to tangling in some process equipment. Thus, extraction of recombinant proteins from leaves or roots of tobacco plants both offer their advantages and disadvantages.

Tobacco (*Nicotiana tabacum* var. *Petit Havana*) is the model transgenic crop being used in our research.

1.9. LARGE SCALE PRODUCTION

1.9.1. GREENHOUSE VERSUS OPEN FIELD PRODUCTION

Open fields are the traditional system for biomass production. The reduced requirement for initial capital investment results in a lower overall cost for the production of biomass. The disadvantages of this system include the limited control on matters of people access, weather conditions and exposure to pests and pathogens. Limited containment would also decrease the confidence of regulators in the safety of the

growth conditions for the transgenic plants. This may lead to an increase in the requirements for the conditions of growth and delay FDA approval for the field production of monoclonal antibodies.

In comparison, greenhouses would require greater control than conventional greenhouses to ensure biosafety, and would therefore mean a greater initial capital investment as well as maintenance costs. A well-regulated greenhouse facility, however, would allow for better control of access of persons to the site, and strict containment and environmental procedures should lead to more homogenous growth of plants and decrease the need for pesticides. Finally, stringent containment facilities for this method of biomass production would increase the confidence of regulators leading to shorter approval times.

1.9.2. FIELD PREPARATION AND HARVESTING

The agronomic know-how for farming *Nicotiana tabacum* is deep-rooted. There are several types of tobacco which are classified according to several factors such as climate, soil, cultural practices, variety, curing procedures, and its intended use (Whitty, 2006). Flue-cured, the primary tobacco grown in Florida, is used in cigarettes. The main types of tobacco used in cigarettes in the US are "Flue-cured tobacco" or "Burley tobacco". (The information below is specific to a case study in Florida, Whitty, 2006).

Tobacco is usually grown on well-drained soils because excess moisture in poorly-drained soils can result in crop damage or loss, and excessively-drained soils can cause dehydration and nutrient leaching from the soil. Due to the very small size of tobacco seed (over 300,000 per ounce) (Whitty, 2006), plantbeds or greenhouses are initially used to shield germinating seed and young plants from dehydration or cold weather. Critical to this is moisture maintenance since the seeds are sowed onto the surface of the soil. The plantlets are then ready to be transplanted within 50-90 days. Within the greenhouse, styrofoam trays that float on water are often used (Whitty, 2006). For this, pelleted seed are positioned on potting media in styrofoam trays. The trays are sectioned, allowing the root system of each plant to be separated from that of other plants. The trays then float on a pool of water and nutrients and pesticides (if required).

As an alternative to greenhouses, plantbeds can be used which requires farmers to remove existing crop or weed residue using tillage equipment. Often, a mix of methyl bromide is used for soil fumigation to kill microbes, nematodes, and seeds of weeds. Alternatively, crop rotation with other crops such as grass is done to reduce reliance on pesticides and other pest control practices. These are all biosafety concerns that need to be thought out carefully for transgenic plants. Pelleted tobacco or fresh seed is then sown in rows or evenly spread over the surface of the soil (Whitty, 2006). To ensure efficient contact of the seed with the soil, the soil surface is then patted. Although, some fertilizer is added before seed sowing, it is usually added after the plants have started growing. If required, pesticides are also applied.

It was estimated that under greenhouse conditions, each plant produces 20 or more leaves in 60-90 days. These plants are manually or mechanically topped to remove immature flowers, causing the top leaves of the plant to become larger and thicker. Flower topping causes a loss of apical dominance, increasing the risks of axillary buds developing at each leaf axis. Any axillary buds are manually removed or destroyed with chemical growth regulators (Whitty, 2006).

Leaf harvesting usually begins at roughly the same time as topping, and is done manually or mechanically. Usually bottom leaves of the plant are removed first followed by the middle leaves, then top leaves, since the chemical composition of these leaves vary (Whitty, 2006). This method of harvesting according to leaf position on the stalk is usually done over 6-10 weeks. In the case of transgenic tobacco expressing recombinant protein, it is suggested that the leaves are immediately placed in freezer boxes for brief storage before processing. Normally there will be three to five harvests during the harvest period within the current tobacco farming industry, which occurs when the leaves have become yellow, thus the harvesting strategy and schedule for transgenic tobacco plants for recombinant protein production is likely to differ.

One mechanical method of harvesting, used in both plantbeds and greenhouses is known as "clipping" and involves the use of a mower to remove the top section of the plants (Whitty, 2006). If this is repeatedly done, it ensures that the plants are all approximately the same height when transplanted.

For transplanting, plants are manually pulled from plantbeds or greenhouse trays, and planted in rows that are about 40 inches apart (Whitty, 2006). Plants are spaced about 20 inches apart in the row. Alternatively, a tractor-drawn mechanical transplanter can be used, where the plants are placed in clips or other devices for placing the plants in the soil. Insecticide and fertilizer are often applied at this stage.

Cultivation of tobacco usually occurs two to four times a year for weed control. For tobacco plants the frequency of irrigation increases as the plants grow. Approximately, 0.25-1.0 inches of irrigation are applied at each application which may sometimes be needed every 3-4 days (Whitty, 2006).

1.9.3. CHOICE OF SITE

There are several factors that could influence the choice of site, including the local availability of labour and the existence of a processing infrastructure. In addition, there should be adequate storage facilities and transport to ensure fast and effective harvesting, and minimise the times between harvesting and processing. The degree of containment is essential and must be able to meet the high standards set by the FDA authorities for commercial production of monoclonal antibodies in transgenic plants both for open field and greenhouse production.

1.9.4. HYDROPONIC SYSTEMS

Hydroponics is generally defined as the cultivation of plants in the absence of soil. This can be considered as an alternative growth system if transgenic plants are capable of secreting significant quantities of a recombinant protein per unit volume. These systems enable the protein to be recovered from either the root exudates or leaf guttation fluid, processes known as rhizosecretion and phyllosecretion respectively (Borisjuk *et al.*, 1999; Komartynytsky *et al.* 2000). The ability of plant tissues, such as leaves or roots, to secrete recombinant proteins in their exudates in this way, enables proteins to be continuously accumulated.

It is thought that rhizosecretion is a diffusion based process driven by the concentration gradient between the apoplast and the medium (Borisjuk *et al.*, 1999). The recombinant proteins GFP (Green Fluorescent Protein), bacterial xylanase and human placental alkaline phosphatise (SEAP) have all been produced by rhizosecretion in transgenic tobacco. These proteins were successfully secreted, retaining their biological activity and accumulating to higher amounts in the medium than in root tissue. For example, SEAP reached a maximum yield of 20μg per dry root mass per day (Borisjuk *et al.*, 1999).

In addition, Drake *et al.*, (2003) demonstrated rhizosecretion of antibodies. However, this type of strategy is likely to be applicable only for small-scale production in high-containment facilities as field deployment would result in large amounts of recombinant protein leaching into the soil and groundwater (Twyman *et al.*, 2003).

On the other hand, hydroponics would eliminate the need for vast farmland and allows crops to be produced in greenhouses. Hydroponic techniques would also allow for precise water and nutrient application directly to the roots of each plant. The conditions of growth for hydroponic based systems must be sterile and stable environmental conditions must be maintained (Komartynytsky *et al.* 2006). The technology is being developed by the US biotechnology company, Phytomedics Inc. (http://www.phytomedics.com/). One of their technologies, RHIZEX™ is a greenhouse-based hydroponic plant cultivation technology that enables environmental containment and reproducible and consistent production of recombinant proteins and botanical therapeutics.

1.10. GUY'S 13 MODEL

The model recombinant protein used for this investigation is Guy's 13, a murine monoclonal IgG1 antibody which recognises a conformational epitope of the major cell surface protein (SA I/II) of *Streptococcus mutans* (Smith and Lehner, 1989). The SA I/II epitope recognised by Guy's 13 is 105.1_{13} (van Dolleweerd *et al.*, 2003).

Ma *et al.* (1994) produced the light (κ) and heavy (γ) chains of Guy's 13 individually in tobacco, crossed the best expressors to generate monomeric Ig expressing plants in the next generation. In these plants, Guy's 13 were expressed at levels up to about 1% (v/v) of total soluble protein. Following on from this, Ma *et al.* (1995) successfully generated transgenic *Nicotiana tabacum* plants that expressed a murine Guy's 13 monoclonal antibody light (kappa) chain, a hybrid immunoglobulin A-G heavy chain, a murine joining chain, and a rabbit secretory component. Following successive sexual crosses between these plants and filial recombinants, plants were generated that expressed all four protein chains at the same time to form a complex. Furthermore, this fully assembled, functional, high molecular weight secretory immunoglobulin recognised the native streptococcal antigen I/II cell surface adhesion molecule. Interestingly, whereas two different cell types (B cell and epithelial cell) are required in mammals to assemble secretory antibodies, plants use one cell type for this purpose (Ma *et al.*, 1995). In addition, this secretory IgA/G chimeric immunoglobulin was engineered with an additional IgG CH2 domain to facilitate purification of the antibody by protein G affinity chromatography (Larrick *et al.*, 2001).

The ability of SIgG A/G and Guy's 13 to prevent oral recolonisation of *S. mutans* has been scientifically demonstrated (Ma *et al.* 1998). Furthermore, in a number of clinical trials, this antibody has been shown to prevent colonization in the human oral cavity. The market demand in the UK and the US for Guy's 13 is predicted to be high (Ma *et al.*, 1995). Despite improvements in mammalian cell culture, (see Sections 1.5 and 1.6), the worldwide manufacturing capacity is limited. This is mainly due to the fact that the cost of goods is dependent on the scale of operation, volume of demand and processing time (among other factors).

Currently, the commercial name for sIgA/G is CaroRX™ owned by Planet Biotechnology. Planet Biotechnology estimate that tooth decay caused by bacterial infection takes up approximately 70% of U.S. dental service expenditures, (an annual expenditure of about $50 billion). They approximate that the combined treatable population in the U.S. and Europe is around 115 million people. CaroRX™ is currently in phase II clinical trials under a U.S. FDA-approved Investigational New Drug (IND) application. Guy's 13

IgG1 is the model monoclonal antibody used in our research, and this immunoglobulin can exist in several different forms in the tobacco cell.

1.11. TARGETING STRATEGY FOR IgG ACCUMULATION IN THREE DIFFERENT SUBCELLULAR COMPARTMENTS

1.11.1. SECRETED FORM OF IgG

Unmodified IgG is produced and secreted by tobacco cells into the apoplasm of the cell by default (Frigerio *et al.*, 2000). This occurs in all organs of the plant. Secretion from the roots is known as rhizosecretion. Rhizosecretion of recombinant proteins was also demonstrated by Borisjuk *et al.* (1999). Drake *et al.* (2003) demonstrated that it was possible to target a functional, full-length monoclonal antibody complex from transgenic *Nicotiana tabacum* roots so that it was secreted. To prove that this IgG1 was rhizosecreted, the hydroponic medium surrounding the roots was measured for plants expressing IgG1 and a membrane-bound version of this antibody (mIgG). The membrane bound IgG was not detected in the medium, indicating that despite extraction from leaves, it was not rhizosecreted, but Guy's 13 IgG (denoted in all the text in subsequent Chapters as the secreted form) was detected both in the medium surrounding the roots and from extracted leaves. In seed-derived hydroponic cultures, the mean production of antibody in MS medium with 8 g/l gelatine was 0.28 μg per 25 ml medium per day with a mean of 11.7 μg per gram dry weight per day (Drake *et al.*, 2003).

As additional evidence that Guy's 13 IgG is secreted, a pulse chase analysis of transgenic protoplasts expressing Guy's 13 IgG was performed. Frigerio *et al.* (2000) performed a pulse chase analysis of transgenic tobacco protoplasts expressing Guy's 13 IgG (secreted form). Transgenic tobacco protoplasts were then isolated and radiolabelled with [^{35}S]-Met and then chased. Antibody was immunoprecipitated and run on a non-reducing gel. An antigen antibody assay of lysed cells and of the medium surrounding the cells revealed that the IgG was being secreted from the cell into the medium.

This was shown as decreasing intensity of bands after 16 hours and 24 hours in the cell, and a corresponding gradual increase in the cell's surrounding media. There were also no degradation products in the cell, further proving that intact IgG was being secreted.

1.11.2. MEMBRANE-BOUND IgG

The membrane bound immunoglobulin (mIgG) also investigated for the purposes of extraction in this thesis, was designed and introduced into transgenic tobacco by Vine *et al.*, (2001), using cDNA encoding the full-length Guy's 13 murine γ1 heavy chain with its native leader sequence, transmembrane and intracellular domains. Consequently, the heavy chains of membrane associated forms are slightly larger than those of secreted IgG due to the presence of additional 71 amino acid residues at the COOH terminus. These extra amino acid residues are organised into 3 domains, a 17 residue acidic extracellular portion, a 26 residue hydrophobic intra-membrane portion and a 28 residue hydrophilic intracellular portion (Yamakawi-Kataoka *et al.* 1982).

To make the final transgenic plant expressing mIgG, Vine *et al.* (2001) crossed plants expressing the mIgG heavy chain with plants expressing the light chain of Guy's 13 (Ma *et al.*, 1994) and the resulting plants were screened for successful expression of this modified form of IgG. (It should be noted here that the signal sequence meant that the modified IgG was targeted to the secretory pathway, of which the membrane forms a part). The assembly of light and heavy chains of the IgG into full-length functional antibodies occurs in the endoplasmic reticulum in plants and mammals, and is then directed to the cell membrane by the extra transmembrane sequence on the heavy chain. Vine et al (2001) reported a mean recovery of mIgG from plants of 1.1% (v/v) of total soluble protein.

Studies were carried out by Vine *et al.* (2001) to establish that unlike the normal recombinant IgG which is secreted by the cell, this modified form of the polypeptide was associated with the cell membrane via its heavy chain. Firstly, the effect of the inclusion of detergent was analysed. The extraction buffer used by Vine *et al.* (2001) to homogenise leaf tissue for immunoglobulin detection

included a non-ionic detergent, 1% (v/v) Nonidet P40 (NP40). The reason for the inclusion of this detergent was to establish whether or not this IgG was membrane bound, since it is known that a detergent is necessary for the solubilisation of membranes.

Vine *et al.* (2001) found that the inclusion of this detergent for the extraction of Guy's 13 heavy chain with no added transmembrane sequence, had no effect on the concentration of IgG (secreted form) released. However, for plants expressing mIgG, detection of mIgG's heavy chain was only possible if NP40 was included in the extraction buffer. Thus, the need for detergent during extraction (to solubilise the cell membrane) was demonstrated for the membrane form but not for the secreted form. In addition, as another proof of cell membrane localisation of mIgG, immunofluroescence of transgenic leaf protoplasts were studied (Vine *et al.*, 2001). These protoplasts were labelled with either FITC anti-mouse κ for light chain detection or FITC anti-mouse λ for heavy chain detection. The surface of untransformed protoplasts were illuminated red due to the presence of chlorophyll in chloroplasts, however, the attachment of mIgG to the membrane resulted in bright green surface staining of protoplasts under immunofluroescence.

Although Vine *et al.* (2001) demonstrated that mIgG was bound by its heavy chain to the cell membrane, it did not exclude for the fact that it may also be present in other parts of the cell. It has previously been proven that modified IgGs targeted for secretion, can also be retained in the endoplasmic reticulum and the vacuole (Frigerio *et al.*, 2000). Another uncertainty that remains is whether the transmembrane sequence on this murine IgG includes signals that are specifically recognised by plants, however, it is thought that the detection of a large number of mIgG at the cell membrane indicates a default secretory pathway to the cell surface.

It is thought possible that the attachment of mIgG to the cell membrane may cause destabilization of the membrane since mIgG was more readily extracted from cell membranes than mγ1 (only the heavy chain of mIgG attached) (Vine *et al.*, 2001). However, Vine *et al.* (2001) also observed that contrary to this, the protoplasts isolated from plants expressing mIgG appeared to have the same level of robustness

as wild type protoplasts. Nonetheless, only about 20% of the protoplasts were found to express the foreign antibody.

Vine *et al.* (2001) observed that retention of the heavy chain of IgG to the membrane had no effect on the assembly of the polypeptide within plants contrary to claims by Hiatt *et al.* (1989) that heavy and light chains of full-length immunoglobulins had to be targeted to the endoplasmic reticulum and plant secretory pathway for correct assembly. Subsequent to targeting of recombinant antibodies to a subcellular component, its final cellular distribution has not yet been fully characterised. However, a large amount is known to accumulate in the relatively stable environment of the apoplastic space (Hein *et al.*, 1991). The following fate of these antibodies is also unknown, possibilities of which are degradation, transport to other areas of the plant, or even reinternalisation (Vine *et al.*, 2001).

It is interesting to note that the secreted form of IgG (described in Section 1.11.1) and mIgG are most similar to that found in nature, since in mammalian B lymphocytes and plasma cells, IgG molecules are present in two forms: as secreted antibody or as a surface antigen receptor.

Potential uses of recombinant proteins attached to the cell membrane include interference with microbial invasion leading to disease resistance, greater understanding of membrane proteins, use of cell suspension cultures or protoplasts in large scale adsorption of antigens, and better phytoremediation and environmental clean-up (Vine *et al.* 2001). However, the main advantage of the membrane-bound antibody over its secreted form is the fact that it is retained by the cell, and thus would be more suitable for transgenic plant production in the field, as this would prevent the antibody from being secreted into the environment, and thus is more likely to suit regulations.

1.11.3. IgG-HDEL

The third form of Guy's 13 that is investigated in this thesis has a HDEL sequence engineered onto to the C-terminus of its heavy chain to ensure its retention in the endoplasmic reticulum. Addition of the HDEL- or KDEL- sequence to recombinant antibody or antibody fragments is a well established strategy for targeting these recombinant proteins to the endoplasmic reticulum in order to optimise expression yields (Conrad and Fiedler, 1998). Tagging of the KDEL sequence, for example, allows the retention of scFv in the endoplasmic reticulum, where yields are maximised to 6.8% (v/v) of total soluble protein (Fiedler *et al.*, 1997). In fact, the expression of full-length antibodies in transgenic plants has required the use of a signal sequence which targets them to the ER, and is then secreted to the apoplasm (Hiatt *et al.*, 1989). Evidence has shown that targeting of a secretory antibody in this way allows the expression of 5-8% (v/v) of TSP despite it being apparently incorrectly retained in the ER (Frigerio *et al.*, 2000).

The endoplasmic reticulum (ER) presents an oxidizing environment with a great quantity of molecular chaperones, whilst there are few proteases. These are probably the most important factors affecting efficient protein folding and assembly. Nuttall *et al.* (2002) demonstrated that antibodies targeted to the secretory pathway in transgenic plants interact specifically with the molecular chaperone BiP (binding protein). In the absence of additional targeting information, the expressed protein is then secreted to the apoplast via the Golgi apparatus. The size of the protein then dictates whether it is retained in the apoplast or is secreted from the cell.

However, antibody stability in the apoplast is lower than in ER lumen. Thus, antibody expression levels can be increased if the protein is retained in the ER lumen using an H/KDEL C-terminal tetrapeptide sequence. It has been reported that accumulation levels are 2–10-fold greater compared with an identical protein lacking the H/KDEL signal (Schillberg *et al.*, 2002). A further advantage of this form of the antibody is that they are not modified in the Golgi apparatus, meaning that they have high-mannose glycans but not the plant-specific xylose and fucose residues. (This is discussed further in Chapter 3).

1.11.4. THE ADVANTAGES AND DISADVANTAGES OF MONOCLONAL ANTIBODIES TARGETED TO DIFFERENT SUBCELLULAR COMPARTMENTS IN TERMS OF EXTRACTION

The various advantages and disadvantages of targeting and accumulating the same monoclonal antibody to three different subcellular compartments within tobacco were investigated in this thesis. These subcellular compartments were the apoplasm, the plasma membrane and the endoplasmic reticulum. This is summarised below in Table 1.2 below. There are advantages and disadvantages of each form of the monoclonal antibody (MAb). The default pathway for IgG is secretion, and an advantage of this MAb is that it is the least modified form, and is therefore expected to be the easiest to validate. The membrane-bound IgG (mIgG) would prevent the secretion of this MAb into the environment, and would therefore be more suited to field production. The HDEL tagged IgG would allow for retention in the endoplasmic reticulum, leading to enhanced expression. This form of the MAb however, has a different extent of glycosylation to IgG and mIgG because it does not complete the secretory pathway.

Antibody construct	Location in the plant cell	Features	Reference
1. IgG	Secreted	Least modified form of antibody	Frigerio *et al.*, 2000
2. mIgG	Plasma membrane	No secretion into environment-regulations	Vine *et al.*, 2001
3. IgG-HDEL	Endoplasmic reticulum	Enhanced expression, but different glycosylation to IgG and mIgG	Schouten *et al.*, 1996

Table 1.2: The immunoglobulin constructs investigated in this thesis

1.12. PROCESSING OF RECOMBINANT PROTEINS FROM PLANTS (UPSTREAM, PROTEIN RECOVERY AND PURIFICATION)

Key issues in process development are to shorten the time taken to supply product for clinical trials and to develop a process which can provide sufficient product to meet market demands at an acceptable price per dose (Birch and Racher, 2005). The main stages in the process are shown in Figure 1.2.

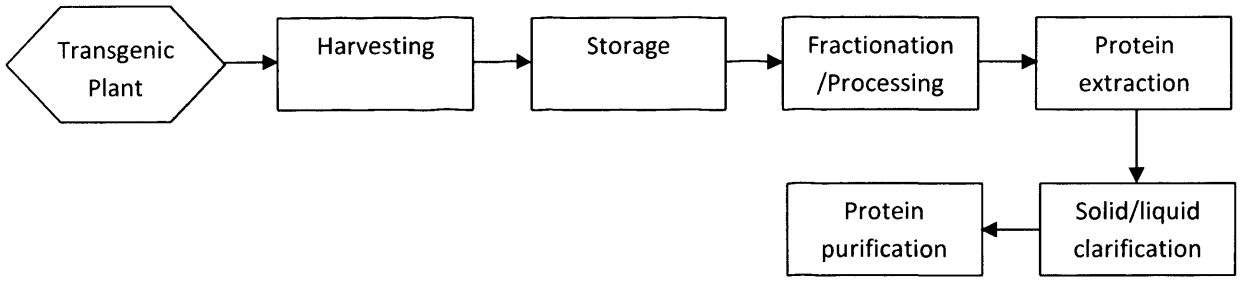

Figure 1.2: A generic process chain for transgenic plants. (Adapted from Menkhaus *et al.*, 2004).

In summary, downstream processing (DSP) is defined by 3 main stages namely, extraction, protein recovery and purification. As soon as recombinant protein expression in plants had emerged as a promising platform upstream, downstream processing (DSP) costs were highlighted as the main determining factor of whether transgenic plants could be a feasible host system at large scale, (Whitelam, 1995). Although economic analysis of transgenic plants for pharmaceutical production is currently limited, there has been small-scale evidence to suggest that the overall production costs are incurred during DSP, i.e. over 80% of the overall processing costs (Mison and Curling, 2000; Evangelista *et al.*, 1998). For example, 94% of the annual operating costs (AOC) for producing and purifying ß-glucuronidase (GUS) from transgenic maize are sustained during seed fractionation (6% of AOC), protein extraction (40% of AOC), and purification (48% of AOC) (Mison and Curling, 2000; Evangelista *et al.* 1998). Thus, with the imminent arrival of a number of transgenic tobacco lines expressing various monoclonal antibodies, the establishment of a model process for purification is increasingly urgent. In addition, optimisation of

downstream processing is important for enhancing the potential of this technology at large-scale and to maximise on its advantages as a competing production system to other well-established systems such as mammalian systems, bacteria, or yeast.

However, to date, relatively little work has been carried out on the optimisation of downstream processing for recombinant protein production from plant tissues. Nevertheless, there is vast information on the extraction of native plant proteins (Jervis *et al.*, 1989). Some information on downstream processing for transgenic tobacco has also been gathered. Unfortunately, not all cases involved transgenic plants, but rather consisted of extracts of native plants that were spiked with foreign protein. Below is a brief summary of this.

1.12.1. STORAGE/PLANT FRACTIONATION

The main objectives of processing transgenic plants are to efficiently extract and purify the expressed recombinant protein in suitable quantities and at a low cost. This may initially involve cleaning, conditioning and grinding of leaf tissue in order to extract the recombinant protein. To date, the grinding of the recombinant protein (secreted or intracellularly retained) has not been found to significantly affect the integrity of the protein (Menkhaus *et al.*, 2004).

Unlike transgenic seed or grain crops that can be stored for years pre-processing, fresh leaves such as that of tobacco are more challenging in this respect. However, there have been some reports of success. For example, Fiedler *et al.* (1997) demonstrated that after a week of storage of leaves that had been dried at room temperature, there was antigen binding activity of single chain variable fragment (scFv) was maintained. Likewise, Khoudi *et al.* (1999) showed that a monoclonal antibody, C5-1, expressed in alfalfa was stable in dry hay 12 weeks after harvest.

1.12.2. PROTEIN EXTRACTION AND RECOVERY

The purpose of protein extraction and recovery is to release the recombinant protein from the plant material into an aqueous environment for further processing. The actual extraction strategy varies significantly with plant species which may be modified to assist purification. For example, SemBioSys Genetics (http://www.sembiosys.com/) developed an oleosin-fusion platform, in which the target recombinant protein is expressed as a fusion with oleosin in oilseed crops. The fusion protein can then be extracted from oil bodies with a simple method involving endoprotease digestion so that the recombinant protein is separated from its fusion partner (Moloney and Boothe, 2003).

For green leaf tissue such as tobacco , however, the most commonly used method of extraction has been wet grinding or homogenisation. This extraction method requires no pre-grinding and high levels of active recombinant protein can be released in short times (Menkhaus *et al.*, 2004).

To date, there have been no detailed studies on comparing extractability of heterologous proteins (or native proteins) that were intracellularly retained versus their secreted form (Menkhaus *et al.*, 2004). Most studies have found that the addition of salts, detergents, and protease inhibitors slightly enhanced recombinant protein extraction, but pH was the main influencing factor. It has been found that the pH of the extraction buffer has a significant effect on total protein extracted from tobacco leaves. From pH 3 to 9, the total native tobacco protein extracted varied from 1.0% to 1.6% (w/w) of the biomass, and thus the purification burden (contaminant proteins needed to be removed) changed significantly (Balasubramaniam *et al.*, 2003).

The stability of the protein in the aqueous environment (after extraction) is also an important factor to be considered. Detrimental compounds include proteases and phenolics that either cause denaturation or irreversible structural modification (Jervis and Piermont, 1989). However, there has only been one example of a really unstable protein in aqueous environment, after isolation from plants, namely, GUS which was found to rapidly degrade after extraction from alfalfa, regardless of the inclusion of protease inhibitors (Austin *et al.*, 1994).

The initial step in protein recovery is to remove the solids from the leaf extract, i.e. clarification. This would involve unit operations such as centrifugation or filtration. Most studies at laboratory scale have involved high speed centrifugation. However, the option of employing expanded bed adsorption (EBA), a novel process unit capable of combining clarification, concentration and preliminary purification in a single discrete step has also been investigated. Plant processing offers challenges. For example, as plant solids are in general, larger, denser, and highly concentrated following extraction (typically 10-30% wt %), the inlet to EBA column is easily clogged, difficulties with column elution may arise, and bed collapse may occur as result of solid interactions (Bai and Glatz, 2003a; Menkhaus and Glatz, 2004a). For each plant species-specific case, it is necessary to establish engineering design parameters including type of column inlet and resin properties.

1.12.3. PURIFICATION

Monoclonal antibodies with therapeutic applications require high degrees of purification, i.e. 95-98% purity (Headon and Walsh, 1994). Plant-related impurities include pesticides, other chemicals used during crop growth and microbial contamination (Miele, 1997). In the majority of processes, product purification has involved chromatography. However, non-chromatographic methods have also been examined due to the current challenges of handling residual solids, improving column life, handling sub-optimally clarified feed, and the current high cost of chromatography.

There have also been efforts to reduce this purification challenge by genetic manipulation of the host. For example, canola, corn, pea, and soy have all been manipulated to increase the efficiency of purification (Menkhaus *et al.* 2004). Zhang *et al.* (2001) utilised the natural acidity of the protein, GUS, to purify it using anion exchange chromatography in combination with charge-modified GUS or immobilised metal affinity chromatography (IMAC) with histidine-tagged GUS to produce a product of very high purity. Another example is the purification of basic T4 lysozyme from canola or soy by cation exchange

chromatography with genetically engineered charge modifications to the target protein so that the elution peak was significantly different to that of native proteins (Zhang and Glatz, 1999).

For antibodies, purification is most commonly enhanced, by utilising the high antibody-antigen specificity. Thus, the purification of expressed antibody or antibody fragments from various plant tissues is relatively simpler with higher resolution compared to that of other non-affinity purification processes. This usually involves a single step of Protein A or Protein G affinity purification yielding a product that typically has a purity of 99% (Menkhaus *et al.*, 2004). For non-IgG antibody types, an additional IgG CH2 domain can be engineered to the molecule to enable Protein A/G affinity chromatography. In addition, other specific protein-binding ligands, such as Protein L against κ variable region are being developed (Bjorck, 1998; Nilson *et al.*, 1992; Akerstrom *et al.*, 1989).

Most work on protein purification specifically from tobacco has involved chromatography. Tagging GUS with the calmodulin protein (CaM), permits GUS to be purified on a phenothiazine affinity column, giving rise to a 20-fold increase in purity (Desai *et al.*, 2002). Histidine-tagged proteins are also a common method of purifying recombinant proteins from tobacco by immobilised metal ion affinity chromatography (IMAC). For example, His6-tagged lactate dehydrogenase was purified in this way, resulting in a 61% increase in purity, and a 48% increase in overall yield (Mejare *et al.*, 1998).

Multi-step chromatographic methods have also been used to purify proteins from tobacco. For example, Krishnan *et al.*, (2002) used anion and cation exchange chromatography to purify a recombinant trichosanthin (a ribosome-inactivating protein) from tobacco. Similarly, Gazaryan *et al.*, (1996) purified the tobacco native protein, anionic peroxidise, to a single band on an SDS-PAGE gel with 80% recovery, using anion exchange and size exclusion chromatography. Other processes, however, that have been designed for purification from tobacco are more complicated, involving a greater number of downstream processing steps, thus reducing the yield for achieving a high purity level product. For example, a process designed for the purification of a soluble salicylic acid binding protein from tobacco involved one anion

exchange, two size-exclusion and one blue dextran-agarose affinity steps, resulting in a 250-fold purification but a 16% yield (Chen *et al.* 1993).

However, due to the nature of components in tobacco extract, complicating direct application to a chromatographic column, the main challenge for large scale purification from tobacco is the development of more economical and scalable pre-chromatographic unit operations. Furthermore, almost all chromatographic purifications from tobacco to date have been done at laboratory scale with clarified extract, often resulting in a high degree of resin fouling. Alternatives to chromatography include precipitation (used for purification of GUS from canola (Zaman *et al.* 1999) and pea (Menkhaus *et al.* 2004a), and aqueous two-phase separation (used for purification of egg white lysozyme from tobacco) (Balasubramaniam *et al.* 2003).

Overall, any process design for the production of a recombinant protein from plants needs to consider regulatory requirements such as those detailed by the Food and Drug Administration (FDA) from the outset.

1.13. WHY IS THE OPTIMISATION OF EXTRACTION IMPORTANT?

As mentioned above, downstream processing (DSP) is represented by 3 main stages namely, extraction, protein recovery and purification. The initial phase of extraction is arguably the most important part of DSP, since it determines the initial level of MAb available for purification, the level of protein and other contaminants requiring removal, handling volumes, the sequence of following DSP stages, and the degree of waste removal and control required, and hence it is the focal point of this study.

In defining an optimal extraction procedure for recombinant MAbs from tobacco plants, there are a variety of parameters to consider. These include the mechanical disruption technique, buffer composition, pH, temperature, as well as many others. The extraction process should release an efficient concentration of the active component, with minimal release of contaminants into the process stream. In addition, the design of this step should consider the fact that plants unlike some other host systems

involve large volumes of biomass and extraction buffer offering further challenges to the downstream process (Menkhaus *et al.* 2004).

1.14. INSIGHT INTO SOME METHODOLOGIES EMPLOYED IN THIS THESIS

1.14.1. ULTRA-SCALE DOWN TECHNIQUES

Most often in literature featuring transgenic plants, recombinant antibody expression level is determined by applying a specific extraction protocol to the plant tissue at small-scale, and then measuring concentration by immunoglobulin detection. This concentration is then directly translated into the plant expression level by comparing to a reference basis, such as total soluble protein. However, the problem with this is that this does not take into account the efficiency of the extraction protocol.

In this work, small scale techniques are used to design extraction procedures for a potential large scale process which could be used for the recovery of Guy's 13 MAb from plants. This is necessary because it is impossible to design an optimised process (e.g. lowest cost, highest recovery of intact protein, easiest form of process validation etc.) without performing initial experiments at smaller scale.

Ultrascale technologies is a representation of the large scale process, but at much smaller scale (e.g. microlitres or millilitres, instead of thousands of litres), by the use of specially designed small devices. Ultrascale down techniques will be used to design the large scale process which could be used for the recovery of this protein from plants. Alternatively, non-mechanical techniques that can be proven to be reproducible at small-scale will be used. This is necessary because it is impossible to design an optimised process (e.g. lowest cost, highest recovery of intact protein, easiest form of process validation etc.) without doing initial experiments at smaller scale. Small-scale studies can be used to predict and verify the performance of industrial sized downstream processing equipment.

In summary, ultra-scale down techniques enables the rapid early stage evaluation of manufacturing choices with millilitre quantities of process material (Varga *et al.*, 1998; Boychyn *et al.*, 2000).

1.14.2. MICROMANIPULATION TECHNIQUES

Micromanipulation is used in this study to measure the mechanical force required to break the roots (indicative of root strength). This is a technique by which particles, of 1μm in diameter or greater can be compressed, and their force deformation behaviour determined (Thomas *et al.*, 2000). This tool can be used to give information on the mechanical properties of animal, bacteria, yeast, and plant cells (from suspension cultures).

Unlike other available techniques for individual cell mechanical property measurement, such as the Young's modulus measured by aspiration (Jones *et al.* 1999), viscoelasticty by cell poking (Goldmann, 2000) and turgor pressure by a pressure probe (Tomos, 2000), micromanipulation techniques are capable of measuring the mechanical properties of cells at large deformations, particularly to bursting. During tissue and/or cell disruption during processing, the cells are subject to high shear forces. The main principle of micromanipulation is the compression of a single particle (such as a cell in its aqueous environment) between two parallel surfaces. One of these parallel surfaces often represents the flat end of an optic fibre probe and the other surface, a microscope slide (as shown in the Figure 1.3).

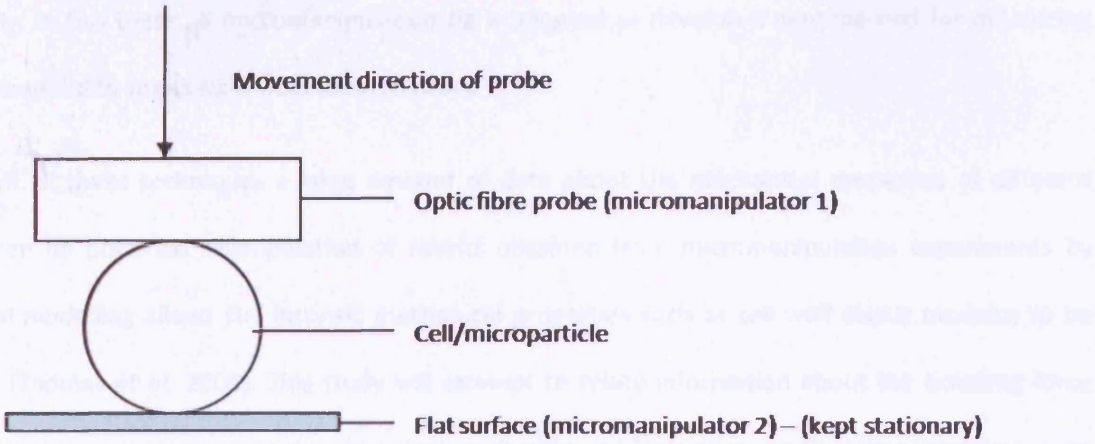

Figure 1.3: Compression of a single cell between two parallel surfaces. (Adapted from Thomas *et al.*, 2000).

The probe is driven by a micromanipulator towards the slide. The resulting force imposed on the particle is measured by a force transducer. Forces between 0 and 500μN can be measured with an accuracy of ± 0.01μN. Larger forces such as 10mN can also be measured. The transducer is mounted on a fine micromanipulator that allows accuracy of positioning of ±0.2 μm, reflecting the approximate precision of estimates of the distance between the parallel surfaces, and hence particle deformation. The results are represented graphically by a force-displacement curve, where the peak of the force represents the point just before the particle is burst or damaged. To allow for the effects of hydration, plant cells can be measured in mannitol instead of water. In addition, to minimise the time dependent behaviour of such systems, these micromanipulation techniques have now been optimised so that mechanical property measurements can be made on the shortest possible time scale, i.e. at speeds of up to 1000 μm/s.

Aside from measurement of mechanical properties of individual cells by compression, micromanipulation techniques also exist to measure the mechanical properties of small tissue, such as filamentous fungi. In this case, the same principles of force measurement are applied but, the force is exerted by pulling, with one fixed end and a probe that induces the force on the tissue, by moving

horizontally. In this thesis, a micromanipulation rig is adapted to develop a new method for measuring the force required to break individual tobacco roots.

From all these techniques a large amount of data about the mechanical properties of different particles can be obtained. Manipulation of results obtained from micromanipulation experiments by mechanical modelling allows the intrinsic mechanical properties such as cell wall elastic modulus to be estimated (Thomas *et al.* 2000). This study will attempt to relate information about the breaking force and hence energy requirements to disrupt a single root obtained from micromanipulation experiments to energy requirements in a small-scale cell disruption device using modelling techniques that in turn can be used to optimise large-scale mechanical disruption techniques that could form an integral part of a bioprocess.

Chapter 2- Materials and Methods

2.1. RECIPIES

All materials were supplied by SIGMA, Poole, Dorset, UK unless stated otherwise.

2.1.1. MEDIA

LB medium

1% (w/v) Bacto™ tryptone (Becton Dickinson, Oxfordshire, UK), 0.5% (w/v) Bacto™ yeast extract (Becton Dickinson, Oxfordshire, UK), 1% (w/v) NaCl, pH 7.0) containing 50μg/ml carbenicillin.

YM medium

1% (w/v) mannitol, 0.04% (w/v) yeast extract, 0.01% (w/v) K_2HPO_4, 0.04% (w/v) KH_2PO_4, 0.01% (w/v) NaCl, and 0.02% (w/v) $MgSO_4.7H_2O$, pH 6.8), containing 200μg/ml spectinomycin.

2.1.2. AGAR

LB solid medium for plates

1.5% Bacto™ agar (Becton Dickinson, Oxfordshire, UK), pH 7.0 in LB media, containing 50μg/ml carbenicillin.

YM solid medium for plates

1.5% Bacto™ agar (Becton Dickinson, Oxfordshire, UK), pH 7.0 in YM media, containing 200μg/ml spectinomycin.

RM3 agar

4.4 g/L Murashige and Skoog basal medium, 30 g/L sucrose, 0.1 mg/L α-Naphthaleneacetic acid, 1 mg/L 6-Benzylaminopurine, supplemented with kanamycin (200μg/ml) and carbenicillin (500 μg/ml).

MS agar

4.4 g/L Murashige and Skoog basal medium, 30 g/L sucrose, 8 g/L Bacto™ agar (Becton Dickinson, Oxfordshire, UK), containing kanamycin (200 µg/ml) and carbenicillin (500 µg/ml).

2.1.3. BUFFERS

50X Tris-acetate EDTA buffer (TAE)

24% (w/v) Tris base, 5.7% (v/v) Glacial acetic acid, 10% (v/v) 0.5M ethylenediaminetetraacetic acid (EDTA).

Electrotransfer buffer

25 mM Tris-base, 192 mM glycine, 0.1% (w/v) SDS, 20% (v/v) methanol.

20x Phosphate-buffered saline (20x PBS)

36 mM KH_2PO_4, 200 mM Na_2HPO_4, 2.74M NaCl, 54mM KCl; pH 7.4 with NaOH. Autoclaved.

10x SDS electrophoresis buffer

0.25 M Tris-base, 1.92 M glycine, 1% (w/v) SDS, pH will be 8.3.

5x SDS sample buffer

0.3125 M Tris.HCl pH 6.8, 10% (w/v) SDS, 50% (v/v) glycerol, 0.75 M β-mercaptoethanol, 0.125% (w/v) bromophenol blue.

Buffers used for extraction technique comparison

The standard extraction buffer was 1X phosphate buffered saline, with the exception of extraction of membrane-bound immunoglobulin G (IgG) where 1% Triton X-100 was also added.

Buffers used for detergent analysis

Triton X-100 was added to phosphate buffered saline at concentrations of 0.0001%, 0.001%, 0.01%, 0.1% or 1% (v/v).

Buffers used for temperature investigation

The standard extraction buffer was 1X PBS, with the exception of extraction of membrane-bound IgG where 1% Triton X-100 was also added.

Buffers used for pH analysis

In order to analyse the importance of buffer pH on the extractability of IgG from transgenic plant leaf tissue, buffer pHs ranging from about 3 to 10 were investigated. All buffers were at 0.1M for constant ionic strength: glycine-HCl (pH 2.91), sodium citrate (pH 3.8, 4.0. 5.0, 6.0), sodium phosphate (pH 6.0, 7.0, 8.0), and sodium carbonate/bicarbonate (pH 10.0). In these experiments, extraction from leaf discs was performed by grinding in buffer. In addition, to ensure that there was no antigen-antibody interference at low pH, following centrifugation, the pH of the supernatants were neutralised to pH 7 by the addition of 1M HCl or 10M NaOH.

2.1.4. WASH OR STAIN/DESTAIN SOLUTIONS

Wash solution

0.1% (v/v) Tween-20 in H_2O.

2.1.5. SOLUTIONS FOR ELECTROPHORESIS

10% Tris/Glycine SDS-Polyacrylamide Gel Electrophoresis solution (Resolving gel)

40% (v/v) distilled water, 33% (v/v) 30% acrylamide mix (Acrylamide/Bis-acrylamide, 50% solution, 37.5:1, Electrophoresis reagent, 25% (v/v) 1.5M Tris (pH 8.8), 1% (v/v) of a 10% (w/v) SDS solution (Sodium

dodecyl Sulphate), 0.04% (v/v) TEMED (electrophoresis reagent) and 1% (v/v) of a 10% (w/v) APS solution (Ammonium persulphate).

Stacking gel

68% (v/v) distilled water, 17% (v/v) 30% acrylamide mix (Acrylamide/Bis-acrylamide, 50% solution, 37.5:1, Electrophoresis reagent), 13% (v/v) 1.0M Tris (pH 6.8), 1% (v/v) of a 10% (w/v) SDS solution (Sodium dodecyl Sulphate), 0.1% (v/v) TEMED (electrophoresis reagent) and 1% (v/v) of a 10% (w/v) APS solution (Ammonium persulphate).

2.1.6. WORKING REAGENTS

TMB (3,3',5,5'-tetramethylbenzidine) substrate mix

25% (v/v) 0.2M Na2HPO4.2H2O, 25% (v/v) 0.1M Citric acid, and 50% (v/v) distilled water and 3 tablets of TMB, followed by 1:1000 dilution of 30% (w/w) hydrogen peroxide).

BCA working reagent

50 parts of BCA reagent A (containing sodium carbonate, sodium bicarbonate, bicinchoninic acid and sodium tartrate in 0.1 M sodium hydroxide) was mixed with 1 part of BCA Reagent B (containing 4% cupric sulphate), (BCA Protein Assay, Pierce Chemical Co., Rockford, IL)

2.2. PLANT SYSTEM

The plants used in this study were *Nicotiana tabacum* (var. *Petit Havana).*

2.3. PRODUCTION OF IgG-HDEL EXPRESSING TRANSGENIC PLANTS FOR THE GENERATION OF INTRACELLULARLY RETAINED MONOCLONAL ANTIBODIES

2.3.1. RECOMBINANT MONOCLONAL ANTIBODIES INVESTIGATED

The model recombinant protein used for this investigation was Guy's 13, a murine IgG1 monoclonal antibody which recognises a conformational epitope (van Dolleweerd *et al.* 2003) of the major cell surface protein (SA I/Π) of *Streptococcus mutans* (Smith and Lehner, 1989). Ma *et al.* (1994) originally produced Guy's 13 IgG transgenic tobacco plants, and demonstrated expression levels up to 1% of total soluble protein or ~24 mg/kg of leaf fresh weight. Two forms of Guy's 13 IgG have been engineered and expressed in tobacco. Each was targeted to a different subcellular compartment (Figure 2.1). IgG is produced and secreted by tobacco cells by default (Frigerio *et al.*, 2000). However, the addition of a mammalian membrane anchoring sequence prevents secretion, and results in the retention and accumulation of membrane IgG (mIgG) on the plasma membrane (Vine *et al.*, 2001). In this study, transgenic IgG (Ma *et al.* 1995) and mIgG (Vine et al 2001) seed from these previous studies were used. In addition, a HDEL tagged version of Guy's 13 was prepared. The C-terminal tetrapeptide (HDEL) tag has been used extensively in the past to retain recombinant proteins in the endoplasmic reticulum (Conrad and Fiedler, 1998).

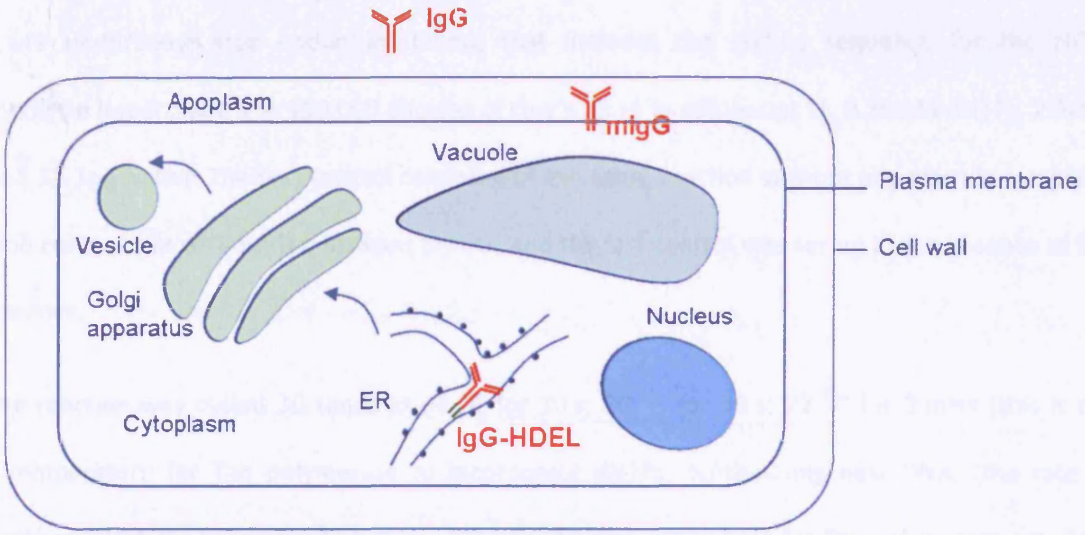

Figure 2.1. Schematic of plant cell and subcellular compartments demonstrating target sites of accumulation of 3 forms of IgG. IgG refers to the Immunoglobulin G that accumulates in the apoplasm and is then secreted by the cell; mIgG refers to IgG that is targeted to and retained in the plasma membrane; IgG-HDEL refers to IgG that is targeted to and retained in the endoplasmic reticulum (ER).

2.3.2. CLONING AND GENETIC ENGINEERING FOR IgG-HDEL - PREPARATION OF GUY'S 13 γ1 HEAVY CHAIN

Recombinant *E.coli* transformed with the gene encoding Guy's 13 γ1 (Ma *et al.*, 1994) was grown in LB media overnight at 37°C. Plasmid DNA was prepared (Qiagen, Crawley, UK) and used as a template (diluted 1: 100,000) for PCR amplification of the Guy's 13 heavy chain.

2.3.3. CLONING AND GENETIC ENGINEERING FOR IgG-HDEL- PCR CLONING

The amplification reaction utilised 2 units of Taq polymerase (Bioline, London, UK), 100 pmol of the (degenerate) forward primer, FRIγ: 5'-tggtacctcgagcCAGGTSMARCTGCAGSAGTCWG-3' (XhoI cloning site underlined, residues corresponding to the murine heavy chain are shown in uppercase) and 100 pmol of

the reverse primer, Guy's 13 H#2: 5'-cctcgaattc*tta*AAGTTCATCATGcttcccaggagagtgggagaggct-3' (EcoR I cloning site underlined, stop codon in italics), that includes the coding sequence for the HDEL tetrapeptide (in uppercase), 1 in 100,000 dilution of Guy's 13 γ1 in pBluescipt Π, 0.25mM dNTPs, 2.5mM $MgCl_2$ and 1X Taq buffer. The first control consisted of the same reaction without any plasmid template, the second control was without the forward primer, and the last control was set up in the absence of the reverse primer.

The reaction was cycled 30 times at 94 °C for 10 s; 56 °C for 30 s; 72 °C for 3 mins (this is the optimal temperature for Taq polymerase to incorporate dNTPs, synthesising new DNA, (the rate of fidelity (rate at which the thermophilic enzyme incorporates the wrong base for Taq polymerase may be 1 in 1000), in a PCR machine (TECHNE PROGENE, UK).

The polymerised DNA fragments were separated according to size by electrophoresis on a 1% (w/v) agarose gel in TAE. The expected DNA fragment size was 1.4kb (Guy's 13 γ1-HDEL PCR). The desired band was purified by gel extraction using a QIAquick Gel Extraction kit (Qiagen, Crawley, UK). Purified Guy's 13 γ1-HDEL PCR product and pBluescript Π sk+ (Invitrogen, Paisley, UK) were both digested with Xho I and EcoR I restriction enzymes (10 units each) with 1X React 2 buffer (Invitrogen, Paisley, UK) and 1X BSA (Invitrogen, Paisley, UK) at 37°C for 2 hours, and the digested fragments were purified using a QIAquick PCR purification kit (Qiagen, Crawley, UK), and concentrated by ethanol precipitation.

For ethanol precipitation, 200µl of digested and purified DNAs, were mixed with a 1/24 volume (8.33 µl) of 5M NaCl and 2 volumes of 100% ethanol (400 µl) and were left at -20 °C for 30 mins. Following centrifugation at 20,000 x g at 4°C for 30 mins, the supernatants were carefully discarded and 400µl of 70% ethanol was added, and the tubes mixed carefully by inverting. The tubes were then re-spun at 20,000 x g for 20 mins at 4°C, supernatants discarded, and the tubes air dried at 37 °C overnight.

The PCR product was then ligated into pBluescript Π sk+. To carry out this ligation step, digested and purified pBluescript Π sk+ was incubated overnight at 16 °C with 2.5X the volume of digested and

purified Guy's13 HDEL PCR product and half the volume each of ligase, 10X ligation buffer, and sterile water.

2.3.4. *E.COLI* TRANSFORMATION

The recombinant pBluescript Π was used to transform *E.coli* DH5 α cells. 3μl of each ligation mix and a control of pBluescript template were mixed with 20μl of DH5α competent cells, left on ice for 20 mins, subjected to heat shock at 42°C for 1 min, and then cold-shocked on ice for 2-3 minutes. These mixes were incubated at 37°C for an hour with 300μl of SOC media. *E.coli* was grown on LB agar plates (containing 0.05 μg/ml carbenicillin in the presence of of 2% X-gal and 1M IPTG, at 37°C overnight. From the plates with pBlueScript containing Guy's13 HDEL in *E.coli* DH5α, 12 white colonies were picked and added to 3mL volumes of LB media containing 0.05 μg/ml and were mixed vigorously overnight at 37°C.

Plasmids (pBluescript Π SK+ containing Guy's 13 γ1-HDEL) were purified from the transformed *E.coli* cells using QIAprep Spin Miniprep Kit (Qiagen, Crawley, UK), and were digested with Xho I and EcoR I to confirm the correct size of the insert (approximately 1.4kb). 50 % (v/v) pBluescript Π sk+ containing Guys13-HDEL were incubated at 37°C for 2 hours with 10U of Xho1 and 10U of EcoR1, 1X React 2, 1X BSA and sterile water. (A control was included which consisted of pBluecript Π sk+ without the insert.

15 μl of each digest were run on a 1% (w/v) agarose-TAE gel (with a 1kb marker included) to check that the insert of Guy's13-HDEL (1.4kb) was present. 2 clones were then selected and these bands were excised from the gel and purified by gel extraction as referred to above.

2.3.5. CONFIRMATION OF CLONED INSERT BY AUTOMATIC SEQUENCING

The cloned Guy's13 γ1-HDEL heavy chain construct was confirmed by DNA sequencing (ABC sequencing, Imperial College London, London, UK) in two plasmids.

2.3.6. SUB-CLONING INTO PLANT VECTOR PL32

The Guy's 13-HDEL insert was sub-cloned into the plant binary transformation vector pL32, a derivative of pMON530 (Rogers *et al.*, 1987), restricted with the same enzymes. Transgene expression in pL32 is driven by the CaMV 35S promoter. The cloning results in the fusion of a murine immunoglobulin heavy chain leader sequence (provided by the vector) to the amino terminus of the Guy's13 γ1-HDEL heavy chain, which targets the transgene product to the plant endomembrane system.

E.coli DH5α containing pL32 was grown up overnight at 37°C in LB media containing 0.525μg/ml spectinomycin. pL32 plasmid DNA was purified using a Sepharose CL-6B (SIGMA, Poole, Dorset, UK) Spin column. 22μl of purified pL32 was digested by incubation with 10 units of Xho1 and EcoR1, 1X React2 buffer, and 1X BSA, at 37°C for 2 hours.

10μl of the digest were then run on a 1% Agarose-TAE gel to check for the correct sized fragment, and the 12kb band of digested pL32 was purified by gel extraction. Guy's13-HDEL was ligated into pL32 by incubation with 2.5X the volume of the digested and purified pL32, and half the volumes of T4 ligase, 10X ligation buffer, and sterile water.

To check for the correct clone and to create a glycerol stock for storage, Guy's13 γ1-HDEL ligated into pL32 was used to transform *E.coli* DH5α cells. To do this, 3μl of each ligation were incubated with 20μl of DH5α FIQ' cells, before streaking onto LB-agar plates, containing 100μg/ml spectinomycin. 35 positive colonies were picked and each incubated overnight at 37°C with 3ml of LB media containing 100μg/ml of spectinomycin. pL32 inserted with Guy's13 γ1-HDEL was then purified from the overnight cultures using QIAprep Spin Miniprep Kit.

To check that all 35 clones of pL32 with the Guy's13-HDEL insert were correct, these were digested as previously described and ran on a 1% (w/v) agarose-TAE gel with digested pBlueScript Π sk+-Guy's13-HDEL and pL32 as markers.

2.3.7. TRANSFORMATION OF *AGROBACTERIUM TUMEFACIENS*

Guy's13 γ1-HDEL heavy chain in pL32 was used to transform *Agrobacterium tumefaciens* (ElectroMax™ *Agrobacterium tumefaciens* (LBA4404) competent cells, Invitrogen, Paisley, UK) by electroporation (Hoekema *et al.* 1983).

25 µl of *Agrobacterium tumefaciens* cells mixed with 1µl pL32-Guy's13 γ1-HDEL was added to a sterile (pre-cooled) cuvette (Bio-Rad, Hertfordshire, UK). Another cuvette with only cells (and no recombinant plasmid inserts) was also added to the device, as a control. Electroporation was at 2.5V for a time constant of 4.5-4.9 ms (BioRad Gene Pulser II, UK). Immediately after electroporation, 1 ml of YM broth (which had previously been incubated at 28°C for 3-4 hours) was added to the electroporated cells, mixed, and transferred back into the original microcentrifuge tubes, which were subsequently incubated at 28°C for 3-4 h (with gentle shaking).

Electroporated (and transformed) Agrobacterium (in YM) was then spun at 5,000 x g for 5 min and the supernatant removed, so that the pelleted cells could be resuspended in 100µl of sterile YM media. These cells were then plated out onto previously prepared plates of YM (agar) containing 200µg/ml of spectinomycin and incubated at 28°C for 3 days. 6 colonies were picked, incubated into 5ml LB media containing 200µg/ml spectinomycin, and shaken vigorously at 28°C, for 2 days. To check for the correct insert, plasmids were then purified from the cell culture using the QIAprep Spin Miniprep Kit (according to the manufacturer's instructions for large plasmids), and purified plasmids were digested using Xho1 and EcoR1. Following digestion at 37°C for 2 h, samples were run on a 1% (w/v) agarose-TAE gel to check for correct insert. Glycerol stocks were made after every stage of transformation by mixing glycerol with cell culture in a 3:7 volume ratio and storing at -80°C.

2.3.8. PLANT TRANSFORMATION

Nicotiana tabacum (var. *Petit Havana*) leaf discs were transformed as described (Horsch *et al.*, 1985). A recombinant *Agrobacterium* culture was prepared by inoculating 50ml of LB media. 10 medium-sized (approximately 90 cm^2), fully expanded leaves were cut from wild type *Nicotiana tabacum* and sterilised with 150 ml of 25% (v/v) Domestos bleach solution for 10 mins. Using aseptic techniques, the leaves were rinsed 3x with sterile deionised water. Each leaf was then placed onto a sterile Petri dish, stomatal side down, and cut into approximately 0.5 cm x 0.5 cm square sections using a sterile scalpel. The leaf discs were transferred to the 50 ml of a 36 h (log) culture of recombinant *Agrobacterium tumefaciens* strain, and the mixture swirled to ensure that all the discs were covered well.

After 15mins, the leaf discs were transferred to solidified RM3 agar medium supplemented with kanamycin (200 μg/L) and carbenicillin (500 μg/L) in order to stimulate callus formation and regeneration of shoots. The plates were sealed with Nescofilm (Fisher, UK), and incubated at 28°C for 48 h in a plant incubator (Percival Scientific, UK).The leaf discs were then transferred aseptically to fresh RM3 plates containing kanamycin and carbenicillin at 200μg/L and 500μg/L respectively, and incubated at 28°C in the plant incubator for 3-4 weeks so that shoots could form.

2.3.9. REGENERATION AND CHARACTERISATION OF GUY'S 13 IgG-HDEL TRANSGENIC PLANTS

Developed shoots were then aseptically transferred to rooting medium (MS agar) to form roots. These young plantlets were then transplanted to soil (non-aseptic conditions) and were left for about 3 weeks for the development of young plants. These young plants were then screened for expression of Guy's13-HDEL heavy chain by leaf extraction, and analysis of the extract by Western Blotting and ELISA, as outlined below in section 2.3.10 and 2.4.1.

Plants which screened positive for the expression of Guy's13-HDEL heavy chain were left to develop to maturity, i.e. flowering stage. Plants expressing assembled Guy's 13-HDEL antibody were produced by cross-fertilisation of Guy's 13 γ1-HDEL heavy chain-expressing plants (produced in this work)

with Guy's13 light-chain-expressing plants (described previously in Ma *et al.*, 1995). The progeny were screened by an antigen-specific ELISA (as outlined below). Plants found to be positive for the fully-assembled antibody were self-crossed for generation of a seed stock.

2.3.10. IMMUNOGLOBULIN CHAIN CHARACTERISATION- WESTERN BLOTTING (REDUCING)

Screening of the plants for expression of the correct relative molecular mass (Mr) of IgG-HDEL, IgG and mIgG was done by Western Blotting. 10% (v/v) SDS-PAGE gels were prepared according to the manufacturer's instructions (MINI-PROTEAN® 3 cell, Bio-Rad Laboratories, Hertfordshire, UK).

Plant extracts of transgenic and wild type plants were prepared by grinding 3 leaf discs in 200µl of sample buffer (1X SDS sample buffer (diluted in deionised water from the 5X stock) with 10% (v/v) ß-metacaptethanol for reducing conditions, with or without 1% (v/v) Triton X-100. As a positive control, 16 µL of murine Guy's 13 hybridoma diluted to 1/100 in 1XPBS (positive control) or positive control (mouse IgG kappa, SIGMA, POOLE, DORSET, UK) were added to 4µL of buffer (1ml 1X SDS with or without 100 µL of ß-metacaptethanol) for reducing or non-reducing analysis.

All samples and positive control were then boiled for 3mins, centrifuged at 14,000 rpm (25200 xg) for 10 mins, at 20 °C. 20 µL of each supernatant were added to separate wells in the gel, along with the positive control and 5µl of the marker (Protein Precision Blue Plus, Bio-Rad, Hertfordshire, UK). To separate the protein samples and the marker, the apparatus was run at 150 V, 40 mA (20 mA per gel), for 1 hour. For immunodetection, the separated protein samples were transferred onto nitrocellulose using a semi-dry blotting apparatus (Hoefer, Newcastle-under-Lyme, UK). The apparatus was then set to 50 V, 0.8 mA/cm2 of filter paper, constant current, and run for an hour for transfer of the separated proteins on the gel to the nitrocellulose paper.

The blots were rinsed with distilled water and blocked with 5% non-fat dry milk in 1X PBS overnight at 4°C, with gentle shaking. Detection of proteins bound to the nitrocellulose was by incubation

with a mix of goat anti-mouse IgG γ (Caltag Laboratories, Invitrogen, Paisley UK) and goat anti-mouse IgG κ (Caltag Laboratories, Invitrogen, Paisley UK) each diluted 1:500 in dilution buffer (1X PBS with 0.1% (v/v) Tween-20, and 1% (w/v) non-fat dry milk), incubated at room temperature for 2 hours, followed by 3 washes with 0.1% (v/v) Tween 20 with gentle shaking for 5 mins each, and a final rinse with deionised water. These blots were then incubated with alkaline phosphatase labelled Donkey anti-sheep IgG (H+L) (diluted 1:1000 in dilution buffer) (Jackson ImmunoResearch, Stratech Scientific Unit, Newmarket, Suffolk, UK) at room temperature for 2 hours, and rinsed 3X with 0.1%(v/v) Tween-20 as described above. Visualisation was with nitroblue tetrazolium/5-bromo-4-chloro-3-indolyl phosphate (BioRad 25X AP colour development buffer, Bio-Rad, Hertfordshire, UK). Immunoglobulin chain detection by Enzyme-linked ImmunoSorbent Assay (ELISA) for immunoglobulin heavy chain (described below in this section) and for functional, fully-assembled antibody (described in Section 2.4.1) were also used to screen the IgG-HDEL plants and to demonstrate functional binding to antigen by the latter.

Immunoglobulin heavy chain detection

The IgG-HDEL plants were initially screened for the presence of the immunoglobulin's heavy chain. Leaf discs were ground on ice, in 1X PBS. Following centrifugation at 25200 x g for 5 mins, 100μl of the supernatant was added as duplicates in serial 5-fold or 4-fold dilutions to 96-well microtitre plates (NUNC, Fischer Scientific, UK) that had been previously coated and blocked. Coating was with sheep anti-mouse IgG γ (1:1000, AU272, The Binding Site, UK) at 37°C for 2 hours with 50μl of coating antibody per well. The plates were rinsed with distilled water thrice and blocked overnight at 4°C or at 37°C for 2 hours with 2.5% (v/v) BSA in 1X PBS. The plates were then washed six times with 0.1% (v/v) Tween 20 (in distilled water). These plant extract samples were incubated on the plates at 37°C for 2 hours or 4°C overnight. The plates were then re-washed six times with 0.1% (v/v) Tween 20 (in distilled water).

Bound immunoglobulin chains were detected by incubation with 50μl per well of horseradish peroxidase-labelled goat anti-mouse IgG-gamma-HRP (1:4000, Jackson ImmunoResearch, Stratech

Scientific Unit, UK) for detection in 1X PBS, and subsequently incubated for 2 h at 37°C. Following washing six times with 0.1% (v/v) Tween 20 (in distilled water), TMB (3,3',5,5'-tetramethylbenzidine, SIGMA, POOLE, DORSET, UK) was added as the substrate. After about 10 minutes, the reaction of the substrate with the secondary antibody was stopped by adding 25 μL per well of 2M Sulphuric acid, resulting in a colour change of the liquid in the wells from blue to yellow. The optical density (OD) of the wells was then measured using a Microplate reader (Sunrise, TECAN, UK) with the absorbance wavelength set at 450nm.

Antibody concentration was calculated by comparison of binding curves with pre-existing standards (Guy's 13 hybridoma supernatant, 1:100, or mouse IgG k, 0.001g/L, SIGMA, POOLE, DORSET, UK), and referred to the fresh weight of each tissue sample harvested.

2.4. CONSIDERATIONS FOR EXTRACTION OF MONOCLONAL ANTIBODIES TARGETED TO DIFFERENT SUBCELLULAR COMPARTMENTS IN TRANSGENIC TOBACCO PLANTS

2.4.1. SCREENING AND ASSAY DEVELOPMENT FOR IMMUNOGLOBULIN CHAIN DETECTION-ENZYME-LINKED IMMUNOSORBENT ASSAY (ELISA)

Functional fully-assembled Immunoglobulin detection

Please see Appendix B for optimisation of the dilution factor for surface antigen I/Π and the concentration of the positive control (Guy's 13 hybridoma) for the antigen-specific ELISA assay. Appendix C describes the method of determining the concentration of the positive control, (Guy's 13 hybridoma), and Appendix D details the method used to quantify IgG yield from ELISA raw results.

Optimal antigen-specific ELISA assay used in all related experiments

After centrifugation, plant supernatants were transferred to microtitre plates (Immulon, Nunc, Fisher Scientific, Leicestershire, UK) for an assay that detects fully assembled and functional (antigen-binding) IgG. The microtitre plates had been previously coated with 50μl per well of a recombinant fragment of streptococcal antigen I/II at 1:5000 dilution (van Dolleweerd *et al.*, 2003), incubated for 2 hours at 37°C, rinsed thrice with distilled water, blocked overnight at 4°C with 5% (w/v) non-fat dry milk in 1X PBS (as this proved more effective than 2.5% (w/v) BSA for this assay), and rinsed six times with 0.1% (w/v) Tween 20. Plant samples were assayed in duplicate (100 μl of plant sample (transgenic or wild type) and Guy's 13 hybridoma positive control) in first row wells (row A), and in 4-fold serial dilutions. Incubation was for 2 hours at 37°C or 4°C overnight. The plates were washed six times with 0.1% Tween 20 (in distilled water). Bound immunoglobulin was detected by incubation with horseradish peroxidase-labelled goat anti-mouse IgG-gamma chain antiserum (1:5000, Jackson ImmunoResearch, Stratech Scientific Unit, Newmarket, Suffolk, UK) for 2 h at 37°C, followed by addition of TMB (3,3',5,5'-tetramethylbenzidine, SIGMA, Poole, Dorset, UK) as the substrate as described above, Section 2.4.1. The colour reaction was stopped after about 5 minutes, with 25 μl of 2M sulphuric acid, and the absorbance was determined at 450nm. Antibody concentration was calculated by comparison of binding curves with a pre-existing standard (Guy's 13 hybridoma supernatant).

2.4.2. CONFIRMATION OF THE HDEL FUNCTION

In order to confirm the HDEL function, i.e. that IgG-HDEL is retained in the endoplasmic reticulum (ER), the recombinant MAb was analysed by ELISA to detect the presence or absence of high mannose and complex glycans which would be added in a post-ER compartment. Microtitre plates were coated with surface antigen I/II (diluted to 1:5000 in 1XPBS) and incubated at 37°C for 2 hours. Coated plates were then rinsed thrice with distilled water, and blocked with 5% (w/v) milk in 1XPBS overnight at 4°C. The plates were rinsed 6 times with 0.1% (v/v) Tween 20 (in distilled water). Plant extracts from IgG and

IgG-HDEL plants were prepared by grinding 6 leaf discs in 900µl of 1XPBS buffer, on ice. The ground samples were centrifuged at 25200 xg at 4°C for 5 minutes, and 100µl of the supernatant in serial dilutions were added to the ELISA plates. Incubation was at 37°C for 2hours. To detect complex glycans, a rabbit anti-horseradish peroxidase (SIGMA, Poole, Dorset, UK) was added, diluted 1/500 dilution in PBS/5% (w/v) milk. As a glycosylation control, Concanavalin A (SIGMA, Poole, Dorset, UK) which binds high mannose and possibly short complex N-glycans (10µg/ml in Tris buffered saline with 3mM $MnCl_2$, 3mM $CaCl_2$) was added at 37°C for 2 hours, followed by a rabbit anti-con A antiserum (SIGMA, Poole, Dorset, UK) for a further 2 hours at 37°C. For both complex and high mannose glycan assays, the plates were washed and incubated with alkaline phosphatase labelled anti-rabbit IgG antiserum for 2 hours at 37°C. Detection of binding was with the substrate p-nitrophenyl phosphate (*SIGMAFAST*^{TM}, SIGMA, Poole, Dorset, UK) and absorbance values were read at 405nm.

2.4.3. MAINTENANCE OF PLANTS AND SAMPLING TECHNIQUE

In the initial ranging experiments, plants in soil expressing mIgG (membrane bound) and IgG (secreted) were already available as mature plants in soil. Six clones of mIgG were screened for expression of the recombinant antibody concerned. Wild type *Nicotiana tabacum* (var. *Petit Havana*) were also available as mature plants in soil. All transgenic plants in soil were treated in the same way as normal plants in soil for maintenance.

There were six clones of mIgG, which had all been previously screened (and were re-screened here) for expression of the recombinant antibody concerned. Wild type *Nicotiana tabacum* (var. *Petit Havana*) were also available as mature plants in soil. More wild type plants were planted from seed in soil for later experiments. All transgenic plants in soil were treated in the same way as normal plants in soil for maintenance. Plants were maintained under controlled light at 28 °C, using a 16 hour light cycle.

Plants in hydroponics however, required maintenance under sterile conditions. In order to grow a plant in hydroponics, a shoot from the established plant in soil was excised and immersed into 30% (v/v)

bleach (Domestos, Sainsbury's, UK). This shoot was left in the bleach for approximately 20 minutes and the jar was swirled at regular intervals to ensure that the explant was well-sterilised. Under sterile conditions, the shoot was then subjected to serial rinsing by transfer of the shoot to six adjacent jars of microwaved distilled water to ensure all traces of bleach had been removed. This sterilised shoot was then transferred to a sterile petri dish. The white areas (usually at the end of the shoot representing "dead" tissue) were excised using a sterile scalpel. This was then placed upwards in solidified culture medium (MS (Murashige and Skoog) media with agar) in a sterile jar. This shoot was left in culture for about 1-2 weeks in a plant incubator (25°C, 16 photoperiod, Pervical, Perry, Iowa, USA), after which growing buds and possibly some roots of a small plant began to form.

At this stage, it was possible to transfer the small plant to hydroponics. Under sterile conditions, the roots were "threaded" through the hole of a platform (as described in Drake et al, 2003), so that the small plant was held upright. This was then transferred to a sterile clear container, MS liquid media added to a level just beneath the platform, and the container shut tightly. The plantlet was then left to grow in the plant incubator to a young plant (~ 8 cm).

For IgG extraction experiments, all transgenic plants and wild type *Nicotiana tabacum* (var. *Petit Havana*) were grown from seed to mature plants in soil. The plants were grown in commercial compost (Homebase Multipurpose, Hombase, Stafford, UK) at 26°C with a 16 hour photoperiod. Plants in this study were between 20 and 100 cm in height, but in comparative experiments, plants of the same age and developmental stage were always used. Leaf discs were produced by puncturing a single leaf using a microcentrifuge tube and cap, giving a leaf disc area of 7.85×10^{-5} m^2. One sample consisted of 3 leaf discs taken from 3 different leaves: a top leaf (near the plant apex, at about 90% of total plant height), a middle leaf (at ~60% of total plant height), and a bottom leaf (at ~30% of total plant height). (The total fresh mass of the 3 leaf discs was recorded). For a single investigation, leaf discs from the same three leaves were taken each time, but samples were taken in a random order.

Since results showed that there was significant plant-plant variability, data was presented from single plants. These data however were representative of multiple replicate experiments (as indicated in Chapter 4). The inherent variability was mitigated by expression of IgG as a percentage of total soluble protein, in which case we have presented data from 3 plants. For IgG and mIgG we have used homozygous seeds from a single clone, to minimise variability. For IgG-HDEL, all plants studied were derived from the same transformation event and was with the same transgenic light chain expressing plant.

2.4.4. REPRODUCIBILITY STUDIES

In order to establish whether or not manual grinding (described in detail below, Section 2.4.5) was a reproducible technique at small-scale and thus an applicable technique for proceeding with investigating all the parameters important for extraction, the reproducibility of results in terms of extractable IgG yield from 10 replicate extractions was tested. These experiments were carried out on the same 3 leaves of 3 randomly chosen plants expressing IgG, IgG-HDEL or mIgG.

2.4.5. COMPARISON OF EXTRACTION TECHNIQUES

Grinding in buffer

A thin plastic pestle (pellet pestle, blue polypropylene, SIGMA, Poole, Dorset, UK) purposely designed for a microcentrifuge tube was used to separately grind a single leaf disc in 200μL of buffer which was kept on ice. (Alternatively, 2 or 3 leaf discs were ground in 400μL or 600μL of buffer respectively). A schematic of the plastic pestle is shown in Figure 2.2 below, and the dimensions of a single microcentrifuge tube are shown in Figure 2.3 below.

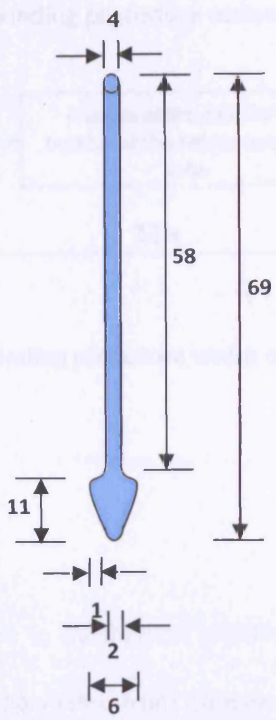

Figure 2.2: Pestle designed for a microcentrifuge tube (pellet pestle, blue polypropylene, Z359947-100EA, SIGMA, Poole, Dorset, UK); Dimensions are shown in mm.

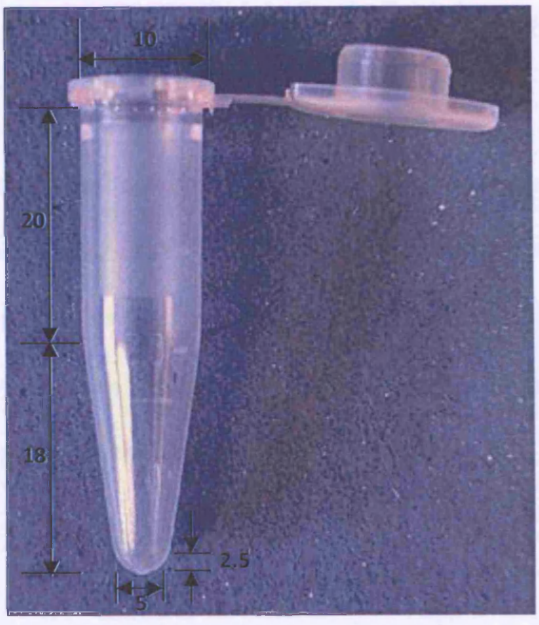

Figure 2.3: Microcentrifuge with a 1.5mL working volume. Dimensions shown in mm.

Figure 2.4 below describes the actual grinding procedure utilised. Each tissue was subject to 12 grinds.

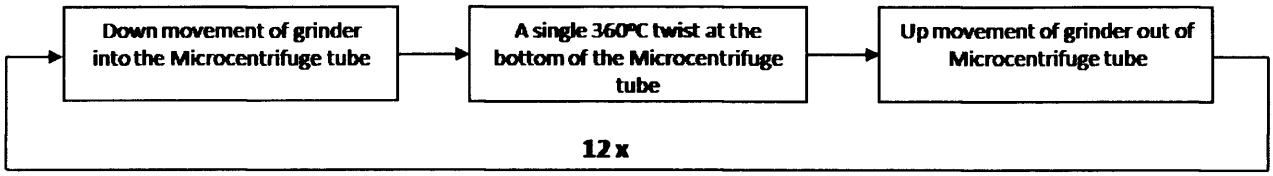

Figure 2.4 The grinding procedure which consisted of 12 cycles.

Freeze-thawing

Freeze-thawing as an alternative to mechanical grinding for extraction of the protein of interest was also investigated. Leaf discs were harvested from transgenic plants as described above. When all the samples had been prepared, all batches were frozen at -20°C for 1h and 40mins. (Note: Care was taken in both cases to ensure that the samples were placed in the same location in the freezer each time). The frozen samples were left to thaw for 20mins at room temperature. This has been defined throughout this thesis as "wet freeze-thaw". Alternatively, leaf discs were frozen at -20°C "dry" i.e. without buffer, where after exposure to room temperature for 10mins, buffer was added to extract the monoclonal antibody (MAb). This was defined as "dry freeze-thaw".

In addition, the effects of freeze-thawing in combination with grinding were investigated to assess whether the concentration of protein release could be enhanced by freeze-thawing, where grinding (12 times) was performed post-thawing, as described above. This has been described in the results and discussion sections as "wet freeze-thaw then grind" or "dry freeze-thaw then grind". ELISA assays as described above (Section 2.4.1) were then performed.

Grinding in liquid nitrogen

Grinding in liquid nitrogen involved placing the leaf discs in an empty microcentrifuge tube, using large tweezers to dip this into liquid nitrogen (-196°C), and to immediately subject the leaf tissue to 12 "grinds" as described. Buffer in its appropriate volume (i.e. 600µl for 3 leaf dsics) was then added to extract the MAb.

Summary

The most commonly used extraction techniques at laboratory scale involve manual grinding of leaf samples. This is either performed in a disposable micro-centrifuge tube with an extraction buffer on ice, or by grinding leaf tissue in liquid nitrogen to a fine powder followed by the addition of an extraction buffer. Both techniques have been used here, with the former technique being regarded as the current "gold standard" comparator. In addition, 5 further extraction techniques were investigated. The small scale extractions (Figure 2.5) were performed with samples that were prepared as described above, followed by

1. Grinding in buffer ("gold standard"): 3 leaf discs in 600µl extraction buffer in a micro-centrifuge tube were subjected to 12 successive grinds using a plastic pestle, on ice.
2. Grinding in liquid nitrogen: 3 leaf discs in liquid nitrogen in a micro-centrifuge tube were reduced to a fine powder by 12 successive grinds using a plastic pestle. 600µl extraction buffer was then added.
3. Passive elution: 3 leaf discs were incubated in 600µl extraction buffer for 1 hour on ice.
4. Dry freeze-thaw: 3 leaf discs were frozen at -20°C for 1 hour 40 mins and thawed at room temperature for 10 mins before adding 600µl extraction buffer.
5. Dry freeze-thaw and grind: "dry freeze-thaw" as described above, followed immediately by grinding in a micro-centrifuge tube by 12 successive grinds using a plastic pestle.
6. Wet freeze-thaw: 3 leaf discs were frozen in 600µl extraction buffer at -20°C for 1 hour 40 mins,

and then thawed at room temperature for 30 mins.

7. Wet freeze-thaw and grind: "wet freeze-thaw" as described above, followed immediately by grinding in a micro-centrifuge tube by 12 successive grinds using a plastic pestle.

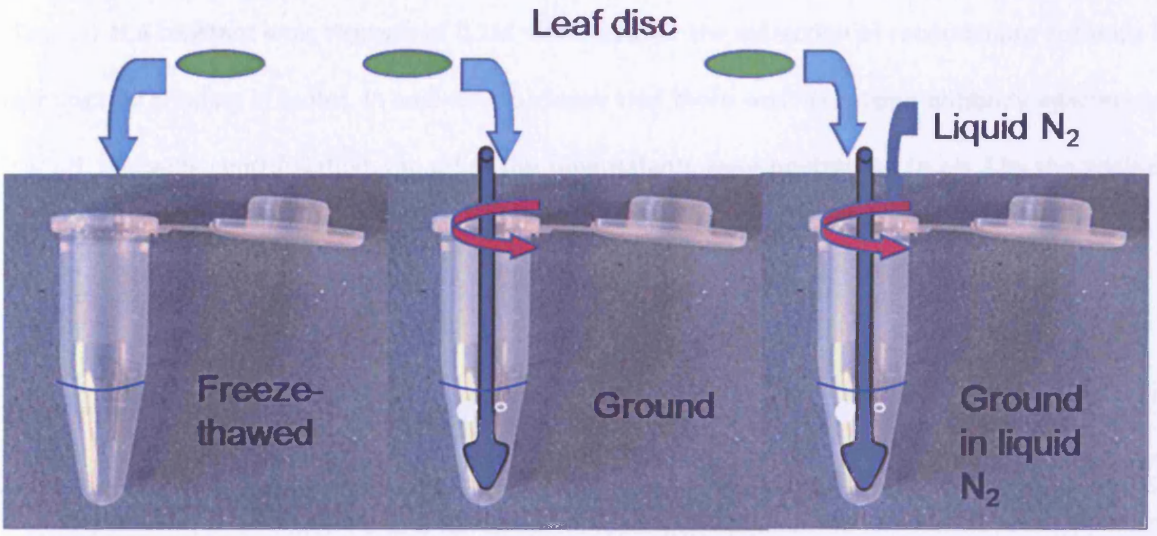

Figure 2.5 Leaf discs were freeze-thawed, ground in buffer or in liquid nitrogen.

After processing, all samples were centrifuged at 14,000 rpm (25200 xg) for 5 minutes at 4°C. The supernatants were collected and used to quantify recombinant IgG yield and total soluble protein as described below.

2.4.6. THE EFFECT OF PHYSICOCHEMICAL BUFFER PROPERTIES ON EXTRACTION

Buffers used for extraction technique comparison, detergent analysis, and temperature and pH investigation are outlined at the beginning of this chapter. Detergent analysis was performed by both passive elution and grinding in buffer, whereas the temperature investigation was carried out by grinding in buffer. In order to analyse the importance of buffer pH on the extractability of IgG from transgenic plant leaf tissue, buffer pHs ranging from about 3 to 10 were investigated with buffers as outlined at the beginning of this chapter. Leaf discs were cut and left in buffer for 1 hour (i.e. passive elution). The

samples were then centrifuged and the supernatants added to ELISA plates in order to determine the difference in the level of functional IgG extracted with pH.

To confirm that ionic strength was not important, buffers (detailed in Buffer recipe section of this chapter) at a constant ionic strength of 0.1M were used for the extraction of recombinant antibody from leaf discs by grinding in buffer. In addition, to ensure that there was no antigen-antibody interference at low pH, following centrifugation, the pH of the supernatants were neutralised to pH 7 by the addition of 1M HCl or 10M NaOH.

2.4.7. TOTAL SOLUBLE PROTEIN QUANTIFICATION

Total protein concentrations in soluble plant extracts were determined by the bicinchonic acid assay (BCA Protein Assay, Pierce Chemical Co., Rockford, IL, USA). Eight dilutions of bovine serum albumin (BSA) standard (starting concentration 2 mg/ml, in 0.9% saline and 0.05% sodium azide) were prepared to account for a protein concentration range ranging from 20 to 2000μg/ml. 25μL of each standard or unknown sample replicate (in 2-fold dilutions) were added to a microwell plate, and mixed and incubated at 37°C for 30mins with 200μL of BCA working reagent. The plate was then cooled to room temperature, and the absorbance read using a plate reader 562nm.

2.4.8. STATISTICAL ANALYSIS USED TO ANAYLSE EXTRACTION RESULTS

Statistical analysis of all data was assessed using the Anderson-Darling normality test. Since all IgG yield data was found not to be of normal distribution, Analysis of Variance (General linear model) was carried out using Minitab®, version 13 software (Minitab Ltd. Coventry). Statistical significance was set at $\alpha = 0.05$ in all cases except where specifically detailed $\alpha = 0.1$. Generalised linear model ANOVA (Minitab®, version 13, UK) was also performed to assess reproducibility of extraction techniques relative to inherent plant to plant variability.

2.5. HARVESTING STRATEGIES FOR MONOCLONAL ANTIBODIES FROM TRANSGENIC TOBACCO PLANTS

2.5.1. MAINTENANCE OF PLANTS AND SAMPLING TECHNIQUE

Harvesting strategies were investigated for the IgG (secreted) and IgG-HDEL (intracellularly retained in the endoplasmic reticulum) transgenic tobacco plants. These plants were grown and maintained from seed as described above (section 2.4.3). Plants in this study were between 5 and 100 cm in height. Leaf discs were produced as described above (Section 2.4.3). In the time of harvest/wound effect experiments, one sample consisted of 3 leaf discs taken from 3 different leaves: a top leaf (near the plant apex, at about 90% of total plant height), a middle leaf (at ~60% of total plant height), and a bottom leaf (at ~30% of total plant height). (The total fresh mass of the 3 leaf discs was recorded). For a single investigation, leaf discs from the same three leaves were taken each time, and the order of samples recorded. For experiments studying the variation of IgG expression at different heights (top, middle and bottom) of a single plant, older plants were used (>30 cm), since it was easier to distinguish between those 3 regions, in that way, and instead of 3 leaf discs, a sample consisted of 2 leaf discs taken from two different leaves from the same height level of the plant (i.e. top, middle, or bottom).

2.5.2. PLANT HEIGHT AND LEAF AREA MEASUREMENT

Plant height was approximately measured (to the nearest cm) as the distance between the start of the plant stem (end of root section, covered with soil) at the base of the plant to the top of the plant (highest section of the stem, not including flowers). A single leaf area, however, was estimated as the product of the leaf's height and width (HXW) multiplied by a correction factor, where leaf height was measured on the leaf's central nerve. This is an accepted method of estimating leaf area (Bozhinova, 2006) with a correction factor that is usually applied which value varies slightly with variety and leaf

position. On average this value has been found to be about 0.75 for *Nicotiana tabacum*, which we have used (Schurr, 1997).

Detailed measurements were made on a plant of mid-range height (34 cm) in terms of height of the top, middle, and bottom sections, and leaf areas, total number of leaves, and average total leaf mass at each of these three different height sections within the plant. These results were subsequently used together with reported estimations of total leaf mass per plant for the related environmental growth conditions for a plant that was >10-20 cm in height and a plant that was 90-100 cm in height, in order to estimate the total monoclonal antibibody yield per plant and its variation with age of the plant.

2.5.3. EXTRACTION PROCEDURES AND BUFFERS USED IN HARVESTING INVESTIGATION

The techniques used in this investigation were grinding in buffer and passive elution, as described above (Section 2.4.5). The extraction buffer consisted of 1X phosphate buffer saline, with 1% (v/v) Triton X-100. For comparing IgG (secreted form) and IgG-HDEL in top, middle and bottom leaves, 1XPBS only was used with extraction via passive elution. For experiments investigating wound effect in young and old plants expressing IgG-HDEL the extraction buffer was 1XPBS with 1% Triton X-100 and the extraction technique was grinding in buffer. The wound effect in young and old plants expressing IgG (secreted form), was performed with passive elution in 1XPBS with 1% Triton X-100. After processing, all samples were centrifuged at 25200 xg for 5 mins at 4°C. The supernatants were collected and used to quantify recombinant IgG yield and total soluble protein as described above (section 2.4.1 and 2.4.7 respectively).

2.6. CHARACTERISATION OF MECHANICAL PROPERTIES OF TRANSGENIC TOBACCO ROOTS EXPRESSING A RECOMBINANT MONOCLONAL ANTIBODY AGAINST TOOTH DECAY

2.6.1. MICROMANIPULATION TECHNIQUE DEVELOPMENT

It was decided to develop a micromanipulation technique to break single roots to breakage for force measurement. Key to this was, understanding the nature of the root specimen in hand by image analysis of typical tobacco roots that were taken using a LEICA microscope (Microsystems Ltd., Milton Keynes, UK), and verifying values for typical root dimensions. In addition, the initial total root length that should be manipulated via micromanipulation was optimised, and cyanoacrylate glue application (as used in a similar experiment for pulling funghi by micromanipulation (Professor Colin Thomas, personal communication) for attaching the root to glass fibre that was attached to the T-shaped probe (discussed in detail in Section 2.6.3 below) was also optimised. Factors that were optimised by "trial and error" for glue attachment included the method of glue application to the root, the amount to be applied, how to apply this whilst limiting the amount of time that the root was exposed to the air, and for ensuring the successful attachment of the root to the probe. The complete set up of the rig for pulling single roots to breakage and measuring the force utilised for this was optimised by adapting a rig that had previously been used by Liu *et al.* (2002) to measure the force required to break and disrupt fouling deposits, using a T-shaped stainless steel probe which acted to scrape the fouled sample off a surface.

Initial experiments indicated that a 25g force transducer was necessary to account for the maximal peak force for breakage generated by some of the roots. The applicability of the technique to dehydrated and re-hydrated roots was also tested, and the time that the root spent outside a wet environment was limited to 15 mins for optimisation of the technique detailed in Section 2.6.3. Probe compliance was also accounted for as described in section 2.6.3.

2.6.2. PLANT MATERIAL PREPARATION FOR MICROMANIPULATION STUDY

Seven transgenic plants expressing Guy's 13 monoclonal antibody (secreted IgG) and two wild type *Nicotiana tabacum (var. xanthii)* plants were grown in soil from seed. All plants used in micromanipulation experiments were young, i.e. at pre-flowering stage, and had a mean height of 14-25 cm. The exact preparation and screening of transgenic plants is described elsewhere (Drake *et al.*, 2003). The plants were grown in commercial compost (Homebase Multipurpose) at 26°C with a 16 hour photoperiod. Before making measurements on plant roots, the soil was gently loosened, to pull the plant gently out of the soil causing minimal damage to the roots. The roots were then rinsed under gentle running water to remove soil particles, and then left upright in a beaker of distilled water for the duration of the experiment.

2.6.3. OPTIMISED SINGLE ROOT PULLING BY MICORMANIPULATION PROCESS

A single root (approx. 1 cm in length from its tip) was excised from a tobacco plant, its colour noted (i.e. white, yellow-brown, light brown or dark red-brown), and its fresh mass measured on a fine balance. Its diameter at each 0.1 cm point along its 1cm length was then recorded under a light microscope using a graticule (x 40 magnification) so that both the mean root diameter and approximate diameter at breakage could be estimated. The diameter at the breakage point was approximated by measurement of the remaining root length post breakage and using the record of the diameter at each 1mm length of the 10mm root. Although only the first 10 mm of the root (as measured from the root tip) was measured each time for the sake of experimental consistency, the total length of the original root (from the base of the plant to the root tip) was also approximately measured each time. The process (root excision to mass and diameter measurements) was optimized to limit the total time that the root spent outside an aqueous environment to 10 mins.

The root was then positioned so that most of it was immersed in buffer (1X phosphate buffer saline i.e. the same buffer used to extract the MAb from the roots), in a Petri dish. The end of the root that was

not in the buffer was blotted dry with a paper towel so that approx. 2mm of the root could be threaded into a hollow glass fibre (Harvard apparatus, 1.0mm outer cross-sectional diameter x 0.58 mm inner cross-sectional diameter) and cyanoacrylate glue applied. This was then allowed to dry at room temperature for 4 mins, and final curing was in the buffer for an additional 4 mins.

In order to position the rod close to the root before gluing, it was clamped to a micromanipulator, (MicroInstruments, Oxon, UK) as shown in Figure 2.6. (Photos of the rig are shown in Figure 2.7 and 2.8). This then became the fixed end of the equipment. Using another micromanipulator, a second rod was then located co-axially with the first. In practice, this second rod was not attached directly to the micromanipulator, but by gluing to the output aperture of a transducer (Model BG-1000, Kulite Semiconductor, Leonia, NJ. USA) which was itself mounted on a three dimensional micromanipulator (MicroInstruments, Oxon, UK), this was the movable end of the equipment. See figure 2.6. The "free" end of the attached root was then positioned next to the "free" end of the glass rod and glue was applied. This was left to dry for an additional 10 mins, leaving the root fixed between the two rods and micromanipulators.

The second rod was then moved so that the root was pulled at a constant speed of 2.2 mms^{-1}. The force exerted on the root was recorded with a sampling rate of 100 Hz by a PC 30-D data acquisition board (Amplicon Liveline, Brighton,UK), and the extension of the root was recorded on video for image analysis (Q600, Leica Cambridge, UK).

Four measurements of the transducer probe compliance were carried out, by driving the probe at a controlled speed of 2.2 mms^{-1} to touch a hard object. This resulted in four voltage (force)-time curves (data not shown) from which the slopes of these curves were calculated and averaged. Unit Compliance was the product of probe speed and data acquisition time divided by the product of the slope and transducer sensitivity. The true displacement was thus calculated from the measured displacement ($2.2mms^{-1}$ x measured pulling time) reduced by the product of compliance and maximum force (peak breaking force). True displacement was used to calculate work done as is described below. 134 roots

were measured from 7 individual plants (all about 14 cm in height) expressing the secreted form of IgG. A measurement on a single root took approximately 30 mins. A close up of the root set up post-pulling by micromanipulation is shown in Figure 2.8.

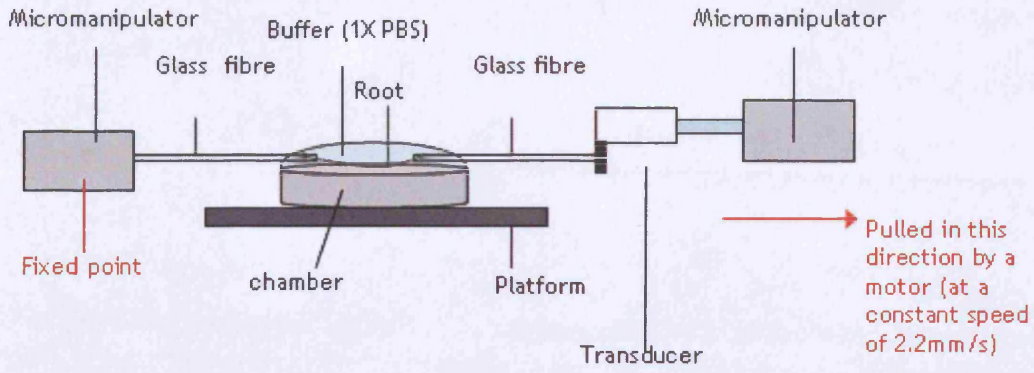

Figure 2.6 A schematic of the set up of the root in the micromanipulation rig.

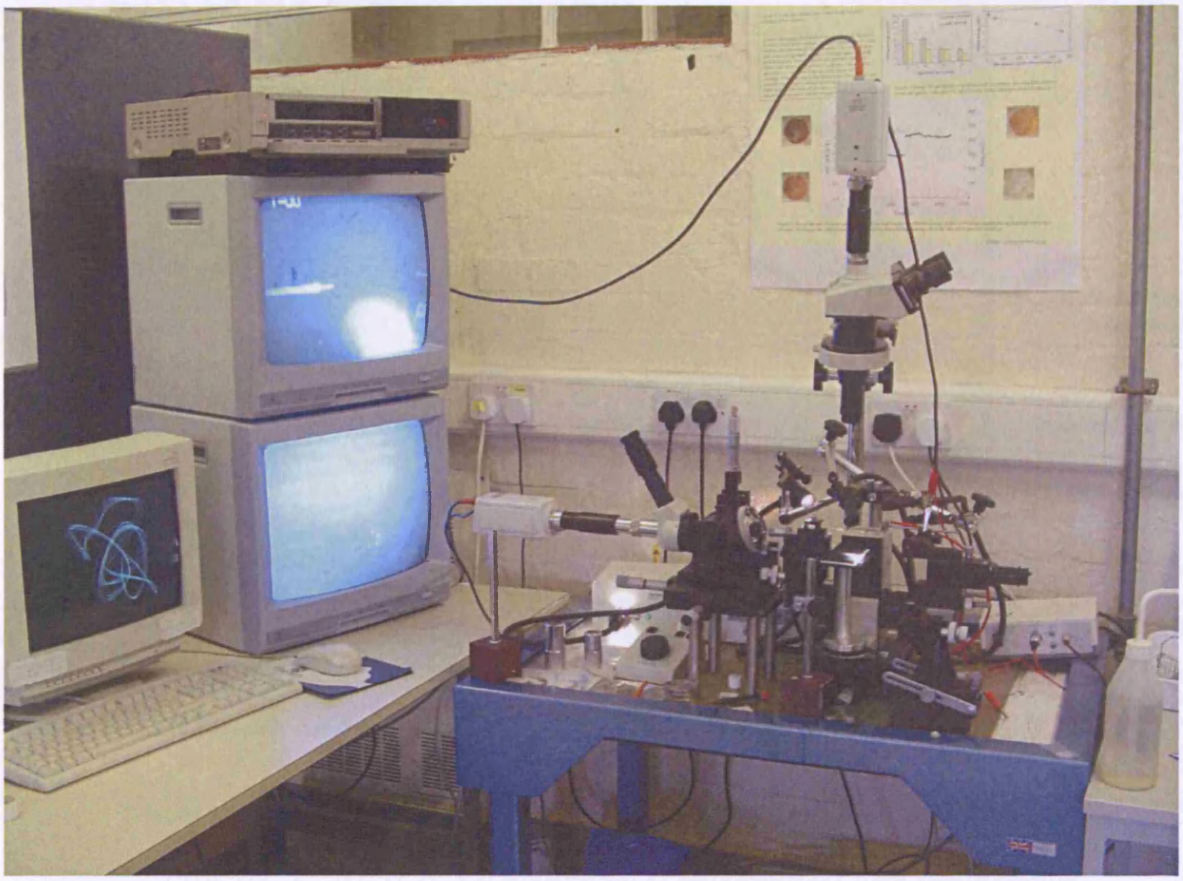

Figure 2.7 A photo of the micromanipulation rig, including the video of the broken root post-pulling by micromanipulation.

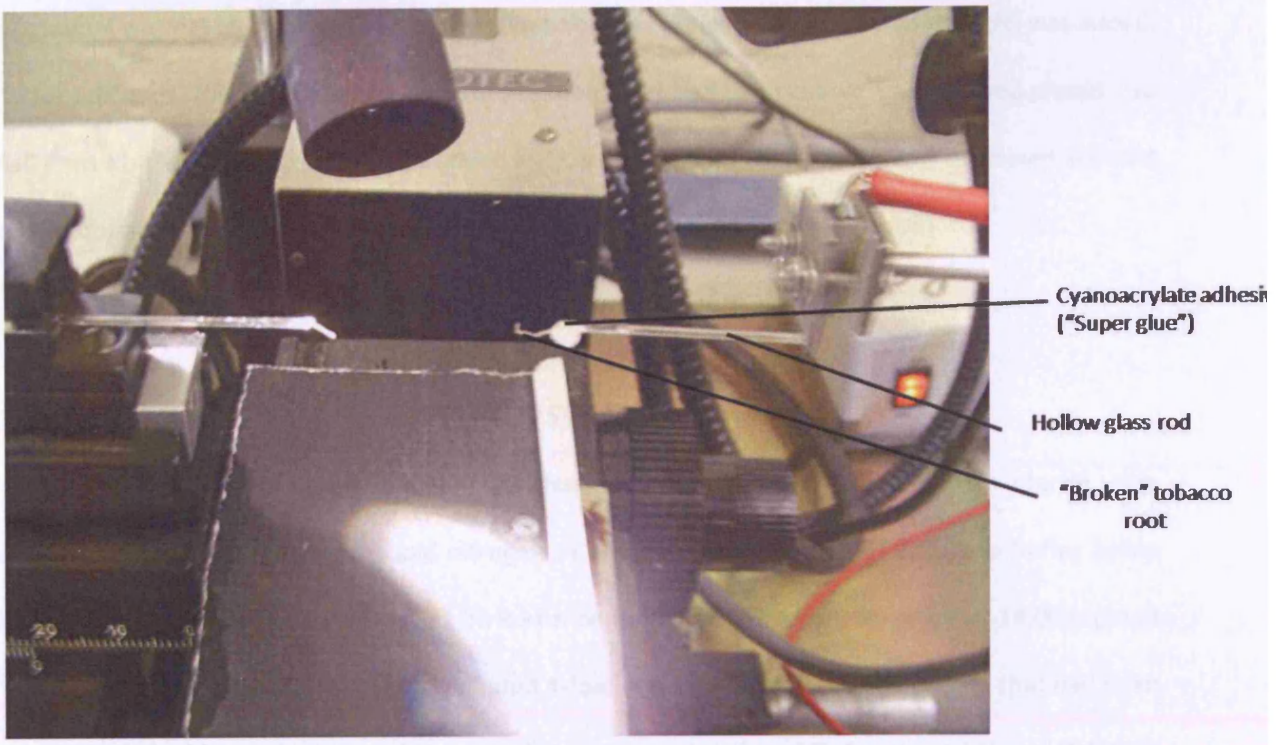

Figure 2.8 A close-up of the broken root post-pulling by micromanipulation set up

2.6.4. ENVIRONMENTAL SURFACE ELECTRON MICROSCOPY (ESEM)

The broken ends of roots (after pulling by micromanipulation) were fixed in 2.5% glutaraldehyde in 0.1M sodium cacodylate buffer, pH 7.3 for 2 days at 4°C. Observations were conducted in a Phillips FEI XL30 FEG-ESEM microscope. Specimens were introduced into the specimen chamber at 5.2 Torr at 2°C (equivalent to a relative humidity of 100%). After equilibration, the root was brought into view by slowly reducing the vapour pressure to 4.7 Torr (90% humidity).

2.6.5. PHLOROGLUCINOL STAINING

Phloroglucinol-HCl staining (Wiesner reaction, Speer, 1987) was performed on root sections of the differently coloured transgenic tobacco roots that were taken from plants that were of a similar age and under the same growth conditions as described above. To prepare the Phloroglucinol stain, 2.0g of

phloroglucinol was dissolved in 80ml of 20% ethanol, to which 20ml of concentrated HCl (2N) was added, in a fume cupboard. This was then added to root sections that had been cut with a blade and placed into a small Petri dish and left at room temperature for 2 mins. Stained (red colour) and unstained sections were then observed under a LEICA microscope (Microsystems Ltd., Milton Keynes, UK).

2.6.6. IgG MEASUREMENT IN DIFFERENT ROOT SYSTEMS-ELISA

20 mg of each of the different root types classified according to colour, (refer Chapter 6) were excised and immediately ground in liquid nitrogen to a dry powder, 400µl 1X Phosphate Buffer Saline (PBS) was added and then the tube was left on ice for an hour. Following centrifugation at 14,000 rpm at 4°C for 5 mins, the supernatant was serially diluted 4-fold in the wells of a microtitre plate that had been previously coated with a recombinant fragment of streprococcal antigen I/II (fragment 105.1_{13}) (1:5000), and the ELISA continued as described above in Section 2.4.1.

2.6.7. STATISTICAL ANALYSIS USED TO ANALYSE MICROMANIPULATION RESULTS

Statistical analysis of the data was carried out using the Anderson-Darling normality test, followed by non-parametric Kruskal-Wallis analysis of variance (ANOVA), as most data was found not to be of normal distribution (Minitab®, v.13 software). Non-normal data involved the comparison of population medians instead of means. This was done to analyse the interrelationship between all parameters. With Kruskal-Wallis analysis it was possible to compare 4 groups (e.g. of colour) at the same time. However, where only 2 groups were to be compared, Mann-Whitney analysis was also carried to confirm the Kruskal-Wallis results. Interrelationships between force, work done or stress with mean root diameter, approximate diameter at breakage, fresh mass, or original root length were analysed by means of Spearman rank correlations. IgG yield data however, was found to be of normal distribution and thus, Analysis of Variance (General linear model) was carried out using the same software. Statistical significance was set at $\alpha = 0.05$. For the Spearman rank correlation test, the correlation coefficient for

ranked values was computed using Mintab®, v.13 software. Since, the sample size was large (>10), the statistic was approximated by a *t*-statistic and compared with *t*-critical value of 1.645 (for P = 0.05, and large sample number). If the *t*-statistic was greater than with *t*-critical or less than – (*t*-critical), it was concluded that there was a correlation. The strength of the association between pairs of variables was determined by coefficients of determination (r-squared), (r-squared ≥ 50%, strong correlation, r-squared ≥ 25% - <50%, moderate correlation, and r-squared <25%, weak correlation).

All graphs are plotted as bar graphs showing the mean (bar) ± Standard Error of the Mean (SEM). Data in the text is also represented as ± SEM.

2.7. ESTIMATION OF ROOT TENSILE STRENGTH FOR THE EXTRACTION OF MONOCLONAL ANTIBODIES FROM TRANSGENIC TOBACCO PLANTS

2.7.1. PLANT MATERIAL PREPARATION FOR ULTRA-SCALE DOWN ROOT SHEAR EXPERIMENTS

Seven transgenic plants expressing Guy's 13 monoclonal antibody (secreted IgG) and two wild type *Nicotiana tabacum (var. Petit Havana)* plants were grown in soil from seed. All plants used in experiments were young, i.e. at pre-flowering stage, and had a mean height of about 14-27.5 cm (average 23 ± 6 cm), (i.e. a similar plant height and age range of plants used in previous micromanipulation experiments (section 2.6.2). The exact preparation, screening, and maintenance of transgenic plants, and root harvesting method were as described in Sections 2.6.1 and 2.6.2.

2.7.2. DESIGN OF THE SCALABLE SHEAR DEVICE USED TO SHEAR LEAF DISCS OR 1CM ROOT PIECES

The apparatus used in this study was a flat-bottomed, cylindrical mixing tank made from Perspex (Figure 2.9). The actual outer casing on this device was very large, so that the internal diameter and the total height of the chamber were 0.055 m and 0.01 m respectively. A lid covering the liquid surface was

fitted, to allow the tank to be operated as a liquid-solid mixer at impeller speeds in excess of the critical speed for surface aeration and to prevent splashing. The impeller diameter was large (D/T = 0.545) which meant that high radial velocities of the flow could be achieved. The root particle to liquid (1XPBS) volume ratio was 5% (w/v), i.e. 0.35 g of root pieces (each in 10 mm sections) in 7ml of 1X PBS. This low particle concentration reduced the number of particle-particle interactions, so that there were a greater number of particle-blade interactions.

In addition, 4500 rpm ($75s^{-1}$), was chosen since it was above the visually determined, just-suspended speed (N_{js}), i.e. the minimum impeller speed required to keep the particles from resting on the base of the vessel for longer than 1-2s (Zwietering, 1958).

(a)

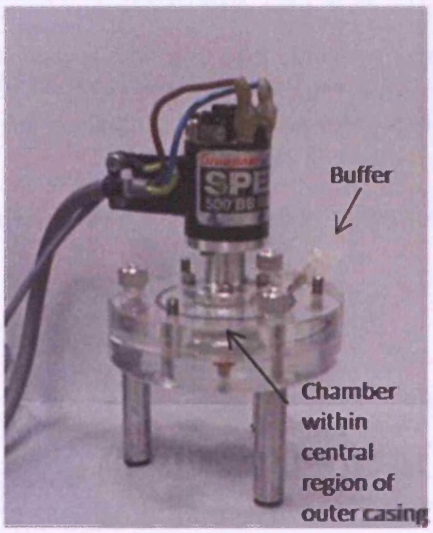

(b)

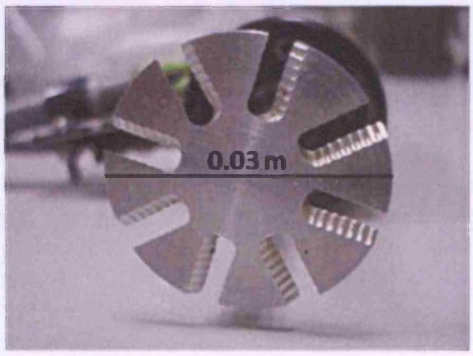

(c)

Disc diameter, D	30mm
disc thickness = blade thickness	0.15mm
chamber diameter (inc O-ring), T	55mm
chamber thickness	10mm
chamber volume without disc and shaft	24mL
distance between disc and chamber walls	13mm
distance of disc from top and bottom of chamber	5mm
number of blades	8
liquid height	10mm

Figure 2.9 a The mechanically stirred shear device used to extract MAb from transgenic tobacco roots. b The impeller consisting of 8 blades each with 2 serrated edges c Dimensions of the mechanically stirred breakage device.

2.7.3. **POWER NUMBER ESTIMATION**

Since we used a novel impeller, unlike common impellers such as the Rushton impeller, it was necessary to estimate the power number, necessary for establishing energy dissipation within the device. The power number was measured as described for power consumption measurement of a miniature bioreactor by Gill *et al.*, (2008). A similar arrangement has also been described by Nienow and Miles (1969). Effectively, the shear device filled with root and buffer (1XPBS) mix as described above (Section 2.7.2) was positioned on top of a large air bearing dynamometer, in the centre. A very high impeller speed of (19200 ± 80 rpm or 22000 ± 160 rpm) was required so that movement in the shear device caused a significant movement of the air bearing, so that a metal attachment (arm) of the air bearing could move and hit a pre-calibrated force transducer (FS Series, Honeywell, USA). The magnitude of the torque was recorded using software that was developed at HELL Ltd. (courtesy of Naveraj Gill). This was repeated in triplicate and at 2 different speeds for an estimation of the power number. The power number for our impeller design was estimated as being 0.11.

Power draw was calculated from the torque via equation 2.1:

$$P = FR\omega \tag{2.1}$$

where P is power requirement, F is the applied force, R is the length of the arm (of the air bearing) pressing against the force sensor, and ω is the angular velocity derived from equation 2.2,

$$\omega = 2\pi N \tag{2.2}$$

where N is the stirrer speed.

2.7.4. ROOT SHEAR EXPERIMENT WITH SHEAR DEVICE

Root tissue from transgenic *Nicotiana tabacum* plants (prepared as previously described) were cut into 1 cm sections and approximately 0.35g of these root pieces (exact initial masses recorded) were then sheared in 7ml of 1X PBS buffer at 4500rpm for a length of time, t. The times lengths investigated were 30, 120, 240 and 480 seconds. Since a single plant did not possess enough roots for a single experiment, 16 plants (of the heights outlined above) were used for this analysis. But, root tissue was taken from the same plant/plants was taken as far as possible.

As there is variation in IgG expression from plant to plant, it was necessary to use grinding in liquid nitrogen as a control using root samples from the same plants. This was done in a much smaller root tissue per unit volume (but with root tissue and extraction buffer in the same mass to volume ratio, i.e 0.03g root pieces in 600μl of 1X PBS buffer. After each individual "run" in the shear device, the device was stopped, and the sheared debris and liquid removed and put into a centrifuge tube. The tube was then left on ice, until all the samples were prepared. These were then centrifuged at 4000rpm, for 20 mins at 4°C. Following centrifugation, 1ml of the supernatant was put into a microcentrifuge tube and left on ice before analysis. The supernatant was analysed for IgG using an Enzyme-Linked Immunosorbent Assay (ELISA) (as previously described above, Section 2.4.1).

2.7.5. ESTIMATION OF PERCENTAGE OF INTACT ROOTS

Following each shear experiment and centrifugation the remaining intact roots, i.e. those that were still 10 mm in length were removed, gently blotted dry to remove excess surrounding liquid (as were the initial roots) and re-weighed. The percentage of remaining intact roots was calculated as the final mass of intact roots over the initial root mass which was about 0.35g.

2.7.6. ROOT DEBRIS LENGTH ANALYSIS

Root debris length analysis was done using the Image J software (Rasband *et al.*, 1995). It can be downloaded as freeware from http://rsb.info.nih.gov/nih-image. All intact roots had been removed before this part of the analysis. The root debris at the bottom of the centrifuge tube was gently mixed, and a plastic pipette was used to place a small amount on to a microscope slide. This was then covered with a coverslip, and viewed via a LEICA microscope at a magnification of 2.5 times. Images of each sample were taken in triplicate of each triplicate sheared sample from each time point. The following root debris length determination process (including roots less than 10mm in length only) was developed using the Image J software. The image was converted to a greyscale image and then thresholded to include all root debris particles in the image. See Figure 2.10. The thresholded image was encircled using the freemanual selections tool to exclude the part of the image that was not root debris. The outside of the selected section was then cleared. Using the Binary option, any holes in the root debris pieces were then filled. Using the 0.1 mm divisions of a ruler, a graticule was drawn onto a microscope slide, and a line drawn using the straight line selection tool over one of these divisions. The number of pixels representing the length of this line (over the 0.1 mm division) was determined using the Analyse, measure tool. This was repeated at least 3 times in order to determine the average number of pixels per unit mm e.g. 144 pixels/mm. The scale was then set as such, and the measurement parameters set. Here, Feret (the longest distance of the particle as defined by the software) was selected and redirected to the original image and the decimal place for recording the results was set to 5 decimal places. To analyse the particles, the minimum particle size was selected as 0.01 mm^2. The results were then copy-pasted into an Excel file for analysis. This process is illustrated in Figure 2.10.

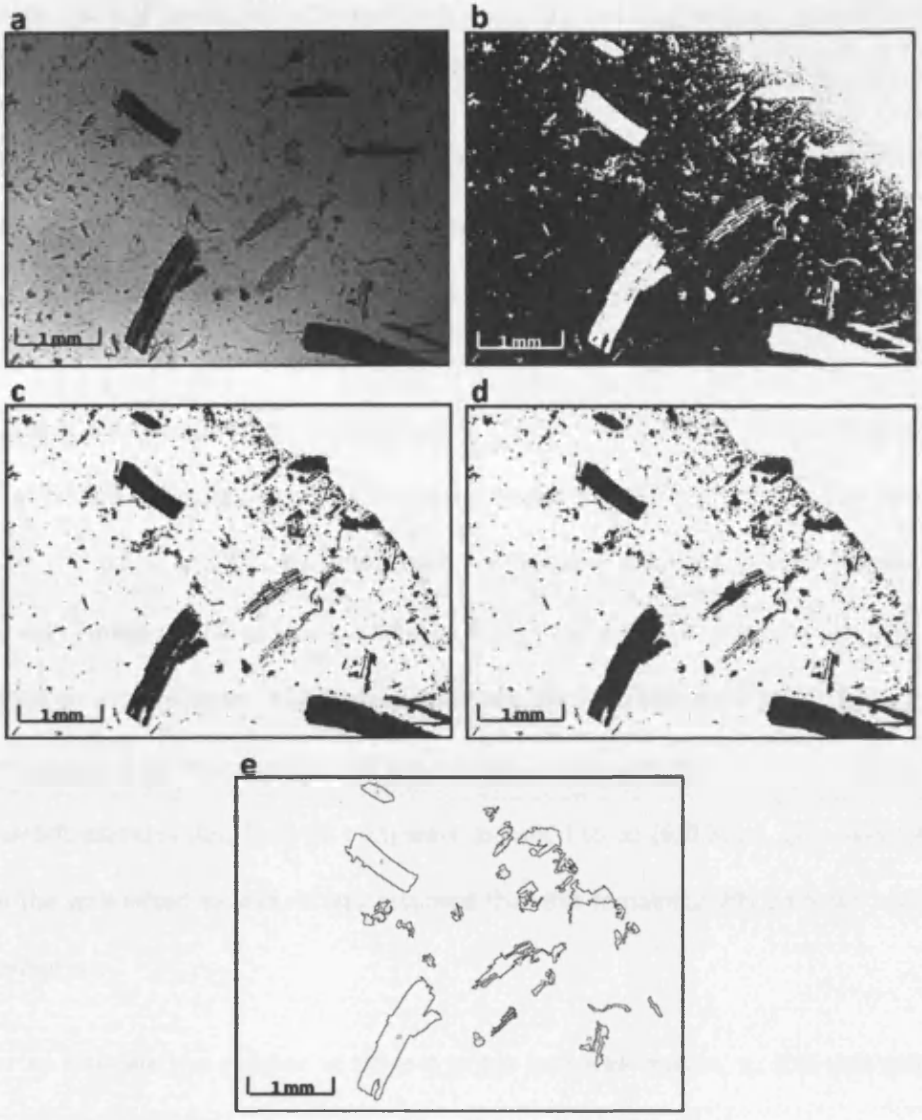

Figure 2.10: Methodology for root debirs size analysis. Light microscopic images were taken at 2.5X maginification, for indidual samples at each time point. Image J software was used to analyse the root debris size. a-e represents the flow diagram of the image processing algorithm for the analysis of root debris. a: An image of resulting root debris post-shearing for 240secs . b: The thresholded binary image (i.e. the root particles are highlighted in white, aginst a black background) c: The root debris selection in c is bordered,anything outside that selection is cleared (note the top right hand corner of the image), and the image is inverted, so that the root particles are now highlighted as black against a white background. d: any holes in the root particles are filled, by selecting "process"; "binary"; and "fill holes" options in the software, to ensure that each whole root debris particle is included in the size analysis (i.e. a single particle is not mistaken for two due to a hole in light image of the root). e: This final image is redirected to the original image (a), so that differences in the size between a and e, could be measured. (Only particles less than 0.01mm^2 were measured, and FERET (the longest distance within each particle) was considered to be the length).

2.7.7. ESTIMATION OF THE NUMBER OF ROOTS OF EACH SIZE IN THE SYSTEM AND PARTICLE SIZE ANALYSIS

The number of root debris of all sizes was estimated as follows. Firstly, the number of intact roots remaining was estimated as the total mass of intact roots remaining after shearing divided by the average mass of a single intact root, (i.e. 0.00281g). Each of these roots are intact and thus represent a length of 10 mm. The number of root debris (defined here as anything below 10 mm) and each of their corresponding length was measured as outlined above ("Root debris length analysis"), which gave a certain number of particles, denoted here as x. However, in order to estimate the number of root debris in the whole system (7 ml), it was assumed that there was a loss of 1 ml due to experimental error and inevitable liquid loss during sampling, giving a total of 6 ml. In addition, it was assumed that 0.1 ml of sample was placed on a microscope slide for measurement, and this was done in triplicate, i.e. 0.3 ml. Thus, x particles measured by Image analysis of microscopic images are representative of 0.3 ml. Thus, the number of debris particles (less than 10 mm) were assumed to be (6/0.3) i.e. 20x. Since the sample was taken from the well-mixed system, it was assumed that the remaining 20x particles had the same particle size distribution.

In order to estimate the number of times a single root was broken, n_r, this was estimated by equations (2.3) to (2.4) below.

$$n_r = \frac{n_d}{n_{ni}} \tag{2.3}$$

where n_d is the actual number of root debris, and n_{ni} is the number of roots subject to breakage (not intact), as determined by

$$n_{ni} = \frac{(initial\ mass\ of\ intact\ roots - final\ mass\ of\ intact\ roots)}{average\ mass\ of\ a\ single\ root} \tag{2.4}$$

Coincidence counts were eliminated since there was an adequate dilution of particle sample (5% (wt/v)). All particle size distribution data were corrected for background noise due to non-root (e.g. soil) particles. Three repeat trials were conducted at each operating time, and samples were equally analysed in triplicate.

2.8. PROCESS OPTIONS BASED ON EARLY IgG TARGETTING, HARVESTING AND EXTRACTION DECISIONS

The commonly used commercial batch simulation package, SuperPro Designer (version 4.5) (Intelligen Inc, Scotch Plains, NJ, USA) was used to design a process based on optimal extraction parameters identified in this research work for the extraction of IgG, mIgG and IgG-HDEL from the leaves of transgenic tobacco plants.

Chapter3- Production of IgG-HDEL expressing transgenic plants for the generation of intracellularly retained monoclonal antibodies

3.1. INTRODUCTION

Plants expressing IgG (secreted form) (Ma *et al.*, 1994) and membrane-bound IgG (mIgG) (Vine *et al.*, 2001) have previously been generated and were available as stably transformed plants in soil. The objective of this Chapter was to generate plants expressing recombinant IgG, in which the tetrapeptide-HDEL was fused to the heavy chain. The K/HDEL tag is well-known to anchor associated recombinant proteins in the membrane of the endoplasmic reticulum via a specific receptor (Conrad and Fiedler, 1998; Fiedler *et al.*, 1997). It has been used extensively to stabilise recombinant proteins (including MAbs) thereby enhancing the levels of accumulation (Stoger *et al.*, 2005), and this strategy has been proposed for commercial production.

3.2. PCR CLONING

A Guy's 13 heavy chain PCR product of the desired size (approx 1.4kb) was amplified (Figure 3.1 Lane A). No bands were amplified in the control samples (lanes B, C, and D). Following purification of the PCR band, ligation into pBluescript II SK+ vector and transformation of *E. coli* DH5α cells, a number of positive transformants were identified (Figure 3.2). As a marker for the correct sized insert, the original PCR product was used (far right lane). All but one sample appeared to have an insert of the expected size.

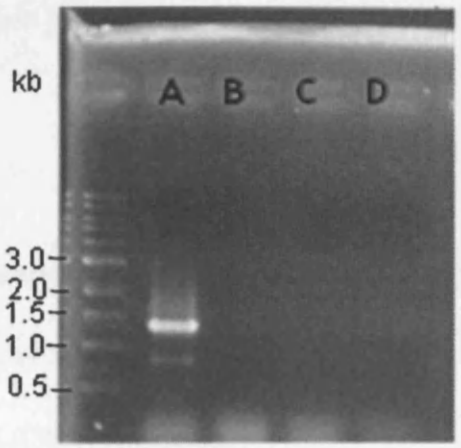

Figure 3.1: Agarose gel electrophoresis and ethidium bromide staining of PCR products. (Lane A = Guy's 13 heavy chain in pBluescript II SK+ (template DNA) amplified by the forward primer and reverse primer; Lane B (as A, but without template DNA in the initial PCR reaction mix; Lane C (as A, but without the reverse primer in the PCR reaction mix; Lane D = as A, but without the forward primer in the PCR reaction mix.

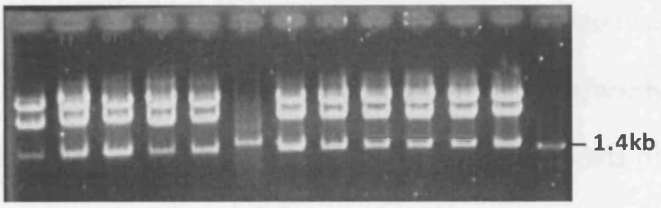

Figure 3.2 Screening of transformed E. coli DH5α. Plasmid DNA was purified and digested with restriction enzymes XhoI and EcoRI and electrophoresed in a 0.5% (w/v) agarose gel, and visualised by ethidium bromide staining. An insert of the approximately 1.4kb is expected for positive transformants.

3.3. CONFIRMATION OF CLONED INSERT BY AUTOMATIC SEQUENCING

Two of the potential positive *E. coli* transformants were selected, and plasmid DNA was used for automatic sequencing. The results for one of these clones are shown in Appendix A. Although the data confirmed that the Guy's 13 heavy chain-HDEL sequence in pBluescript II SK+ was cloned, a single silent mutation was also identified, as well as a further mutation that results in a predicted phenylalanine substitution to leucine in the CH2 domain at nucleotide position 1542. It is unknown whether this mutation is functionally significant, however, as the mutation is within the constant region of the heavy

chain and not involved in the antigen binding site, it should have no effect on the antibody's functionality or targeting.

3.4. SUB-CLONING INTO PLANT VECTOR pL32, TRANSFORMATION OF *AGROBACTERIUM TUMEFACIENS* AND PLANT TRANSFORMATION

The cloned Guy's 13 heavy chain-HDEL sequence was sub-cloned into the plant vector pL32, and then transformed into *E.coli* DH5 α. From a plate of 39 colonies, 36 colonies were picked and grown in culture overnight. The DNA was re-isolated, digested using Xho1 and EcoR1, and electrophoresed on a 1% (w/v) agarose-TAE gel, and visualised by ethidium bromide staining, revealing at least 18 positive clones (Figure 3.3). The cloned Guy's 13 heavy chain-HDEL sequence sub-cloned into the plant vector pL32 was then used for *A. tumefaciens* transformation using electroporation (Hoekema et al, 1983). Six clones of transformed *A. tumefaciens* were identified by the same method described above (Figure 3.4). Subsequently, leaf discs were transformed with the recombinant *A. tumefaciens,* and once shoots had formed they were transferred to root-inducing media, so that small plantlets could form, and then be transferred to soil pre-screening.

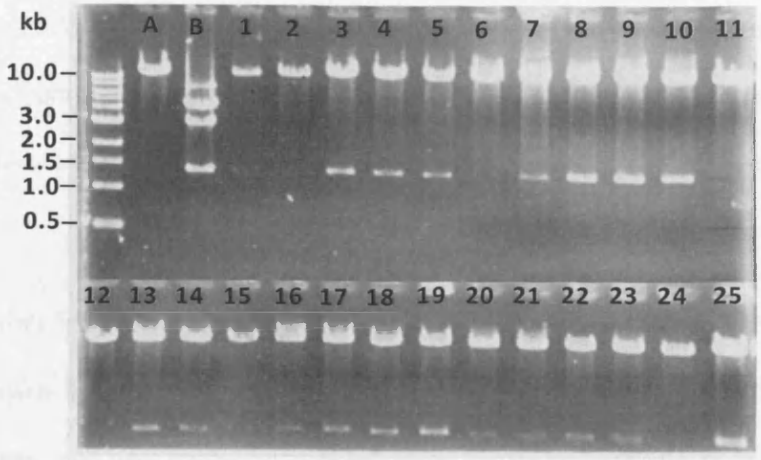

Figure 3.3 Screening of transformed E. coli DH5α for Guy's 13 heavy chain-HDEL cloned into pL32. As markers, pure pL32 (lane A) and pBluescript containing the Guy's 13-HDEL insert (lane B) were also included. The numbered lanes are the purified and digested pL32 containing Guy's 13-HDEL. Samples 3-5, 7-10, 13-14, 16-23 and 25 shows the correct insert (~1.4 kb).

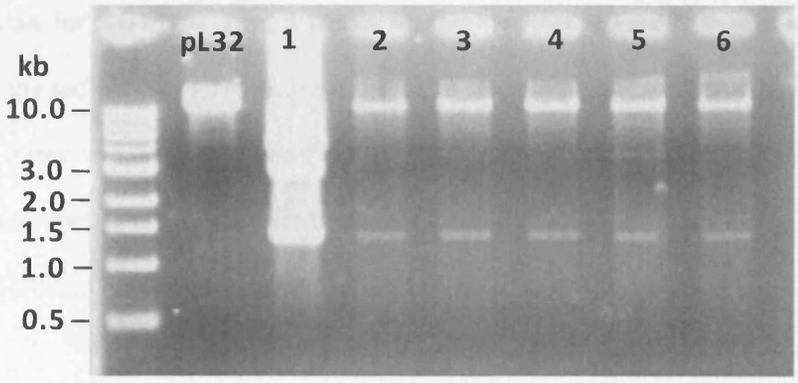

Figure 3.4 Screening of transformed *Agrobacterium* for Guy's 13 heavy chain-HDEL cloned into pL32. As markers, pure pL32 was also included. The numbered lanes are the purified and digested pL32 containing Guy's 13-HDEL. All samples shows the correct insert (~1.4 kb). (The concentration of DNA added to the gel in lane 1, is too high, hence the unclarity of the bands).

3.5. SCREENING FOR EXPRESSION OF IgG-HDEL HEAVY CHAIN PLANTS AND CROSSING WITH IgG-LIGHT CHAIN PLANTS TO REGENERATE FULLY-ASSEMBLED IgG-HDEL ANTIBODY

Plants were screened using enzyme-linked immunosorbent assays that were specific for IgG heavy chain detection (Figure 3.5). A total ten individual transgenic plants were identified as positive. Figure 3.5 demonstrates results from 3 of the plants. These Guy's 13 γ1-HDEL heavy chain expressing plants were then used for cross-fertilisation with existing transgenic plants expressing the Guy's 13 light chain (Ma *et al.*, 1994).

Putative IgG-HDEL transformed plants were screened by Western blotting to identify MAb heavy and light chains. Figure 3.6a shows reducing SDS-PAGE of extracts from IgG-HDEL plants showing expected bands of heavy and light chains being 50KDa and 25KDa respectively, for plants 1, 2 and 4. No recombinant protein expression was observed in plant 3 extract. For the IgG-HDEL positive plants, no differences were observed whether the plant extract was prepared with or without detergent (D). These plants were also screened by an antigen-specific ELISA. Figure 3.6b demonstrates the results for an

antigen-specific ELISA for IgG-HDEL. The 3 plants represented for IgG-HDEL expression, show similar titration curves to the murine Guy's 13 positive control, in contrast to the wild type plant that shows no antigen detection (negative control). In total, out of 18 progeny plants screened by an antigen-specific ELISA, 14 expressed functional Guy's 13 antibody. Plants found to be positive for the fully assembled antibody were self-crossed for the generation of a seed stock.

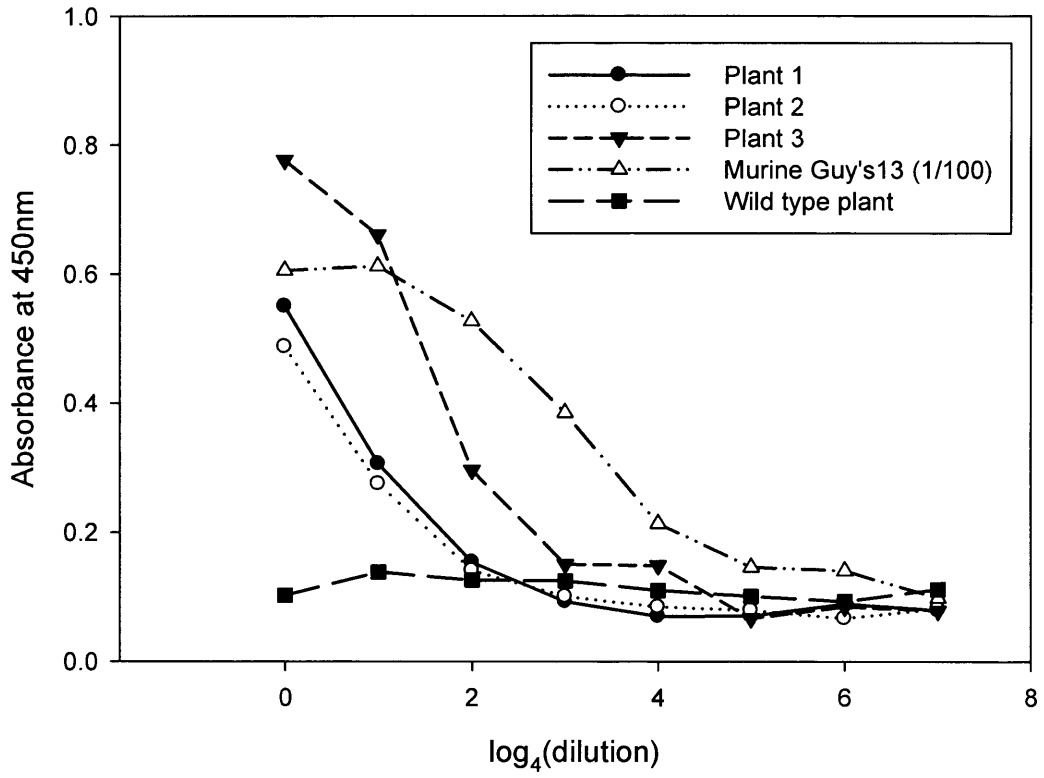

Figure 3.5: Heavy chain specific ELISA results for 3 IgG-heavy chain-HDEL plants. Plant extracts were prepared by grinding leaf discs in buffer (no detergent included). Binding of plant extracts to anti-mouse IgG γ was detected using an HRP labelled anti-mouse IgG (Fc gamma specific) antiserum (1:4000). Control samples are murine Guy's 13 culture supernatant and an extract from a wild type plant.

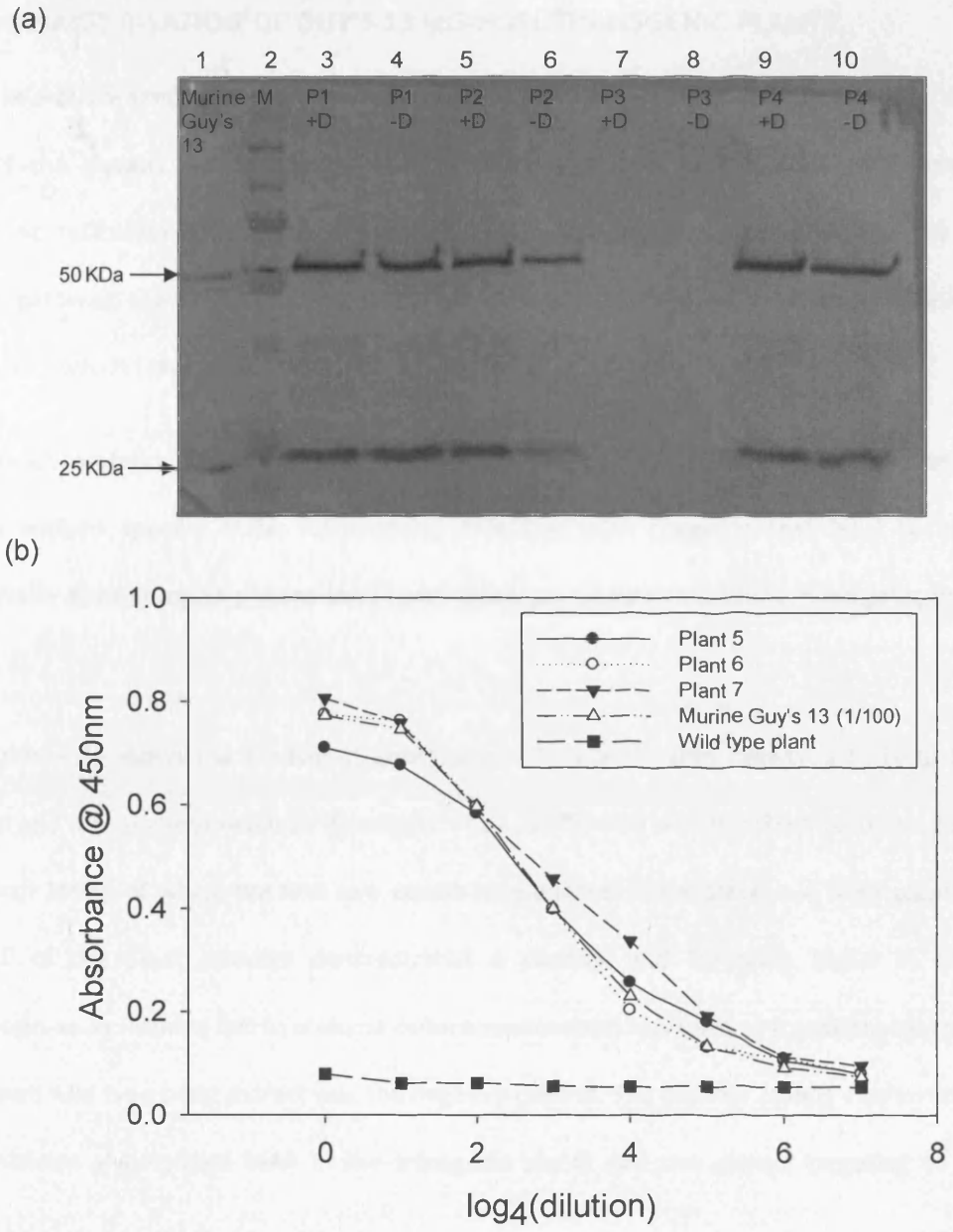

Figure 3.6 IgG-HDEL expression in transgenic plants. (a) Western blot run under reducing conditions, with immunodetection using anti-murine- heavy and light chain anti-serum. (Lane 1: murine Guy's 13 hybridoma supernatant (1/100 dilution); lane 2: Protein markers; lanes 3, 5, 7, 9 – samples from 4 individual plants extracted with 1% v/v Triton X-100 (+D). Lanes 4, 6, 8 and 10 – paired samples from 4 individual plants extracted without detergent (-D).

(b) Antigen specific ELISA results for 3 IgG-HDEL plants. Plant extracts were prepared by grinding leaf discs in buffer (no detergent included). Binding of plant extracts to specific antigen was detected using an HRP labelled anti-mouse IgG (Fc gamma specific) antiserum (1:4000). Control samples are murine Guy's 13 culture supernatant and an extract from a wild type plant.

3.6. CHARACTERISATION OF GUY'S 13 IgG-HDEL TRANSGENIC PLANTS

A selectively simple way to assess the functionality of the –HDEL peptide-tag is to determine the nature of the glycans associated with the IgG-HDEL antibody. As the antibody is retained in the endoplasmic reticulum (ER), with only limited access to the Golgi apparatus and the downstream secretory pathway, the presence of complex type glycans is limited, but these should be high mannose glycosylation, which takes place in the ER.

The glycosylation status of the recombinant MAb Guy's 13 IgG-HDEL was therefore determined using an antigen specific ELISA followed by detection with reagents that bind to high mannose (concanavalin A) or complex glycans (anti-horseradish peroxidase antiserum) (Chargelegue *et al.*, 2000); (Figure 3.7).

Figure 3.7a shows the binding of Concanavalin A- a lectin with specific affinity to terminal α-D-mannosyl and α-D-glucosyl residues (Baenziger *et al.*, 1979) and possibly short complex glycans (Wilson and Altman 1998), of which the first two would be predicted to be present in both plant IgG and IgG-HDEL. All of the plant samples demonstrated a positive and titratable signal in this functional glycosylation assay. Murine IgG hybridoma culture supernatant was used as a positive control, and a non-transformed wild type plant extract was the negative control. The positive results confirm the expression of recombinant glycosylated MAb in the transgenic plants and the correct targeting to the secreted pathway.

The same plant samples were also used in an antigen-specific capture ELISA with detection of complex glycosylation (Figure 3.7b). We have previously demonstrated the structures of the complex glycans associated with plant derived Guy's 13 IgG (Cabanes-Macheteau *et al.*, 1999), and three IgG transgenic plants were used as positive controls in this assay. Murine hybridoma derived IgG does not incorporate plant complex glycans (Cabanes-Macheteau *et al.*, 1999) and as expected, no binding was observed. The wild type negative control plant demonstrated no binding. The absence of complex glycan detection in the 3 IgG-HDEL plants provides evidence for the correct function of the heavy chain C-

terminal HDEL tag, retaining the recombinant IgG in the ER membrane; and preventing trafficking further through the secreted pathway into the Golgi complex and the addition of complex glycan residues.

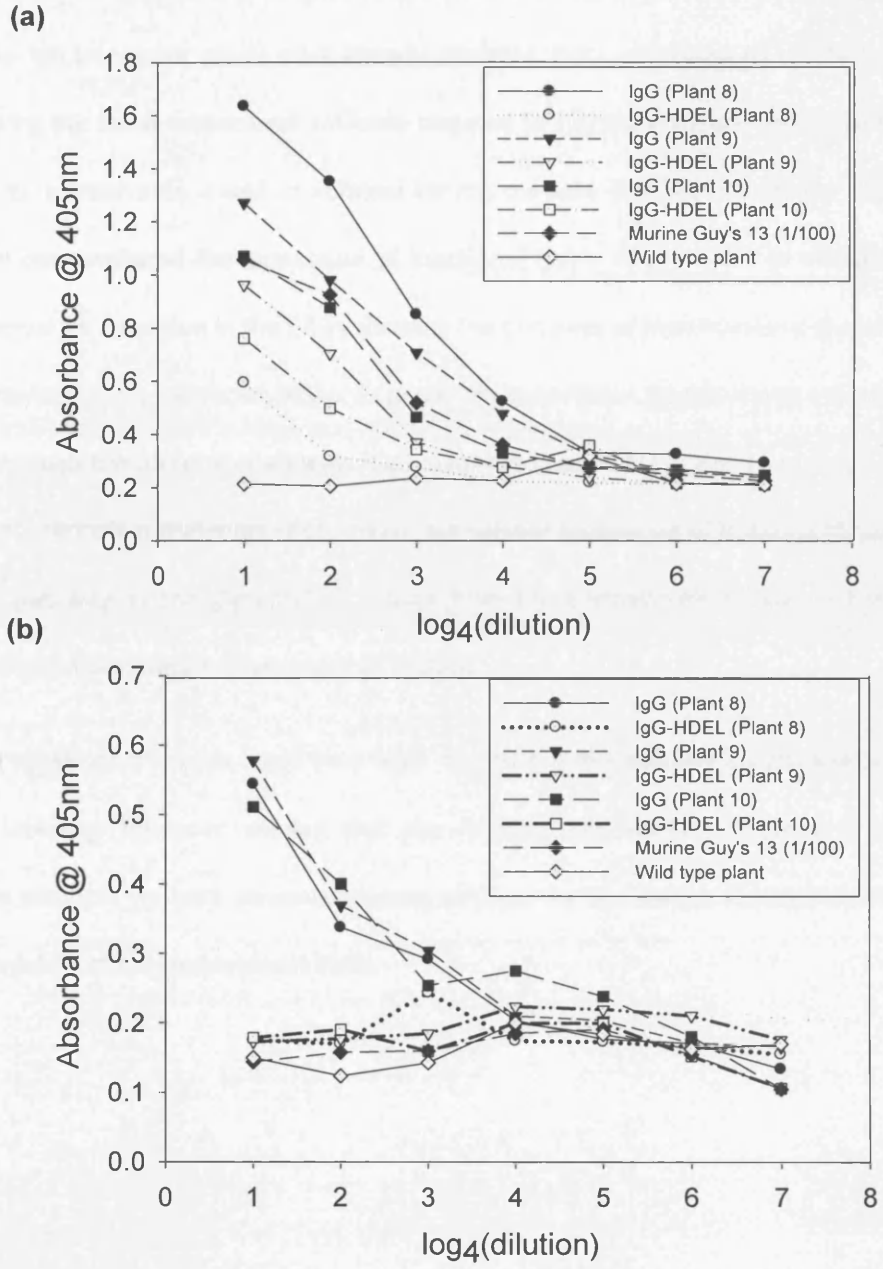

Figure 3.7 Glycosylation of IgG-HDEL. (a) Glycosylation control: Detection of high mannose glycosylation. Extracts from 3 IgG plants and 3 IgG-HDEL plants were incubated on ELISA plates coated with specific antigen. Detection of binding was with concanavalin A followed by rabbit anti-concanavalin A, followed by an alkaline-phosphatase labelled anti-rabbit anti-serum. (b) Detection of complex glycans. Samples were incubated in microtitre wells coated with specific antigen. Detection of binding was with rabbit anti-horseradish peroxidase, followed by an alkaline-phosphatase labelled anti-rabbit anti-serum.

3.7. DISCUSSION

The targeting of recombinant IgG to 3 sub-cellular compartments in plants has been described in the literature (Ma *et al.*, 1995; Vine *et al.*, 2001; Conrad and Fiedler, 1998). For this study, secreted IgG and membrane IgG transgenic plants were already available. Here we produced a third line of transgenic plants expressing the same monoclonal antibody targeted to the endoplasmic reticulum membrane. The use of an –HDEL tetrapeptide is well established for this purpose (Conrad and Fiedler, 1998; Denecke *et al.*, 1992). We demonstrated the expression of functional Guy's 13 IgG-HDEL in transgenic plants, and provided evidence for retention in the ER by showing the presence of high mannose glycosylation, but the absence of extended complex glycosylation. As plants are eukaryotes, glycan chains are added to proteins as they pass through the secretory pathway. High mannose glycans are added to proteins including IgG in the endoplasmic reticulum (Helenius *et al.*, 2004), but further processing of N-linked glycans occurs along the secretory pathway as the glycoprotein moves from the endoplasmic reticulum through the Golgi apparatus to its final destination (Gomord *et al.*, 2004).

Further localisation studies could have been carried out, for example by electron microscopy with Immunogold labelling. However, we felt that the –H/KDEL tag function in plants is extremely well-established. In addition, we have generated strong evidence for the correct function of the HDEL tag and the correct targeting of the recombinant MAb.

Chapter4- Considerations for extraction of monoclonal antibodies targeted to different subcellular compartments in transgenic tobacco plants

4.1 INTRODUCTION

Monoclonal antibody (MAb) production from transgenic tobacco plants offers many advantages over other heterologous production systems, creating the prospect of production at a scale that will allow new prophylactic and therapeutic applications in global human and animal health. However, information on the major processing factors to consider for large scale purification of antibodies from transgenic plants is currently limited, and is in urgent need of attention.

The purpose of this Chapter was to investigate methods for the initial extraction of recombinant IgG antibodies from transgenic tobacco leaf tissue. Three different transgenic plant lines were studied, in order to establish the parameters for optimal extraction of MAbs that accumulate in the apoplasm, at the plasma membrane or within the endoplasmic reticulum. For each transgenic line, seven techniques for physical extraction have been compared. The factors that determine the optimal extraction of antibodies from plants have a direct influence on the initial choice of expression strategy, so must be considered at an early stage. The use of small scale techniques that are applicable to large scale purification was a particularly important consideration. (The result of this work has been published, Hassan *et al.*, 2008b).

4.2 STRATEGY FOR EXAMINING THE EXTRACTION OF MONOCLONAL ANTIBODIES FROM TRANSGENIC PLANTS

4.2.1 OVERALL STRATEGY

For the investigation of extraction of monoclonal antibodies from transgenic tobacco plants, successful and optimised protocols were established for immunoglobulin detection of fully-assembled functional IgG, (Chapter 2, Section 24.1). A deliberate design of this enzyme-linked immunosorbent assay

(ELISA) method, was to capture the antibody with specific antigen and detect with labelled gamma-specific anti-IgG, in order to ensure the measurement of only assembled and functional antibody with the elimination of any unassembled IgG heavy chains or light chains or a possible Fab fragment that may have arisen due to proteolytic cleavage. Having identified a number of factors that may affect the extraction of monoclonal antibodies from transgenic tobacco plants, the following flowchart (Figure 4.1) was pursued.

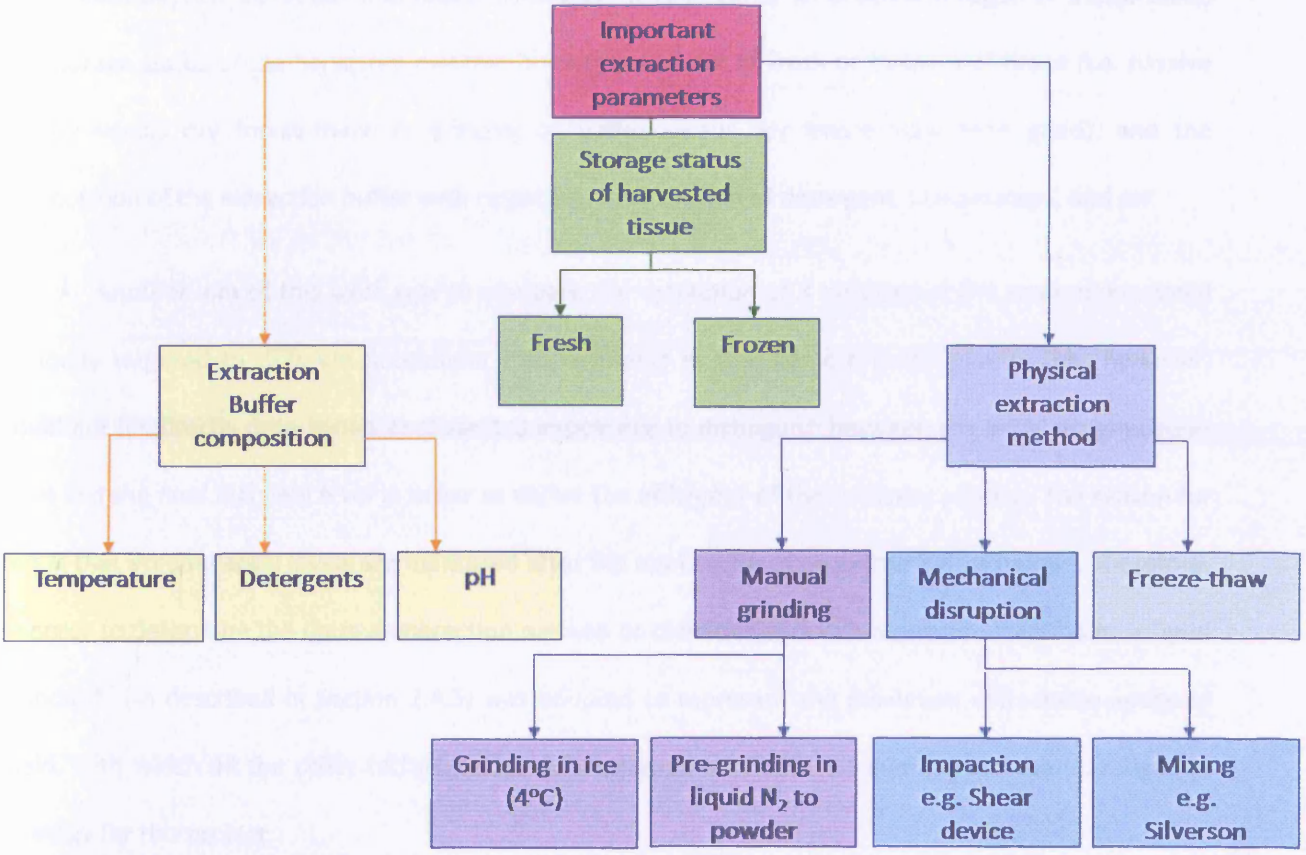

Figure 4.1: Factors investigated to compare ease of extractability in transgenic tobacco leaves.

Initially it was thought that the first step of this investigation should be to choose the best mechanical disruption method for this purpose. Each small scale device would be investigated for pre-identified criteria for an ideal extraction technique, and the results compared by ELISA assay to assess concentration of functional antibody. However, because of the requirement of larger amounts of biomass in these mechanical laboratory scale techniques (at least 100 fold greater) translating into a smaller range of investigatable parameters per unit time, in addition to the limited literature on the efficiency of mechanical procedures for monoclonal antibody extraction, the reproducibility and comparability of

microcentrifuge scale techniques such as grinding in buffer to investigate all the parameters important for extraction, was tested first. As detailed in the following section (Section 4.3), grinding in buffer, passive elution, dry or wet freeze-thaw and these techniques in combination with grinding were found to be reproducible for extractability of IgG at microcentrifuge scale in order to perform informative initial studies, and were therefore used to proceed with the above plan. This chapter explores the employment of different physical extraction methods including grinding in buffer or in liquid nitrogen or freeze-thaw, the storage status of the harvested material looking at the use of fresh or frozen leaf tissue (i.e. passive elution versus dry freeze-thaw, or grinding in buffer versus dry freeze-thaw then grind), and the composition of the extraction buffer with respect to the inclusion of detergent, temperature, and pH.

Another aim of this work was to compare the extraction of 3 versions of the same monoclonal antibody targeted to different subcellular compartments in transgenic tobacco plants. This, however, could not be directly determined because it is impossible to distinguish between the initial accumulation level and the final recovery level in order to derive the efficiency of the recovery process. The reason for this is that accumulation levels are measured after the application of an extraction technique. Therefore, in order to determine the optimal extraction method or condition for each monoclonal antibody, a "gold standard" (as described in Section 2.4.5) was adopted to represent the maximum extractable antibody yield, with which all the other techniques could be compared. Table 4.1 summarises the investigation strategy for this project.

Reproducibility **(Reasons for establishing a "gold standard")**	♦ Plant vs. plant within the same transgenic line and approximately the same age ♦ Leaf vs. leaf within individual plants
Extraction technique **(Defined in Chapter 2 (Section 2.4.5)**	♦ Passive elution ♦ Dry freeze-thaw ♦ Wet freeze-thaw ♦ Grinding in buffer ♦ Dry freeze-thaw then grind ♦ Wet freeze-thaw then grind ♦ Grinding in liquid nitrogen
Buffer physiochemical properties	♦ Detergent ♦ Temperature ♦ pH
Antibody targeting strategy	♦ IgG (secreted) ♦ mIgG (membrane bound) ♦ IgG-HDEL (Endoplasmic reticulum)
Plant management	♦ Age of plant (discussed in Chapter 5) ♦ Plant organ (leaf vs. root) (discussed in Chapters 6 and 7)

Table 4.1 Investigation strategies for this project

4.3 REPRODUCIBILITY OF EXTRACTION TECHNIQUES

4.3.1 ESTABLISHING WHETHER THE SMALL-SCALE EXTRACTION TECHNIQUES USED ARE REPRODUCIBLE

Grinding plant tissue in buffer is the most commonly used methodology for extraction of recombinant proteins from transgenic plants at a laboratory scale. Before this could be used as a "gold standard" for comparison with other extraction techniques, it was necessary to determine the reproducibility of this method. In addition, in order to perform a valid comparison between different techniques for extraction, it was also important to test the reproducibility of the other small scale extraction techniques.

Thus, three of the extraction techniques, (passive elution, grinding in buffer, and wet freeze-thaw), were subjected to a test of reproducibility, following the method of Montgomery, (2005). At least three different plants expressing either IgG or IgG-HDEL were selected and 10 random extractions were taken from 3 randomly chosen leaves located at the top, middle and bottom of the plant. An analysis of variance (ANOVA) Generalised linear model (Minitab, version 13, UK) was performed to compare the differences between successive extractions with plant to plant variation (Table 4.2).

The variability of multiple extractions from the same plant (b) never reached significance regardless of the extraction technique. Therefore, the extraction techniques are sufficiently reproducible for the planned small-scale investigation. The inter-plant variability (a) was always significant (except in one case). On this basis, experiments were designed to use individual plants. Repeat experiments were performed to confirm our findings, but the data presented is usually based on one representative experiment.

		Passive elution	Grind in buffer	Wet freeze-thaw
IgG	a) IgG variation between individual plants (n = 3 for passive elution and grinding, n = 5 for wet freeze-thaw)	P < 0.0001	P < 0.0001	P = 0.050
	b) IgG variation within the same plant and leaves (10 extractions)	P = 0.703	P = 0.061	P = 0.159
IgG-HDEL	a) IgG variation between individual plants (n = 3 for all techniques)	P = 0.001	P < 0.0001	P = 0.130
	b) IgG variation within the same plant and leaves (10 extractions)	P = 0.75	P = 0.937	P = 0.554

Table 4.2 Reproducibility of extraction techniques: plant-plant variation versus variation between multiple extractions from the same plant. The results are from analysis of variance (ANOVA) (Generalised linear model, Minitab, version 13).

4.4 THE EFFECT OF INCLUSION OF DETERGENT IN THE EXTRACTION BUFFER ON RECOMBINANT ANTIBODY EXTRACTION

The detergent chosen for investigation was Triton X-100. It is known that non-ionic detergents are required to extract membrane-bound proteins. In general, nonionic and zwitterionic detergents are milder and less denaturing than ionic detergents and are used to solubilize membrane proteins where it is critical to maintain protein function and/or retain native protein:protein interactions for enzyme assays or immunoassays. CHAPS, a zwitterionic detergent, and the Triton-X series of non-ionic detergents are commonly used for these purposes (Sivars *et al.*, 2000). Non-denaturing detergents such as Triton X-100 have rigid and bulky nonpolar heads that do not penetrate into water-soluble proteins; consequently, they generally do not disrupt native interactions and structures of water-soluble proteins and do not have cooperative binding properties. The main effect of non-denaturing detergents is to associate with hydrophobic parts of membrane proteins, thereby conferring miscibility to them.

It was previously demonstrated that the inclusion of a detergent in the extraction buffer is required for extraction of recombinant mIgG from transgenic plants (Vine *et al.*, 2001). Here, we also investigated the addition of Triton X-100 on the extraction of IgG and IgG-HDEL (Figure 4.2).

For mIgG extraction, in the absence of Triton X-100, very little immunoglobulin could be extracted in transgenic plant extracts. For mIgG, the immunoglobulin yield increased with increasing Triton X-100 concentration and at 1% (v/v) the mIgG yield was up to 4-fold greater. Due to the variability in the 1% Triton X-100 samples, the differences in mIgG yields compared with lower detergent concentrations did not reach statistical significance (Figure 4.2a). However, the yield with 0.1% Triton X-100 compared with no detergent approached significance ($P = 0.068$). Figure 4.2b shows the yield of mIgG as a % of TSP. Again, there was no statistical significant increase in MAb yield as a % of TSP with detergent concentration, with the exception of 0 and 0.1 % (v/v) where a significant increase was observed ($P = 0.045$).

In IgG transgenic plants, an increase in Triton X-100 from 0% (v/v) to 1% (v/v) lead to an almost 3-fold decrease in IgG yield and this approached statistical significance ($P = 0.077$) (Figure 4.2c). Figure 4.2d shows IgG yield as a % of TSP, also decreases significantly with increasing detergent concentration, ($P = 0.028$ between IgG yield at 0% (v/v) and 1% (v/v) Triton X-100).

In IgG-HDEL plants, the effect of increasing concentration of Triton X-100 is shown in Figure 4.2e. There was a significant increase in IgG-HDEL yield between 0 and 0.1% (v/v), ($P = 0.018$). Yield of IgG-HDEL as a % of TSP (Figure 4.2f) however, did not vary significantly with detergent concentration.

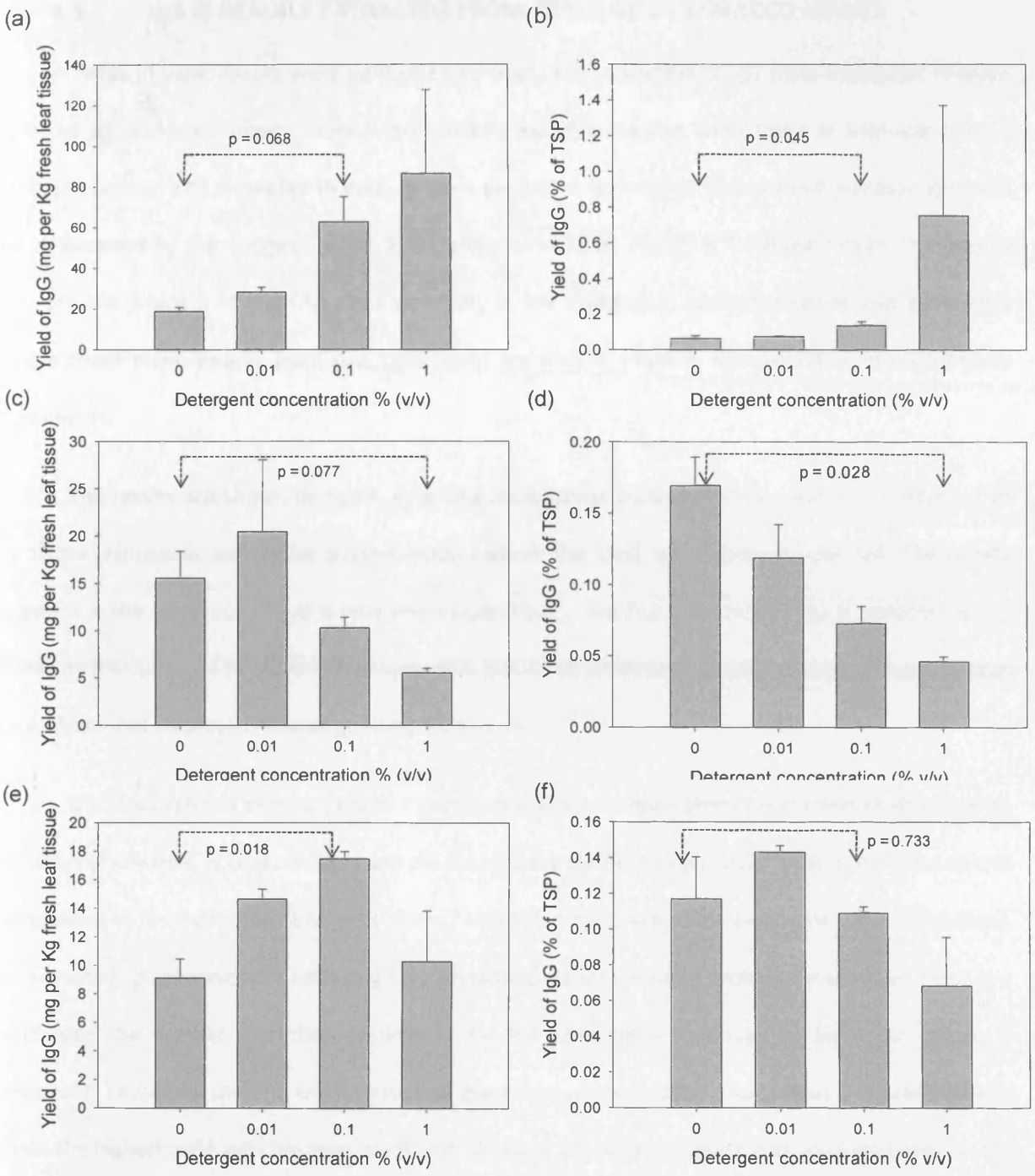

Figure 4.2 Effect of detergent concentration on the extraction of membrane-bound IgG (mIgG) (a), IgG (c) and IgG-HDEL (e) from transgenic tobacco plants. Samples were extracted by grinding in buffer containing Triton X-100. Yield of IgG as a percentage of total soluble protein from transgenic plants expressing mIgG (b), IgG (d) and IgG-HDEL (f). Representative results for single plants are shown, and are the mean ± standard error of the mean (SEM) of triplicate samples.

4.5 IgG IS READILY EXTRACTED FROM TRANSGENIC TOBACCO LEAVES

A series of experiments were performed to assess the extraction of IgG from transgenic tobacco leaves by different techniques. In each experiment, leaf disc samples were taken in triplicate from 3 plants (9 samples) and subjected to each of the 7 extraction techniques. Monoclonal antibody IgG yield was determined by the antigen-specific ELISA and expressed as mg/kg of fresh leaf tissue. In order to eliminate the problem of plant to plant variability in IgG expression, each experiment was performed using a single plant. Results from one experiment are shown, which is representative of six replicate experiments.

The results are shown in Figure 4.3a. The monoclonal antibody (MAb) yield was similar for all extraction techniques, except for passive elution where the yield was approximately half. The results suggest that the extraction of IgG is relatively simple. Thus, a significant amount of IgG is released simply by leaving the cut tissue in buffer. Techniques that just relied on freeze-thaw released similar amounts of IgG as those that employed harsher grinding techniques.

It is also useful to express yield as a percentage of total soluble protein extracted, as this gives an indication of the level of contaminants and the subsequent purification burden (Figure 4.3b). Here data is represented as the mean and SEM for 3 plants. With the mildest extraction technique, (passive elution), the extracted IgG represents a relatively high percentage of total soluble protein. In contrast, there is a trend with the harsher extraction techniques for the MAb IgG percentage to be lower, which is presumably caused by the unwanted release of plant host proteins. On the basis that it is preferable to obtain the highest yield with the least purification burden, the results suggest that dry-freeze-thaw is the technique of choice for releasing IgG from leaf discs.

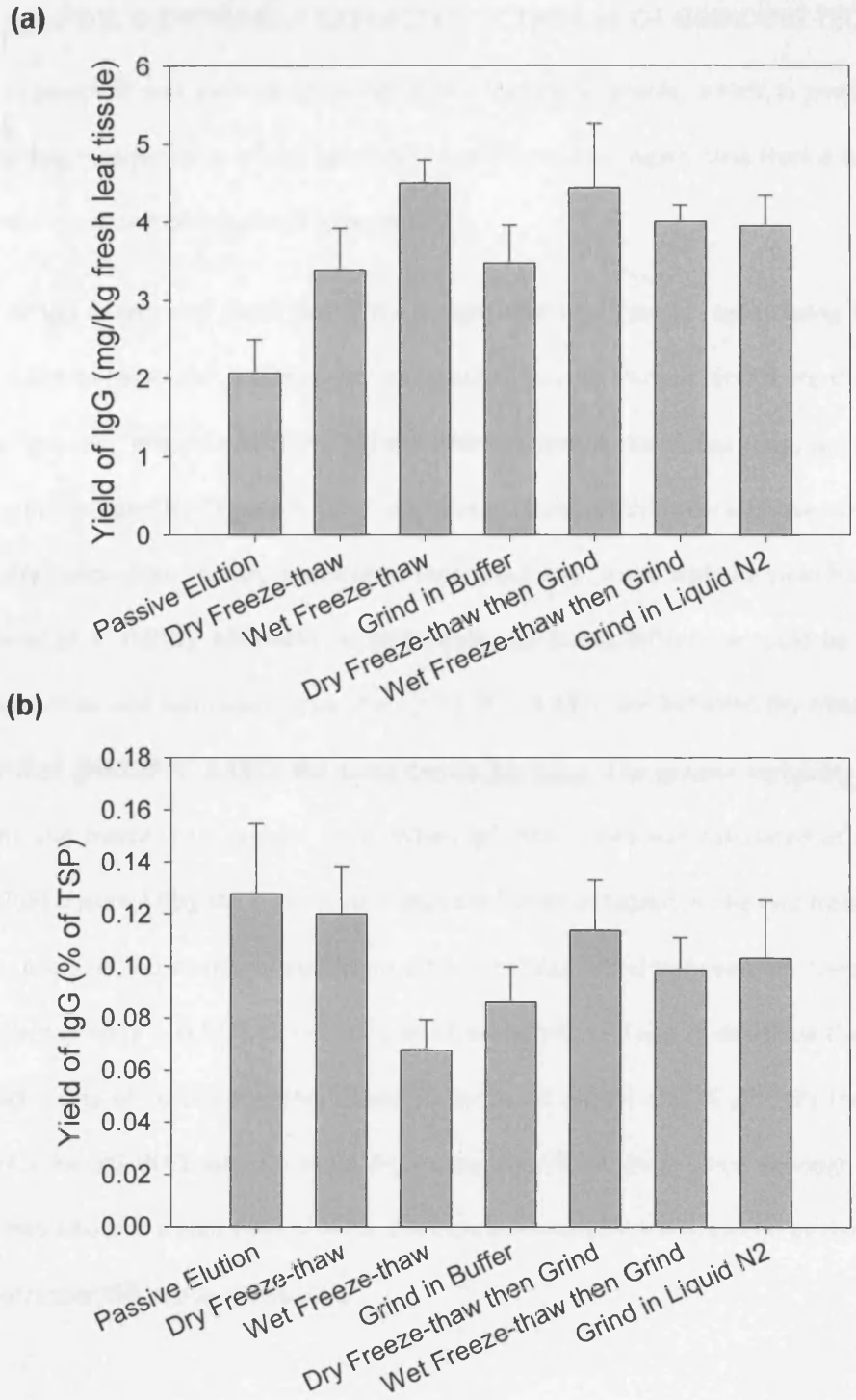

Figure 4.3: Recombinant monoclonal antibody (MAb) extraction from IgG transgenic plants by seven techniques. (a) Results of IgG yield are from a representative experiment using a single plant, and are the mean ± standard error of the mean (SEM) of triplicate samples, expressed as milligram of MAb per kilogram of fresh leaf tissue. (b) Results of IgG as a percentage of total soluble protein are the mean and SEM from nine samples (i.e. three plants and three separate extractions per plant.

4.6 IgG-HDEL IS OPTIMALLY EXTRACTED BY THE USE OF GRINDING TECHNIQUES

A similar experiment was performed on IgG-HDEL transgenic plants, which in contrast to IgG, indicated that grinding is required to release IgG-HDEL MAb (Figure 4.6). Again, data from a single plant is shown, which is representative of 6 replicate experiments.

The yield of IgG in terms of fresh leaf tissue weight was significantly higher using the grinding techniques ($P = 0.021$ between the "passive" groups including passive elution, dry freeze-thaw, and wet freeze-thaw, and "grinding" groups including grind in buffer, dry freeze-thaw then grind, wet freeze-thaw then grind, and grind in liquid N_2) (Figure 4.6a). A significant statistical difference between yield of IgG-HDEL MAb from dry freeze-thaw and dry freeze-thaw then grind was found, with the yield from the latter being 3-fold greater ($P = 0.013$). Although, no statistically significant difference could be determined between wet freeze-thaw and wet freeze-thaw then grind ($P = 0.237$), nor between dry freeze-thaw and wet freeze-thaw then grind ($P = 0.135$), the same trends are seen. The greater variability is probably introduced by the wet freeze-thaw process itself. When IgG-HDEL yield was calculated as a % of total soluble protein (TSP) (Figure 4.6b), the highest yield appeared to be obtained by the two freeze-thaw and grind techniques, however, no statistical significant difference was found between dry freeze-thaw and dry freeze-thaw then grind ($P = 0.543$), or between wet freeze-thaw and wet freeze-thaw then grind ($P = 0.147$). Taking both sets of results together (yield in terms of mg/kg and % of TSP) the extraction technique of choice for IgG-HDEL appears to be dry freeze-thaw then grind, since although wet freeze-thaw then grind may also give a high yield of MAb, the increased variability introduced by the wet freeze-thaw process may render this process unfeasible.

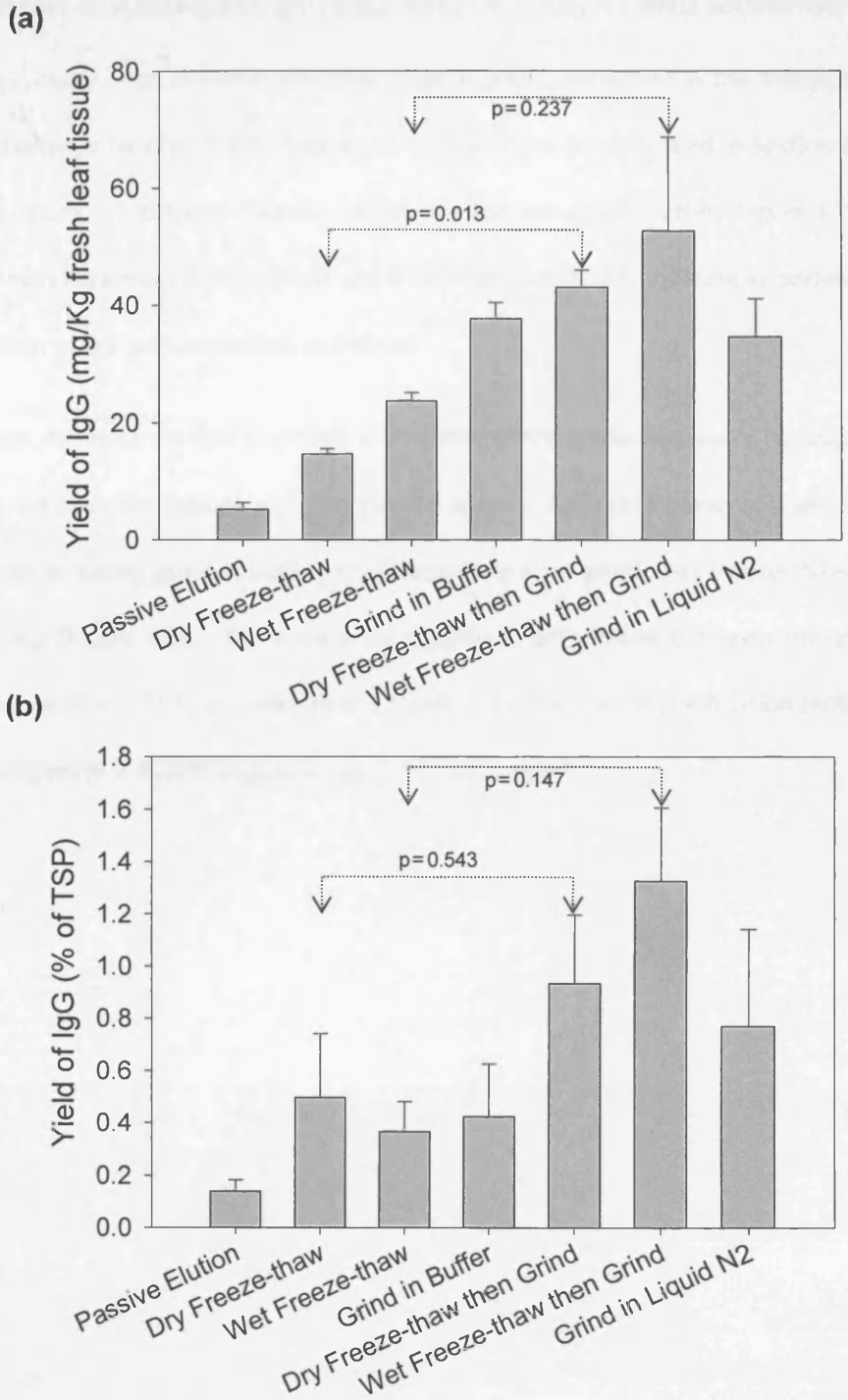

Figure 4.6 (a) Recombinant monoclonal antibody (MAb) extraction from IgG-HDEL transgenic plants by seven techniques. Results of IgG yield are from a representative experiment using one plant, and are the mean ± standard error of the mean (SEM) of triplicate samples, expressed as milligram of MAb per kilogram of fresh leaf tissue. (b) Results of IgG as a percentage of total soluble protein are the mean and SEM from nine samples (i.e. three plants and three separate extractions per plant).

4.7 MEMBRANE-BOUND IgG (mIgG) REQUIRES DETERGENT AND GRINDING

It has previously been demonstrated that mIgG is poorly extracted in the absence of detergent in the extraction buffer (Vine *et al.* 2001). This was confirmed here (as described in Section 4.4). To compare extraction techniques, 1% triton X-100 was included in the extraction buffer (Figure 4.7). As above, IgG yield data is shown here from a single plant and is representative of 3 replicate experiments, all showing the same variation of IgG with extraction technique.

The results demonstrate that a technique including grinding was necessary for mIgG extraction ($P = 0.020$ between the "passive" groups including passive elution, dry freeze-thaw, and wet freeze-thaw, and "grinding" groups including grind in buffer, dry freeze-thaw then grind, wet freeze-thaw then grind, and grind in liquid N_2) (Figure 4.7a). There were no significant differences between the yield, from the 4 grinding techniques ($P = 0.763$), nor was there a significant difference in purification burden between the 4 grinding techniques ($P = 0.423$) (Figure 4.7b).

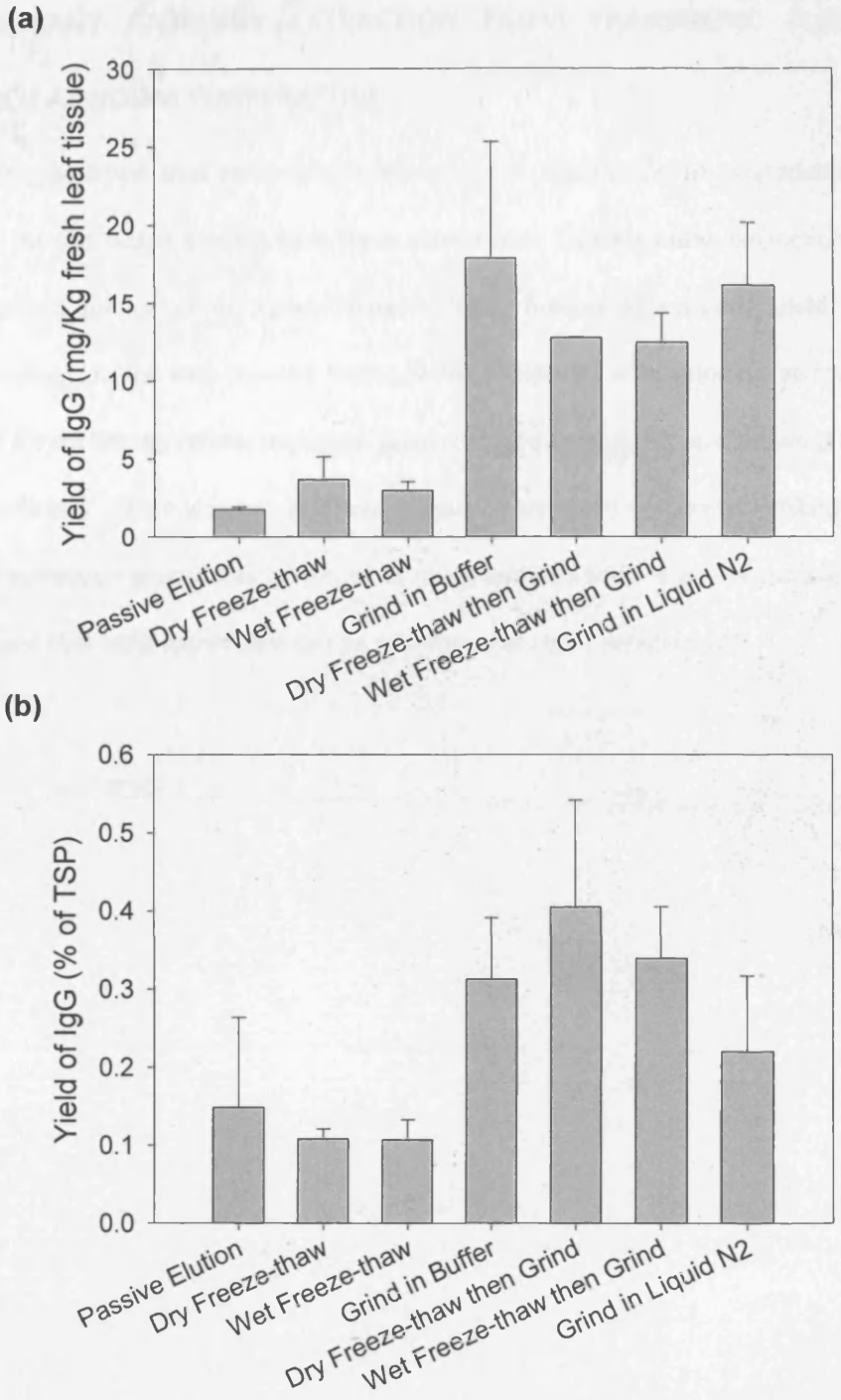

Figure 4.7 (a) Recombinant monoclonal antibody (MAb) extraction from membrane-bound IgG (mIgG) transgenic plants by seven techniques. Results of IgG yield are from a representative experiment using one plant, and are the mean ± standard error of the mean (SEM) of triplicate samples, expressed as milligram of MAb per kilogram of fresh leaf tissue. (b) Results of IgG as a percentage of total soluble protein are the mean and SEM from nine samples (i.e. three plants and three separate extractions per plant). In all cases, 1% Triton X-100 was included in the extraction buffer.

4.8 RECOMBINANT ANTIBODY EXTRACTION FROM TRANSGENIC PLANTS CAN BE PREPARED AT ROOM TEMPERATURE

It is widely believed that recombinant proteins are susceptible to degradation by proteases released during the extraction process from fresh plant tissue. Consequently, extraction procedures are generally performed on ice or in liquid nitrogen. Here, functional antibody yield from extraction procedures (grinding) on ice with ice-cold buffer, were compared with grinding at room temperature (Figure 4.8). Data from IgG, IgG-HDEL, and mIgG plants assayed in triplicate are shown (Figure 4.8a, 4.18b and 4.18c respectively). There was no significant difference between functional antibody yield, between performing the extraction procedures on ice, or at room temperature for any of the plants or IgG types. The results suggest that MAb extractions can be performed at room temperature.

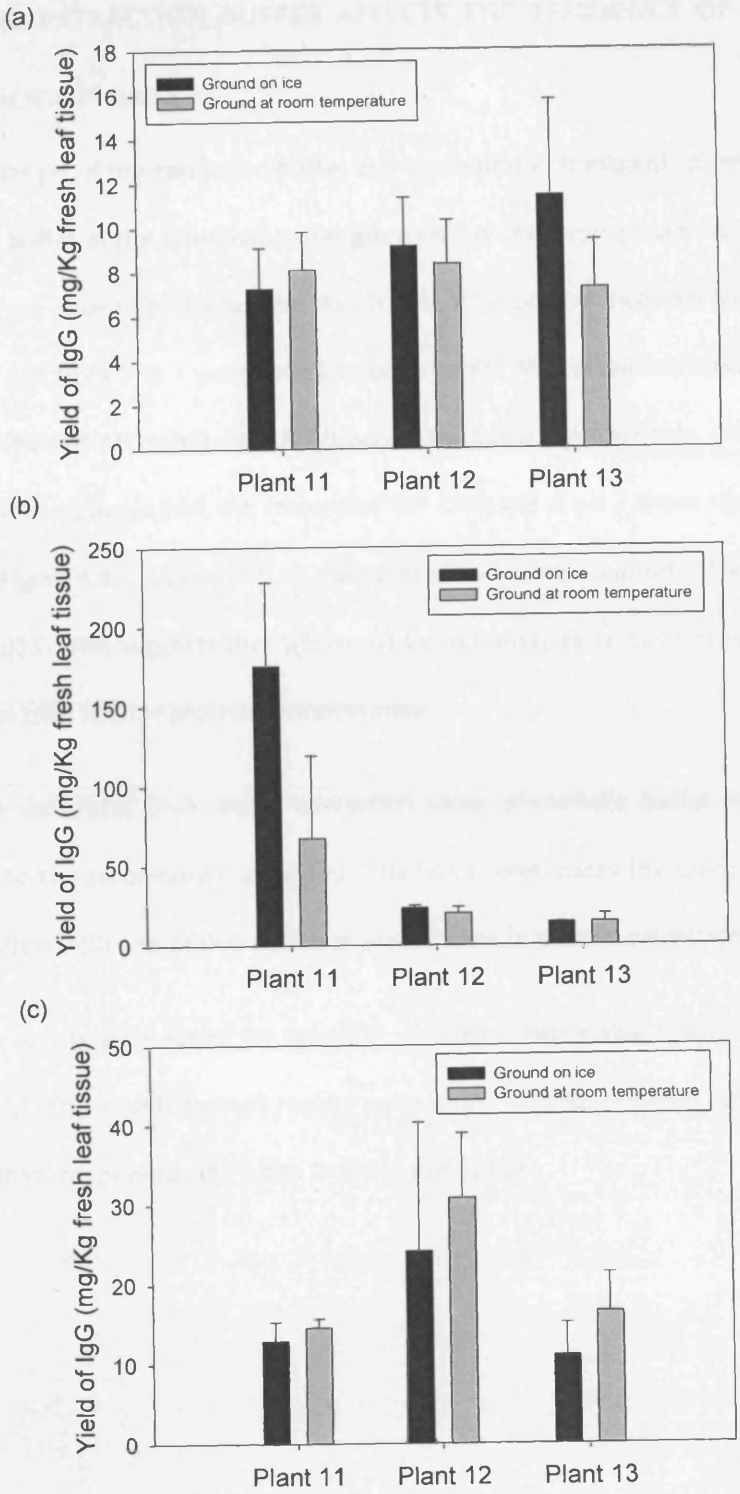

Figure 4.8 Effect of temperature on the extraction of recombinant monoclonal antibody (MAb) from transgenic plants: (a) IgG; (b) IgG-HDEL; (c) membrane-bound IgG (mIgG). The data, represented as milligrams of MAb per kilogram of fresh leaf tissue, are from three representative plants with the mean ± standard error of the mean (SEM) of triplicate samples from each plant. The black and grey bars represent grinding on ice and at room temperature, respectively.

4.9 THE pH OF THE EXTRACTION BUFFER AFFECTS THE EFFICIENCY OF IgG EXTRACTION FROM TRANSGENIC PLANTS

The effect of the pH of the extraction buffer was examined in transgenic plant samples. Three leaf discs were ground in buffer of the same ionic strength with the pH varying from 2.8 to 10. The data for 3 individual IgG plants are shown in Figure 4.9a. At pH 3-4, little or no functional IgG could be detected. However, a range of pHs from 5 to 7 were found to be suitable. When the extraction buffer approached the IgG1's pI (8-9.5 (Buis *et al.*, 1997), less MAb was extractable. Interestingly, when the total soluble tobacco protein levels were measured, the amount of TSP released at pH 7.4 was significantly higher than at pH 6 ($P = 0.017$) (Figure 4.9b). In addition, the amount of TSP released at pH 7.4 was significantly lower than at pH 8 ($P = 0.025$). This suggests that IgG would be optimally extracted between 5-6 for maximum IgG yield and minimal total soluble protein contamination.

This work demonstrates that simple extraction using phosphate buffer maintained at pH 5.0 efficient for extracting the recombinant antibody. This fact corroborates the claim of Larrick *et al*, 2001 that low cost salt buffers with one or two additives are efficient in protein extraction.

Again, similar results were found for IgG-HDEL and mIgG expressing tobacco plants, (Figures 4.10 and 4.11 respectively). The membrane-IgG results were more variable however, and this may be due to the addition of another component, 1% Triton X-100 in the buffer.

(a)

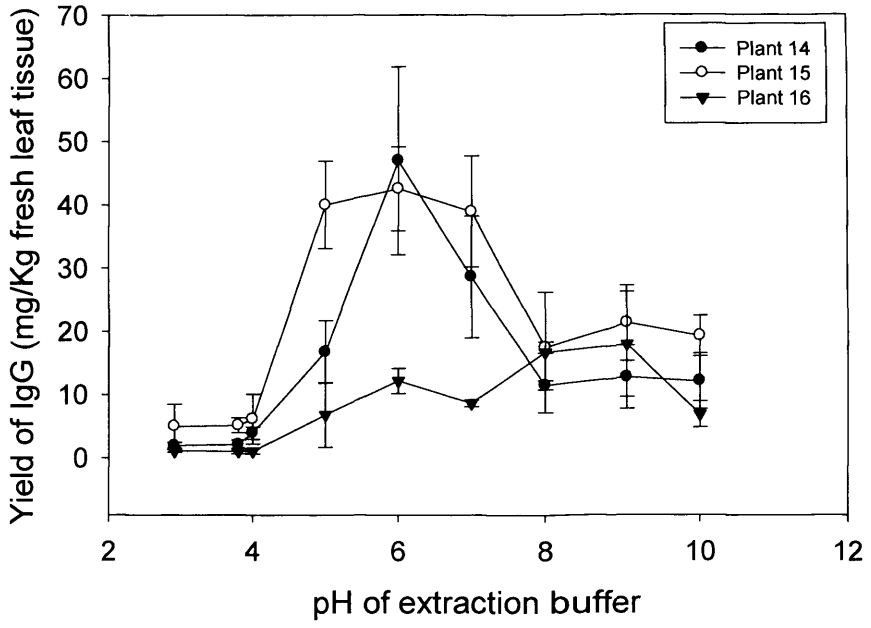

(b)

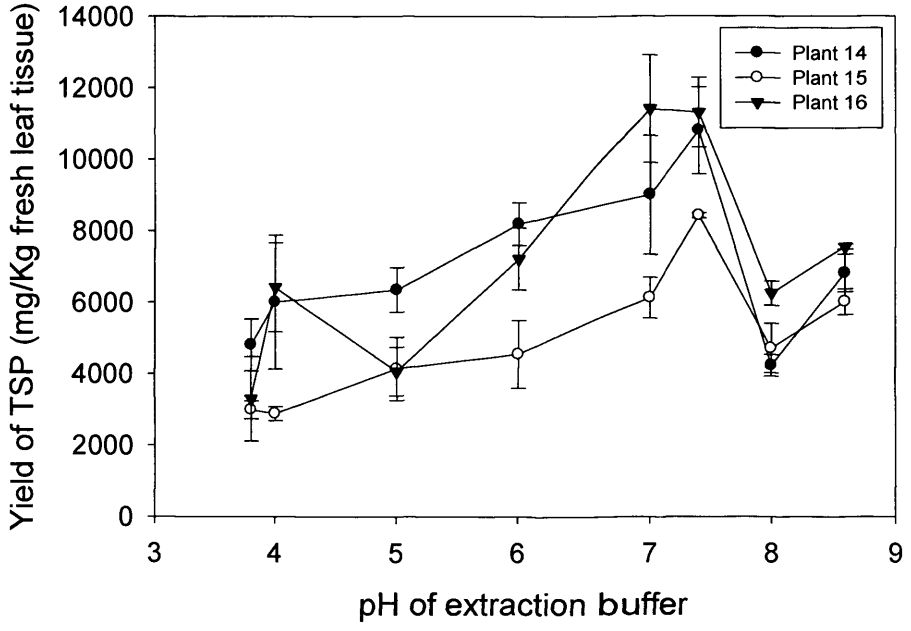

Figure 4.9 (a) Effect of pH on the extraction of IgG from transgenic tobacco plants. Samples were extracted by grinding in buffers of different pH. Results are shown as milligrams of MAb per kilogram of fresh leaf tissue. (b) Effect of pH on the release of total soluble protein from transgenic tobacco plants expressing IgG. Samples were extracted by grinding in buffers of different pH. Results are the mean ± standard error of the mean (SEM) of triplicate samples from three representative plants.

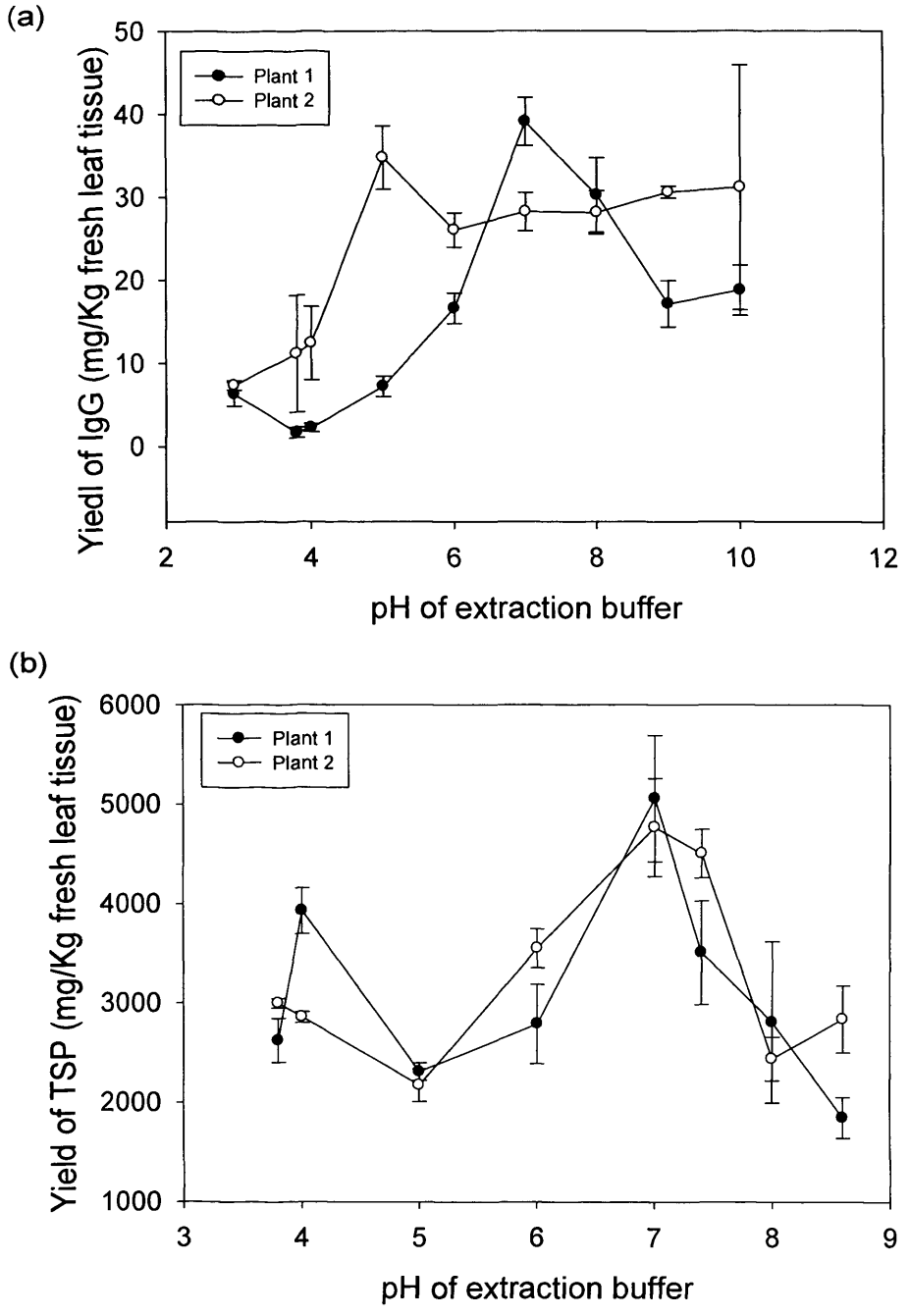

Figure 4.10 (a) Effect of pH on the extraction of IgG-HDEL from transgenic tobacco plants. Samples were extracted by grinding in buffers of different pH. Results are shown as milligrams of MAb per kilogram of fresh leaf tissue. (b) Effect of pH on the release of total soluble protein from transgenic tobacco plants expressing IgG-HDEL. Samples were extracted by grinding in buffers of different pH. Results are the mean ± standard error of the mean (SEM) of triplicate samples from two representative plants.

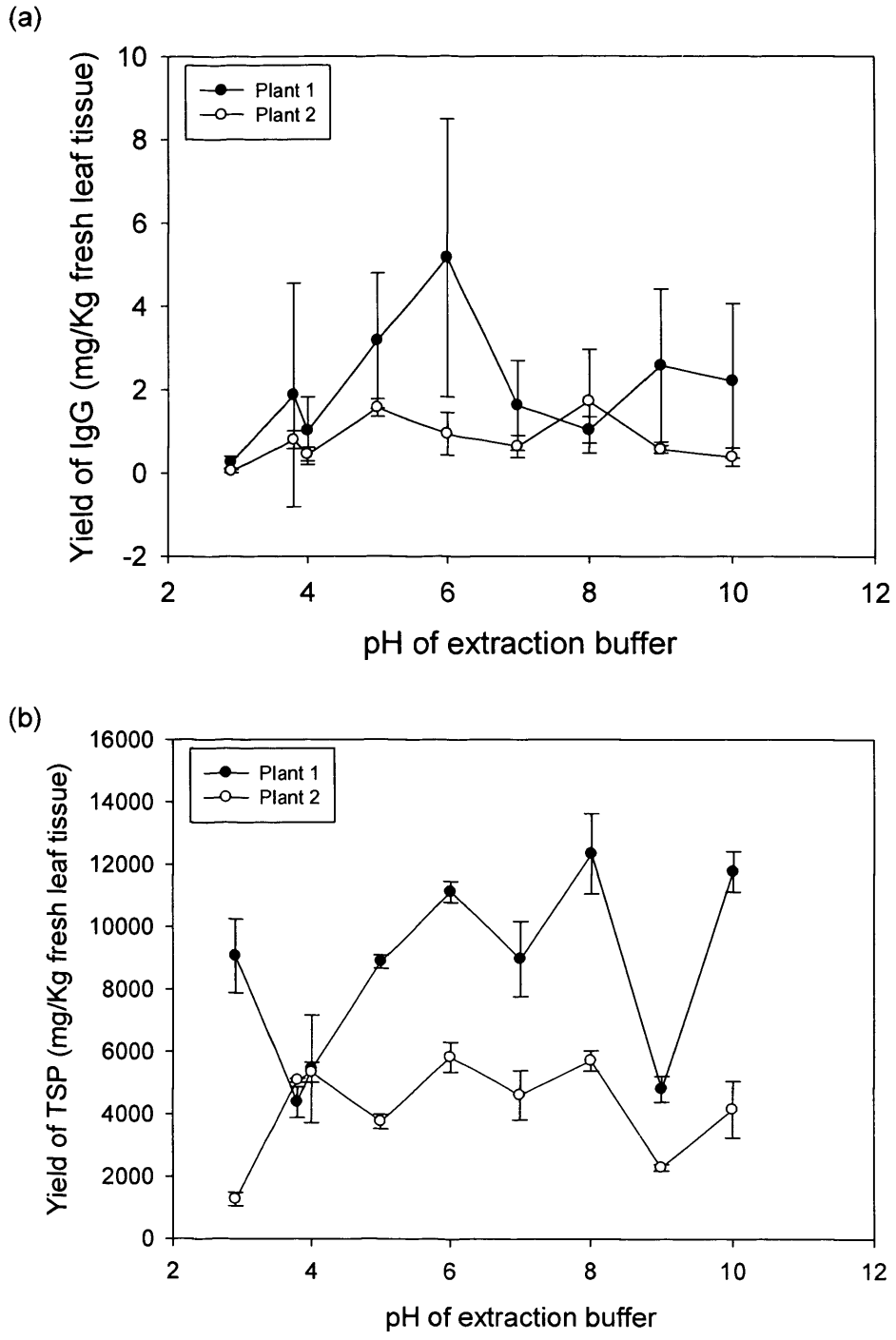

Figure 4.11 (a) Effect of pH on the extraction of mIgG from transgenic tobacco plants. Samples were extracted by grinding in buffers of different pH. 1% (v/v) Triton X-100 was included in the extraction buffer. Results are shown as milligrams of MAb per kilogram of fresh leaf tissue. (b) Effect of pH on the release of total soluble protein from transgenic tobacco plants expressing IgG-HDEL. Samples were extracted by grinding in buffers of different pH. Results are the mean ± standard error of the mean (SEM) of triplicate samples from two representative plants.

4.10 DISCUSSION

Having established the 3 transgenic plant lines, we investigated the use of different extraction techniques for each form of IgG. To date, there have been no detailed studies comparing extractability of either heterologous or native proteins that were targeted to different cellular locations in transgenic plants. The major factors to consider initially are 1) the tissue disruption technique and 2) the extraction buffer composition.

At laboratory scale the most common disruption technique for extraction of recombinant proteins produced in green tobacco leaf tissue is manual grinding in buffer with a pestle and mortar. High levels of active recombinant protein can be released quickly in this way, (Menkhaus *et al.* 2004a). However, the presence of vascular tissue in mature leaves can make grinding more difficult. Another widely used method at small-scale is to grind frozen leaves in liquid nitrogen to a dry powder and resuspend in an aqueous buffer for protein release (Blaszczyk *et al.*, 2002; Desai *et al.*, 2002).

Liquid nitrogen (that has a critical temperature of -146.9°C) is more commonly used for cryopreservation. Unlike freezing, crystallisation is avoided and instead vitrification occurs, during which water is solidified into an amorphous glass rather than a crystal (Storey and Storey, 2005). The glass encompasses all of the dissolved solutes in the water and consequently vitrified cells avoid any stresses associated with normal freezing, such as osmotic, ionic strength, or volume stresses (Storey and Storey, 2005). Grinding in liquid nitrogen was investigated in this Chapter, because it is currently, the second most commonly used method for recombinant or native protein extraction from transgenic leaf tissue. At small-scale, this involves freezing the leaves and grinding them to a dry powder in liquid nitrogen before putting them into an aqueous buffer environment for protein release (Blaszczyk *et al.*, 2002; Desai *et al.*, 2002). However, the use of liquid nitrogen is not a feasible option at large scale due to its hazardous nature. Grinding in liquid nitrogen is unlikely to be a feasible option at large scale due to high cost implications. In this study 5 other techniques or combinations of techniques were investigated.

It was not possible to directly determine IgG accumulation without first applying an extraction protocol for ELISA analysis. However, we have assumed that our "gold standard" (in this case grinding in buffer) was representative of the maximal extractable IgG. The results illustrated variation in the degree of extraction with the applied technique. Although there was plant-plant variability, the results were consistent for comparing different extraction techniques on the same individual plants.

It is important that the extraction step is successful in removing as much of the initial impurities as possible whilst recovering maximal amounts of antibody because application of a crude tobacco extract to a chromatography column is not feasible due to column fouling and plugging over extended use (Holler *et al.* 2008). If a crude extract was to be applied, this would necessitate the use of an intermediate scalable non-chromatographic step to clarify the crude extract, thus increasing the overall number of steps in the process which will be translated into lower overall product yields and higher costs (Jervis and Pierpont, 1989).

This study showed that for a recombinant murine IgG that is secreted and accumulates in the apoplast, dry freeze-thaw is a suitable technique for extraction from transgenic tobacco leaves in terms of yield and release of indigenous plant proteins. This could be a beneficial finding for processing, since it means that no mechanical shearing technique is required, and simply freezing the leaf discs at -20°C, and then adding buffer to thaw is sufficient. In addition to IgG yield, the level of contaminant plant proteins and other impurities released by the same step is also important. In order to simplify downstream processing, a high IgG yield is desirable with the least amount of contaminants. The purification profile in terms of IgG as a % of TSP, shows that less severe techniques of passive elution and dry freeze-thaw are more favourable for this form of IgG. Economically also, it is expected that freezing leaf discs pre-addition to buffer could help process scheduling and is most likely to be cheaper than an energy intensive mechanical breakage device.

It is apparent that leaf discs with a damaged edge ease the level of extraction. In order to imitate the cut surface area of the leaf discs (~0.31 cm^2) at large scale it is suggested that the leaves could be

shredded pre-extraction for example via an industrial tobacco shredding or cutting equipment (US patent 3659620, 3946954). It should therefore be borne in mind, that although the passive (non-grinding) extraction techniques were effective at laboratory scale, the leaf samples used had a high cut surface to volume ratio, which would need to be considered when scaling up to large scale purification from whole plants.

However, it is also clear that dry freeze-thaw is making a significant contribution to IgG release, since our observations have shown a significant difference in IgG released from passive elution and dry freeze-thaw. For the secreted form of IgG, passive elution is only capable of producing 60% of yields by dry freeze-thaw. For intracellular IgG-HDEL, however, passive elution can only produce 30% of the extractable yields by dry freeze-thaw. Even for the membrane-bound antibody passive elution produces about 50% of obtainable yields via dry freeze-thaw.

Unlike in our studies where, freeze-thawing is examined for its ability to release intracellular protein, as a possible extraction technique, most literature on this process to date has had the opposite purpose of trying to maintain the cell's viability under the inevitable freeze-thawing process that is often used for example, in strain preservation. In addition, within any process at pilot or large scale, freezing is often the step that precedes harvesting or protein recovery by cell disruption, as an efficient storage step. In fact, as the scale of production increases this required storage time is usually extended, making freezing instead of refrigeration a necessity. However, there have been some cases where freeze-thawing has been used for extraction instead of maintenance of cell viability, for example, for the recovery of intracellular products from yeast (Black, 1951) and other microorganisms (Koepsell, 1942).

The ability of cells to remain viable after freezing and thawing is thought to be determined by their physiological state prior to freezing. Park *et al.* (1997) investigated factors affecting survival of yeast cells during the freeze-thaw process. Before freezing, the process of "supercooling" occurs during which there is no loss in cell viability. However, as soon as the process of freezing begins, loss of viability becomes an exponential function of the freezing duration. The fact that yeast cell damage is an exponential function

of freezing suggests that there is an ongoing process affecting the cell's integrity that exists well beyond the time taken for the cell's surrounding medium to freeze and reach the external temperature (Park *et al.*, 1997). Prolonging the supercooling state at -20 °C was also found to have no effect on the viability of cells in the early-exponential growth phase during which the cells are most sensitive to freeze-thaw stress (Park *et al.*, 1997).

The thawing process may also cause cell damage. For example, oxidative stress may be caused by reactive oxygen species formed during the thawing process. However, Park *et al.* (1997) found that there was no difference in viability between thawing at room temperature and at 0 °C. Overall, freezing is thought to be the main cause of freeze-thaw damage.

Plant cells, like yeast, are eukaryotic cells, and thus are expected to behave quite similarly during freeze-thawing. The mechanism of cell damage during the freeze-thawing process is dependent upon the rate of freezing. At high freezing rates, intracellular freezing occurs resulting in cell damage due to ice crystal formation. At low rates of freezing, however, extracellular ice crystal formation predominates, causing the cell's membrane to become flaccid, leading to intracellular dehydration by osmosis towards the outside of the cell where, the concentration of water is comparably low (Figure 4.12). Freezing rate is determined by an individual cell's characteristics including its shape, structure, surface area-to-volume ratio, and membrane permeability.

Similarly to yeast cells, plant cells (from culture) were found to have a high resistance to freeze-thawing when the medium was supercooled to -20 °C, indicating that ice nucleation is a prerequisite for loss of viability in the freezing stage (Goldstein *et al.*, 1996). Thus it was concluded that ongoing loss of viability was due to external freezing leading to dehydration or intracellular ice formation and not simply as a result of the subzero temperatures (Park *et al.*, 1997).

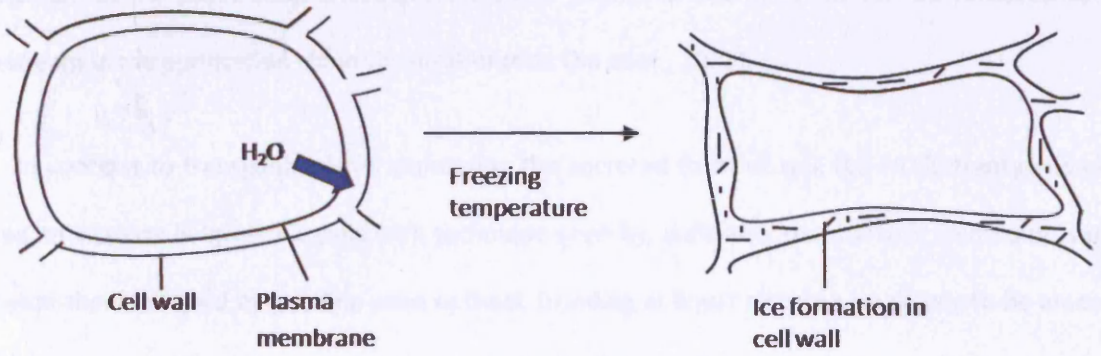

Figure 4.12: Ice crystal formation due to freezing (Adapted from Mazur, 1984).

The membrane is the primary site of damage caused by freezing. Cellular dehydration as a response to freezing results in the formation of membrane lesions. Freeze-induced dehydration causes the membrane structure to be altered, by bringing the plasma membrane into close apposition with membranes of organelles such the chloroplast, causing destabilisation of the membrane. The extent of cellular damage is determined by the freezing rate, the temperature at which the ice crystals form, and the subcellular location of freezing.

During the analysis of the purification burden data represented here as IgG as a % of total soluble protein, it is important to note that the impurities presented by the plant hosts do not consist solely of native proteins. Tobacco leaves consist of 10.3% cellulose, 9.5% organic acid, 8.1% protein, 5.2% potassium, 3.9% nicotine, 3.5% lignin (a phenolic compound), 3.2% calcium, 3.2% pectin, 2.8% amino acids, 2.1% nitrate, 1% solanesol, 0.8% phosphate, 0.7% magnesium, 0.6% nucleic acids, 0.4% ammonia, 0.3% starch, and 0.1% sugars (in wt %) (analysed for Burley tobacco, Torikaiu *et al.* 2005). These, non-protein contaminants need to be considered in further studies, since lipids can cause fouling of membrane filtration and carbohydrates may result in lower filtration rates and microbial growth (Azzoni *et al.* 2005). Additionally, phenolics and phytic acid may form complexes with proteins, or foul chromatography columns (Cheyran, 1980; Jervis and Pierpoint, 1989; Kusnadi *et al.*, 1998a) further

downstream in the purification chain. Nevertheless, phenolics and alkaloids can be removed further downstream in the purification chain via ultrafiltration (Xu *et al.*, 2002).

In contrast to transgenic plants expressing the secreted form of IgG, IgG-HDEL transgenic plants showed an increase in IgG-HDEL yield with technique severity, indicating that harsher techniques such as dry-freeze-thaw followed by grinding were optimal. Grinding in liquid nitrogen is unlikely to be amenable to scale up and considerable variability is introduced by the wet freeze-thaw process. Commercially, dry freeze-thaw followed by grinding probably represents the system of choice, because as with IgG, it offers potential solutions for storage before processing. The enhancement of antibody yield gained by the use of the –HDEL tag strategy needs to be balanced with the additional requirement for grinding during extraction in identifying an optimal strategy of producing IgG in plants.

Milburn *et al.*, (1994) investigated the effects of freeze-thawing recombinant and untransformed strains of Saccharomyces cerevisiae prior to disruption by either high pressure homogenisation or bead milling. The results of these studies showed that freeze-thawing pre-disruption caused the cells to become four times more resistant to homogenisation and twice as resistant to bead milling. It was found that this effect was independent of the time that the cells remained frozen.

For mIgG transgenic plants, there is a marked difference in antibody yield between the less severe techniques (passive elution, dry freeze-thaw and wet freeze-thaw), and the harsher techniques which all involve grinding. If immediate processing is possible, grinding in buffer would be chosen, however if storage pre-processing is required dry freeze-thaw pre-grinding is possible. In fact, it is possible to use both these techniques, depending upon the manufacturer's process scheduling. However, a major barrier is that the extraction of mIgG requires the addition of a detergent.

Despite the likelihood of a greater degree of damaging ice crystals per leaf surface area in wet freeze-thaw than dry freeze-thaw, the increase in absolute IgG yield is small in each (dry freeze thaw

produces about 91%, 87% and 83% of the wet freeze-thaw amount for IgG, IgG-HDEL and mIgG respectively).

Grinding samples on ice or at room temperature was found to have no effect on IgG yield for all three MAbs. Similarly, Khoudi *et al.* (1999) found that the MAb, C5-1 produced in alfalfa was 100% stable in crude extracts at room temperature. In their experiments, the transgenic alfalfa was ground in distilled water, and left for 2 hours at room temperature pre-analysis. This is encouraging, as it indicates that IgG is stable at room temperature, an obvious cost benefit at industrial scale.

A variety of aqueous extraction buffers have been reported in the literature. These buffer solutions can be complex, containing salts, detergents, reducing agents, and protease inhibitors. Some studies aiming at large-scale process development report the use of a few specific buffers, usually phosphate buffer, at pH 7.5, (Bai *et al.*, 2001; Balasurbramaniam *et al.*, 2003; Evangelista *et al.*, 1998; Yildirim *et al.*, 2002; Zhang *et al.*, 2001), which was the approach adopted in this study.

Non-ionic detergents are often used to extract membrane-bound proteins. The main effect of non-denaturing detergents is to associate with hydrophobic parts of membrane proteins, thereby conferring miscibility to them. They therefore act by solubilising the cell membrane, whilst leaving proteins intact. All detergent monomers have a hydrophobic tail and an uncharged hydrophilic head (Bhairi and Mohan, 2007). The hydrophilic head groups either consist of polyoxyethylene moieties as in the BRIJ® and TRITON® series of detergents or glycosidic groups as in octyl glucoside and dodecyl maltoside. At low concentrations of detergent, these become embedded within the lipid bilayer of the membrane, disrupting it slightly, however after the critical micelle concentration which is specific to the type of detergent, micelles form consisting of a mixture of detergent and lipid monomers. Non-ionic detergents confer miscibility to proteins by associating with their hydrophobic parts. Unlike ionic detergents, salts (or ionic strength) have minimal effect on the micellar size of the non-ionic detergents, but the critical micelle concentration (CMC) (defined as the lowest concentration above which monomers cluster to form micelles) of the detergent does increase significantly with rising temperature. The performance of non-

ionic detergents is dependent on several factors, including its concentration, ionic strength, alkyl chain length, pH, purity, temperature, and the presence of organic additives (Bhairi and Mohan, 2007).

At concentrations below the critical micelle concentration (CMC), detergent monomers bind to water-soluble proteins. Above the CMC, binding of detergent to proteins competes with the self association of detergent molecules into micelles. Consequently, there is effectively no increase in protein-bound detergent monomers with increasing detergent concentration beyond the CMC. Triton X-100 has a CMC of approximately 0.015%. This may explain why beyond this concentration (tested here as 0.1% v/v), there is no longer an increase in IgG yield for most forms of IgG.

As expected, and has been shown before for another non-ionic detergent, NP40, (Vine *et al.*, 2001), mIgG yield increased with detergent concentration, with a statistical significant increase (at 90% confidence levels) in IgG yield per gram of fresh leaf tissue or IgG as a % of TSP (at 95% confidence levels) between 0 and 0.1% (v/v) detergent concentrations.

For IgG located and targeted to the apoplasm, detergent concentration had no effect on absolute IgG yield, but there was a significant drop in IgG as a % of TSP as detergent concentration was increased indicative of the increasing release of contaminant proteins with increasing detergent dosage. This was reflected by an increasing green colour of the supernatant, indicating that more chlorophyll was also being co-extracted with the IgG. Thus, unlike for the membrane-bound IgG, it is a clear disadvantage to add detergent for extraction of the native form of IgG.

For IgG-HDEL like mIgG, there was a significant increase in MAb per unit mass of fresh leaf tissue between 0 and 0.1% (v/v) Triton X-100 with a 2-fold increase at the higher detergent concentration. On the other hand, IgG-HDEL as a % TSP profile was the same for extraction in 0% or 0.1% (v/v) Triton X-100, as a result of more total soluble protein being released with increasing detergent concentration. However, since MAb yield is likely to be more important for processing than limiting the initial amount of co-extracted impurities, there is a favourable case for the inclusion of detergent for the extraction of this form of the MAb.

Nevertheless, although detergent may aid IgG-HDEL extraction it is not a necessity as it is for the membrane-bound form, mIgG. This can be explained, as membrane-bound IgG has a hydrophobic transmembrane-spanning region (26 amino acids) which causes the protein to be anchored in the similarly hydrophobic cell membrane. The protein becomes inserted into the membrane as it is being translated and, crucially, this is not normally a reversible process because the energy requirement is too great to release the hydrophobic transmembrane domain from the membrane into the aqueous environment. However, adding detergent solubilises the membrane. Thus, instead of the protein remaining as part of the lipid bilayer it is, instead, incorporated into detergent micelles, thus extracting the protein from the membrane.

In contrast, HDEL-tagged protein resides in an aqueous environment (the ER) and is not membrane-spanning. The mechanism by which an HDEL-tagged protein is kept in the ER is via a specific ER membrane-bound receptor. The binding of an HDEL-tagged protein to the HDEL receptor is dependent upon achieving the right conformational environment within the ER (Tang *et al.*, 1992), and mechanical disruption of plant cells is sufficient to release the IgG-HDEL. The increase in yield of IgG-HDEL at 0.1% Triton X-100 may be reflected by the fact that although this MAb is not bound in the membrane, it is intracellularly retained in the ER, meaning that the plasma membrane barrier needs to be disrupted to release the protein, unlike the native form of IgG which is easily accessible from the apoplasm (external to the plasma membrane).

A complication of the inclusion of detergent in an extraction process is the necessity to remove it during the manufacturing purification process. Contrary to other detergents that can be removed from the recombinant protein by dialysis or gel exclusion chromatography on Sephadex G-25 (Horowitz *et al.* 1985), Triton X-100 cannot be removed in this way because it forms such large micelles (Horowitz *et al.* 1985). Nevertheless, this commonly used detergent at large scale can be removed by ion exchange chromatography. If however dialysis or gel filtration is desired over ion exchange chromatography, Octyl ß-Glucoside and Octyl ß-Thioglucopyranoside are alternative nondenaturing, non-ionic, dialyzable detergents.

However, another disadvantage of the addition of detergent is the simultaneous release of the phospholipid membrane in addition to lipids that act to compartmentalize various sections of a cell, in turn releasing other intracellular contaminants (Maire *et al.*, 2000). This is evident in the increasing green colour of the solution indicating the extra release of chlorophyll with increasing detergent concentration. Lipid removal is desired prior to protein purification processing to decrease non-specific fouling of downstream chromatographic matrices or ultrafiltration membranes. Thus, it is preferable to avoid the inclusion of detergent in processes, if possible.

Most studies have found that the addition of salts, detergents, and protease inhibitors can all affect protein extraction, but pH appears to be the major factor (Balasubramaniam *et al.* 2003). The pH study on IgG showed that with the exception of very low pHs of 3, and 4, there is a wide variety of usable pHs i.e. from 5 to 7. There could be several reasons for the very low levels of IgG at pH 3-4. Gore *et al.* (1992) found that fusion proteins of IgG were unstable in phosphate buffer at pH values <5.5. In addition, there is a possibility that IgG unfolds and then aggregates at this low pH. Vermeer *et al.* (2000) observed that for IgG, F_c fragment was most sensitive to low pH (pH 3.5, in glycine buffer). They found that these transitions were independent and the unfolding was followed immediately by an irreversible aggregation step. However, since our results show that both extractable levels of IgG and total soluble protein are low at pH 3 and 4, it is also a possibility that the applied low pH buffer is causing these proteins to co-precipitate with native proteins. Pulatov *et al.* (1978) observed the maximum precipitation of protein (derived from cotton-plant treated with 5% ammonium chloride) at pH 3-3.5, with 90% of the dissolved protein substances precipitated.

Since a protein's solubility is at its minimum at its isoelectric point (p*I*) when it carries no net charge, it is less likely to be extracted when the buffer pH is at or near its p*I*. This work demonstrates that simple extraction using phosphate buffer maintained at pH 5.0 is efficient for extracting the recombinant antibody. This corroborates the claim of Larrick *et al.* 2001 that low cost salt buffers with one or two additives are efficient in protein extraction. For these studies, all pH buffers had the same ionic strength, since ionic strength has been shown to have a significant effect on protein partioning (Asenjo *et al.*,

1994). In addition, two different buffer systems were included at pH 6.0, i.e. citrate and phosphate buffer systems, which generated similar IgG yields, demonstrating that the buffer system itself was not an important factor for IgG extraction.

Most plant proteins were extracted at pH 7 and there is a significant reduction at pHs 5-6 and 8-9. This is consistent with previous findings (Balasubramaniam *et al.* 2003), who also found that most of the co-extracted native proteins in tobacco were acidic. In fact this is thought to be mainly due to ribulose 1,5 bisphosphate carboxylase-oxygenase (Rubisco), (the chloroplast storage protein) which is responsible for greater than 25% of the total protein, and about 50% of the total chloroplast protein (Garger *et al.*, 2000; Shewry and Fido, 1996).

It has previously been shown that increasing buffer pH increases the extractability of total soluble protein from transgenic corn, most likely due to the fact that most water-soluble corn proteins have a p*I* around 5.0 (Azzoni *et al.* 2002). A similar study of the extraction of aprotinin from transgenic corn seeds, found a sudden drop in yield at pH 8, which was reported to be similar to the protein's pI (Azzoni *et al.* 2002, Zhong *et al.*, 1999). This phenomenon was explained by the effect of the pH on the extracellular microenvironment, where most of the aprotinin accumulated. The data here for tobacco suggests that at commercial scale, it would be unfavourable to use very low pH conditions of pH 3 and 4, however, the optimum pH is 5.0 for highest IgG yield and lowest amount of native protein.

This study has shown that the specific IgG target location in the tobacco leaf cell has an important impact on the determination of an optimal extraction procedure, which needs to be considered in developing production strategies. Here we considered some of the main requirements for extraction for each targeting strategy, but we do not make the comparison between different transgenic plants expressing different antibody variants (i.e. IgG versus IgG-HDEL versus mIgG) because as yet, the highest expresser amongst these is unknown.

The use of simple methods was a deliberate decision as simple techniques are the easiest to emulate at large scale, and are usually more economical than complicated techniques. Although, grinding

in buffer or liquid nitrogen are commonly used techniques in the laboratory, freeze-thawing leaf discs dry or within buffer, and "passive elution" are novel techniques which have not previously been discussed in the literature. In fact all prior literature have assumed that it is necessary to cause maximum physical damage to leaf tissue by manual grinding, or mechanical shearing for example using milling equipment (e.g. Fitzmill Comminutor, Valdés *et al.* 2003). It is assumed that this would release the maximum amount of antibody. However, there are several reasons why such harsh methods should not be used. Firstly, there is the economical dimension in terms of operating costs of such mechanically intensive equipment. Secondly, increased shearing will result in increased contaminant release, increasing the purification burden, possibly resulting in lower overall product yields and higher overall downstream costs. Thirdly, the complete mulching of leaf tissue will generate a high degree of fibre that will inevitably foul chromatographic columns, and filtration membranes (Menkhaus *et al.*, 2004a; Holler *et al.*, 2007). In addition, the overall viscosity of the liquid material, would decrease its flowrate through pipes (necessitating the use of more energy intensive and hence more expensive pumps). Lastly, we sought to utilise gentler techniques, since there is evidence that increased air-liquid interfaces generated by high shear forces can cause significant damage to proteins in solution (Thomas *et al.*, 1979; Virkar *et al.*, 1981; Narendranathan and Dunnill, 1982). Thus, the ability to use gentle techniques such as dry freeze-thaw to extract the MAb are likely to be welcomed by process engineers.

It is a significant finding that a non-mechanical extraction method may be applicable at large scale for extraction of the secreted form of IgG, since this may offer economic savings at this initial stage of downstream processing. Furthermore, the application of preliminary ultra-scale down techniques for large scale processing optimisation is essential in order to save time and costs (Boulding *et al.*, 2002; Lee *et al.*, 2002; Neal *et al.*, 2003).

4.11 CONCLUSIONS

Optimal extraction technique varied with target location of IgG in the plant cell, and the dependence of antibody yield on the physical extraction methodology employed, the pH of the extraction buffer, and the extraction temperature, was demonstrated in each case. Addition of detergent to the extraction buffer may improve yields, but this was also found to be dependent on the IgG's site of accumulation within the plant cell.

We have demonstrated that the initial targeting strategy has a strong influence on extraction strategy, and thus also on the subsequent purification chain. These findings will therefore help to inform the decision making process for the production of MAb from transgenic plants, which will ultimately depend on multiple factors. These will include the overall levels of MAb accumulation, extractability, purification burden and the desirability of peptide or polypeptide tags in the final product.

Chapter 5- Harvesting strategies for monoclonal antibodies from transgenic tobacco plants

5.1 INTRODUCTION

One of the main issues that is often overlooked in the production of pharmaceuticals in transgenic plants is harvesting. Fresh tobacco tissue offers more harvesting challenges in comparison to dry seed crops, because of the considerations arising from handling fresh wet tissue. Thus, there is a need to carry out the harvest and processing procedure quickly. Another harvesting consideration, in a biopharmaceutical production setting, is that in order to meet biosafety requirements for the prevention of cross-pollination or gene-flow, the tobacco plants are not likely to be allowed to flower in order to meet containment requirements. This will probably require the harvesting of leaf tissue before plants are mature enough to flower, or cutting flower tops as soon as they form. In terms of practice, contrary to traditional tobacco, manual methods of harvesting are unlikely to be suitable for transgenic tobacco which, are more likely to require mechanical harvesting (Kostandini *et al.* 2006). An example of a mechanical method of harvesting, used in both plantbeds and greenhouses is "clipping" which involves the use of a mower to remove the top section of the plants (Whitty, 2006).

The objective of this Chapter is to address the main questions of harvesting that need to be considered including when to harvest and which part of the plant to harvest. These harvesting factors are investigated at small-scale for the production of a secreted IgG and the HDEL tagged endoplasmic reticulum retained form of this IgG in transgenic tobacco.

5.2 WHEN TO HARVEST?-YOUNG VERSUS OLD PLANTS AND THE IMPORTANCE OF SENESCENCE

At large scale it is likely that all (or most) of the leaves of a plant will be harvested together. Thus, leaves were simultaneously extracted from top, middle and bottom leaves, as in the extraction experiments described in Chapter 4, in order to compare overall variation in IgG expression with plant age. Figure 5.2 compares young (4 weeks from germination) and old plants (18 weeks from germination) for extractable levels of secreted IgG (Figure 5.1).

Figure 5.2 shows the difference in IgG yield between young and old plants. The result shows that the young plants express the secreted IgG to 31mg/Kg fresh leaf tissue, i.e. approximately 6X greater than the old plants (5mg/Kg fresh leaf tissue) when extraction is performed by grinding in buffer. Extraction by passive elution gave a similar result (13mg/Kg fresh leaf tissue for the young plant and about 4mg/Kg for the old plant).

(a)

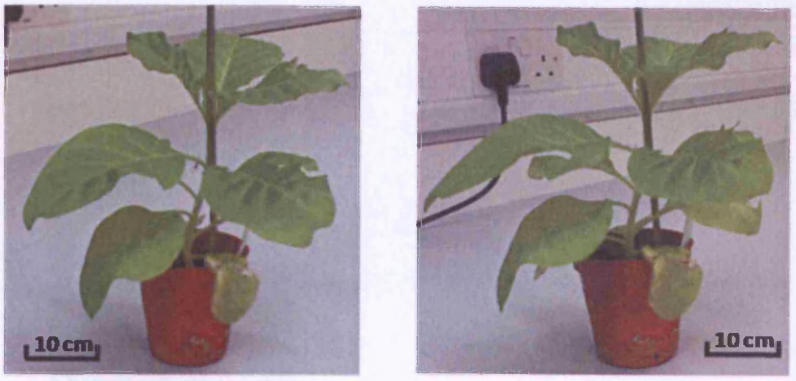

(b)

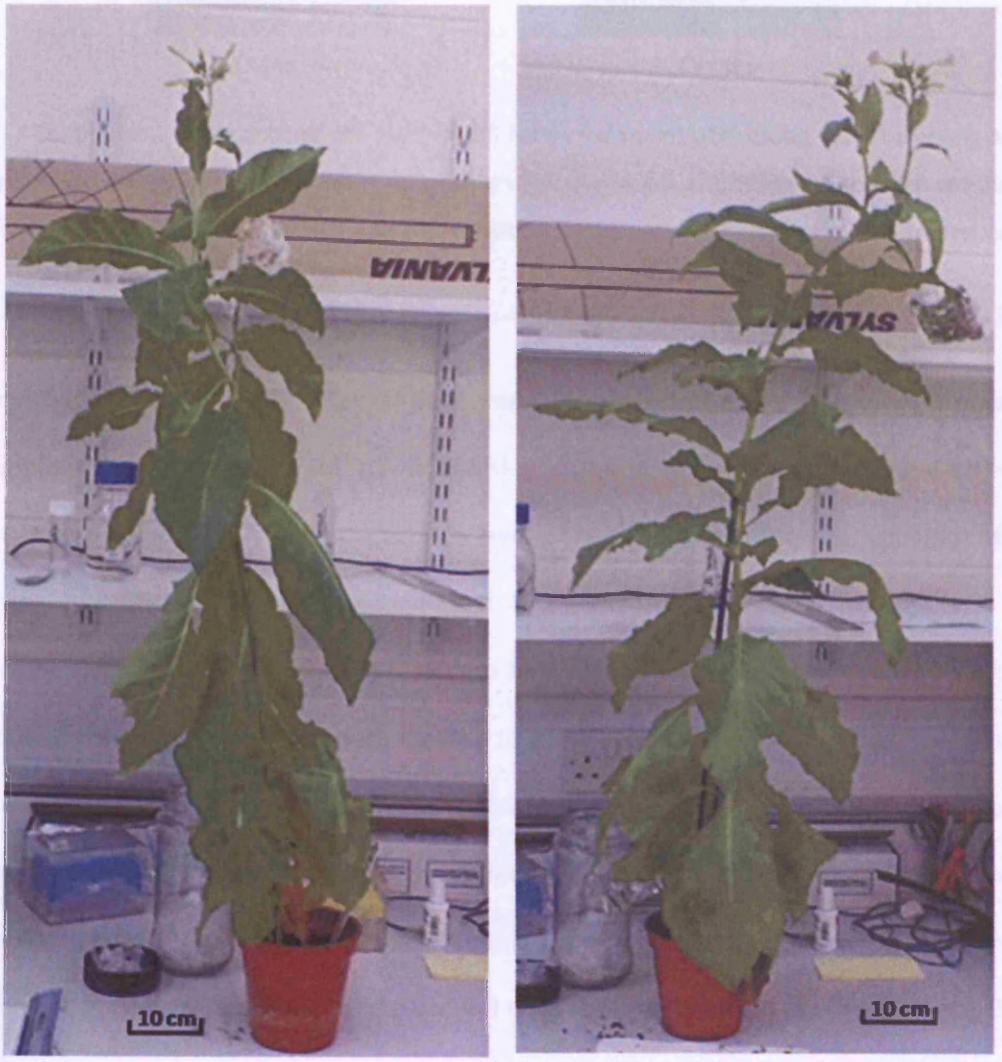

Figure 5.1 (a) Young transgenic *Nicotiana tabacum* plants (~ 2-4 weeks old) expressing IgG-HDEL in soil (b) Old transgenic *Nicotiana tabacum* plants (~ 16-18 weeks old) expressing IgG-HDEL in soil.

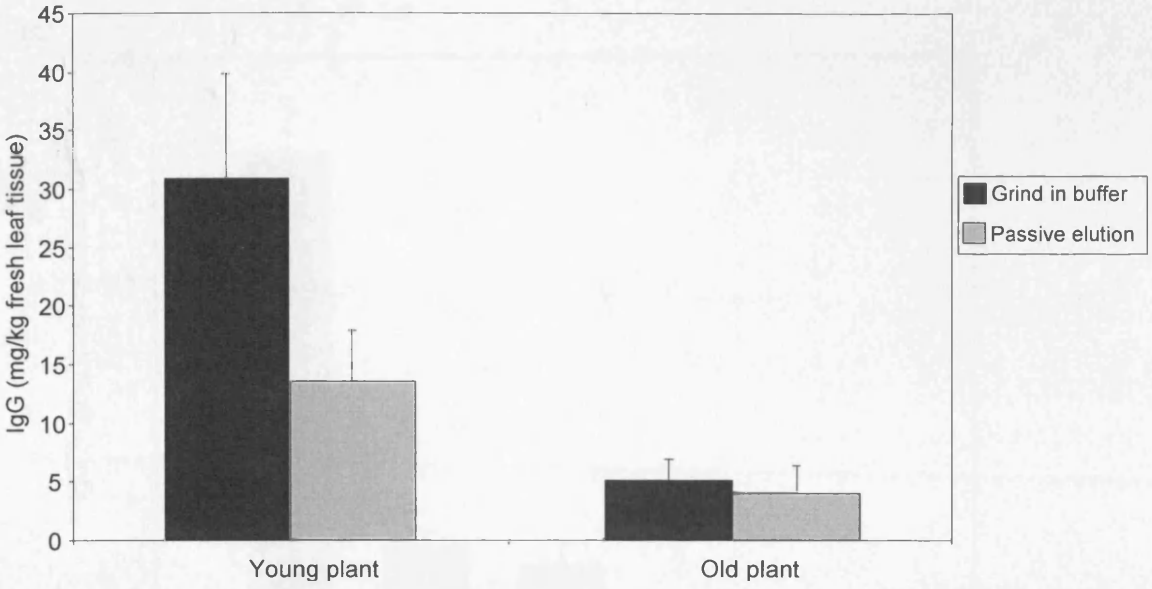

Figure 5.2 Comparison of the extractable yield of IgG (secreted form) with plant age. The young and old plants were approximately 4 and 18 weeks old respectively. (Averages and SEMs represent 4 old plants and three young plants). (1% Triton X-100 was included in the extraction buffer in this analysis).

This result was confirmed in a further experiment, investigating a wider range of plant ages. For plants expressing the secreted form of IgG, it was shown that recoverable IgG (secreted form) is age-dependent (Figure 5.3a). The highest extractable level of IgG is derived from the youngest plants, i.e. plants that are approximately less that 2-4 weeks old. There was then a 10 fold drop in IgG level as plants reached approximately 4-7 weeks (21 to 40 cm in height) and this IgG level was maintained at 7-11 weeks (41 to 60 cm) in height), followed by another 10 fold decrease in IgG from 61 to 90 cm (about 11-16 weeks old). The lowest IgG levels are seen in oldest plants (post-flowering), i.e. in 11-16 week old plants (from germination). Figure 5.3b shows the variation in IgG as a % of total soluble protein with plant age. There was a significant change in leaf total soluble protein per fresh weight of leaf tissue with age, and this is reflected in the decrease in IgG levels and increase in purification burden with age. The same experiment was prepared in IgG-HDEL-transgenic plants (Figure 5.4). Surprisingly, the extractability of IgG-HDEL was approximately constant with plant age (for the age range of about 2 to 18 weeks).

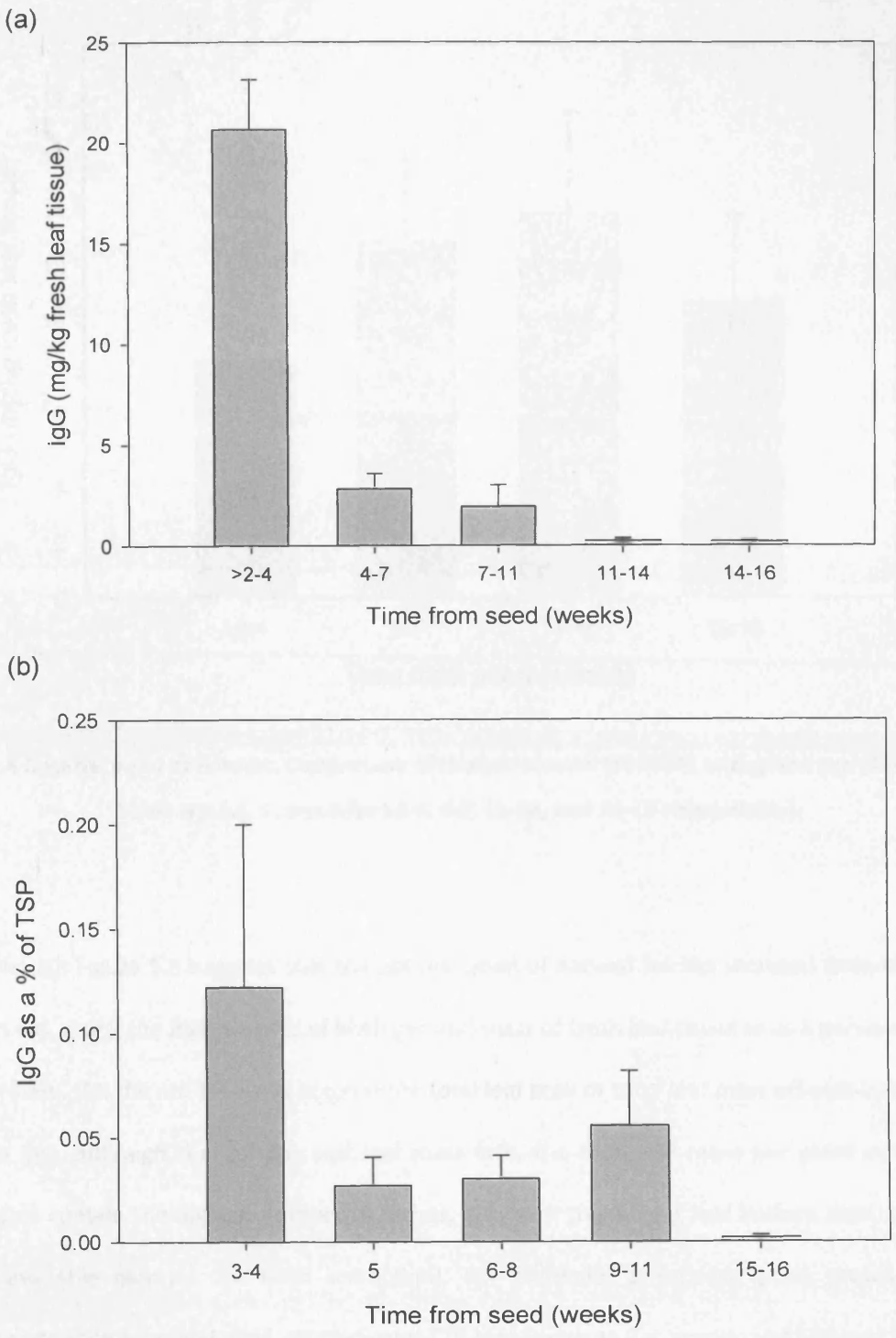

Figure 5.3 Optimal point of harvest. Comparison of the extractable IgG (secreted form) and total soluble protein (TSP) with plant age. (a) IgG (Averages and SEMs are of 28, 13, 8, 9, and 25 plants for time ranges of >2-4, 4-7, 7-11, 11-14, and 14-16 weeks respectively) and (b) TSP (representative of the purification burden). (Averages and SEMs are of 3, 5, 5, 4, and 3 plants for time ranges of 3-4, 5, 6 to 8, 9-11, and 15-16 weeks respectively).

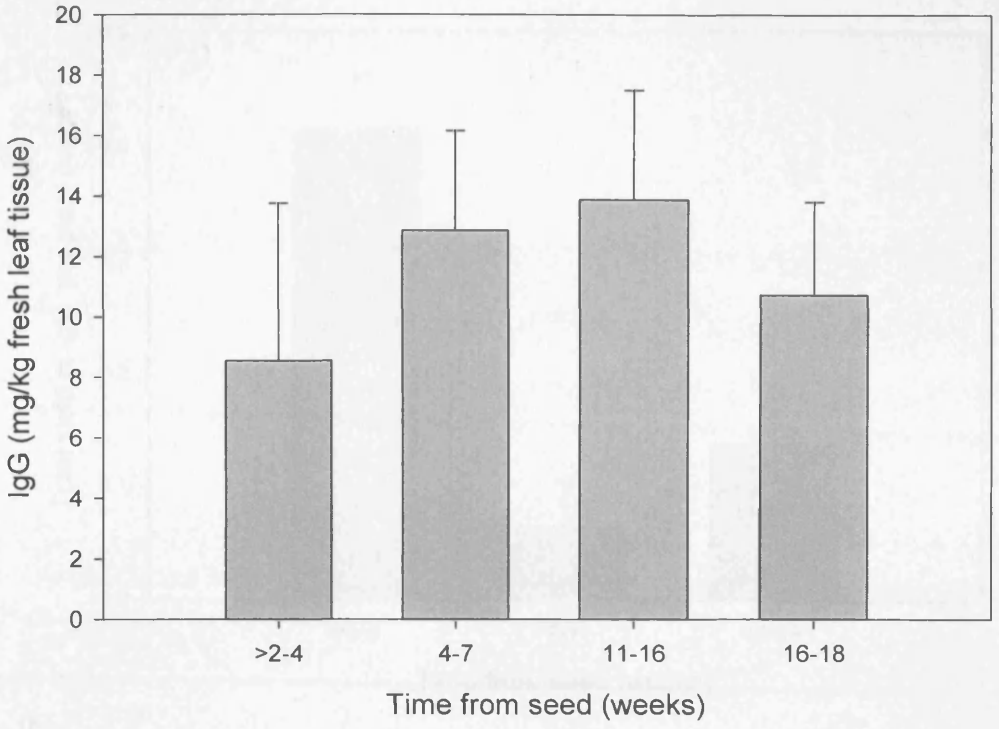

Figure 5.4 Optimal point of harvest. Comparison of the extractable IgG-HDEL with plant age (Averages and SEMs are 4,6, 5, and 8 for >2-4, 4-7, 11-16, and 16-18 respectively).

Although Figure 5.3 suggests that the optimal point of harvest for the secreted form of IgG was at 2-4 weeks old, giving the highest yield of MAb per unit mass of fresh leaf tissue or as a percentage of total soluble protein, this did not take into account the total leaf area or total leaf mass offered by the plant. As the plants age, although the IgG per unit leaf mass falls, the total leaf mass per plant increases. (The tallest plants contain the highest number of leaves, also with the largest leaf surface area, and thus the greatest available biomass for MAb extraction). For example, a tobacco plant grown under our greenhouse conditions would yield approximately 20 g of leaves at 2-4 weeks, and 600 g of leaf biomass at 16-18 weeks (Julian Ma, personal communication), and measurements of a single 36 cm plant in this study (i.e. 6-7 weeks old) gave a total leaf biomass of about 28 g. Based on this, estimates of absolute IgG yield per plant in milligrams was calculated for IgG and IgG-HDEL expressing plants (Figure 5.5a and b respectively).

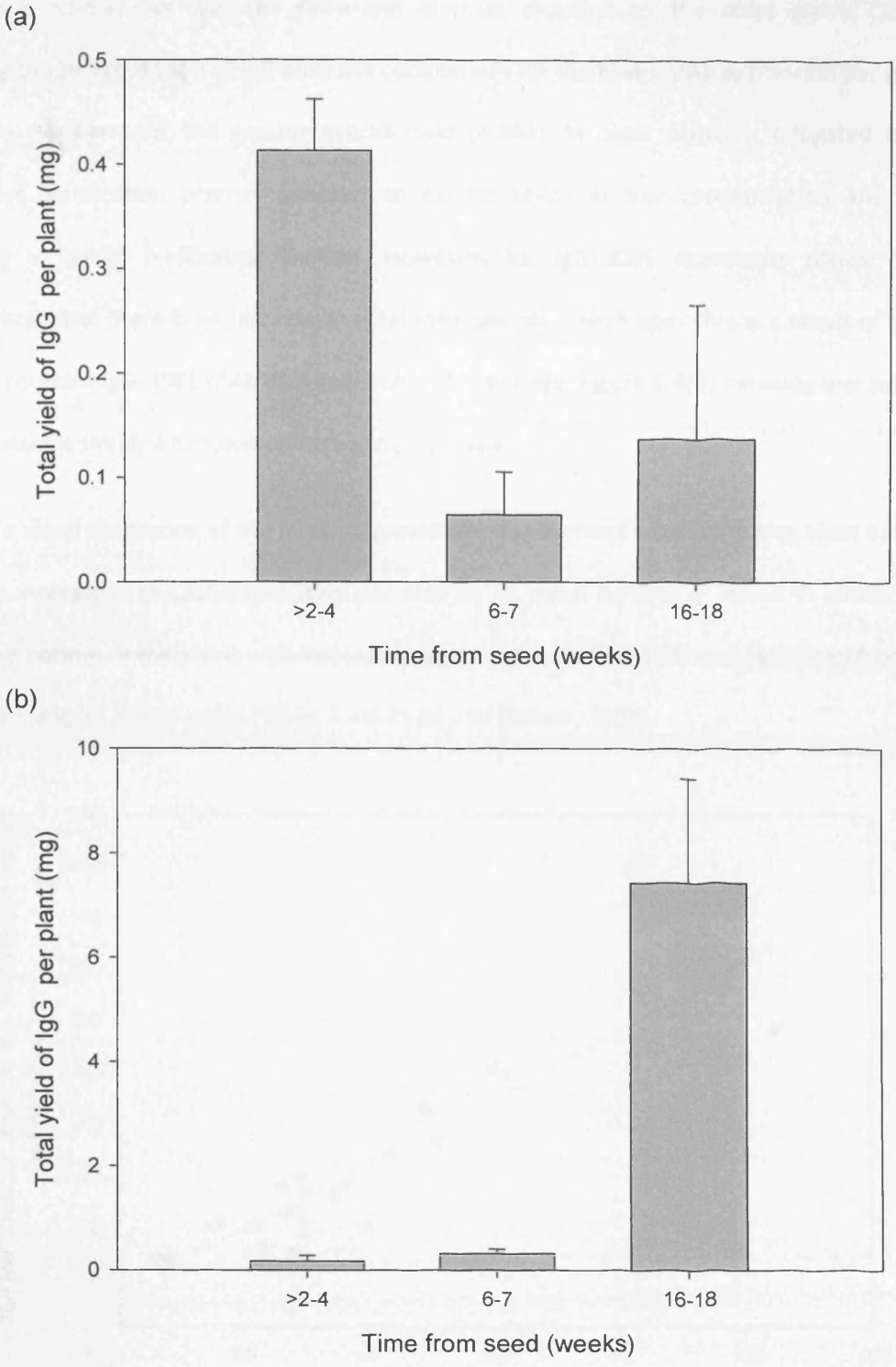

Figure 5.5 Estimated total extractable IgG per plant with plant age. (a) IgG (secreted form) (Averages and SEMs are of 28, 4, and 7 plants for time ranges of >2-4, 6-7, and 16 to 18 weeks respectively) and (b) IgG-HDEL (Averages and SEMs are 4, 4, and 8 for >2- 4, 6-7, and 16-18 respectively).

Figure 5.5a shows that the extra leaf biomass provided by the older plants (16-18 weeks) expressing the secreted form of IgG does not compensate for the lower MAb expression per gram of fresh leaf tissue. Furthermore, the greater overall yield of MAb in older plants is mitigated by the more complicated purification process required to extract MAbs at low concentration and from fluids containing a higher purification burden. However, for IgG-HDEL expressing plants, Figure 5.5b demonstrates that there is an increase in total MAb per plant with age. This is a result of the fact that there is a constant IgG-HDEL MAb accumulation with plant age (Figure 5.4b), meaning that total IgG-HDEL yield per plant is simply a function of increasing plant age.

As a visual illustration of the increasing available leaf biomass with increasing plant age, Figure 5.6 shows the increase in the estimated total leaf area for an equal number of leaves (3 located at the top, middle and bottom of the plant) with increasing plant height. Leaf area (A) was estimated from the length of the leaf blade (L) and its width (W) as A = 0.75 x L x W (Schurr, 1997).

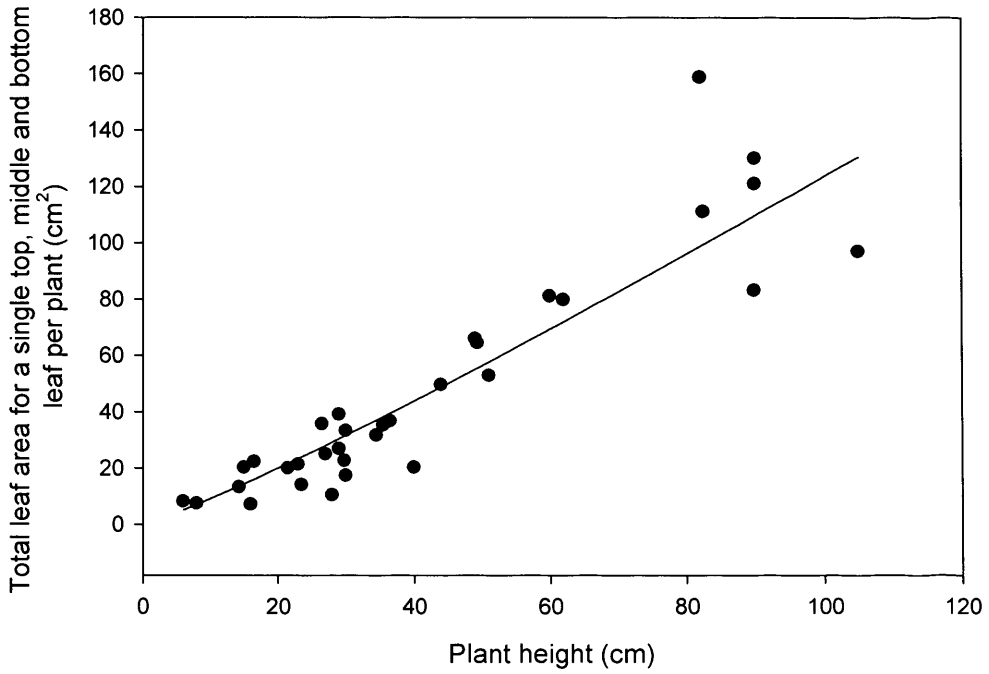

Figure 5.6 Available leaf area with plant height. Estimated total leaf area for 3 leaves located at the top, middle, and bottom of the plant, with increasing plant height for plants expressing the secreted form of IgG. (Leaf area was simply estimated as a product of the height and width of the leaf, multiplied by a coefficient of 0.75). (A power curve has been drawn through the data, as a line of best fit, $R^2 = 0.83$).

5.3 WHICH PART OF THE PLANT TO HARVEST? - A COMPARISON OF IgG LEVELS IN TOP, MIDDLE AND BOTTOM LEAVES

In light of the findings that plant age and wounding were important factors in IgG yield, the IgG yield from leaves at different positions in the plant were investigated. For old plants (all of which were over 60 cm in height) (Figure 5.7) there was a significant difference in recoverable IgG levels between the top, middle and bottom leaves. This figure shows IgG variation with approximate height for the same plants and indicates that on average the middle and bottom leaves have only a third and a fifth of the IgG per unit mass of fresh leaf tissue present in the top leaves respectively.

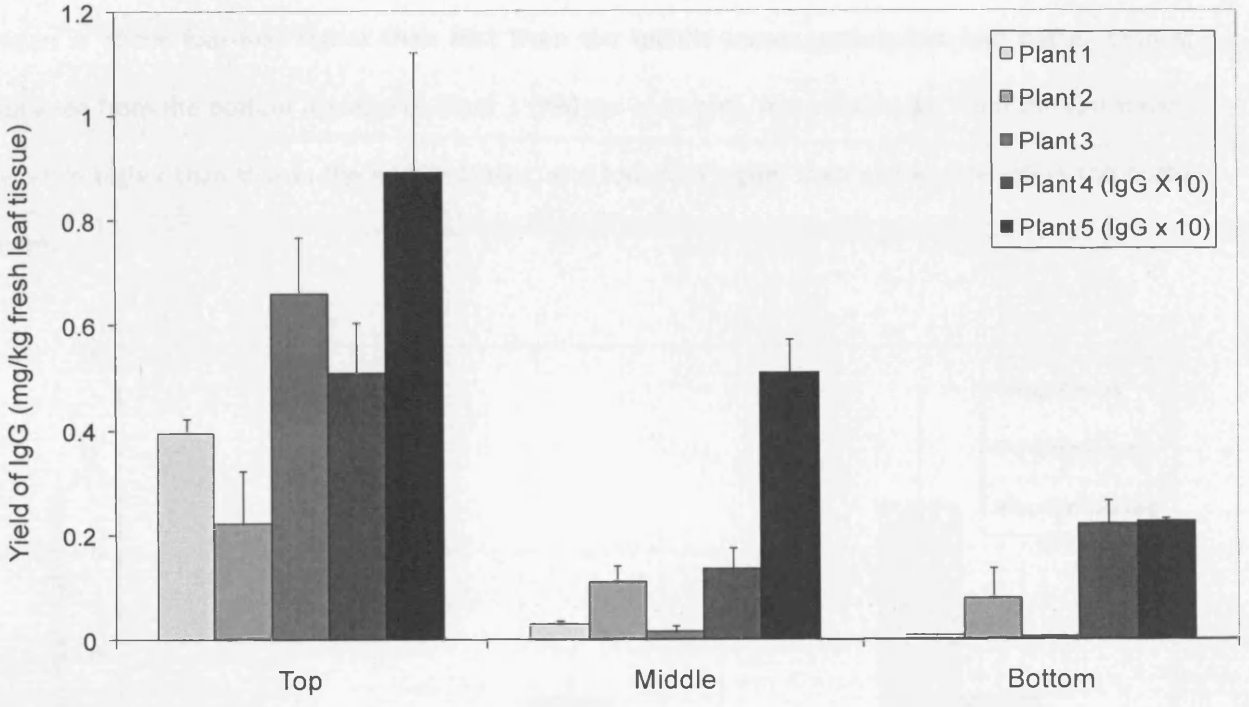

Figure 5.7 Effect of leaf age within a plant on extractable level of IgG. Comparing IgG extracted per gram of fresh leaf tissue from the (a) top, (b) middle and (c) bottom of the plant. Data is shown for 5 different plants (15-18 weeks old from seed) expressing the secreted form of IgG. (Averages and SEMs are of triplicate values). (Plants 4 and 5 had 10 times the IgG yield displayed here).

Figure 5.8 shows data that comprises three findings in 3 plants of different ages. For plants expressing the secreted form of IgG, the top leaves had a significantly higher IgG than the middle and

bottom leaves of the same plant. In these experiments, 2 leaf discs were harvested, from 2 leaves at the same height level, but with their leaf tips pointing horizontally in opposite directions. Figure 5.8 clearly shows that the top leaves express greater amounts of the secreted IgG than the middle leaves, which in turn express more IgG than the bottom leaves. It should be noted that similar levels of IgG are observed in top and middle leaves of plants that are only 30 cm in height, since at this total height level there is little distinction between the top and middle portions of the plant. However, a significant reduction is seen for the bottom leaves of this plant, with these leaves only possessing a third of the IgG level in the top or middle leaves. For plants that are over 85 cm there was a significant drop in IgG in the middle and bottom leaves relative to the top leaves: For plant 2 (~85 cm in overall height), IgG recovery from the top leaves is about four-fold higher than that from the middle leaves, and is two-fold higher than IgG obtained from the bottom leaves; For Plant 3 (~90 cm in height), recoverable IgG from the top leaves is two-fold higher than that in the middle leaves, and four-fold higher than extractable IgG in the bottom leaves.

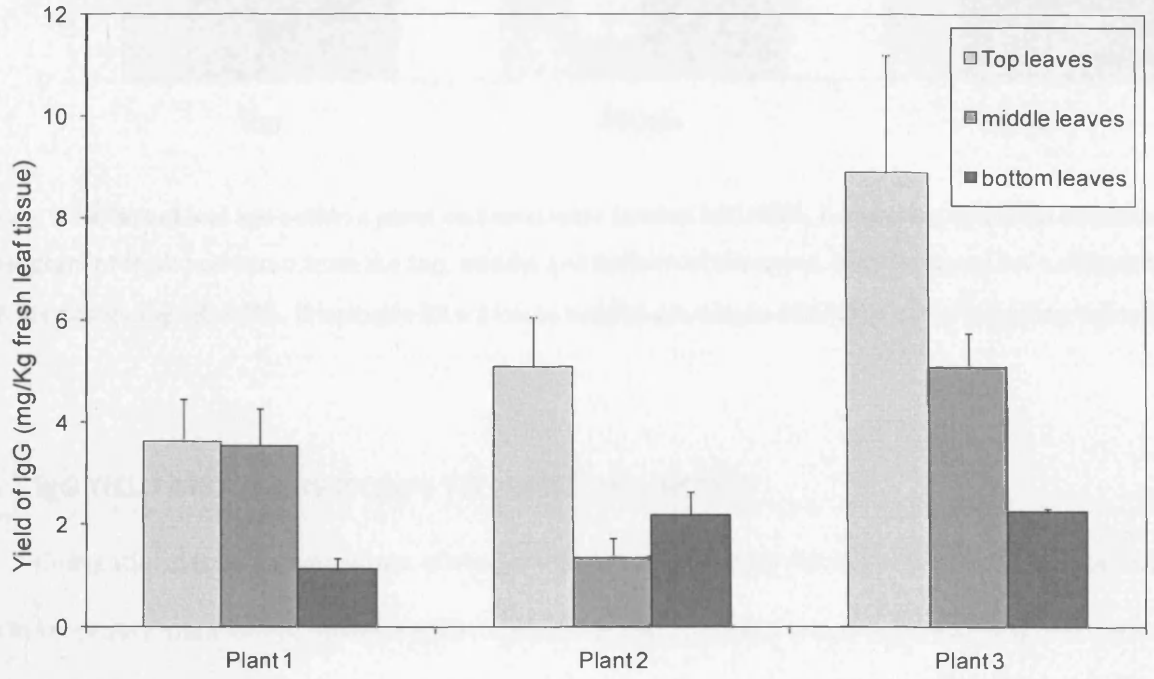

Figure 5.8: Comparing IgG in top, middle and bottom leaves of plants expressing IgG (secreted form). Plants heights are approximately 30, 85 and 95cm for plants 1, 2 and 3 respectively. Averages and SEMs are of triplicate samples.

For IgG-HDEL expressing plants however, (Figure 5.9), there was no clear difference in IgG expression with leaf position within the plant. On average, the middle leaves have 1.1 times the IgG yield per gram of fresh leaf tissue of the top leaves and the bottom leaves have an average of 1.5 times the IgG yield of the top leaves, and no clear trends are seen.

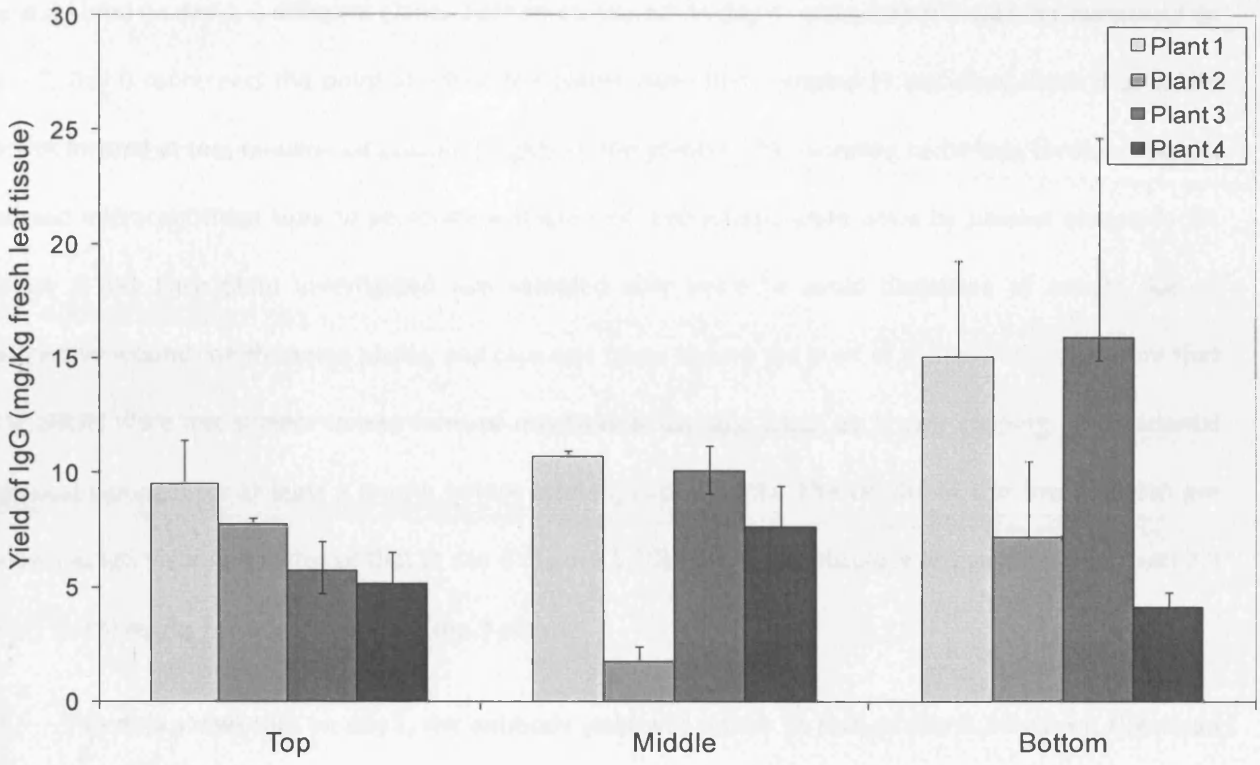

Figure 5.9 Effect of leaf age within a plant on extractable level of IgG-HDEL. Comparing IgG-HDEL extracted per gram of fresh leaf tissue from the top, middle and bottom of the plant. Data is shown for 4 different plants expressing IgG-HDEL. (Plants are 82 ± 5 cm in height). (Averages and SEMs are of triplicate values).

5.4 IgG YIELD AND THE RESPONSE TO PLANT WOUNDING

Conventional tobacco agriculture allows plants to grow intensely for optimal harvest of large leaves rich in secondary metabolites. Having demonstrated that this approach would not be appropriate (at least for secreted IgG), the next objective was to determine if repeated harvesting (clipping) of young plants might maximise the yields from individual plants.

Plants expressing IgG (secreted form)

The IgG levels (expressed as mg per unit mass of fresh leaf tissue) from different plants expressing the secreted form of IgG, were measured at different intervals after initial sampling. From a total of nine young plants <2 weeks from germination (16 ± 5 cm) all measured for MAb yield at day 0, 3 plants were re-measured on day 1, 3 different plants were re-measured on day 4, and another 3 were re-measured on day 6. Day 0 represents the point at which the plants were first sampled (3 leaf discs, from 3 different leaves located at top, middle and bottom heights of the plants). The sampling technique involved using a capped microcentrifuge tube to perforate a single leaf. Extractions were done by passive elution in 1% Triton X-100. Each plant investigated was sampled only twice to avoid distortion of results due to successive wounds on the same plants, and care was taken before the start of experiments to ensure that the plants were not subject to any form of mechanical damage (such as flower topping, or accidental physical damage) for at least a month before starting experiments. The results of this investigation are shown as IgG yield as a factor of that in day 0 (Figure 5.10). The mean absolute IgG yield at day 0 was 7.9 ± 1.3 (SEM) mg/kg fresh leaf tissue for the 9 plants.

This data shows that on day 1, the antibody yield was similar to that on day 0. However, the mean IgG level at day 4 decreased by less than 50%, and by about 70% at day 6. The results suggest that there is a progressive decrease in secreted IgG yield in response to the first sample on Day 0. There are a number of potential reasons for this "wounding response". These include a decrease in IgG synthesis and/or an increase in degradation of accumulated IgG.

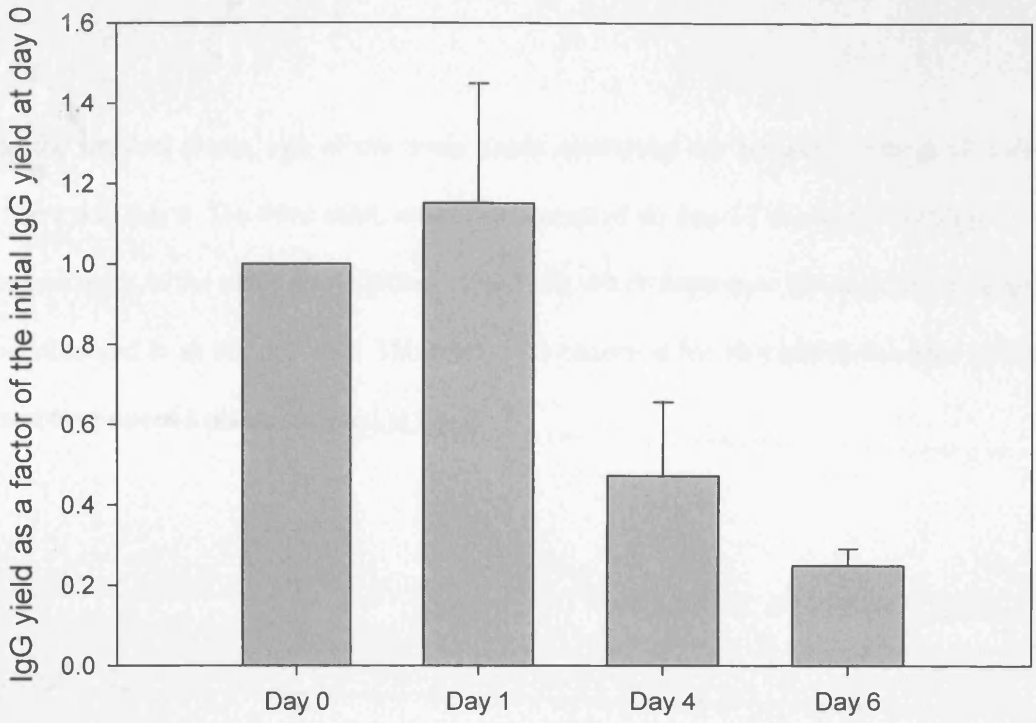

Figure 5.10: Extractable IgG (secreted form) product from young plants at days 1, 4 or 6, as a proportion of yield from first sampling at day 0. Averages and SEMs are of three plants. All plants are under 16 ± 5 cm in height, i.e. 2-4 weeks old from seed.

This study was extended by Professor Julian Ma in a further experiment to determine the duration of this wounding effect. Different top leaves of plants were sampled on Day 0, and subsequent samples were taken from different groups of plants at Days 3, 6, 9, 15 and 22. At Day 15, the mean yield was about 80% of Day 0, but the differences were not quite significant. On Day 22, the mean yield was virtually the same as Day 0 and there was no significant difference. Thus after 15-22 days, the residual effect of the wounding effect was observed (Julian Ma, Personal communication).

The wounding experiment was then repeated for plants of different ages. Table 5.1a shows IgG levels (in mg per unit mass of fresh leaf tissue) measured from individual plants of different ages expressing the secreted form of IgG, on different days (Days 0, 1, 2, 4, 6 and 13). The plants in Table 5.1a

are ordered in terms of increasing plant height, ranging from 16 to 90 cm i.e. approximately 2 to 16 weeks old.

For the smallest plants, two of the three plants confirmed our previous findings of a decrease in yield at Day 2 and Day 6. The third plant, which was sampled on Day 13 showed a significant increase in yield. Unexpectedly, in the older plants (plant 4-plant 20), which were over 28 cm in height, a boost in IgG levels was observed in all but one case. This boost was observed for all 4 plants sampled on Day 1, 2, 4, and 13, and for 2 out of 3 plants sampled at Day 6.

	per gram of fresh weight basis (mg MAb per kg fresh leaf tissue)							IgG Boost or drop?
	height(cm)	Day 0	Day 1	Day 2	Day 4	Day 6	Day 13	
Plant 1	16	0.02					49.89	Boost
Plant 2	21.5	3.79		2.63				Drop
Plant 3	23.5	8.42				1.02		Drop
Plant 4	28	1.81			7.94			Boost
Plant 5	29	3.11					19.66	Boost
Plant 6	29.8	0.20			19.84			Boost
Plant 7	30	0.24		4.72				Boost
Plant 8	30	0.63					81.13	Boost
Plant 9	34.5	0.004				0.11		Boost
Plant 10	35.5	2.00		3.862				Boost
Plant 11	36.5	0.65				1.30		Boost
Plant 12	40	6.51			36.91			Boost
Plant 13	44	1.39		2.66				Boost
Plant 14	49.3	1.21			3.48			Boost
Plant 15	51	8.76					76.30	Boost
Plant 16	60	3.6				1.56		Drop
Plant 17	62	0.69	147.63					Boost
Plant 18	82	0.26	3.27					Boost
Plant 19	82.5	0.02	0.40					Boost
Plant 20	90	0.05	0.17					Boost

Table 5.1a: The effect of wounding on plants expressing the secreted form of IgG. The data is shown as mg MAb per kg fresh leaf tissue. (Apart from day 0 where a single sample was measured as duplicates in an ELISA, all values displayed are averages of triplicate samples per plant, each measured in duplicates in an ELISA).

	Total soluble protein (Kg/Kg)						IgG Boost or drop?
	height(cm)	Day0	Day 2	Day 4	Day 6	Day 13	
Plant 1	16	5.0				4.3	No effect
Plant 2	21.5	4.9	3.3				No effect
Plant 3	23.5	3.4			1.0		Drop
Plant 4	28	3.8		4.9			No effect
Plant 5	29	4.8				3.4	No effect
Plant 6	29.8	4.6		3.0			No effect
Plant 7	30	4.4	5.3				No effect
Plant 8	30	10.6				9.6	No effect
Plant 9	34.5	5.3			5.1		No effect
Plant 10	35.5	5.7	5.2				No effect
Plant 11	36.5	4.3			5.4		No effect
Plant 12	40	9.9		6.1			Drop
Plant 13	44	5.4	18.9				Boost
Plant 14	49.3	8.7		11.2			Boost
Plant 15	51	7.2				22.6	Boost
Plant 16	60	6.7			10.7		Boost

Table 5.1b: The effect of pre-harvest wounding on total soluble protein (TSP) for transgenic plants expressing (secreted form). The data is shown as Kg TSP per Kg of fresh leaf tissue. (Apart from day 0 where a single sample was measured as duplicates in an ELISA, all values displayed are averages of triplicate samples per plant, each measured in duplicates in an ELISA). (Due to the average error of sample of ± 1.6, any yield differences within this range are assumed to be the same, i.e. no effect).

Table 5.1b shows total soluble protein (TSP) for the same samples in Table 5.1a. In contrast, to IgG per Kg of fresh leaf tissue, there was no wound effect for 3 out of 4 young plants (distinguished by 28 cm) or for 7 out of 12 old plants, all showing similar levels of TSP after the initial wound.

Overall, the data suggest that the impact of wounding pre-harvest on IgG yield is dependent on plant age (with a distinction made at 28 cm, i.e. an approximate age of 5 weeks).

Plants expressing IgG-HDEL

The same wounding response studies were prepared on IgG-HDEL transgenic plants. In contrast, to IgG transgenic plants, there is either no wound effect or a slight boost in MAb yields per Kg of fresh leaf tissue for either young or old plants and there is no distinction in behaviour according to plant age. Extractions for this intracellularly retained version of the MAb were done by grinding in buffer with no detergent rather than passive elution with 1% (v/v) detergent.

	per gram of fresh weight basis (mg MAb per kg fresh leaf tissue)					IgG Boost or drop?
	height(cm)	Day 0	Day 1	Day 4	Day 6	
Plant 1	13	13.11	28.85			Boost
Plant 2	15	21.08	21.59			No effect
Plant 3	23	7.86		11.64		No effect
Plant 4	26	23.94		131.12		Boost
Plant 5	27	21.78	28.13			Boost
Plant 6	30	5.03		11.48		Boost
Plant 7	35	6.73			12.10	Boost
Plant 8	37.5	19.44			21.45	No effect
Plant 9	39	11.77			11.65	No effect
Plant 10	84	6.95		8.21		No effect
Plant 11	85	9.84			6.84	No effect
Plant 12	90	24.09	95.58			Boost
Plant 13	91	11.93	25.52			Boost
Plant 14	94	9.54			6.39	No effect
Plant 15	98	18.75	19.08			No effect
Plant 16	99	25.06		30.21		Boost
Plant 17	99	4.99			11.54	Boost
Plant 18	100	4.78		4.27		No effect

Table 5.2: The effect of pre-harvest wounding for plants expressing IgG-HDEL. The data is shown as mg MAb per kg fresh leaf tissue. (All values displayed are averages of triplicate samples per plant, each measured in duplicates in an ELISA). (Due to the average error of sample of ± 4.4, any yield differences within this range are assumed to be the same, i.e. no effect)

5.5 DISCUSSION

This Chapter demonstrated that for old plants (15-18 weeks) expressing the IgG (secreted form), the youngest top leaves showed the highest extractable yield of MAb, with a significant reduction in the lower leaves. Conversely, IgG-HDEL expressing plants showed no variation in MAb with leaf location within the plant. For plants expressing the secreted form of IgG, MAb yield decreased with plant age with the highest yields (on a unit mass basis or a total soluble protein basis) extracted from the youngest plants (>2 to 4 weeks old). IgG-HDEL expressing plants, however, had a constant yield per unit fresh leaf mass with increasing plant age. However, in consideration of the increasing total leaf biomass available per plant with plant age, optimal MAb yields is still from the youngest plants for IgG (secreted), but is from the oldest plants for IgG-HDEL. Mechanical wounding of leaves of young IgG-expressing plants causes an immediate decrease in IgG (secreted) which lasts for about 2 weeks, but an increase in old plants. In contrast, IgG-HDEL expressing plants are unaffected by mechanical wounding.

Younger leaf tissue (obtained from either young plants or from top leaves of old plants) expressing the secreted form of IgG expressed greater amounts of the monoclonal antibody per unit mass of fresh leaf tissue than older tissue. This supports findings by Stevens *et al.* (2000) who showed that both endogenous protein and antibody level declined strongly during leaf tissue development, and explained this by the presence of acidic proteases in older leaves. They suggest that proteolytic degradation during plant development had a significant influence on the yield and homogeneity of heterologous protein produced by transgenic plants.

It is well-established that momentous proteolytic degradation occurs during leaf senescence and as a response to stress when nutrients are reorganised for transport to other parts of the plant or when an increased capacity for synthesis of stress gene products is needed (Stevens *et al.*, 2000). In addition, senescence causes the translocation of nutrients from senescing tissue to young tissue and reproductive organs, thus, senescence usually occurs during the transition from plant maturation to the reproductive stage.

Stevens *et al.* (2000) also carried out their investigation on a secreted IgG1, (MGR48). Interestingly, our values for % of IgG in middle and bottom leaves with respect to top leaves are very similar to those in Stevens *et al.*, (2000); (approximately deduced from Figure 4 in their manuscript showing IgG per gram of fresh weight, under environmental conditions of 25°C and low light, similar to ours), they found that middle leaves had about a third of the IgG in top leaves, and the bottom leaves had approximately a fifth of the IgG in top leaves. This, is a significant finding, since it demonstrates that results of Stevens *et al.* (2000), and this article, might be applicable to all IgG1 monoclonal antibodies, regardless of their specific functionality. Stevens *et al.* (2000) also showed that the proteolytic activity specifically acting on endogenous proteins in basal leaves was significantly higher than in the top and middle leaves. But, they found that although middle leaves had similar proteolytic activity per amount of leaf tissue as the top leaves, they contained much lower amounts of intact antibody. They hypothesised that IgG degradation rate increases with its residence time in leaf tissue (Stevens *et al.* 2000).

Since it is widely known that antibodies are relatively stable proteins, Stevens *et al.* (2000), compared the proteolytic breakdown of equal quantities of hybridoma IgG1 and that derived from transgenic plant tissue that had subsequently been purified, by incubating both in crude wild-type plant leaf tissue extract. They showed that the plantibody heavy chain degraded at a much faster rate than that from hybridoma cells, and they speculated that this was due to the presence of plant-specific N-glycans rather than murine N-glycans.

It should be noted however, that the changes in protein synthesis and degradation that occur during senescence are not the same for all proteins. It is known that the concentration of several enzymes that play a role in nitrogen metabolism, increases during senescence, however other proteins including chlorophyll-binding proteins, ribulose 5-phosphate kinase, and Rubisco actually decease during this stage (Smart, 1994; Buchanan-Wollaston, 1997; Noóden and Guiamét, 1997). Moreover, Rubisco that resides in chloroplasts represents the majority of soluble protein in green leaf tissue. The secreted form of IgG as in Stevens *et al.* (2000) or in our example, however, is assembled and matured in the ER and Golgi apparatus, after which it is secreted into the apoplasm (Frigerio *et al.* 2000, Hein *et al.*, 1991).

Thus, these secreted forms of IgG will be exposed to different pools of proteases (that reside in apoplasm) compared with those in the ER (Stevens *et al.*, 2000). This offers a probable explanation for the fact that a much more stable level of IgG-HDEL was observed with leaf age or stress by wounding in our investigation.

In Chapter 4, it was shown that extraction of total soluble protein from transgenic tobacco plants increased with increasing pH, indicating that most proteins in tobacco are acidic. It has been reported (Stevens *et al.* 2000) that acidic proteases in tobacco catalyse plantibody degradation. Thus, Stevens *et al.* (2000) concluded that antibodies are degraded in the apoplast, thus also explaining our results of an age-sensitive IgG (secreted form) which is targeted to the apoplasm but an age-independent IgG-HDEL which is retained in the ER.

In addition to top, middle and bottom leaf analysis, Stevens *et al.* (2000) also observed that plants that developed more rapidly and had formed flowers, often displayed lower total protein and MAb levels than plants that were less developed, supporting our results for the secreted form of MAb.

Senescence of *Nicotiana tabacum* leaves can be observed by a progressive yellowing of the leaves, and represents the succession of biochemical and physiological events that occurs at the final stage of development, leading to cell death (Smart 1994). Senescence in tobacco is known to be independent of transition to the generative plant phase, or floral development (Thomas and Stoddart, 1980). It is also independent of environmental conditions, and will occur at a particular point in time in the leaf's life, resulting in the breakdown of specific cell constituents (Mascalux *et al.*, 2000). Masclaux *et al.* (2000) found that there was a progressive decrease in chlorophyll, protein and RNA from the top of the plant to the bottom of the plant.

In this thesis, there was a contrasting wound response and its effect on subsequent IgG (secreted form) levels once plants had reached a height of about 28 cm. The difference in IgG response to stress initiated by wounding in young and old plants expressing the secreted form of IgG was a surprise finding. Plant growth patterns are greatly affected by physiological and ecological constraints. Herms *et al.*, (1992)

explained that it was possible to bring together phenotypic and life history theories within the growth-differentiation balance (GDB) framework. Plant activity at a cellular level can be classified as growth (cell division and enlargement) or differentiation (chemical and morphological changes leading to cell maturation and specialisation). Both cell division and expansion are demanding of resources such as light, water, minerals, temperature, photoassimilates, growth regulators, and the regulating effects of neighbouring cells. Differentiation usually occurs after cell division and enlargement. The thickening of leaf cuticle and secondary cell walls, production of wax and cellular inclusions, and secondary metabolism, are examples of cellular differentiation processes. It is known that certain differentiation processes limit herbivory by producing secondary metabolites (Herms *et al.*, 1992).

The basis of the GDB hypothesis of plant defence is that there is a physiological trade-off between processes of growth and differentiation. This trade-off exists because secondary metabolism and structural reinforcement are physiologically restricted in dividing and enlarging cells, and because they divert resources from the production of new leaf area. Therefore plants must grow at a high rate in order to compete, but also need to build-up essential defences in order to survive in the presence of pathogens and herbivores.

Young, developing tissue, may lack the ability to synthesise essential enzymatic machinery. On the other hand, concentrations of some secondary metabolites (particularly low molecular weight phenolics, and alkaloids) are highest during early stages of seedling growth and leaf expansion, and may be synthesised only in young tissue. Previously synthesised and stored secondary metabolites are utilised in times and locations of which their biosynthesis is constrained (Herms *et al.*, 1992). Several studies show concentrations of secondary metabolites to be highest in buds (or at budbreak) and then decline as leaves expand. Secondary metabolites are usually concentrated in epidermal cells, which are among the first cells in leaves to mature.

The reason why plants choose to grow or defend, without the ability of optimally undertaking both simultaneously, is that plants have limited resources that can support their physiological processes, hence

all requirements cannot be met at the same time, and trade-offs occur among growth, maintenance, storage, reproduction and defence (Herms *et al.*, 1992). Consequently, there is sequential growth and maturation of tissues within organs and organs within plants and/or strong inverse relationships between the allocation of resources to growth and non-growth processes. In addition, growth processes demand particularly high levels of limited plant resources. Therefore, during periods of intense growth, secondary metabolism may be substrate and/or energy limited. Furthermore, primary and secondary metabolic pathways share common precursors and intermediates.

Plant growth is heavily dependent upon protein synthesis for the manufacture of photosynthetic, biosynthetic and regulatory enzymes, as well as for structural protein. Thus, phenolics synthesis competes with growth for common substrate. Alkaloid synthesis, with its amino acid precursors, also competes directly with protein synthesis, and consequently with growth.

The ability of older plants expressing IgG (secreted form) to boost their antibody expression may be due to the wound response. It is well-established that plant damage due to mechanical interference or herbivore attack results in the production of proteinase inhibitors (Green and Ryan, 1972, Schilmiller and Howe, 2005). Proteinase inhibitor accumulation would protect the recombinant IgG from proteases that also reside in the leaf apoplasm after every wound, thus causing an increase in overall extractable level of IgG. It should be noted also that the higher IgG level as a result of wounding, is a systemic (rather than local) wound response, due to the fact that on the second day of plant wounding, a different set of leaves (at the top, middle, and bottom of the plant) were wounded than the original set that were first wounded on day 0. This wound response is thought to be modulated by Jasmonic acid.

It has previously been found that mechanical wounding of tobacco leaves can cause a 10-fold increase in jasmonic acid concentration in damaged leaves within 90 min, and a systemic 3.5 fold increase in jasmonic acid in roots 180 min after wounding. In addition, nicotine concentration increased in the leaves up to 5 days after wounding (Baldwin *et al.*, 1997; Ohnmeiss *et al.*, 1997). The indication of these results was that nicotine accumulation is a wound response and that jasmonic acid acts as a signal

molecule between the stimulus in the leaves and the response in the roots. There are other studies, however, that show that application of exogenous auxin can inhibit some wound-induced responses (Mason *et al.*, 1992; De Wald *et al.*, 1994). It was found that auxin significantly decreased the level of methyl-jasmonate inducible accumulation of mRNA of compounds that play roles in nicotine synthesis (Imanishi *et al.*, 1998a, b).

Shi et al (2006) examined the effect of mechanical wounding on nicotine production in tobacco plants. This group performed this study on plants grown either in sand or hydroponics, and damage was caused either by removal of the shoot apex or damage of the youngest unfolded leaves by a comb-like brusher that made 720 punctures. Treatment on plants used in this study was left 90 days after sowing, i.e. relatively old plants. Mechanical wounding caused an increase in overall nicotine level at day 3, and peaked at day 6. They found that wounding by excision of the shoot apex caused a greater increase in nicotine accumulation than leaf peroration. Shi et al (2006) also found that mechanical wounding resulted in an increase in jasmonic acid concentration within 90min in the shoot, and then an increase in the roots (210mins), which was more significantly caused by leaf perforation than shoot damage. They found that the increase in nicotine concentration occurred throughout the plant, particularly in the shoot, whereas the increase in jasmonic acid in the shoot occurred mainly only in region of damaged tissue and not in adjacent tissues. Shi *et al.* (2006) found that removal of lateral buds that generated after shoot excision caused an increase in nicotine concentrations in plant tissues. Removal of mature leaves, however, did not affect nicotine concentration, even though the degree of wounding was comparable to apex removal. This group concluded that nicotine production (also thought to be a result of wounding) in tobacco leaf did not correlate with degree of wounding by cutting the surface or puncturing the leaves, but depended more significantly on the removal of apical meristems, and thus on major sources of auxin in the plant. In addition, applying 1-napthylacetic acid (NAA) on the cut surface post-removal of the shoot apex caused complete inhibition of the increase in nicotine in whole plants and in Jasmonic acid in the damaged stem segment and roots (Shi *et al.*, 2006). An auxin transport inhibitor also applied around the stem directly under the shoot apex of intact plants also caused an increase in nicotine concentration in the whole plant

(Shi *et al.*, 1996). In our study, however, apical meristems were not removed, suggesting that recombinant monoclonal antibody levels post-wounding are not determined by auxin, and may still be due to jasmonic acid production, which may produce nicotine in a very different way to protein.

Interestingly, Gilissen *et al.*, (1996), found that for *Nicotiana tabacum*, once the total plant length was greater than 30 cm, the growth phase at the top of the plant changed from vegetative to generative. The vegetative phase of plants is the initial growing phase of the plant, characterised by the iterative production of leaves from the shoot meristem (Poethig, 1990). The generative phase of the plant, however, occurs later in development, and signifies the point at which the meristem is responsible for reproductive development, producing flowers and differentiating the germ line (Hendersen and Dean, 2004). Flowering-time differs for different plant species, and is dependent on multiple environmental and endogenous signals (Izawa *et al.*, 2003; Simpson and Dean, 2002). (The plants that were assessed in Gilissen *et al.*, (1996) were for *Nicotiana tabacum* cv Samsun NN, grown from seed in a climate room at 21°C, with a 13 hour photoperiod light, and we used *Nicotiana tabacum* (var. *Petit Havana*) grown from seed at 26°C with a 16 hour photoperiod. Although the variety of *Nicotiana tabacum* and growth conditions varies slightly, it is expected that the switch from vegetative to generative phase of the top of the plant may also occur at around 30 cm). This offers a probable explanation for the variation in wound response and its effect on IgG for young and old plants expressing the secreted form of IgG.

5.6 CONCLUSIONS

With increasing interest and potential in transgenic tobacco as a suitable recombinant protein host, optimal harvesting strategy is of paramount importance and needs to be addressed. This chapter considers some harvesting issues, namely time of harvest, which leaves of the plant to harvest for *Nicotiana tabacum* plants expressing a recombinant MAb that is targeted via the plant secretory pathway to the apoplasm (IgG) or is intracellularly retained in the endoplasmic reticulum (IgG-HDEL), and the impact of damage to plants before harvest.

For old plants (15-18 weeks) expressing the secreted form of IgG, the top leaves (representing the youngest leaves) show the highest extractable yield of MAb, and progression to lower leaves of the same plants leads to gradual drops in MAb, most likely a result of senescence and its associated increase in detrimental apoplasm-residing proteases. In contrast IgG-HDEL expressing plants show no variation in MAb with leaf position within individual plants.

Yield of IgG per kilogram of fresh leaf tissue (or IgG as a % of total soluble protein) decreased with plant age for the secreted form of IgG, with optimal yields (on a per unit mass basis) for the youngest plants, i.e. >2 to 4 weeks old. On the contrary, IgG-HDEL expressing plants demonstrated a constant yield per unit fresh leaf mass with increasing plant age. However, yield of MAb per mass, does not take into account the total leaf biomass available per plant, with plant age. When this is taken into account, it is in fact evident that the optimal total MAb yields (mg) for plants expressing IgG (secreted form) is still >2 to 4 weeks. For IgG-HDEL expressing plants, however, since there is a constant MAb yield per kg, the increase in total leaf biomass with plant age, leads to a corresponding increase in the amounts of total MAb per plant.

For plants expressing IgG (secreted form), the mechanical wounding of leaves of young plants leads to an immediate decrease in IgG which nay last for about 2 weeks. In contrast, mechanical wounding the day before harvesting appears to have the opposite effect for older plants expressing IgG (secreted form) since this may lead to boosts in MAb yields. Mechanical wounding, however, does not affect MAb yields per kg of plants expressing IgG-HDEL, which may be favourable for general plant maintenance, as any accidental damage would not be critical.

Overall, IgG-HDEL appears to be present in a greater absolute yield than IgG in transgenic plants. However, it should be noted that the final targeting strategy is influenced by many factors including the: total extractable yield of MAb from plants, co-extraction of native (contaminant) proteins, phenolics, and other contaminants; simiplicity and scalability of the extraction method; associated ease of downstream processing; preference of secretion over intracellular retention (greenhouse vs. Contained field); and

glycosylation acceptability with FDA regulations and *in vivo* consequences of the –HDEL tag, bearing in mind that the default pathway for antibodies in mammalian B cells is secretion.

Chapter 6- Characterisation of mechanical properties of transgenic tobacco roots expressing a recombinant monoclonal antibody against tooth decay

6.1 INTRODUCTION

Until now, the main focus in the literature (and in the previous 3 chapters of this thesis) for monoclonal antibody production in tobacco plants has been on the extraction of the recombinant protein from fresh leaf tissue. Although tobacco leaves represent the majority of the total plant's biomass for large plants and thus would appear to be the obvious tissue choice for extraction, the extraction and recovery of the MAb from tobacco roots may also be an attractive proposition. Roots show similar levels of expression to the leaves; they contain about 70% of the MAb level that is present in the same fresh weight of leaves; (See forthcoming Section 6.10). Furthermore, roots contain lower levels of toxic phenolics and alkaloids, for example, the nicotine content in leaves of *Nicotiana tabacum* are three times the level found in roots of the same plant (Dawson *et al.*, 1959). This would potentially ease downstream processing for removal of these major contaminants. This chapter focuses on the mechanical properties of transgenic tobacco plant roots, which ought to be fundamental to the design of a suitable mechanical extraction process.

In order to characterise the root mechanical properties, micromanipulation was used to measure the mechanical force required to break them (indicative of root strength). Micromanipulation is a technique by which particles, of 1 μm in diameter or greater can be compressed, and their force deformation behaviour determined (Thomas *et al.*, 2000). Although most measurements of mechanical properties on individual cells are by compression, it is also possible to exert forces on a fibre by pulling. Using an adapted micromanipulation rig, a new method for measuring the force required to break individual tobacco roots is described here. The bulk of the work described in this chapter has been published (Hassan *et al.*, 2008a).

6.2 INITIAL PREPARATORY WORK FOR MICOMANIPULATION EXPERIMENTS

6.2.1 TOBACCO ROOT MICROSCOPIC IMAGES AND APPROXIMATE DIMENSIONS

Photographs and dimensional measurements of tobacco roots were taken in order to assess the structures of the roots that would be tested by micromanipulation forces. The structure of single root hairs was also observed, because they are also capable of antibody production in a bioreactor format (Wongsamuth and Doran 1997) and this is an option for production of monoclonal antibodies using transgenic tobacco. Table 6.1 shows the dimensions of a single white *Nicotiana tabacum* root taken from a plant approximately 20 cm in height. The tobacco cells were seen to be arranged in a regular, uniform and compact array within the root. Figure 6.1 shows the structure of the root tip taken at x4 and x10 magnification, Figure 6.2 illustrates the middle of the root, and Figure 6.3 illustrates a single root with its surrounding root hairs taken at both magnification levels.

	length (μm)	width (μm)
root hair size	383	26
whole root diameter	-	588
diameter of middle layer of whole root (consisting stele (xylem and phloem) and Endodermis with Casparian strip)	-	209
size of a single cell within the cortex region of a whole root	99	42

Table 6.1 Dimensions of a single white *Nicotiana tabacum* root taken from a plant approximately 20 cm in height. The root itself was approximately 5 cm long.

(a)

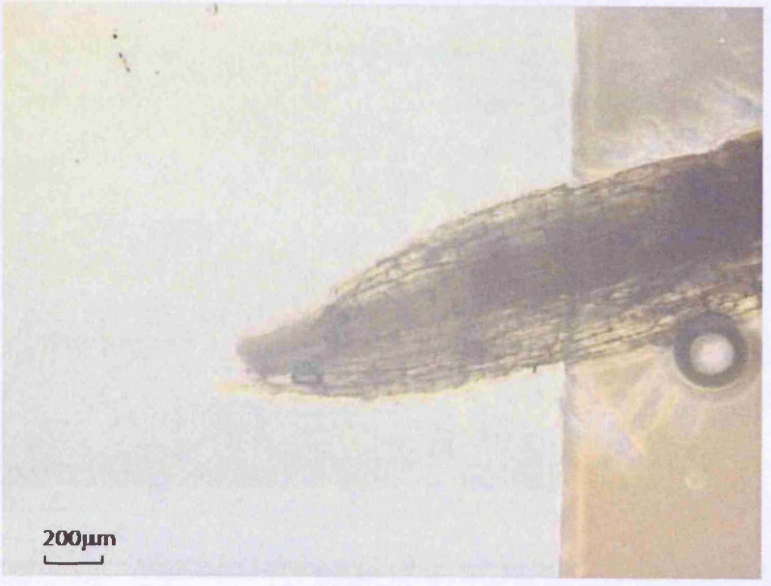

(b)

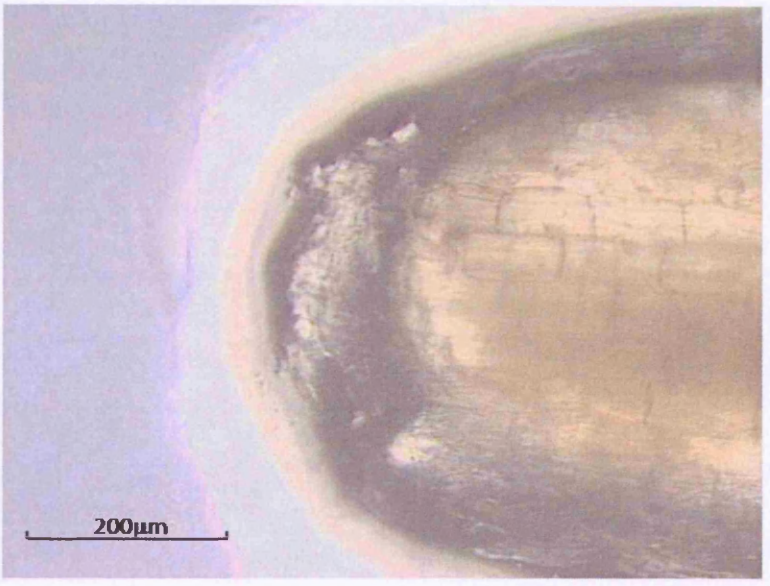

Figure 6.1 Root tip from a *Nicotiana tabacum* plant grown in hydroponics solution imaged at x 4 magnification (a) and at x10 magnification (b).

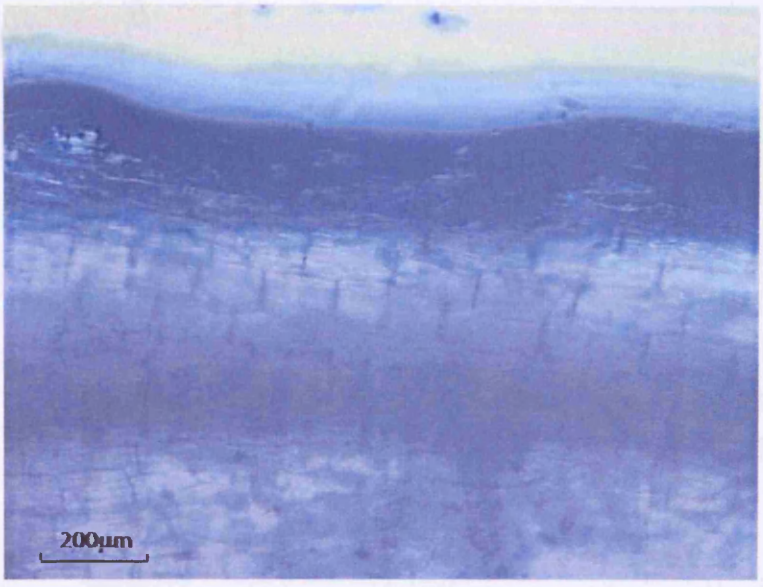

Figure 6.2 The middle of the root from a *Nicotiana tabacum* plant grown in hydroponics solution imaged at x 10 magnification.

(a)

(b)

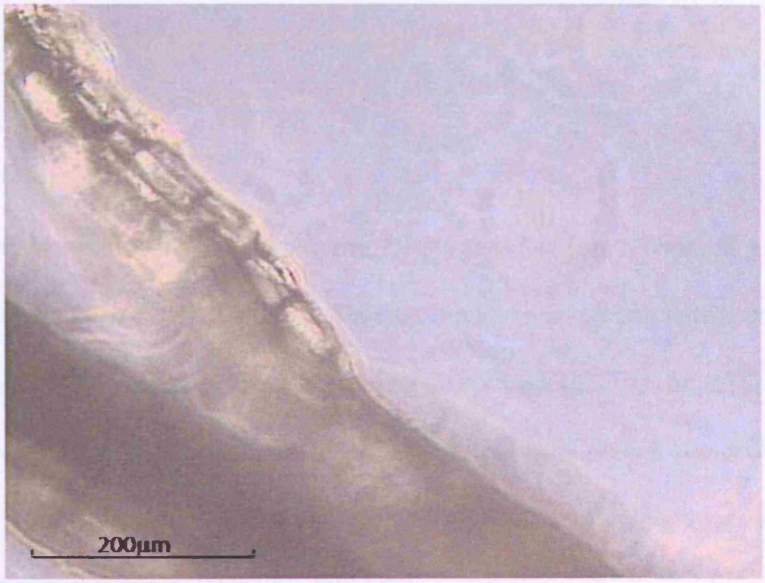

Figure 6.3 Root with root hairs from a *Nicotiana tabacum* plant grown in hydroponics solution imaged at x 4 magnification (a) A single root hair branching from the main root section viewed at x 10 magnification (b).

6.2.2 CHOICE OF MICROMANIPULATION TECHNIQUE

Most micromanipulation equipment which had already been developed at the University of Birmingham, were designed to measure the tensile strength of single cells by compression (Thomas et al, 2000). The possibility of isolating protoplasts from tobacco leaf or root tissue and then allowing the cell wall to was therefore considered. However, use of a High strain-rate compressor rig designed and used for "squeezing" single cells (in a vertical direction) to breakage to determine cell strength was opted out of due to a) the difficulty of generating a large amount of protoplasts (data not shown), b) the difficulty of persuading the protoplasts (with a cell membrane as outer protection only) of re-forming their cell walls, and c) the complicated nature of trying to relate single cells to cells within a whole tissue (root or leaf) framework.

Therefore, it was decided to examine the possibility of using a different micromanipulation technique to pull single transgenic tobacco roots and assess their breakage properties.

6.2.3 PROBE COMPLIANCE

In order to obtain accurate results from the micromanipulation technique for measuring the force required to break single roots it was necessary to measure the compliance of the probe (and associated force transducer) involved in the set up. As described in Chapter 2, Section 2.6.3, four measurements of the transducer probe compliance were performed, by driving the probe at a controlled speed of 2.2 mms^{-1} to touch a hard object. The sensitivity for the 25 gram transducer was 2.5 gf/V. The results of these experiments are shown below in Figure 6.4.

The average slope of the linear regions of the voltage-time curves in Figure 6.4 above was 15.5 Volts/sec. The compliance factor was then calculated using the following equation:

Compliance factor = (probe speed x time of movement)/ (slope x transducer sensitivity) (6.1)

= (2.2 x 0.01)/(15.5 x 2.5)

= 0.00057 mm/g

= 0.57 μm/g

where the product of the probe speed and time of movement is the distance moved. The time of movement was the time from when the probe first touched the hard object until the motion had ended. In subsequent experiments, the actual displacement was taken to be equal to the measured displacement (2.2mm/s x measured time) reduced by the (compliance factor* force). For example, if the force was 250 mN (~ 25 gf), the corresponding compliance was 0.57x 25 = 14.2 μm, and this was then subtracted from the measured displacement to obtain a value for true displacement.

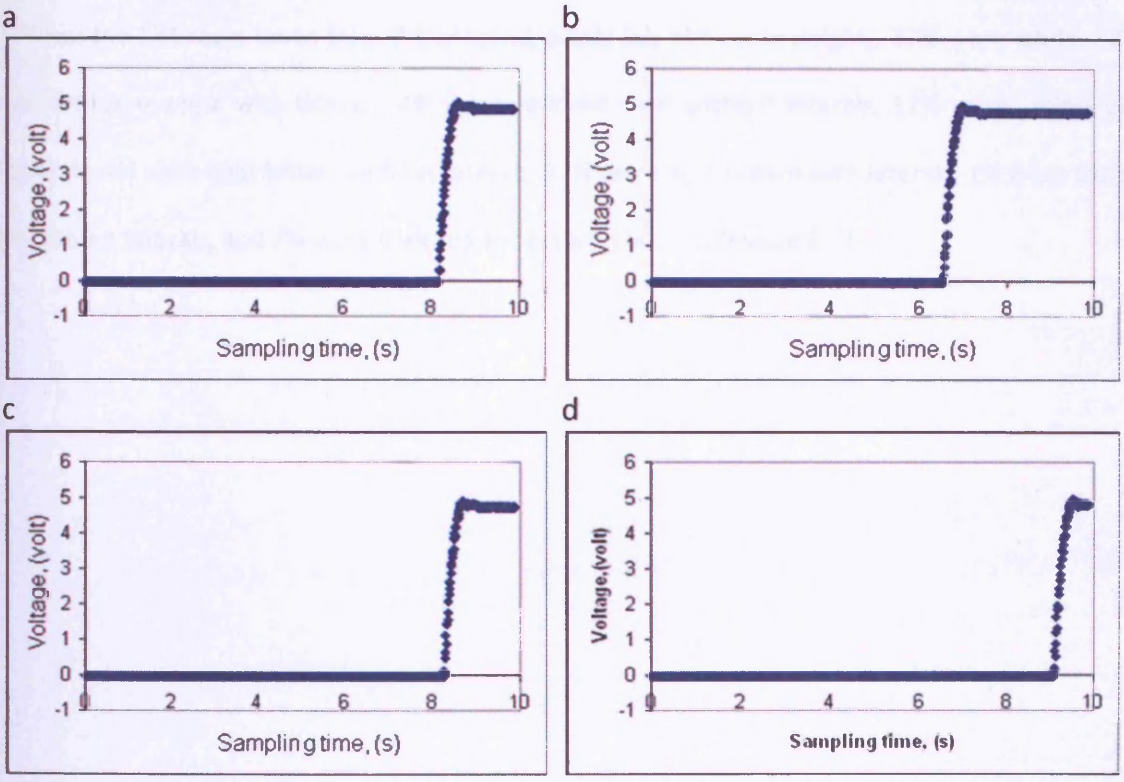

Figure 6.4: Measurement of transducer probe compliance: The probe was driven at a controlled speed (2.2 mm/s) to touch a hard object in order to obtain voltage (force) vs. time curves. a Slope of linear region of the graph is 15.6 Volts/sec; b slope = 15.6 Volts/sec; c slope = 15.0 Volts/sec; d slope = 15.8 Volts/sec.

6.3 ROOT MORPHOLOGY

Tobacco root systems like most root systems are branching structures; i.e. each node (the point of origin of a branch in a root system) has links or edges emanating from it. A schematic of this is shown in Figure 6.5a. All roots measured in this chapter were first or second order lateral roots. The main features of individual roots that show systemic variation are diameter, colour, growth potential, and surface texture. Older roots are usually a various shade of brown, whereas younger roots can be unpigmented ("white") or variously tinged with pink or orange (Fitter, 1996). The roots were therefore divided into 4 distinct colours i.e. white, yellow-brown, light brown, and dark red-brown (as shown in Figure 6.5b). A single tobacco plant (14-25 cm in height) was found to possess a mixture of old and young roots in the proportions mentioned below. This is because *Nicotiana tabacum* plants are perennial, and thus unlike annual plants where fine roots are of a relatively similar age, they are known to exhibit a broad range of root ages at any stage (Wells and Eissenstat 2003).

From the 134 roots taken from 7 transgenic plants (all ~14 cm in height), 37% were white without laterals, 8% were white with laterals, 4% were yellow-brown without laterals, 12% were yellow-brown with laterals, 4% were light brown without laterals, 27% were light brown with laterals, 1% were dark red-brown without laterals, and 7% were dark red-brown with laterals (Figure 6.6).

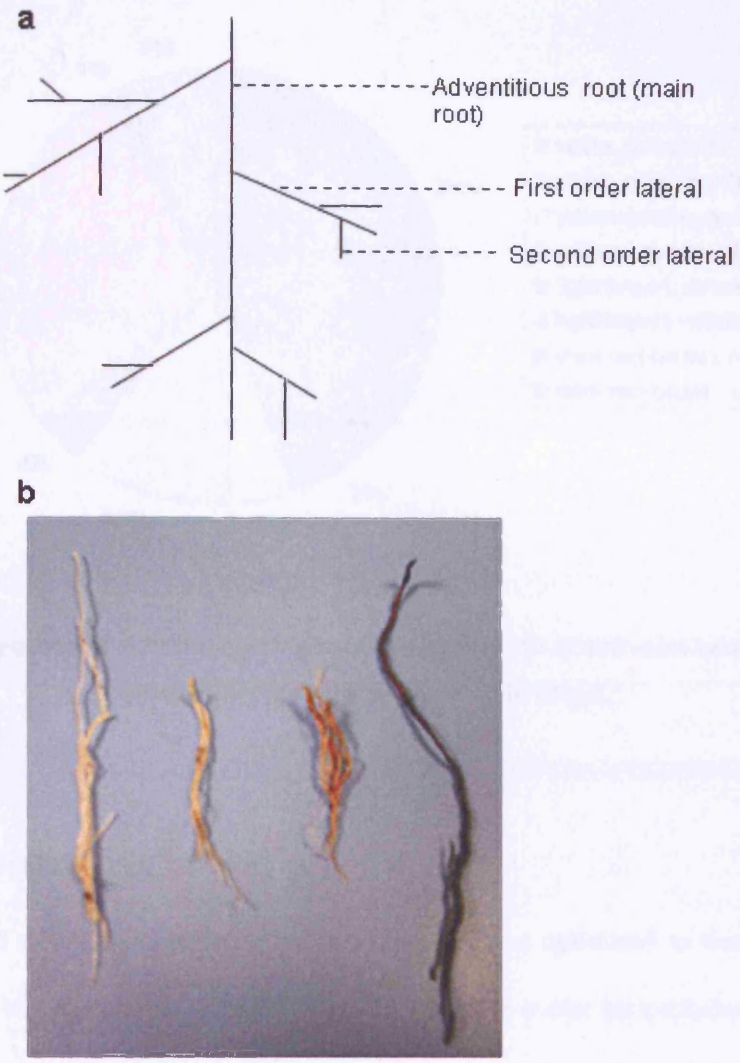

Figure 6.5 a) Schematic of root branching structure (adapted from Fitter, 1996) b) Different coloured roots. Starting from the left hand side, white roots, yellow-brown roots, light brown roots, dark red-brown roots. (Length of root in photo is not representative of the different root types and not to scale).

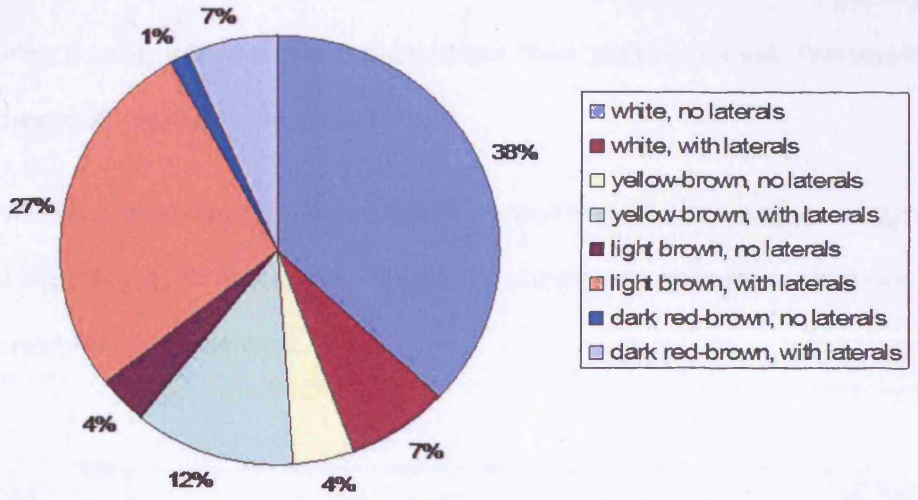

Figure 6.6: The proportion of different types of root in a population of 136 roots taken from 7 different plants expressing the secreted form of IgG.

6.4 RESULTANT FORCE-TIME CURVES

Based on initial results, the micromanipulation method was optimised so that the roots remained hydrated throughout the procedure, and each root was pulled in buffer (as explained in detail in chapter 2, section 2.6.3). Figure 6.7 shows a typical force-time curve for pulling a single tobacco root to breakage in buffer. For all 134 roots pulled, from 7 different tobacco plants expressing IgG and 2 wild type plants, the resultant shape of the force-time curve was always similar to that shown in the representative graph in Figure 6.7. A uniform step-wise increase in the force was observed, possibly representing the individual fibrous layers of the root being "torn apart" one by one as the root was pulled, until the force was big enough to separate all the root fibres completely, and break the root into two sections. There are three reasons why the step-wise increase in force up to breakage point was not believed to be an artefact: a) ESEM images which suggested this mechanism, as explained below; b) the number of steps and their magnitude differed between measurements, and c) this step-wise increase had not been observed for the pulling of single fungi by a similar micromanipulation technique (C.R. Thomas, personal communication).

The fact that the force keeps rising up to a peak force for complete root breakage, indicates that the stress by pulling is being applied to stiffer and stronger fibres after each break. This may be because the core root fibres are stronger than the surface fibres.

Roots of wild type tobacco plants produced similar force-time curves to roots of transgenic tobacco plants (data not shown), suggesting that they have similar mechanical properties, which was expected, since they were morphologically identical.

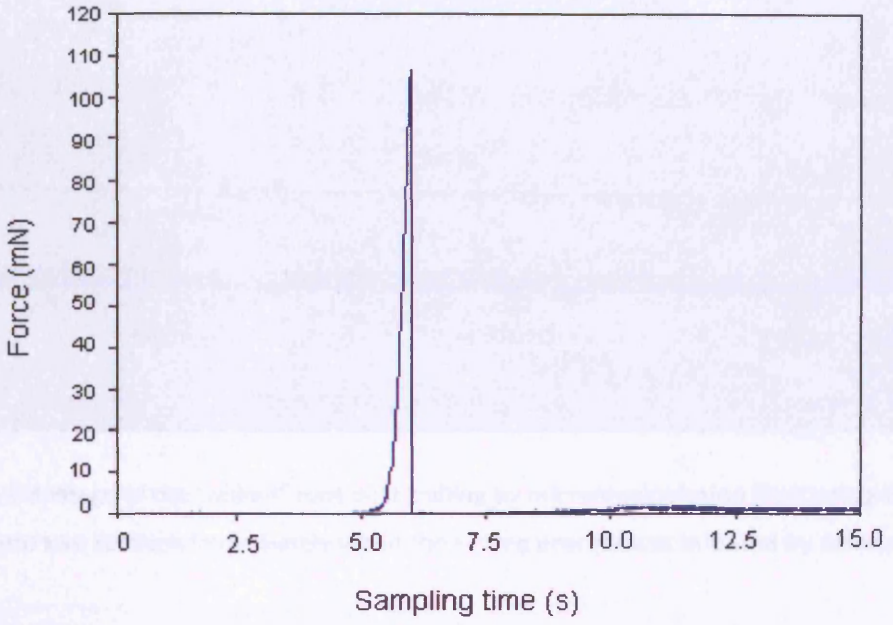

Figure 6.7 A typical force-time curve for single tobacco roots pulled to breakage (represented by the peak on the curve). The breaking point is about 107 mN for a dark red-brown root with laterals.

6.5 ESEM (ENVIRONMENTAL SURFACE ELECTRON MICROSCOPY)

Images of broken ends of roots (hydrated) from micromanipulation experiments were taken using environmental surface electron microscopy (in wet mode), in order to try to better understand the mechanism of root breakage. As explained above, pulling the root at a constant speed of 2.2mm/s does not cause the immediate breakage of the root, but it appears to occur in a stepwise manner as individual surface cells are first detached, until complete root breakage finally occurs at the point of highest force.

Figure 6.8 demonstrates this concept, as pockets of torn fibres of the root can be seen along the root's surface.

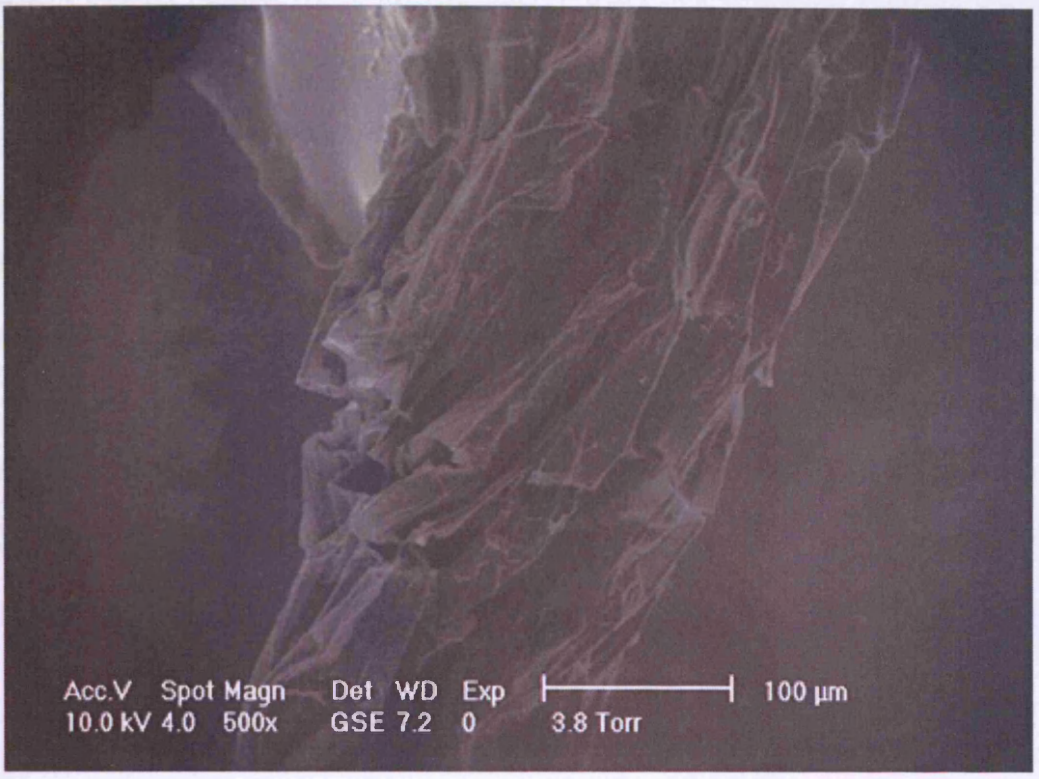

Figure 6.8 An ESEM image of the "pulled" root post-pulling by micromanipulation illustrating that the root was not broken into two sections immediately when the pulling process was initiated by micromanipulation.

6.6 BREAKING FORCE VS. STAGE OF ROOT MATURATION

To underpin the mechanical strength of the roots we considered peak force for breakage, work done and nominal stress. Figure 6.9 shows that a greater peak force is required to completely break the more mature brown roots (118 ± 15 mN) than the younger white and yellow brown roots whose peak forces are approximately the same, (89 ± 14 mN). The peak force required to break the young white and yellow-brown roots increased also to break the "fully-mature" dark red-brown roots with laterals (148 ± 29 mN). The result of the Kruskal-Wallis analysis variance (ANOVA) comparing these different root stages (as defined by their colour) was P = 0.15, suggesting that there is no significant difference between the peak forces required to break the roots at any of the stages. However, when comparing just the two-

defined extremes of the different root stages (i.e. white roots (both with and without laterals) with the dark red-brown roots with laterals), their peak forces for breakage were found to be significantly different, i.e. P = 0.027 (Kruskal-Wallis ANOVA), and P = 0.021 (Mann-Whitney analysis). (The results of dark red-brown roots without laterals are not included in this statistical analysis as their occurrence was very rare i.e. 2 roots out of 136 roots and are therefore only included in the figures as an indication). The presence or absence of laterals had no effect on the peak force for breakage. Overall however, very similar peak forces are required to break all the roots of *Nicotiana tabacum* irrespective of the stage of maturity, i.e. 101 $\pm$ 7 mN. It is important to note here, however, that these different root types are not present in the same proportions as described above, so that even if darker roots require a slightly greater peak force for breakage, their proportion in the total population of roots is small. Their influence in achieving satisfactory breakage in processing might, therefore, be limited.

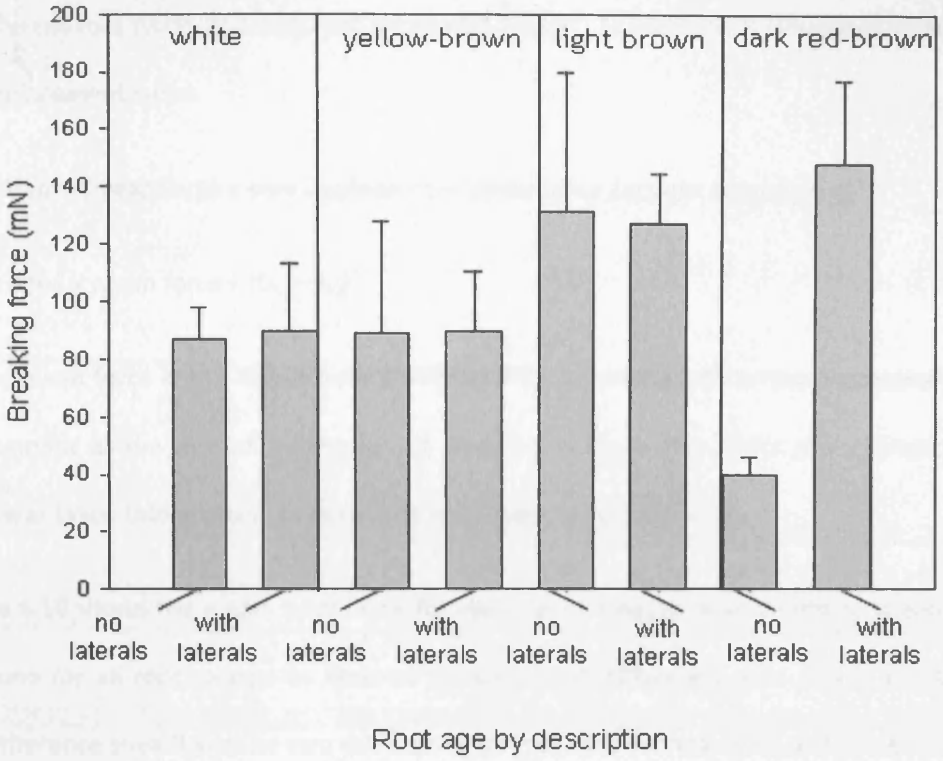

Figure 6.9 The relationship between mean breaking force and root age as represented by their colour and the presence of laterals, in a sample population of 136 roots, taken from 7 different transgenic plants expressing the secretory form of IgG. (Means and Standard Error of the means (SEMs) represent 50 different roots for white roots without laterals, 10 for white with laterals, 6 for yellow-brown without laterals, 16 for yellow-brown with laterals, 5 for light brown without laterals, 37 for light brown with laterals, 2 for dark red-brown with laterals, and 9 for dark red-brown with laterals).

Unlike plant flowers and leaves, roots show few distinctive external features that would permit plant species identification (Fitter, 1996). This suggests that similar root types of species other than *Nicotiana tabacum*, may display similar mechanical properties, indicating that the data in this chapter may be applicable to other plant species.

In bioprocessing, it may be useful to establish minimum energy requirements for root breakage as this may determine the point at which maximum antibody yield is obtained with minimal release of contaminants (defined as any component other than the product of interest). In addition this will

minimise energy utilisation thus helping to save costs. The work done to pull individual roots to breakage point for different root types, at a constant speed of 2.2mms^{-1}. Work done is calculated as the area under the force displacement curve.

Work done = mean force x true displacement (taking into account compliance) (6.2)

Work done = mean force x ($D_t - D_{t0}$) (6.3)

where mean force is the displacement-averaged force (taking into account compliance) and D_t is final displacement at the end of pulling at 2.2 mms^{-1} and D_{t0} is the initial displacement pre-pulling. Compliance was taken into account as described in Chapter 2, Section 2.6.3.

Figure 6.10 shows the mean work done for each root category. Kruskal-Wallis analysis comparing the work done for all root categories showed no significant difference (P = 0.65) and there was no significant difference even if just the two extreme root types i.e. all white roots with dark red-brown roots with laterals were compared (P = 0.28).

Mean work done for the different root categories are shown in Figure 6.10. It should be noted here, that the profile for work done is very different to that of breaking force, since it is estimated on the basis of mean force (as described above) rather than a peak force. Overall, the mean work done for breaking single roots of *Nicotiana tabacum* (regardless of their maturity stage) is approximately 97 $\pm$ 6 μJ per root.

In addition to categorising the root systems in terms of stage of maturity, (as indicated by it brown intensity colour), other properties of the individual roots were examined in order to determine which factor had the greatest influence on the breaking force, i.e. the root strength.

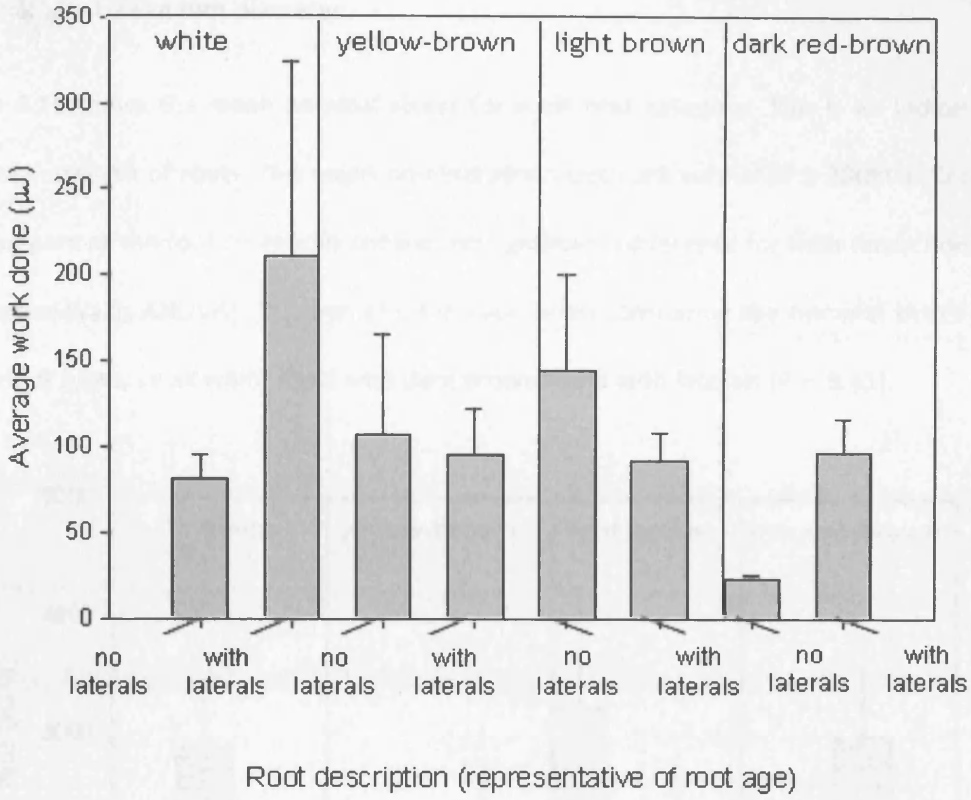

Figure 6.10 The relationship between work done and root age represented by colour and the presence of laterals, for the majority of root types of the population. (Means and SEMs represent 45 replicates for white roots with no laterals, 13 replicates for white roots with laterals, 5 replicates for yellow-brown roots with no laterals, 16 replicates for yellow-brown roots with laterals, 7 replicates for light brown roots with no laterals, 31 replicates for light brown roots with laterals, 2 replicates for dark red-brown roots without laterals and 8 replicates for dark red-brown roots with laterals).

6.7 NOMINAL STRESS

As an alternative parameter of peak force for breakage, the force per unit root cross-sectional area, or nominal stress was calculated. This was calculated as:

$$\text{Nominal Stress} = \frac{F_b}{A_o} \tag{6.4}$$

where, F_b is the peak force for breakage and A_o is the original root cross-sectional area, i.e. (πd_o^2 / 4) where d_o is original mean root diameter.

Figure 6.11 shows the mean nominal stress for each root category. This is an indication of the ultimate tensile strength of roots. The mean nominal stress per root was 2400 ± 200KPa. Kruskal-Wallis analysis to compare all the root categories showed no significant difference for their mean nominal stress (P = 0.29 Kruskal-Wallis ANOVA). This was also the case when comparing the nominal stress of just the two extreme root types, i.e all white roots with dark brown roots with laterals (P = 0.61).

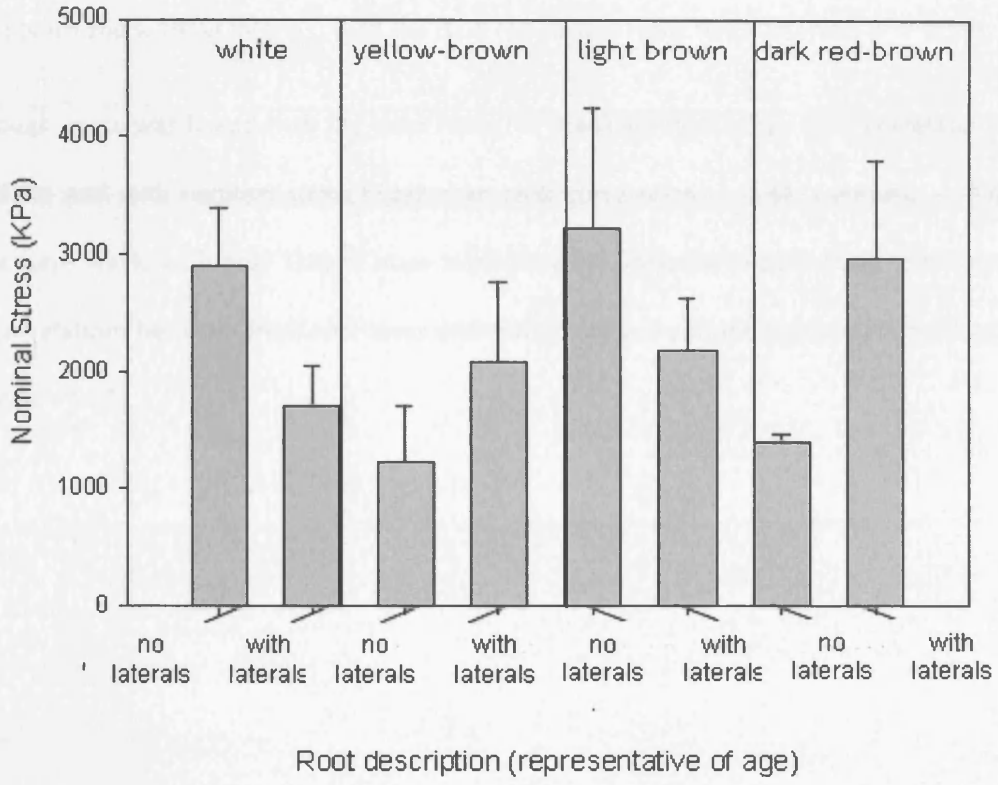

Figure 6.11 The relationship between nominal stress and root age as represented by their colour and presence of laterals, in a population of 129 roots taken from 7 individual transgenic plants expressing the secretory IgG. (Means and SEMs represent 48 different roots for white roots without laterals, 8 for white with laterals, 6 for yellow-brown without laterals, 16 for yellow-brown with laterals, 5 for light brown without laterals, 35 for light brown with laterals, 2 for dark red-brown with laterals, and 9 for dark red-brown with laterals)

6.8 GEOMETRICAL ROOT PROPERTIES OR FRESH MASS

6.8.1 MASS

Figure 6.12 shows variation of mean fresh root mass with root category (described by its colour and the presence or absence of laterals). The result of the Kruskal-Wallis analysis comparing all the different root types classified in this way was P = 0.99, suggesting that there is no significant difference between them. This was also the statistical conclusion for comparing just the white roots (with and without laterals) with the dark red-brown roots (with laterals) (P = 0.98) or for comparing the yellow-brown roots (with and without laterals) with the dark red-brown roots (with laterals) (P = 0.39).

Although, mass was linked with the peak force for breakage (Spearman rank correlation = 0.33, *t*-statistic = 4.00) and with nominal stress (Spearman rank correlation = -0.34, *t*-statistic = -4.02), these correlations were weak, with only 11% of mass explaining the variance in both peak force and nominal stress. No correlations between fresh root mass and work done were found (Spearman rank correlation = 0.14, *t*-statistic = 1.52).

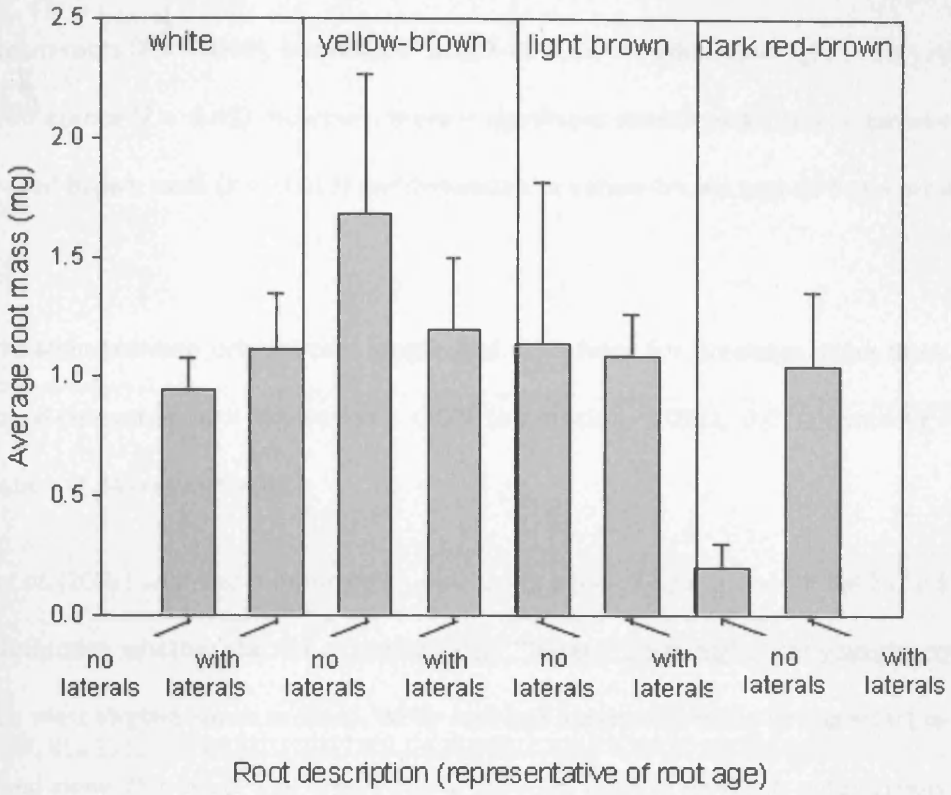

Figure 6.12 The relationship between mean root fresh mass and root age as represented by their colour, in a sample population of 136 roots, taken from 7 different transgenic plants expressing the secreted form of IgG. (Means and SEMs represent 50 white roots without laterals, 11 white roots with laterals, 6 yellow-brown roots without laterals, 16 yellow-brown roots with laterals, 5 brown roots without laterals, 37 brown roots with laterals, 2 dark red-brown roots without laterals, and 9 dark red-brown roots with laterals.

6.8.2 ORIGINAL ROOT LENGTH

Another measurement of root age (in addition to its colour) could be its original root length. Since peak force for breakage has been shown to increase for the most mature, dark-red-brown roots, a possible prediction is that the older the root, the longer its original length, and the higher the peak force for breakage. Figure 6.13 shows the original root length for the different root categories. This figure shows that the whole root length is about 21mm for all the root categories with the exception of the most mature dark red-brown roots where the total root length increases to about 33 mm. A Kruskal-Wallis test on all the varying root categories analysed shows that the original root lengths of the different

root categories are significantly different (P = 0.014) . Statistical difference also exists between the white and yellow-brown roots (P = 0.069), but original length of both the white and light brown roots showed no significant difference (P = 0.45). However, there is significant statistical difference between the white roots and dark red-brown roots (P = 0.013) and between the yellow-brown and dark red-brown roots (P= 0.034).

No correlation between original root length and peak force for breakage, work done or nominal stress were found (Spearman rank correlation = -0.008 (*t*-statistic = -0.091), -0.011 (*t*-statistic = -0.12), and -0.118 (*t*-statistic = -1.34) respectively).

Wells *et al.* (2002) analyzed minirhizotron data using a mixed-age, proportional hazards regression approach to determine whether the risk of mortality (or "hazard") was higher for younger roots than for older roots in a West Virginia peach orchard. While root age apparently had a strong effect on the hazard when considered alone, this effect was largely due to different rates of mortality among roots of different orders, diameters, and depths. Roots with dependent laterals (higher order roots) had a lower hazard than first-order roots. Greater root diameter was also associated with a decreased hazard. When considered alone, age appeared to be a strong predictor of risk: a 1-d increase in initial root age was associated with a 1.26–2.62% decrease in the hazard. However, when diameter, order, and depth were incorporated into the model, the effect of root age disappeared or was greatly reduced.

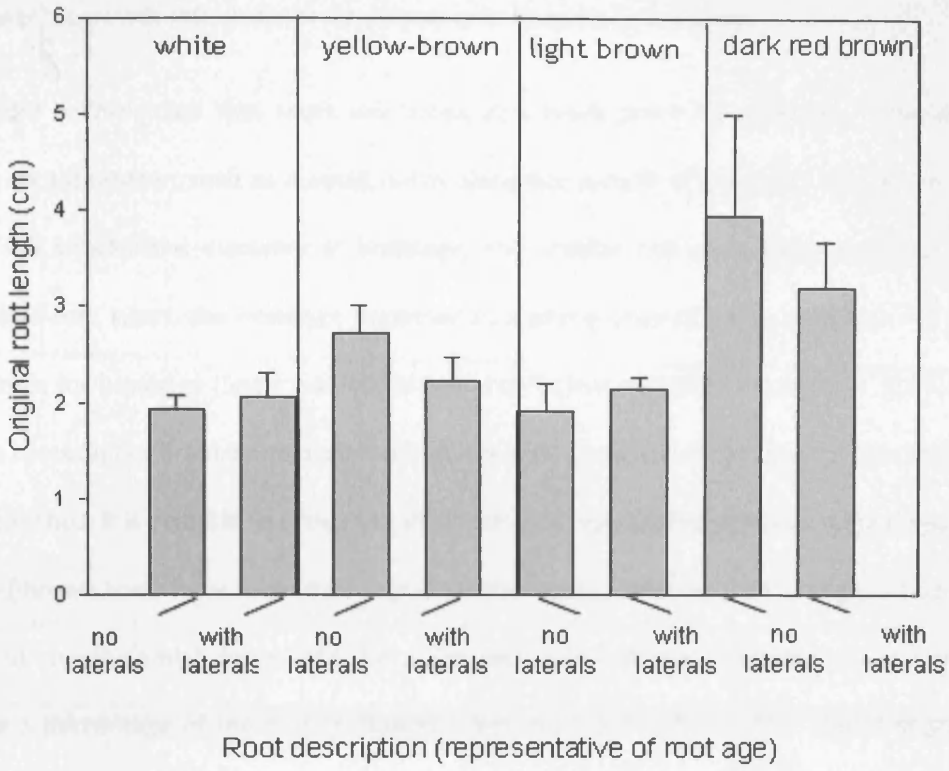

Figure 6.13 The relationship between mean original root length and root age as represented by their colour, in a sample population of 136 roots, taken from 7 different transgenic plants expressing the secreted form of IgG. (Means and SEMs represent 50 white roots without laterals, 11 white roots with laterals, 6 yellow-brown roots without laterals, 16 yellow-brown roots with laterals, 5 brown roots without laterals, 37 brown roots with laterals, 2 dark red-brown roots without laterals, and 9 dark red-brown roots with laterals.

6.8.3 MEAN DIAMETER AND APPROXIMATE DIAMETER AT BREAKAGE

Unlike leaves, roots form new cells constantly just behind the root tip and expand them in the proximal expansion zone. The result of this is a constant stream of new cells through the growth zone of the root tips. This has been shown for tobacco roots (Walter and Schurr, 2005). The spatial distribution of relative elemental growth rate within the root growth zone is more complex than in the dicot leaf. Expansion growth rate within the meristem is relatively low, as repetitive cell divisions take place at rates between one division per day and one per week. In tobacco roots, expansion growth rate increase with

the onset of 25% h^{-1} at 0.7 mm behind the root tip. Beyond this zone of maximal expansion growth, the relative elemental growth rate declines steadily as cells develop to maturity.

It would be predicted that roots will break at a weak point for example, if there is a sudden decrease in root diameter, such as a small notch along the length of the root. This would theoretically mean that the smaller the diameter at breakage, the smaller the peak force required for breaking. However, in all root types, the breakage diameter as a percentage of mean diameter did not correlate with peak force for breakage (Spearman correlation coefficient = -0.018, *t*-statistic = -0.20). This may be because the roots do not break immediately across the entire original diameter into two sections with the applied force. Thus, it is possible to group the different root types using into two main groups; the brown and dark red-brown roots have a low breakage diameter represented as a percentage of the root's mean diameter, but require a high force, and the white and yellow-brown roots that have a high breakage diameter as a percentage of mean root diameter but need a low force. This would suggest that root diameter is less significant for the more mature roots, due to its increasing fibrous properties as lignin is deposited.

Figure 6.14 shows the relationship between the stages of root maturation (as defined by its colour) with mean diameter and approximate diameter at breakage point. For mean root diameter, there was no statistical difference between all the different root categories (P = 0.14, Kruskal-Wallis ANOVA). There was a small statistical difference between the all white roots and all light brown roots (P = 0.049). There was no statistical difference between the mean diameters of the youngest white roots and the oldest dark red-brown roots (with laterals only) (P = 0.13).

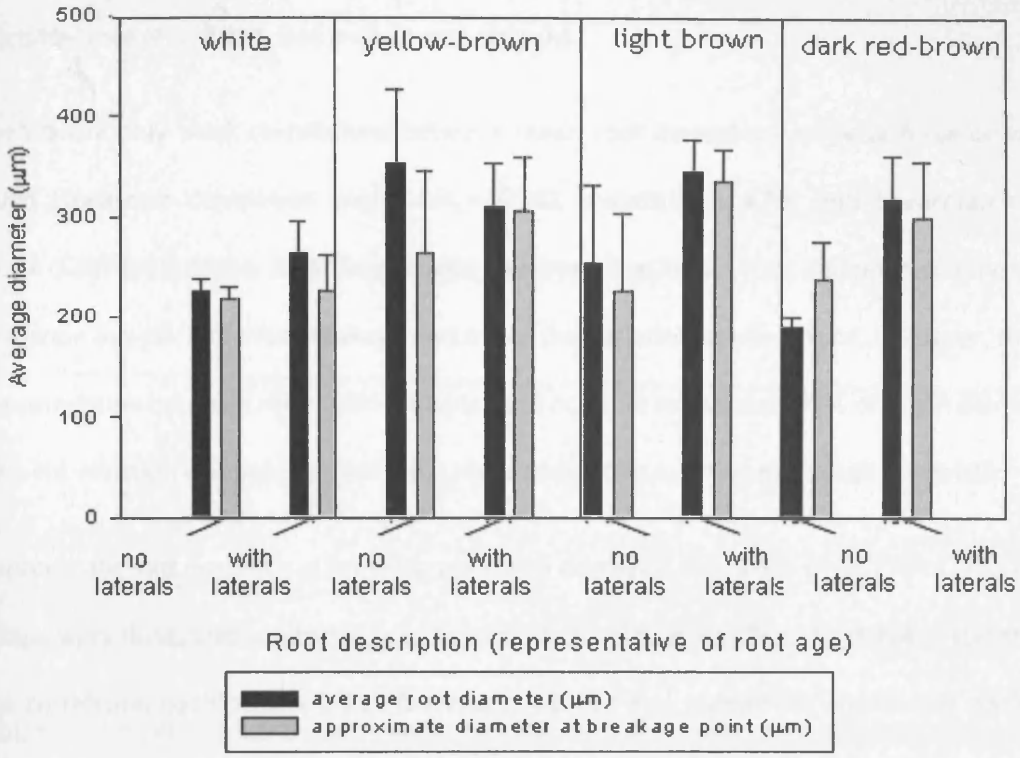

Figure 6.14 The relationship between mean root diameter or approximate diameter at breakage point and root age as represented by their colour, in a sample population of 136 roots, taken from 7 different transgenic plants expressing the secreted form of IgG. (Means and SEMs represent 50 white roots without laterals, 11 white roots with laterals, 6 yellow-brown roots without laterals, 16 yellow-brown roots with laterals, 5 brown roots without laterals, 37 brown roots with laterals, 2 dark red-brown roots without laterals, and 9 dark red-brown roots with laterals.

To determine whether diameter at breakage should be considered as another variable in this study, Kruskal-Wallis analysis was done to compare this with mean root diameter. A statistical difference between these two parameters was observed (P = 0.0001), suggesting that approximate diameter at breakage should be examined as a separate variable. However, as is apparent in Figure 6.14, there was no statistical difference between the approximate breakage diameters of the different root categories (P = 0.60, Kruskal-Wallis, ANOVA). The approximate diameter at breakage point for comparing the white and

light brown roots, and the white roots with the dark red-brown roots (with laterals only) also showed no significant difference (P = 0.094, and p= 0.43 respectively).

There were only weak correlations between mean root diameter and peak force or work done were found (Spearman correlation coefficient = 0.381 (*t*-statistic = 4.73) and Spearman correlation coefficient = 0.289 (*t*-statistic = 3.38) respectively) meaning that mean root diameter could only explain 15% of variation in peak force for breakage and 8% of the variation in work done. However, there was a moderate correlation between root mean diameter and nominal stress, with 36% of mean diameter being responsible for variation in nominal stress (Spearman correlation coefficient = 0.599 (*t*-statistic = 8.46).

Approximate root diameter at breaking point also displayed only weak correlations with peak force for breakage, work done, and nominal stress, (Spearman correlation coefficient = 0.258 (*t*-statistic = 3.06), Spearman correlation coefficient = 0.217 (*t*-statistic = 2.48), and Spearman correlation coefficient = -0.463 (*t*-statistic = -5.89) respectively) meaning that approximate root diameter at breaking point could only explain 7% of variation in peak force for breakage and 5% of the variation in work done, and 15% of variation in nominal stress.

The fact that there are no significant differences between fresh root mass, original root length, or mean root diameter for any of the root categories, displays the uniformity of plant roots which would be an additional advantage of bioprocessing from transgenic tobacco roots for IgG production as an alternative to IgG extraction from leaves. Where only weak correlations exist between two parameters, more measurements by micromanipulation are required to ensure that these correlations are not significant for an even larger sample size.

6.9 LIGNIN

The increase in peak force for breakage between the white roots and the dark red-brown roots may be explained by the increasing deposition of lignin as the roots mature, which confer increased mechanical strength to the root, thus making them more difficult to break. Lignins are heterogenous tridimensional phenolic polymers resulting from the polymerisation of cinnamyl alcohols, known as monolignols (Piquemal *et al.*, 1998). It is water insoluble and thus immobile. It is made in the cell wall, initially being formed in the middle lamella and primary cell wall of cells such as xylem vessel elements and phloem fibres which have thick secondary walls. Thus, the initial site of lignification may be about 10 μm distant (thickness of secondary wall) from the nearest living protoplasm (Fry, 2004). Lignin gives plants its "woody" nature. Its composition varies from plant to plant and across individual cell walls (Hibino *et al.*, 1994; Takabe *et al.*, 1986; Terashima *et al.*, 1986). Hepworth *et al.* (1998) studied lignified xylem tissue (wood) from *Nicotiana tabacum* plants and found that that the content of lignin in tobacco plants (40-45%) is similar to that in a tree. It was suggested that tobacco plant lignin has a much lower crosslink density than that of a tree, allowing large amounts of permanent deformation when load is applied over a long timescale (Hepworth *et al.*, 1998). It has been shown that root apoplasts can be enriched in lignins (Schreiber, 1996). Lignin and phenolics are deposited in the cortex of the roots so that the cortical cells break down and periderm is formed (Burgess *et al.* 1999).

As was mentioned above, fine roots are white when first produced, but then become brown with age and remain in this state, without visible secondary thickening, for the majority of their life span (Hendrick and Pregitzer, 1992; McKenzie and Peterson, 1995; Richards and Considine, 1981). Root "browning" occurs in older roots due to the senescence of the root cortex (Wells *et al.*, 2003). New fine roots are white in colour but become brown several weeks to months after their production (Comas *et al.*, 2000; Wang *et al.*, 1995; Wells and Eissenstat, 2001). A proportion of brown roots eventually become black and shriveled appearance before vanishing, but others are retained and function in successive growing seasons (Wells *et al.*, 2003).

Neither suberisation (the deposition of suberin lamelle in the root endordermis and exodermis) nor the development of the secondary xylem has been directly linked to root browning (McCrady and Comerford, 1998). Instead, browning is associated with the accumulation of condensed tannin in cortical cell walls and the death of the epidermis and cortex, resulting in a dead, tannin-filled sheath around an intact and living stele (McKenzie and Peterson, 1995). Thus, although lignification is not directly linked to the brown colour of roots, the intensity of brown root colour is known to increase with age, and lignification is also a developmental process, and thus can be used as an indication of increased lignification.

Although root browning is a normal developmental process occurring under axenic conditions (Liljeroth, 1995), there are some external factors that can accelerate browning rate. These include interactions with nematodes and fungal pathogens (Allen, 1989; Dunn, 1979; Liljeroth, 1995).

Phloroglucinol staining was done on each root type to demonstrate this increase in lignin with root maturation. Areas of lignin deposition are stained red by Phloroglucinol. Figure 6.15 illustrates the increase in lignin amount with the different root types, as classified in this study. The black areas within the root in these black and white images represent the red stain, indicating areas of lignin deposition. The white root shows the stained region only in the middle of the root (root xylem and phloem). The yellow-brown root shows staining in central xylem and phloem, some of the surrounding cortex, and in the outer epidermal layer also. The light brown root has staining throughout the root section, as does the dark red-brown root, also with complete staining showing presence of lignin in the whole root. It is worth noting here that the browning effect observed in more mature roots is not attributed to the development of secondary xylem such as lignin, but is a result of accumulation of condensed tannin in cortical cell walls and the death of the epidermis and cortex (McCrady and Comerford, 1998; McKenzie and Peterson, 1995). Given the increase in lignin, it is important to establish the effect root ageing has on the expression of IgG, as considered in Section 6.10.

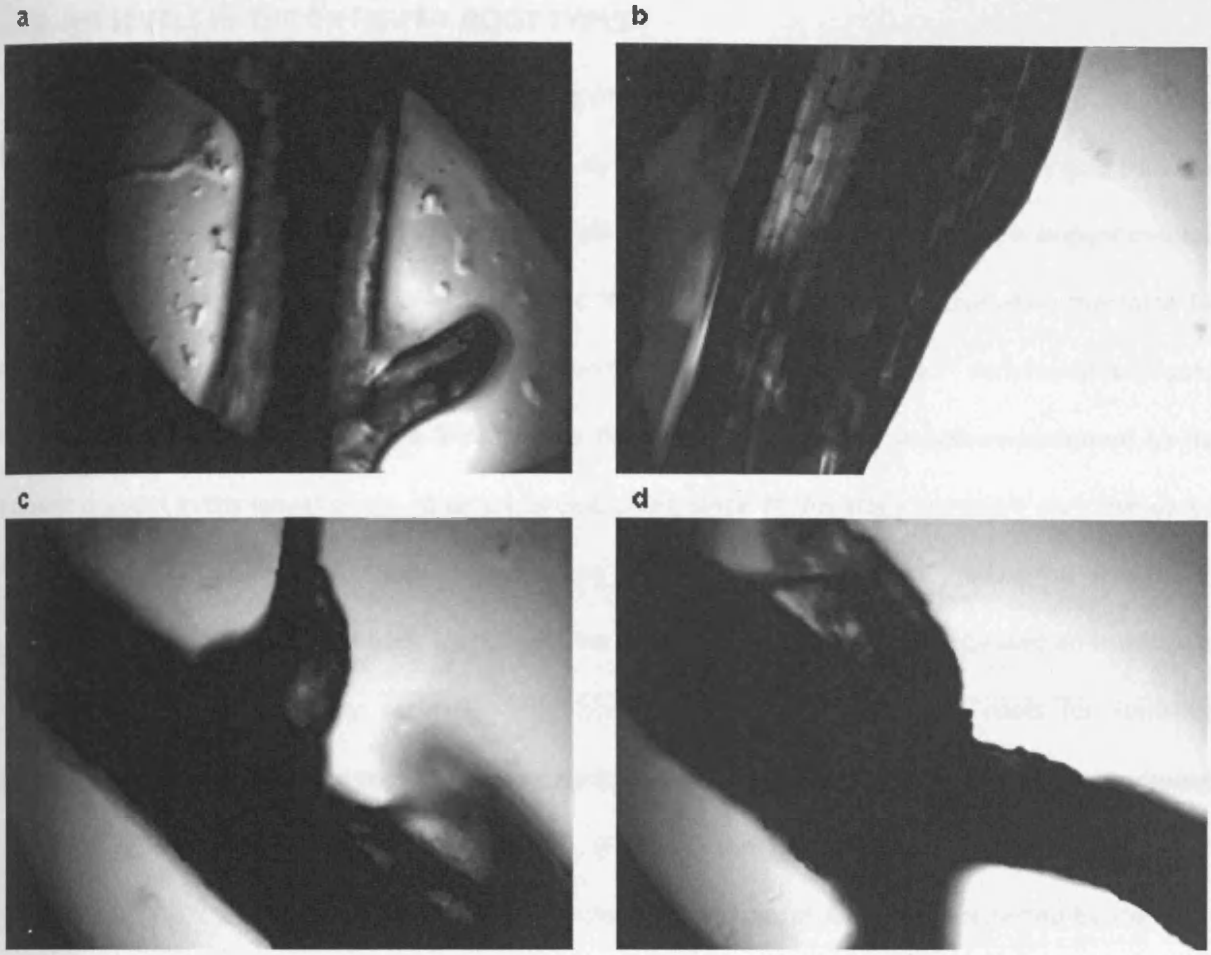

Figure 6.15 Phloroglucinol staining to show increase in lignin amount of different root types as classified according to the degree of brownness. a) white root b) yellow-brown root, c) light brown root d) dark red-brown root

It is thought that the polymer entanglement properties is formed by lignin whilst cellulose, hemicellulose and pectin supply a fully crosslinked backbone structure with more normal elastic and plastic properties (Hepworth *et al.*, 1998). This entanglement of lignin networks provides a good explanation for the increased root strength with increasing lignin deposition.

6.10 IgG LEVELS IN THE DIFFERENT ROOT TYPES

Figure 6.16a shows the amount of IgG per Kg of fresh root tissue for a representative plant. At this microcentrifuge scale, extractions were performed by grinding in liquid nitrogen, since the gold standard employed in chapter 3 of grinding in buffer was insufficient for visible root breakage. It is evident that IgG levels in the different coloured roots of transgenic *Nicotiana tabacum* are approximately the same for white roots through to the light brown roots, but decreases for the "fully-matured" dark red-brown roots. It is not surprising that the dark-red brown roots have the least amount of IgG as compared to the amount present in the leaves of the same transgenic plant, since at this stage there are very few water-filled active cells (Steudle *et al.*, 1998), and most are likely to be "fully-lignified". Since this data is only representative of one plant, and each plant had a varying net yield of IgG, and possessed an insufficient amount of the less frequently occurring root types such as dark red-brown roots for statistical comparison, it was necessary to convert all the data for 6 plants (which were included in this experiment) into IgG as a % of leaves before statistical analysis, (Figure 6.16b). The extractable level of IgG from all root types is 40- 70% of the total IgG in the equivalent fresh mass of leaf discs (extracted by the same method), with the exception of the dark red-brown roots which are only capable of producing 5-9% of the level of IgG in the leaves.

However, no statistically significant difference in IgG levels between any of the coloured-roots was found, ($P = 0.25$, ANOVA, General linear model). The same conclusion was deduced for comparing just the white and dark red-brown roots or just light brown and dark red-brown roots, ($P = 0.081$ or $P = 0.058$ respectively, ANOVA, General linear model). One possible explanation is in that older roots have more laterals containing IgG, thus compensating for areas in the root where lignin formation inhibits soluble IgG expression.

This chapter (summarised in Hassan *et al.* 2008a) addresses a fundamental understanding of the force required to break transgenic tobacco roots. Such knowledge may form the basis for establishing the large scale minimum energy requirements to extract IgG from tobacco roots. The next two chapters addresses relating the energy requirements for breakage of single transgenic tobacco roots by

micromanipulation to the minimum energy requirements in a mechanical shear device, forming part of a process for extraction and recovery of the antibody from the roots.

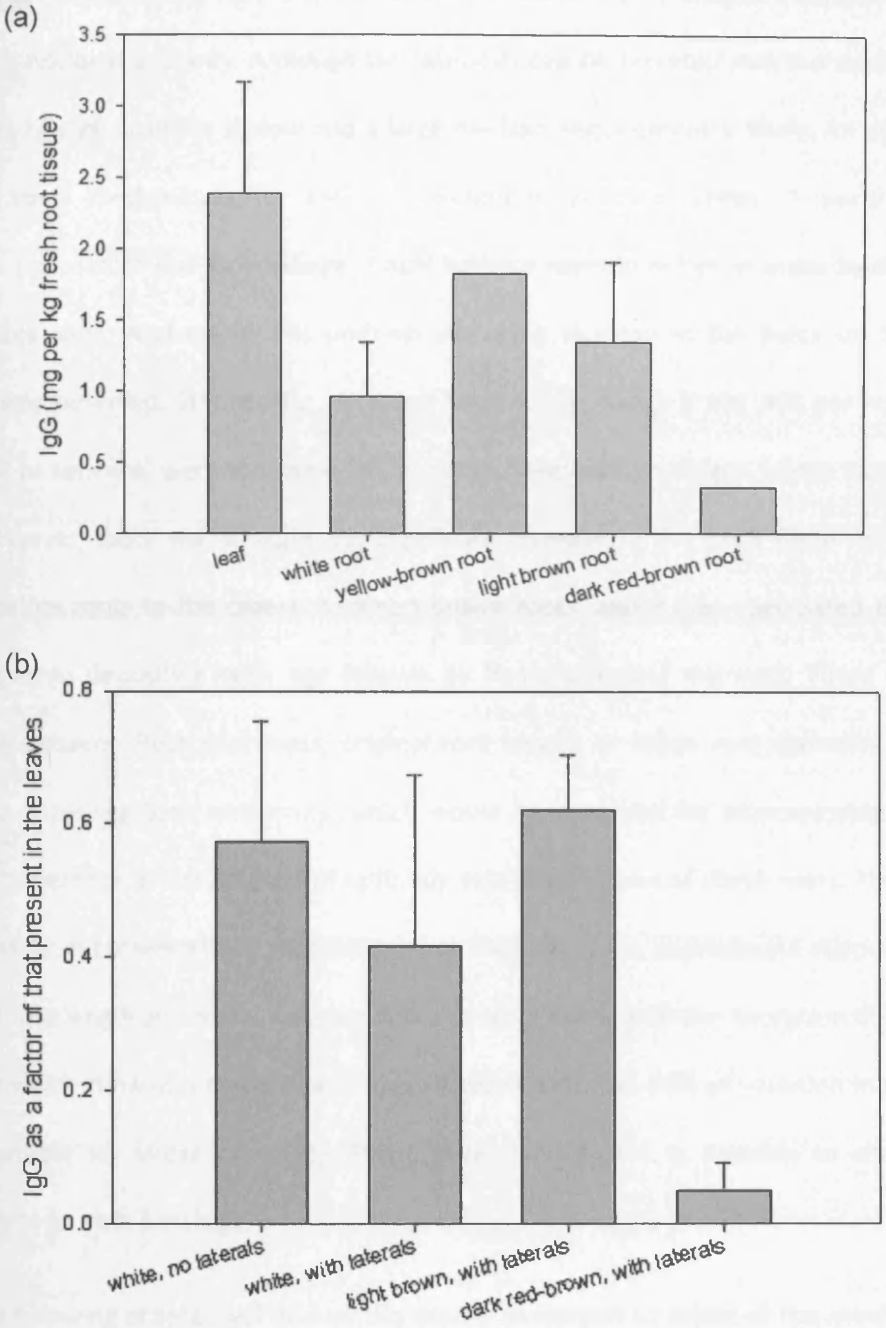

Figure 6.16 (a) IgG in the roots of a representative plant. (Averages and SEMs are triplicates to 4 replicates, except for yellow-brown and dark red-brown roots did not possess enough of these root types for replicates; however similar trends were found for all other plants tested). (b) IgG in 1 cm roots as a factor of that present in the same fresh mass of leaf discs of the same plants (results were taken from 6 plants in soil and averages and SEMs are of triplicate samples).

6.11 CONCLUSIONS

This chapter has described a new approach that allows the determination of the magnitude of force required to break single plant roots. Roots were taken from transgenic tobacco plants, expressing a secreted monoclonal antibody. Although this antibody can be secreted into the medium in a hydroponic system, the rate of secretion is slow and a large medium requirement is likely. An alternative is to break open the roots mechanically for the optimisation of antibody yields. A novel micromanipulation technique was used to pull to breakage, single tobacco roots in buffer in order to determine their peak force for breakage. A characteristic uniform step-wise increase in the force up to a peak force for breakage was observed. Statistically, the peak force for breakage (~101 mN per root) and mean work done (~ 97 μJ per root) were the same for four root development stages, which were identified by their colour. However, there was a slight but significant increase in the peak force for breakage from the youngest white roots to the oldest, dark red-brown roots, and it was speculated that this was due to increasing lignin deposition with age (shown by Phuloroglucinol staining). There were no significant differences between fresh root mass, original root length, or mean root diameter for any of the root categories, displaying their uniformity, which would be beneficial for bioprocessing. There was no also significant difference in the amount of antibody expressed in any of these roots. There were no or only weak correlations between fresh root mass, mean root diameter, approximate diameter at breaking point or original root length and force, nominal stress or work done, with the exception of mean root diameter and stress which showed a moderately negative correlation (i.e. 36% of variation in mean root diameter was responsible for stress variation). These data show that it is possible to characterise the force requirements for root breakage.

The following chapter will discuss the theory developed to relate of the mechanical properties of single root sections, characterised in this chapter, to the minimum energy dissipation requirements in a mechanically stirred shear device to assist in the optimisation of recombinant protein extraction from these roots.

Chapter 7- Theory for root tensile strength estimation in an ultra-scale down mechanical shear device

7.1 INTRODUCTION

There are currently broad uses of monoclonal antibodies (MAbs) within diagnosis, infectious diseases treatment, and cancer (Fischer and Emans, 2000). Up until now, the main expression systems for recombinant MAbs have been mammalian cell culture, myeloma lines and Chinese Hamster Ovary (CHO) cells (Wurm, 2004). The downside of mammalian cell culture is that it is expensive and not sufficiently scalable for some potential applications. Transgenic plants offer a possible alternative. Complex full-length immunoglobulins have been successfully expressed in transgenic tobacco to levels of up to 8% of the total soluble protein (Ma *et al.*, 1994). Transgenic plant advantages include easier upstream scale-up, low upstream cost (in comparison to steel fermenters), and the low risk of mammalian virus contamination (Drake *et al.*, 2003). Here, the extraction of Guy's 13 MAb from transgenic tobacco is studied. This MAb acts against *Streptococcus mutans* (van Dolleweerd *et al.*, 2003), the main causative agent of tooth decay in the mouth.

Most of the literature describing monoclonal antibody production from *Nicotiana tabacum* plants has involved its extraction from fresh leaf tissue (Ko *et al.*, 2004, Ma *et al.*, 2003, Valdés *et al.*, 2003). This is largely because tobacco leaves represent the majority of the total biomass of the plant. However, the extraction of the MAb from tobacco roots may also be viable, since roots show similar IgG levels to the leaves per unit fresh mass (Hassan *et al.* 2008a), and also contain lower levels of toxic phenolics and alkaloids. The nicotine level in tobacco leaves, for example, is three times that in the roots (Dawson *et al.*, 1959), thus potentially posing a greater burden on downstream processing.

Mechanical extraction methods are thought to be necessary to recovery monoclonal antibodies from transgenic tobacco roots. Chapter 8 will investigate the applicability of a mechanically stirred shear device for the extraction of IgG. This device is based on the design of an original shear device (Boychyn *et*

al., 2000) used on liquid material, but differs mainly in that instead of a smooth-edged rotating disc, the disc has 8 blades each with a serrated edge for plant material breakage, and is enclosed in a Perspex chamber. The design of the device was such that it was thought to be efficient at breaking plant material, and is likely to be scalable, as has been shown for the original device (Boychyn *et al.*, 2000). In order to extract the monoclonal antibody in this system, the roots are suspended in buffer.

No literature exists that is specific to the disruption of tobacco roots in a mechanically stirred shearing device, nor is there anything on the possible mechanisms by which such disruption might occur. However, there are several possibilities including: root breakage by turbulence (hydrodynamic forces), root-root, root-impeller, or root-chamber wall collisions, the latter of which includes collision with any internal part of the device excluding the moving impeller. Although in practice, breakage could be due to any or all of these processes, it is important to establish the dominant mechanism of breakage, in order to develop a mathematical model of the disruption process.

Although there is nothing specific on the behaviour of roots in a mechanically stirred shearing device, a significant amount of literature does exist on the breakage or fragmentation of other small biological materials such as yeast or filamentous fungi during homogenisation (Keshavarz-Moore *et al.*, 1987) or fermentation (Jüsten *et al.* 1998b). In addition, there is some literature on breakage of particles by impaction (Kee and Rielly, 1997), which may be implicated in damage to roots via mechanical extraction.

There have been several attempts to model breakage of filamentous fungi in stirred fermenters. The definitive work of Jüsten and co-workers, showed that the main phenomenon was the breakage of short, freely dispersed hyphae from mycelia clumps (Jüsten *et al.*, 1996; Jüsten *et al.*, 1998a) and that the growth, morphology, vacuolation and productivity of Penicillium chrysogenum in fed-batch fermentation depended on the "energy dissipation/circulation function" (EDC) in the fermenter (Jüsten *et al.*, 1996, 1998b). The utility of this mixing parameter was confirmed by Amanullah *et al.* (1998) for work on recombinant protein production by Aspergillus oryzae. Jüsten *et al.* (1996) showed that it was important

not just to consider the freely dispersed hyphae in evaluating fungal morphology in agitated fermentations, because this might lead to the incorrect impression that these forms are broken to create shorter hyphae, rather than being created by fragmentation from clumps. Despite this, Li *et al.* (2002) considered only freely dispersed hyphae in estimating hyphal tensile strength using a model in which breakage was due to hypha-turbulence interactions. The main assumption was that under given process conditions, the equilibrium length of an individual hypha is determined by a balance between hyphal strength (resisting breakage) and hydrodynamic forces (causing breakage). Despite the inappropriate use of this model for describing fungal fermentations, the approach of Li *et al.* (2002) may still be relevant to the present study, because there are no clumps in root section suspensions (and no growth).

An alternative mechanism of breakage for the roots in a mechanically stirred shearing device is impact, or collision of the roots with a solid surface. There are some examples in the literature where the particles are fragile and undergo break-up or abrasion by collision with the blade; in other cases the particles may be harder than the impeller material, so that the blade itself undergoes severe erosion (Kipke, 1980; Weetman, 1994, 1996). For example, size reduction of friable catalysts or agglomerates can be caused by mechanical collisions with the blade, and in crystallisation processes, impacts between crystals and impeller blades may lead to breakage or abrasion and the formation of secondary nucleation sites (Evans *et al.*, 1974; Synowiec *et al.*, 1993). Within these solid liquid mixing systems, the distribution of the impact velocities of the particles depends on their mass and size but also on local hydrodynamic conditions near the impeller blades (Kee and Rielly, 2004). Ploss and Mermann (1989), van der Heijedin *et al.* (1994) and Meadhra *et al.*, (1996) reported that the energy of impact and the target efficiency are functions of particle size and the local hydrodynamics. During solid-liquid abrasion, fluid mechanical effects alter the particle velocity as a solid surface is approached (Humphrey, 1990). It has been demonstrated that there is always a difference between the impact angle and velocity of a particle on a surface and its initial angle and velocity (Laitone, 1979; Kee and Rielly, 1997).

Nienow (1976) investigated the effect of crystal collisions with an impeller on the resulting secondary nucleation rate. The distribution of impact positions on Rushton blades was investigated by

use of an evenly covered grease coating on the impeller which captured the particles. In this case, particles most frequently impacted the inner part of the blades, above and below the disc of the Rushton impeller, and these findings were explained by swirling flow around each blade. Takahashi *et al.* (1992) and He *et al.* (1995) also measured the particle impact positions on Rushton and pitched blade turbines, using a wax crayon method. Contrary to Nienow (1976), they concluded that the outer and lower edges of Rushton turbine blades experienced the highest impact frequency, whereas for downward-pumping pitched blades, the outer, upper edges of the blades endured the most impacts. Kee and Rielly (2004) suggested that these differences may have been caused by transient effects and/or differences in the softness of the coated layers, meaning that different particle impact energy ranges were recorded. Kee and Rielly (2004) used an improved coating technique involving plasticine to obtain the particle impact position distribution on both Rushton and downward-pumping, 45° pitched blades in a mixing tank. The highest particle impact frequencies were found to be below the disc for the Rushton impeller, and on the lower half of the blade, at the inner edge of the pitched blade impeller.

A model describing the motion of a spherical particle at an oblique angle during plastic impact was developed by Hutchings *et al.* (1976), and was later improved by Rickerby and MacMillan (1980) in order to give a better representation of the actual contact area between the particle and target surface during the impact process, so that subsequently a better correlation between experimental results and numerical predictions was achieved (Hutchings *et al.*, 1981).

By modelling the fragmentation of roots as a function of agitation time, the intention was to discover the dominant mechanism, if any. Regardless of the mechanism(s) of root breakage in a mechanically stirred shearing device, damage will depend on root mechanical properties, and some estimate of the mean tensile strength of the roots was also sought. This could be compared with the mean tensile strength of roots as previously determined using micromanipulation (Hassan *et al.*, 2008a). Micromanipulation was previously used to pull single roots in buffer to breakage, and thus determined their mean breakage force (101 ± 7 mN), the work done for breakage (97 ± 6 μJ), and their tensile strength (2400 ± 200 kPa) (Chapter 6). The goal of this study was to establish whether these

micromanipulation results could be used to predict the minimum energy dissipation requirement in a mechanically stirred shearing device for the extraction of Guy's 13 MAb from transgenic tobacco roots.

7.2 THEORY

As described above, there are several possible mechanisms for breakage of root sections in the mechanically stirred shearing device. These include hydrodynamic forces ("shear") resulting from turbulent eddies, or collisions of roots with solid surfaces or even with other roots. However, due to the large relative size and density of the roots in comparision to the buffer in which they are suspended, it is thought likely that their breakage is mainly due to root-solid surface collisions. Although these collisions will occur with any internal solid surface of the device, the assumption is made here that root breakage will predominantly be a consequence of impaction with the moving impeller.

Assuming that the maximum particle velocity is approximately equal to the linear speed of the impeller at the radius of the impact, the maximum impact energy for a particle colliding with the blade at radius r would be

$$E_{max} \approx \frac{1}{2} m_p (2\pi N r)^2 \qquad (7.1)$$

(Kee and Rielly, 2004) where m_p is the mass of a single root, N is the impeller speed (s^{-1}) and r is the impeller radius (m). However, this does not take into account the collision efficiency,η or the probability of a particle colliding with one of the 8 blades. Assuming that every collision of a single root with an impeller blade is successful in causing breakage of the root,

$$work\ done\ for\ breakage = Emax.\eta \qquad (7.2)$$

where η is the collision efficiency, which according to Kee and Rielly (2004) is,

$$\eta = \frac{n_{blade} R_p}{f_c} \tag{7.3}$$

where n_{blade} is the number of blades of the impeller. Takahashi *et al.* (1992) postulated that the start-up transient period, of up to 30s in duration, has a significant effect on impact distribution and thus affects the impact rate. Thus impact rate is given by:

$$R_i = \frac{n_t - n_{30}}{t - 30} \tag{7.4}$$

where n_t is the number of impact marks on a blade of the impeller at time t, and n_{30} is the number of impact marks on a blade of the impeller after 30 secs. This equation was also used by Kee and Rielly 2004, who further suggested that impact rates should be normalised by the number of particles in the tank for each particle size.

$$R_p = \frac{R_i}{n_p} \tag{7.5}$$

Both Takahashi *et al.*, (1992) and Kee and Rielly (2004) investigated particle-impeller collisions by coating the blades of the impeller with black wax crayon in the former and plasticine in the latter, in order that every impact of a particle with the impeller could be recorded. In our case the impeller was not coated with any softer materials, however it was possible to estimate the number of "imaginary" marks on the blade of the impeller from the product of the number of times a single root is broken and the number of roots that collide with the impeller in that time period, divided by the number of blades of the impeller, i.e. assuming that the number of roots that collide with each blade of the impeller at any time point is equal.

$$n_t = \frac{n_r n_{r-i}}{n_{blade}} \tag{7.6}$$

where n_r is the number of times that a single root is broken (an explanation of how this is estimated is described below under Results and Discussion, and $n_{r\text{-}i}$ is the number of roots that collide with the impeller during that time period.

In equation 3, f_c is the frequency with which fluid elements are pumped through the impeller region (Kee and Rielly 2004),

$$f_c = \frac{Fl N D^3}{V} \tag{7.7}$$

For our impeller, the impeller flow number, Fl was calculated from the following equation for radial flow impellers (Platzer and Noll., 1983).

$$Fl = (0.91 P_o \left(\frac{W}{D}\right)^{0.5} \tag{7.8}$$

Once the work done for breakage is estimated from equations (7.1) to (7.8), it is possible to estimate the force for breakage since

$$force\ for\ breakage = \frac{work\ done\ for\ breakage}{distance\ moved\ in\ the\ direction\ of\ the\ force} \tag{7.9}$$

where the distance moved in the direction of the force is assumed to be the maximum possible distance of movement in the radial direction, i.e. the distance between the disc and the chamber walls (0.0125m), (assuming linear elastic behaviour).

Thus the stress due to impeller blade root impact, τ_i is the force for breakage, F_b, per unit root cross-sectional area, i.e.

$$\tau_i = \frac{F_b}{\pi d^2/4} \tag{7.10}$$

It was next attempted to relate this stress due to the impeller blade root impact with the tensile strength of the root. In using the classical strain energy criterion of failure, it is assumed that the root

obeys Hooke's law up to some elastic limit, beyond which non-recoverable "permanent" deformations occur eventually leading to rupture. However, experimental observations (Chapter 6) showed that root deformation by pulling was not entirely elastic up to breakage, since there was a step-wise increase in the force with displacement until the root was completely broken into two sections. Nevertheless, if breakage by any mechanism is assumed to be a first-order process, the dependence of the mean main root length, L, on the agitation time, t, may be expressed as

$$\frac{dL}{dt} = q_{frag}(L_E - L) \tag{7.11}$$

where q_{frag} is a first-order rate breakage constant (s^{-1}) and L_E is the mean main root length at equilibrium, i.e. at very long times. This equation correctly assumes that breakage is the dominant mechanism in determining root length, with negligible permanent deformation of the roots during agitation.

Equation (7.11) can be solved noting that mean root length at time 0, $L = L_0$ and mean root length at equilibrium, $L = L_E$ when $t \rightarrow \infty$.

$$\frac{L - L_E}{L_0 - L_E} = exp(-q_{frag}t) \tag{7.12}$$

Equation (7.12) suggests that $\ln[L - L_E]$ plotted against time, t, should be a straight line with a slope equal to the breakage rate constant k. Equations (7.11) and (7.12) above were taken from Ayazi Shamlou *et al.* (1994a) and Li *et al.* (2002).

Li *et al.*, (2002), investigated the breakage of filamentous fungal hyphae (which are much smaller than our root pieces) during fermentation. Since filamentous fungal hyphae are much smaller than roots ~ 100-300 μm, and also have a density close to that of water, it was concluded that the main mechanism of breakage in their case was hydrodynamic stresses due to turbulent eddies acting on the cell surface. They suggested the following expression for hyphal tensile strength:

$$\sigma_h = \tau_s ln\left(\frac{S}{q_{frag}}\right) + (\tau_s ln K_2) \tag{7.13}$$

where S is the eddy-hyphae contact frequency, q_{frag} is specific hyphal fragmentation rate for freely dispersed hyphae (also described by Nielsen and Krabben, (1995); Li *et al.*, (2002)), τ_s is stress due to turbulent eddies acting on the cell surface, and K_2 is a constant. q_{frag} was determined as described above graphically from equation (7.12). Since K_2 was dependent upon morphology and hydrodynamics during the fermentation, and also on the hyphal tensile strength, Li *et al.*, (2002) suggested using the first term in equation 7.13 to estimate pseudo tensile strength, σ_{pseudo}, thus providing a means by which available experimental data could be used to obtain a relative measure of tensile strength. A similar approach was used here where

$$\sigma_{pseudo} = \tau_i ln\left(\frac{R_p}{q_{frag}}\right) \tag{7.14}$$

The value of relative tensile strength estimated by a mixture of experimental data and theoretical modelling equations above, was then compared with the tensile strength (nominal stress) measured by pulling single transgenic tobacco roots by micromanipulation (Chapter 6) for comparison.

Chapter 8- Estimation of root tensile strength for the extraction of monoclonal antibodies from transgenic tobacco plants

8.1 INTRODUCTION

As discussed in the previous chapter, most literature to date, describing monoclonal antibody production from *Nicotiana tabacum* plants has involved its extraction from fresh leaf tissue (Ko *et al.*, 2004; Ma *et al.*, 2003; Valdés *et al.*, 2003). This is largely due to the fact that tobacco leaves represent the majority of the total biomass of the plant. However, the extraction of the MAb from tobacco roots may also be viable, since roots show similar IgG levels to the leaves per unit fresh mass (Hassan *et al.* 2008a), and also contain lower levels of toxic phenolics and alkaloids.

In Chapter 6, a micromanipulation technique was used to pull single root sections to breakage in buffer and their mean force (101 ± 7 mN), work done for breakage (97 ± 6 μJ), and tensile strength (2400 ± 200 KPa) were determined. The goal of this chapter is to establish whether these micromanipulation results could be used to determine the minimum energy dissipation requirements in a mechanically stirred shear device used to extract Guy's 13 MAb from transgenic tobacco roots. In this chapter, roots are broken in buffer using this device, macroscopically (i.e. 126X the initial number of roots), to characterise transgenic tobacco root breakage and find the optimal operating conditions for MAb recovery. A model was proposed for the crude estimation of the mean tensile strength of the roots that are broken in the device in Chapter 7, and this is compared with the mean tensile strength of roots previously determined using micromanipulation (Chapter 6). The minimum energy dissipation requirement within a scalable mechanically stirred shear device for MAb recovery from transgenic tobacco roots is also estimated.

8.2 MECHANICALLY STIRRED SHEAR DEVICE

In Chapter 6, the mechanical properties of transgenic *Nicotiana tabacum* roots were examined by micromanipulation, because tobacco offers a potential alternative to leaves for IgG production. This chapter investigates the macromanipulation of similar roots in a mechanically stirred shear device (described in Chapter 2, Section 2.7.2). (Macromanipulation is defined throughout this Chapter as the mechanical agitation of 126 roots (1 cm long) in a buffer system to cause root breakage). Figure 8.1 shows data from an experiment were IgG extraction from the same mass (1 g) of leaf discs and roots (sliced into 1 cm root sections), were broken in 20 ml of phosphate buffer saline using the mechanically stirred shear device, operating at 7020 rpm for 30 seconds. After centrifugation, the supernatant was analysed for immunoglobulin detection. This figure shows that the mechanically stirred breakage device is capable of extracting the same amount of IgG as that present in the leaves, whereas grinding in liquid nitrogen only gives 50% of the extractable IgG from the leaves.

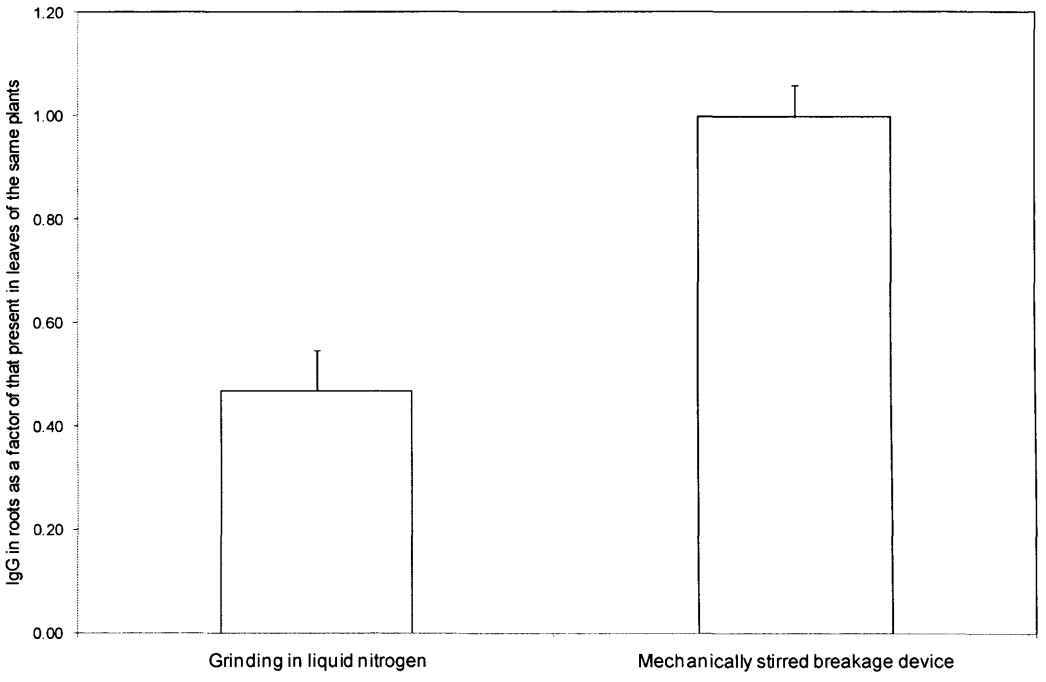

Figure 8.1 Comparison of IgG (secreted form) from the roots of transgenic tobacco as a factor of that present in the leaves of the same plants, extracted either by grinding in liquid nitrogen or with the mechanically stirred breakage device. (Averages and SEMs are of triplicate samples).

The shear device used in experimentation was as described in Chapter 2, Section 2.7.2.

8.3 THE OPTIMAL AGITATION TIME AT $75s^{-1}$ FOR MONOCLONAL ANTIBODY EXTRACTION FROM TRANSGENIC TOBACCO ROOTS

There are many reasons why it is important to limit the mixing time at a constant operational speed. Not only is it economically beneficial in terms of saving energy usage of the device and limiting variable costs, it also limits the possibility of antibody loss due to either heat generation or extended exposure to proteases that are co-extracted from the roots during the disruptive mixing process. Another main advantage of using the minimal agitation time is limiting overall process time, potentially increasing process turnover and overall profits. In addition, it is advantageous to limit fine debris material by agitation for the minimal time period required, since very fine debris may pose a problem in downstream processing by, for example, fouling chromatography columns, and may require extensive filtration to remove them sufficiently (Hearle *et al.*, 1994). In the case of filtration, very fine particles may reduce flux rates due to blinding and fouling of the membrane (Gray *et al.*, 1973). Centrifugation is not affected by such fouling, and thus offers an alternative to filtration.

Figure 8.2 shows that beyond the processing time of 30 seconds in the shear device, the device is more efficient in extracting IgG than grinding in buffer or grinding in liquid nitrogen (used in Hassan *et al.* 2008a), as IgG as a fraction of grinding in liquid nitrogen or grinding in buffer is maintained at a value greater than 1. (Note that the use of the term shear in "shear device" does not refer to the mechanism of breakage but rather to the act of breakage and has been maintained in this investigation since the original IMRC patented device on which our modified version was based on, was of that name). *(IMRC is the Innovative Manufacturing Research Centre).*

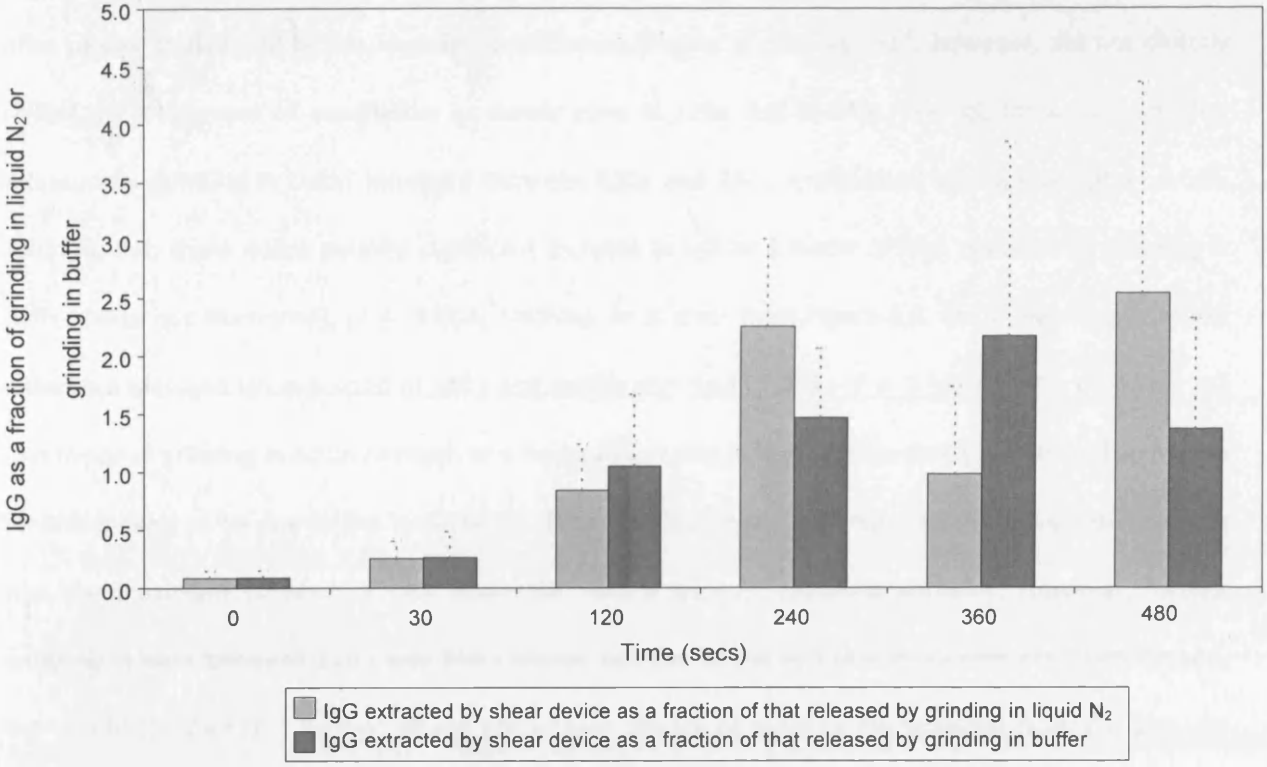

Figure 8.2: The effect of agitation time on IgG extraction from transgenic tobacco roots. IgG data is shown as a fraction of grinding in liquid nitrogen or as grinding in buffer for breakage using the shear device for increasing lengths of time.

Figure 8.3, illustrates the effect of agitation time on antibody extraction, root size reduction, and overall particle number. It is evident that the fraction of remaining intact roots (i.e. those still 1 cm in length) decrease monotonically with time, until 120 s, when it stabilises. The total number of particles (including intact roots and root debris, and estimated as described above), mirrors the decrease in the proportion of intact roots, with a steady increase with time, up to 120 s, when the total number of particles steadies. The total mean root length in the system (estimated as described above), reflects the decrease in the proportion of intact roots in the system, with an expected monotonic decrease until 120 s, when it no longer changes, having reduced the overall root length to approximately 1.6% of its original length. The amount of antibody per gram of fresh root tissue as a fraction of that released by the gold

standard (albeit grinding in liquid nitrogen (Figure 8.3) or grinding directly in buffer (Data not shown)) after mixing as directed by the impeller for different lengths of time at $75s^{-1}$, however, did not directly reflect the attainment of equilibrium or steady state at 120s, but at 240s. The IgG (as a factor of that released by grinding in liquid nitrogen) between 120s and 240s approached significance, ($P = 0.065$, ANOVA). But, there was a definite significant increase in IgG as a factor of that released by grinding in buffer (data not illustrated), ($P = 0.004$, ANOVA). As is clear from Figure 8.3, there was no significant difference between IgG extracted at 240 s and double this time of 480 s ($P = 0.913$ and $P = 0.950$ for IgG as a factor of grinding in liquid nitrogen or a factor of grinding in buffer respectively, ANOVA). The reason for this is likely to be due to the fact that at 120 s, the total mean minimum root length equilibrates, so that the maximum number of cells along the root is broken, releasing antibody. However, further antibody release between 120 s and 240 s occurs, not due to the fact that more cells are being broken, but due to the fact that further mixing encourages release of more of the antibody from the already-ruptured cells. (This particular antibody is located within the apoplasm of the cell; Frigerio *et al.*, 2000).

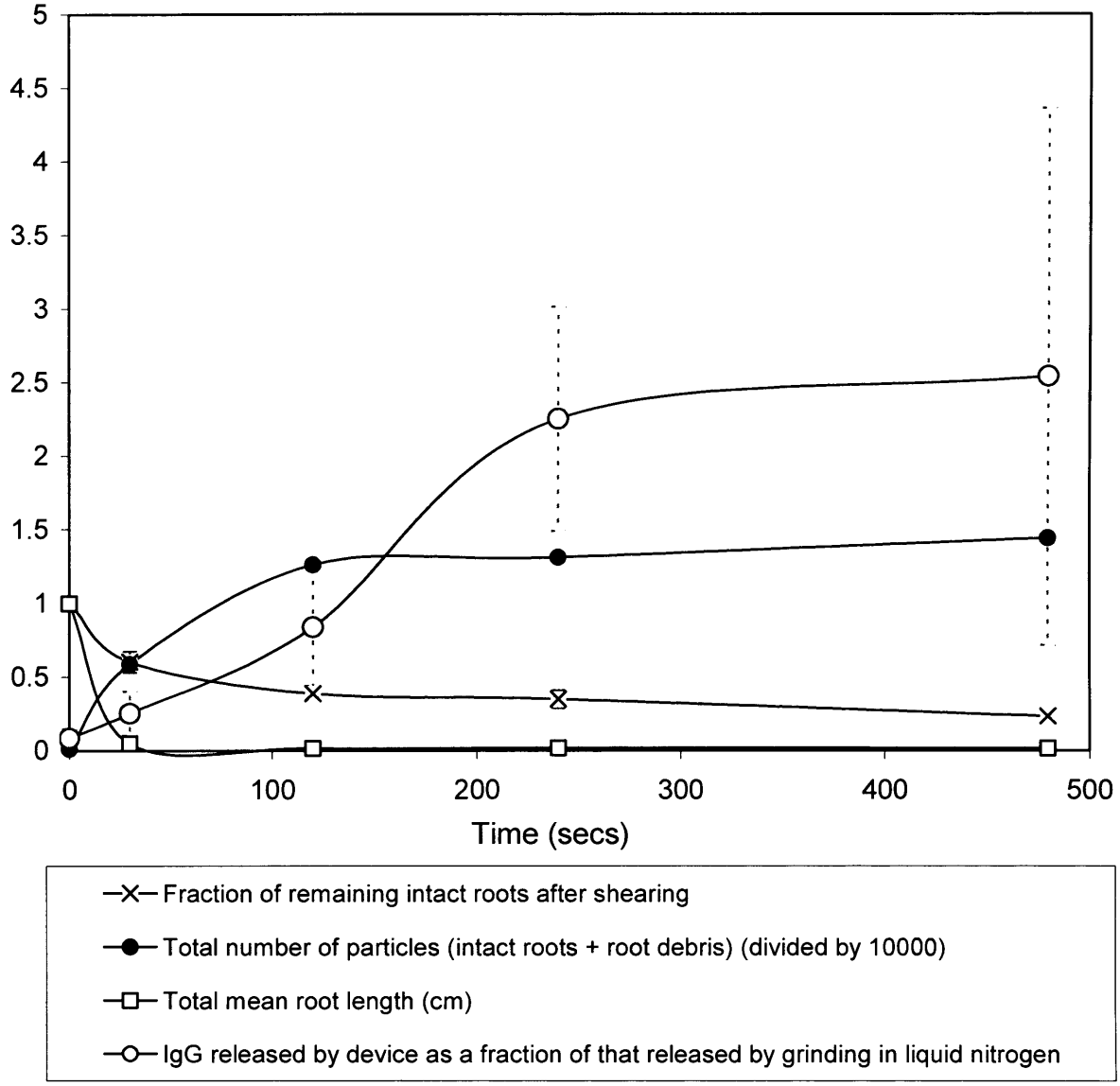

Figure 8.3: The effect of agitation time on IgG extraction from transgenic tobacco roots. The y-axis represents any of the legend key names. (Note the total number of root particles were 10000 times that shown here for the minimum size range investigated). Averages and SEMs are of triplicate samples.

The decrease in the root length during the mechanical extraction process observed in Figure 8.4 appears to follow the first-order process suggested by equation (7.12). Figure 8.5 shows the variation in $\ln[(L_{(t)} - L_E)/ (L_{(t)} - L_E)]$ (a dimensionless group) as a function of time. In plotting this line, it is necessary to have an estimate of the value of the steady-state root length, however, inevitably there will be

uncertainty associated with the determination of L_E because of the experimental errors in root measurements. Despite this, the straight line plot in Figure 8.5 suggest that root breakage (like hypha breakage in fermentation, (Ayazi-Shamlou *et al.*, 1994a)), is a first-order process. The slope of the line in Figure 8.5 is representative of the fragmentation rate (q_{frag}) which equals -0.0226s^{-1}, (illustrating the very fast nature of the mechanical breakage process). In this estimation of q_{frag}, the first 30 seconds of breakage was not included, since Takahashi *et al.* (1992) postulated that the start-up transient period, of up to 30s in duration, has a significant effect on impact distribution. Although speed was not investigated in this analysis, it is expected that as speed is increased the rate of root breakage will increase, however, at very high speeds other factors would have to be taken into account when examining antibody release such as increased temperature generation, and the necessity to control this.

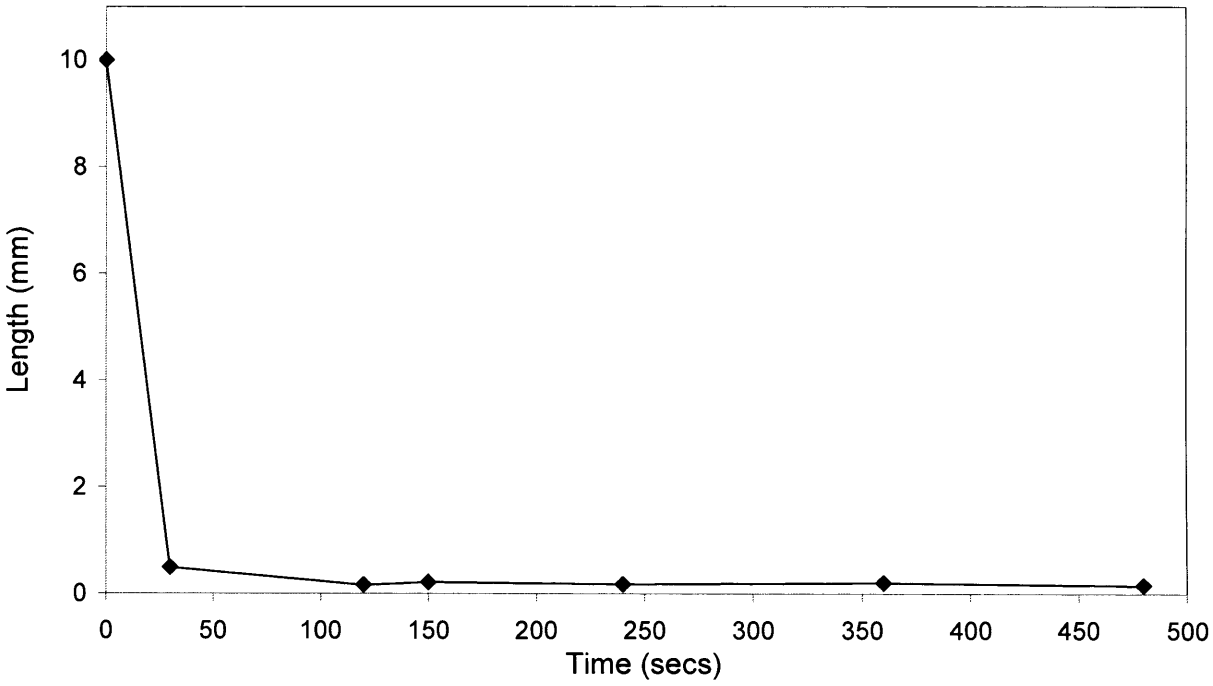

Figure 8.4: Mean root length for root debris and intact roots as a result of roots fragmented at 75s-1 for increasing lengths of time.

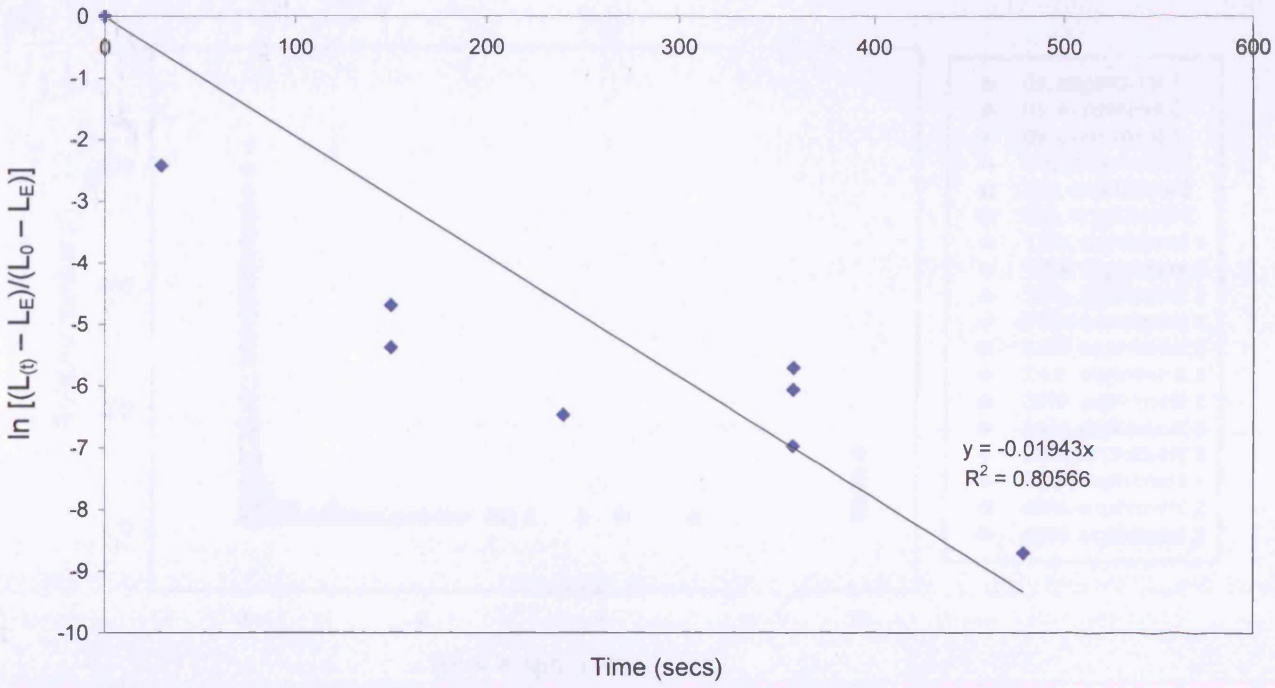

Figure 8.5 Plot of the natural log of $[(L_{(t)} - L_E)/(L_0 - L_E)]$ versus shearing time at a speed of $75s^{-1}$.

To our knowledge whilst there have been some studies looking into fluid-particle systems where breakage is a key parameter affecting particle size, such as oil drops dispersed in an immiscible continuous phase (Delichatsios and Probstein., 1976), protein particles in suspension (Glatz *et al.*, 1986), and breakage of filamentous microorganisms (Ayazi-Shamlou *et al.*, 1994a) there has of yet been no such studies on transgenic plant roots. In all these situations, the time-dependent size distribution of the particles were simulated by using the population balance method or the Monte Carlo simulation technique since they were applied to systems that had particle growth in addition to particle damage. In the mechanically stirred shear device, the root particle size distribution however, is determined solely by the process of root breakage. Figure 8.6a illustrates the particle size distribution of resulting root fragments at each different time point investigated, in triplicate experiments and Figure 8.6b only shows particles that are less than or equal to 0.2 mm.

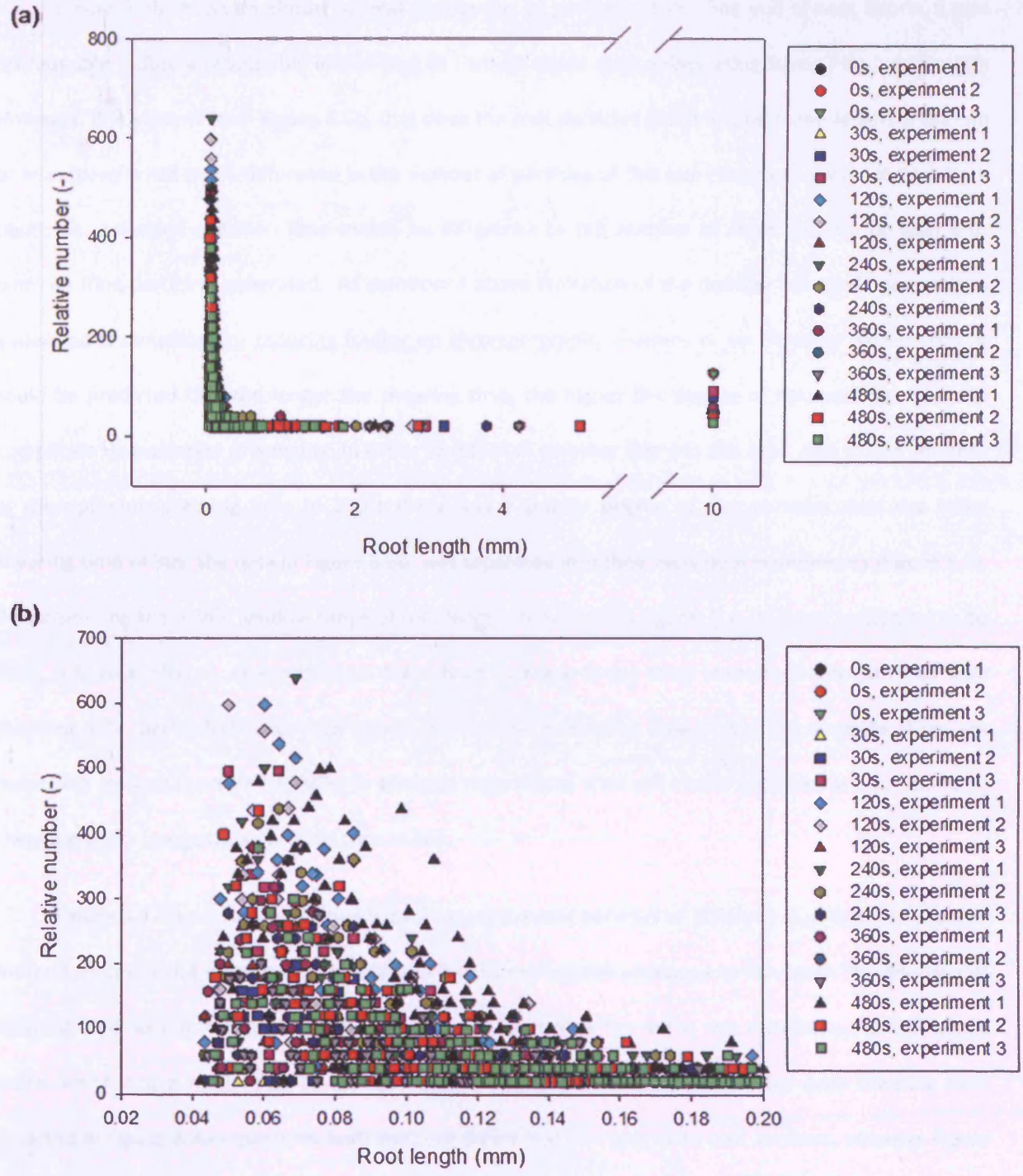

Figure 8.6 Particle size distribution (number basis) of transgenic root pieces damaged at 4500 rpm at varying units of time, t . a: All data represented b: Data showing maximum root length of 0.2 mm only.

Figure 8.6b shows an almost normal distribution of particles at the fine end of root debris. It was not possible to find a reasonable line of best fit through these data points using Sigma Plot (version 10). However, it is evident from Figure 8.6b, that once the root particles reach a total mean length of 0.2mm or less, there is not much difference in the number of particles of this size range generated at each time point; i.e. extended agitation time makes no difference to the number of small (0.2mm or less) root particles (fine particles) generated. As mentioned above limitation of the number of actual fine particles generated is beneficial for reducing fouling on chromatography columns or on filtration membranes. It could be predicted that the longer the shearing time, the higher the degree of fine particles that can complicate downstream processing. In order to establish whether this was the case, and to see whether at the optimum shearing time of 240 s there was a greater degree of fine particles than the initial shearing time of 30s, the data in Figure 8.6b, was separated into their individual experiments (Figure 8.7). By considering the whole window range of root length shown in this Figure, (i.e. 0.05mm to 0.2mm) to be fines, it is clear that in all experiments there is an increase in the total amount of fine particles with shearing time, particularly in comparison to the minimum shearing time of 30s; For example there are more pink squares (particles at 480s) in all three experiments than red circles (particles at 30s). Similarly there are more fine particles at 120s than at 30s.

Figure 8.8 shows the cumulative % over length for root particles of different sizes which is another method of describing particle size distribution for the root debris produced at $75s^{-1}$ with the duration of shearing time as a parameter. The plots in Figure 8.8a include the initial size distribution of the whole roots, which had a modal size of approximately 10 mm. The size distribution for each shearing time depicted in Figure 8.8a represents both the root debris and any unbroken root sections, whereas Figure 8.8b shows the fine end of root debris. Figure 8.8 shows that while there are differences in shape for the particle size distribution curves from assumed different time points, these variations are very small. The curve based upon particle size distribution shows similar gradients at each time point, meaning that a similar proportion of particles occupy each size band, with no variation that is large enough to be considered significant.

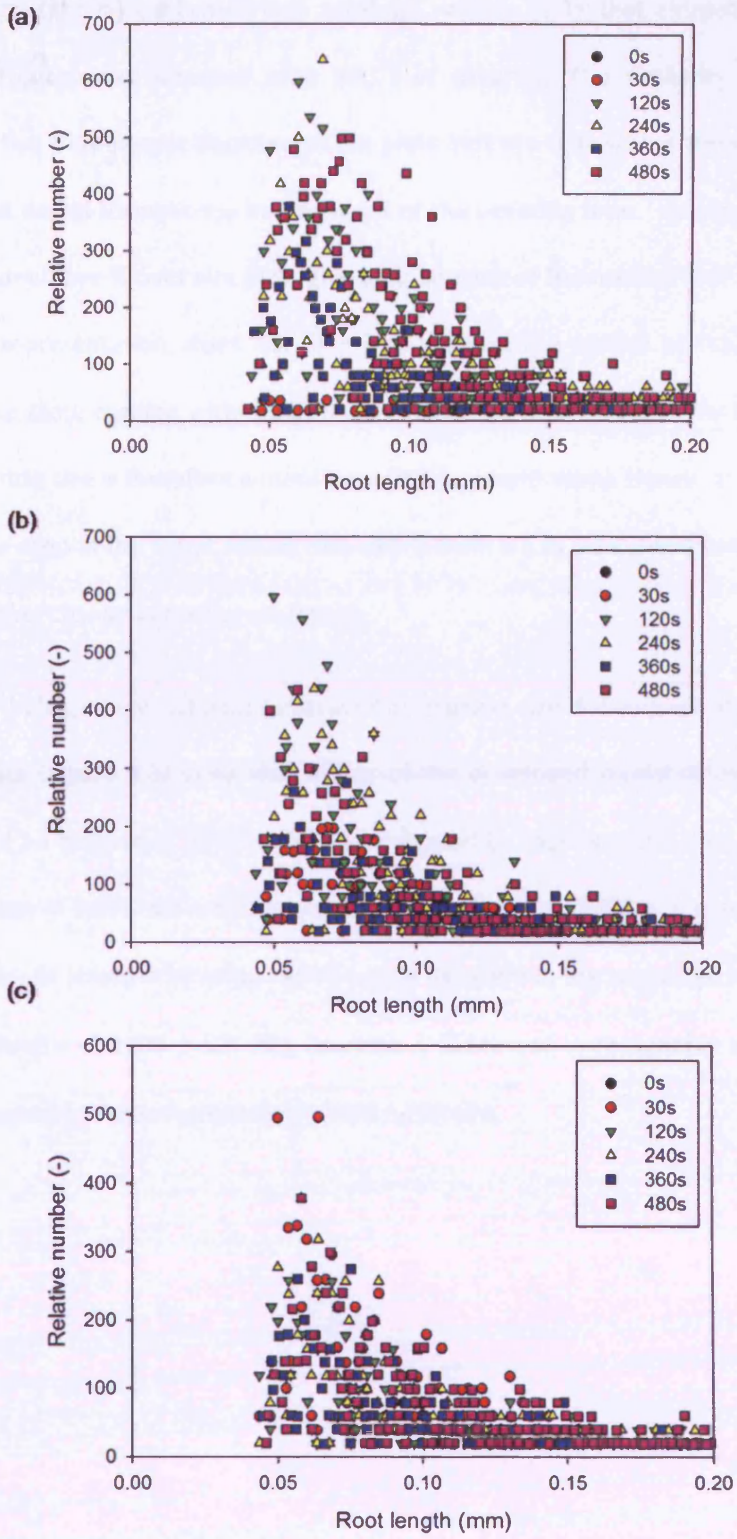

Figure 8.7 Particle size distribution (number basis) of transgenic root pieces damaged at 75s^{-1} at varying units of time, t. Data showing maximum root length of 0.2 mm only. Data shown separately for experiment 1 a, experiment 2 b and experiment 3 c.

IgG release data (above) confirmed that total IgG release (2.3X that extractable level of IgG by grinding in liquid nitrogen) was achieved after 240 s of shearing. The similarity of the particle size distributions for the five time ranges depicted in the plots indicate that within the range of parameters investigated, fine root debris formation is independent of the shearing time. However, it is important to note here that the cumulative % over size plots give an indication of the median root debris size (at 50%), but this method of representation, does not take into account the spread of the distribution, and it possible to obtain the same median with either a very narrow or a very wide distribution (Smith *et al.*, 2007). The mean particle size is therefore a more accurate representation). Hence, as shown in Figure 8.4 above there is a clear drop in the mean size of root debris from 0 s to 30 s, and from 30 s to 120 s, after which there is no further change in mean root length.

Nevertheless, the experimental data generated on particle size distribution of root fragments and the fragmentation rate (Figure 8.5) were vital inputs of the developed model (Chapter 7) so that root tensile strength could be estimated. This model was validated by experimental data obtained by pulling single roots to breakage in buffer via micromanipulation (Hassan *et al.* 2008a). A macroscopic estimation of the relative root tensile strength by using experimental data within the suggested model resulted in an estimated tensile strength of 2100 ± 600 kPa (average ± SEM) was in reasonable agreement with the tensile strength measured by micromanipulation 2400 ± 200 kPa.

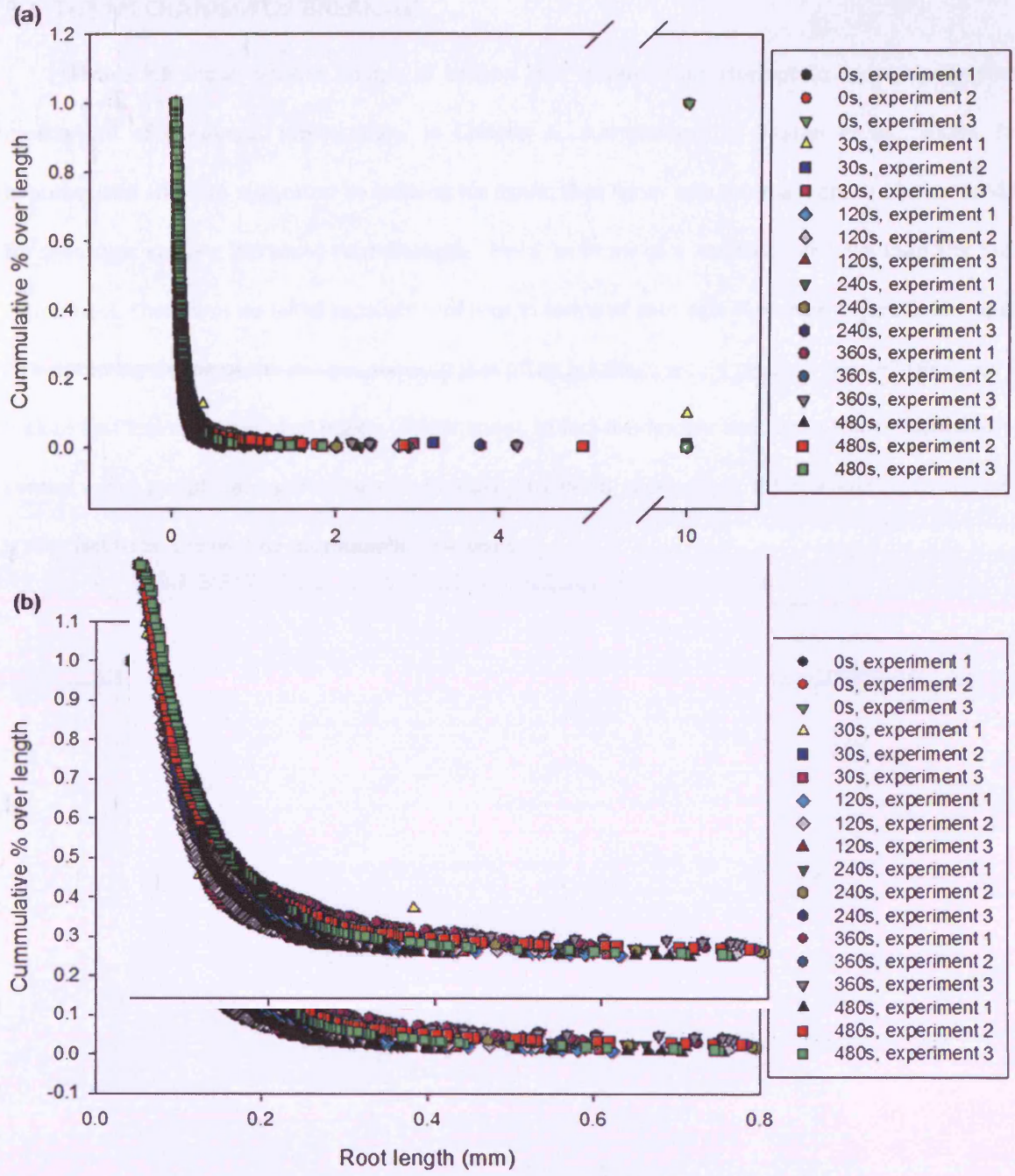

Figure 8.8: Decumulative size distribution for the root debris. a All data shown. b Data shown for a maximum root length of 0.8 mm only.

8.4 THE MECHANISM OF BREAKAGE

Figure 8.9 shows various images of broken root debris in an attempt to try to understand the mechanism of breakage. Interestingly, in Chapter 6, summarised in Hassan *et al.*, 2008a, it was hypothesised and also suggested by staining for lignin, that lignin was the main cause of increased force for breakage, causing increased root strength. Here, at more of a macroscopic level than the previous experiment, there was no initial separation of root in terms of root age. However, Figure 8.9a and d, was a re-occurring theme of the images, showing that often breakage would result in the weaker tissue being broken first leaving the central region (darker zone). In fact it is known that lignin is first deposited in the central xylem and phloem and surrounding cortex (Chapter 6, section 6.9), which could be why this region is the "last to be broken" by root-impeller collisions.

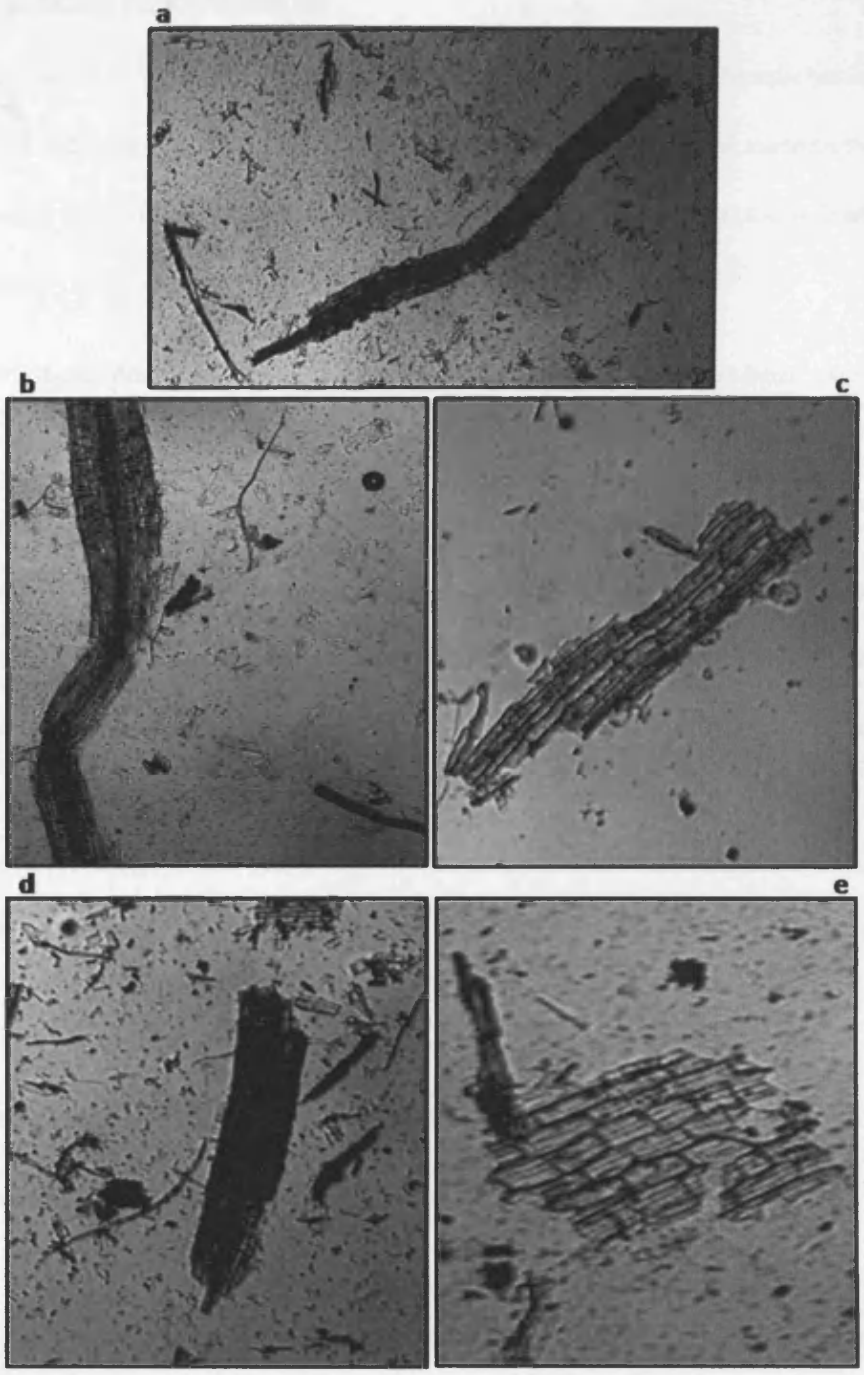

Figure 8.9: Images taken with the LEICA microscope, which may suggest the main mechanism of root breakage in the mechanically stirred breakage device

8.5 WORK DONE FOR BREAKAGE

Equations (7 to 14) lead to an estimation of work for breakage in the mechanically stirred breakage device of 6.3 ± 0.6 mJ which is in fact about 65 times greater in orders of magnitude than the energy for failure directly approximated by micromanipulation (97 ± 6 μJ, (error analysis as SEM), Chapter 6; Hassan *et al.* (2008a)), i.e. on average,

$$work\ done\ for\ root\ breakage\ in\ the\ mechanically\ stirred\ shear\ device = 65(work\ done\ for\ breakage\ by\ micromanipulation) \quad (8.1)$$

This can be explained by the fact that during micromanipulation a pulling force was directly applied to the root in the horizontal direction (Chapter 6), whereas in the mechanically stirred breakage device, breakage by root-impeller collision relied upon random impacts of the root particle with the impeller, the generation of sufficient kinetic energy during the impact to cause breakage leading to root size reduction and an increase in the total number of roots particles in the system. Thus, it is not possible to use the work done for breakage of a single root by micromanipulation to estimate the work done for breakage in the mechanically stirred shear device described here unless the factor of 65X is applied.

8.6 ESTIMATION OF ROOT TENSILE STRENGTH AND ITS RELEVANCE TO MICROMANIPULATION

In order to estimate root tensile strength, the theoretical approach outlined in Chapter 7, was followed. The kinetic energy of the collisions was found to be 70.7mJ. At $75s^{-1}$, the frequency with which the contents are pumped through the impeller region (f_c) is 6.5 s^{-1}, and thus, the collision efficiency which is dependent on both f_c and the total impact rate per impeller blade per particle, R_p, was found to be 0.0895 ± 0.008, giving a work done for of 6.2 mJ per root. (The total impact rate per impeller blade per particle, R_p, (also termed as the collision frequency) was experimentally determined from the number of root-impeller blade impacts at each unit of time, as explained in Materials and Methods, Section 2.7.7, and was found to be 0.0727 ± 0.0068 s^{-1}. The work done for pulling single roots to breakage in buffer

using micromanipulation was found to be 97 ± 6 μJ per root (Chapter 6), illustrating that 65 times this energy is required to break single roots by impeller-root impaction. The reason for this difference in the magnitude of energy required could be due to several factors, such as the fact that pulling is a completely different mechanism to random collisions with a solid surface, and that in the pulling experiment direct energy is being applied to the root to separate the cells. Interestingly, the estimated force for breakage (work done for breakage per unit displacement) was found to be 506 ± 47 mN, i.e. about 5 times the peak force for breakage for single roots pulled by micromanipulation (101 ± 7 mN per root; Chapter 6). The force for breakage is expected to be different because a) the same factors affecting the work done for breakage discussed above, b) the fact that the force for breakage measured in the micromanipulation experiments was a peak force, rather than the total mean force for breakage, and finally (and probably, most importantly), c) the displacement or distance moved in the direction of the force is about 5 times smaller in the micromanipulation experiments (representing the stretching of a root), whereas displacement is much larger due to a root-impeller-blade impact collision.

Contrary to work done and force for breakage that are entirely reliant on the mechanism of breakage, the tensile strength is an inherent property of the root. Nominal stress which is tensile strength of the root was estimated in the micromanipulation experiments as being 2400 ± 200 kPa per root. The pseudo or relative tensile strength was calculated as described in Chapter 7. This was reliant also, on the fragmentation rate (estimated on the basis of total mean root length, q_{frag}) which was found to be -0.0226s^{-1}. The relative tensile strength was found to be 2100 ± 600 kPa which is in fact close to the measured tensile strength by micromanipulation. This, thus, proves the validity of using micromanipulation as described in Chapter 6, to assess the tensile strength of roots that will be subject mainly to root-impeller collisions for breakage in a mechanically stirred breakage device. Thus, it is possible to use the measurement of a single root pulled to breakage in buffer using micromanipulation to estimate the minimum energy required to break a single root, and the minimum energy requirements of the device, as described below.

8.7 MINIMUM ENERGY REQUIREMENTS

Ouzineb *et al.*, (2005), investigated homogenisation for the production of miniemulsions, and suggested that the total work-done by the rotor-stator of the small-scale homogeniser was the sum of work done for breakage of droplets, the work done for coalescence of droplets and work done to generate heat. Similarly, the total work-done by the rotor-stator ($W_{rotor\text{-}stator}$) in our system is:

$$W_{rotor-stator} = W_{breakage} + W_{mixing} + W_{heat} \tag{8.2}$$

It may be possible to use the estimated root tensile strength estimated by measuring single roots in micromanipulation experiments, to estimate the minimum energy required to break the roots in a mechanically stirred breakage device at a set speed. For example, if the rotational speed of the device is set to $75s^{-1}$. Firstly, the tensile strength measured by micromanipulation is 2400 ± 200 kPa. It is then possible to assume that this is of a similar magnitude to the stress of the collision acting on the root (assuming equal and opposite forces acting on single roots during collisions by root-impeller impacts). The force required for breakage of a single root can then be estimated as the product of the stress and the root cross-sectional area (595 mN in this example). Taking the displacement to be the maximum distance that the root can travel in the radial direction (i.e. the distance between the impeller blade edge and the chamber walls (0.0125 m), (a valid assumption since the impeller occupies a large area of the chamber), the work done for breakage of a single root can be estimated (7.44 mJ, in this example). The kinetic energy of the collision is calculated as in equation (7.1) above, and is dependent on the impeller speed and single root mass, and impeller diameter. The work done for breakage of a single root as a fraction of the kinetic energy of a collision gives an estimate on the collision efficiency, (0.105) in this example. Re-arranging equation (7.5) gives R_p, the total impact rate per blade, per particle. R_i is therefore the product of R_p and the total number of roots in the system (126 in this example, giving $R_i \sim 10.8$). Using, this value of R_i, and re-arranging equation (7.4) gives the minimum time required to break the roots at $75s^{-1}$:

$$t_{4500rpm} = \frac{(n_t - n_{30}) + 315.2}{10.8} \tag{8.3}$$

where n_t is the maximum number of particles in the homogeniser, per blade. Looking at Figure 8.3, t_{75s-1} is also equal to the time at which the maximum number of particles is reached, and the minimum total mean length of the roots is reached, and also the point at which the fraction of remaining intact roots over the initial amount of intact roots is unchanged. As a rough estimate, $(n_t - n_{30})$ will be equal to the total number of roots in the system multiplied by the number of blades in the system (i.e 126 x 8). This gives an approximate t_{75s-1} of 124 seconds.

The product of power ($2\pi NT$, 1.138J/s for our device) and t_{75s-1} gives the total work done by the device, i.e.

$$Work_{total} = [0.108(n_t - n_{30})] + 34.146 \quad (8.4)$$

At t_{75s-1} of 124 s, the total work is 140.7 J, which is of course divided into work for mixing, breakage, and work lost due to friction and heat.

8.8 SCALABILITY OF THE MECHANICAL EXTRACTION DEVICE

The ability to scale the mechanically stirred breakage device is critical for its applicability in an industrial setting. $75s^{-1}$ was chosen as the operating speed of the small-scale mechanically stirred breakage device since, this speed was in between the speed for complete suspension (N_{js}) and surface aeration speed (N_{sa}), but was greater than the maximum speed at which no particle impaction occurred (N_{ni}). Takahashi *et al.* (1993) found that,

$$N_{js} \propto N_{sa} \propto N_{ni} \propto D^{-1} \quad (8.5)$$

Although obvious parameters for scale-up of our shear device would be a constant power per unit volume or tip speed of the disc, it is better to develop our own scale-up rules of thumb, based upon process performance. Takahashi *et al.* (1993) also described the scale-up rule for a device where solid-solid collisions result in breakage, as,

$$N_M D_M^{\beta} = N_L D_L^{\beta} \tag{8.6}$$

where the subscripts M and L refer to the small-scale model and larger vessel respectively, N is the impeller speed, and D is the impeller diameter. The exponent β is a parameter varying according to the scale-up condition. According to Takahashi *et al.*, (1993), if β = 0 the scale-up rule is constant impeller speed, if β = 2/3 constant mean energy dissipation rate is the scale-up rule throughout the vessel, if β = 1 it is scaled-up by constant impeller tip speed, and finally, if β =2 the scale-up rule is constant Reynold's number. Takahashi *et al.*, (1993) also found that R_p may also be used as a scale-up parameter. The same number of impacts per second was found at a constant impeller tip speed and that for a constant mean energy dissipation rate throughout the vessel. It is important that a scale-up model is able to duplicate all these identified critical parameters. In light of the above, although a large-scale model has not yet been developed, this small-scale model is expected to be readily scalable.

8.9 CONCLUSIONS

Transgenic tobacco roots offer a potential alternative to leaves for monoclonal antibody (MAb) production. For design of equipment for extraction of the antibody from roots, it is necessary to know the minimum energy required for their breakage. This was assessed by treating 10 mm root sections in a scalable, ultra-scale down, stirred shearing device. Size distributions of the roots when passed through this device at a rotational speed of $75s^{-1}$ were obtained as a function of time. It was postulated that root fragmentation in such a mechanically stirred shear device is due to root-impeller collisions. On this basis, a relationship between the equilibrium mean length of the root fragments and the critical physical parameters affecting it was established using a theory of failure based on a maximum strain energy criterion. Data on the stable size of the root debris agreed well with model predictions based on this criterion. The data further suggested that root breakage was approximately a first-order process. The model suggests that knowledge of root tensile strength is important since it directly determines the minimum energy required to break the transgenic roots. The mathematical model was applied to the data

to estimate mean root tensile strength as 2100 ± 600 kPa (standard error in the mean), and this was similar to the mean tensile strength of the roots as determined previously by a micromanipulation technique i.e. 2400 ± 200 kPa. It appears therefore that measurements of root tensile strength by micromanipulation would be a valid means of finding the minimum energy required to break roots in a mechanical shear device. It is important to note, however, that these results are consistent for this particular set-up e.g. biomaterial type, impeller speed, impeller/vessel type etc., and a change in any of these parameters may affect the similarity of values of root tensile strength derived at micro- and macro-scales. Further work is therefore required to determine whether this is a generic method that will work for ranges of values of all critical input operating parameters and vessel geometries.

Chapter 9- Framework for the harvesting strategy and overall process design of monoclonal antibody production in transgenic tobacco

9.1. INTRODUCTION

One of the most important features of downstream processing for recombinant pharmaceutical proteins from different sources as a whole is that a given end product must meet the same standards and specifications in terms of safety, quality, potency, and efficacy, regardless of the production host. Furthermore, the physiochemical properties of such end products should be identical, so that the intrinsic features used for purification are the same.

The main stages of recombinant protein production from transgenic plants are harvesting, and the downstream processing stages of extraction, protein recovery, and purification. Based on optimal harvesting age, location and frequency, described in Chapter 5, recommended harvesting strategies for a secreted IgG and an intracellularly retained IgG-HDEL are described in this Chapter. The simulation tool (SuperPro Designer version 4.5) was used to design alternative process options for the production of a monoclonal antibody (Guy's 13) in transgenic tobacco plants. This tool allowed the graphical representation of a series of unit operations models as icons that can be interconnected within a specified sequence (Petrides *et al.*, 2002b). For monoclonal antibody (MAb) production from transgenic tobacco leaves, three separate designs were described, which were specific to the three targeting strategies explored in this thesis; namely IgG (secreted form), membrane-bound IgG (mIgG) and IgG-HDEL that is intracellularly retained in the endoplasmic reticulum. A process for the production of IgG (secreted form) was also described for monoclonal antibody production from the tobacco roots. The design of each process was based on optimal extraction conditions for each antibody type from transgenic tobacco plants as highlighted in prior Chapters.

9.2. RECOMMENDED STRATEGIES FOR HARVESTING

For recombinant MAb extraction from *Nicotiana tabacum*, our results suggest a recommendation that a mechanical harvesting method is employed. Leaf harvesting in the tobacco industry is a well-established method in agriculture. To simulate the puncturing of leaf discs from whole tobacco leaves, we suggest that technology from the paper shredding industry is used. Alternatively, it may be possible to combine the process of harvesting and cutting by using driven swath formers (used on leafy crop such as spinach), which allow plants in the upright position to be uprooted (for whole plant harvesting) and gathered in swaths for uniform cutting (Stoll *et al.*, 2000).

Figure 9.1 summarises our recommended strategy for harvesting. The harvesting strategy for both the secreted form of IgG and IgG-HDEL is dependent on the manufacturing handling capability of leaf mass at any one time, the scheduled process time of a single batch, and whether it is desirable to re-use the same plants after a short period of time for several process batches. If these permit the processing of all leaves of the plant at once, or if it is more beneficial to process a small number of leaves of the plant at any one time, will influence optimal harvesting time for both versions of the Guy's 13 MAb.

In the first instance of harvesting all leaves of the plant at once, optimal harvest time for the secreted form of IgG is 2-4 weeks (equivalent to an approximate height of 10-20 cm under our plant growth and maintenance environment conditions). However, in the case that only older plants are available for harvesting (e.g. > 6 weeks or > 30 cm in height), it is advised that only top leaves of these plants are harvested. If choosing the latter option of 9-11 weeks, it is recommended to wound the plant leaves 1-6 days before harvest in order to boost IgG yields. For IgG-HDEL, however, the optimal harvest time is 11-16 weeks and it is not necessary to wound the plants pre-harvest.

In the second example of only harvesting some of the leaves of the plant per batch, the age or heights of the plants are important. If there is a variety of plants ages available, optimal harvest time is 2-4 weeks but care must be taken to limit multiple harvests to days 0, 1 and 13, during which is the "IgG recovery period" for the secreted form of IgG. It should be noted that for these young plants, extra care

must be taken, however, to ensure no physical damage is done to the plants before time of harvest as this may lead to a significant reduction in IgG levels. (Thus, young plants expressing a secreted form of IgG are more preferably grown in a greenhouse setting for a greater control on its surroundings). If however, only older plants (greater than 30 cm in height i.e. 5 weeks for our environmental conditions) are available, the recommended harvesting strategy is to harvest from the top leaves of the plants.

An alternative strategy for the secreted form of IgG is a combination of the above, i.e. to harvest only some of the leaves of young plants (> 2-4 weeks old) and then to leave them to grow to 9-11 weeks, when all the leaves of the plant can be harvested (with pre-wounding the leaves 2 days before week 9 to boost IgG yields).

For IgG-HDEL expressing plants, however, if it is decided to harvest only some of the leaves per plant at any one time, the availability of a variety of plant heights means that the leaf tissue can be harvested at any desired time, (with multiple wounds having no negative/positive effects on IgG yield). If only plants greater than 30 cm in height are available, then any leaves of the plant can be harvested.

An alternative combined strategy for IgG-HDEL expressing plants, is to harvest the topmost leaves on a regular basis (for example, every 2 weeks), and then to harvest all the leaves at 18 weeks when the plants are older, but with most leaves of the plant remaining green and fresh to avoid the extra phenolics that can be present in yellowing leaves.

Although overall IgG-HDEL offers a more flexible harvesting strategy, as it has been shown to have a more stable IgG level with time, and also appears to be independent of senescence or stress caused by mechanical wounding, it differs from IgG in terms of a lack of complex glycosylation, and thus its applicability is dependent upon the manufacturer's and regulator's acceptability of degree of glycosylation necessary for effective immunisation. Addition of HDEL or KDEL sequences at the C-terminal end of a secretory protein is a well-established strategy for its retention in the ER (Gormord *et al.*, 1997; Chapter 3 or Hassan *et al.*, 2008b). For KDEL fused to the heavy chain of antibodies, most N-linked glycans were found to be of the high-mannose type with 6–9 mannose residues but with a small percentage still

containing the immunogenic β1,2 xylose glyco-epitope (Ko *et al.*,2003). Addition of KDEL retention signals on both heavy and light chains of the antibody, however, forms antibodies with entirely non-immunogenic high mannose type N-glycans (Sriraman *et al.*, 2004). On the other hand, the *in vivo* half-life of these antibodies in mice was found to be lower than mammalian antibodies or plantibodies that were able to pass through the complete secretory pathway and thus had complex oligosaccharides. This is likely to be a result of endocytosis and degradation following binding to mannose receptors, as has been observed for antibodies produced in the Lec 1 mutant CHO cells that have high mannose N-glycans (Khoudi *et al.*, 1999). If IgG-HDEL is acceptable, however, this is a much more favourable form of the recombinant protein in terms of processing, since it does not have much influence on harvesting, making the decision process in this category, far easier.

Although we did not investigate membrane-bound IgG in terms of harvesting, we suspect it will be similar to IgG as it completes the secretory pathway, and although it is bound to the membrane, it will be exposed to the apoplasm-residing proteases.

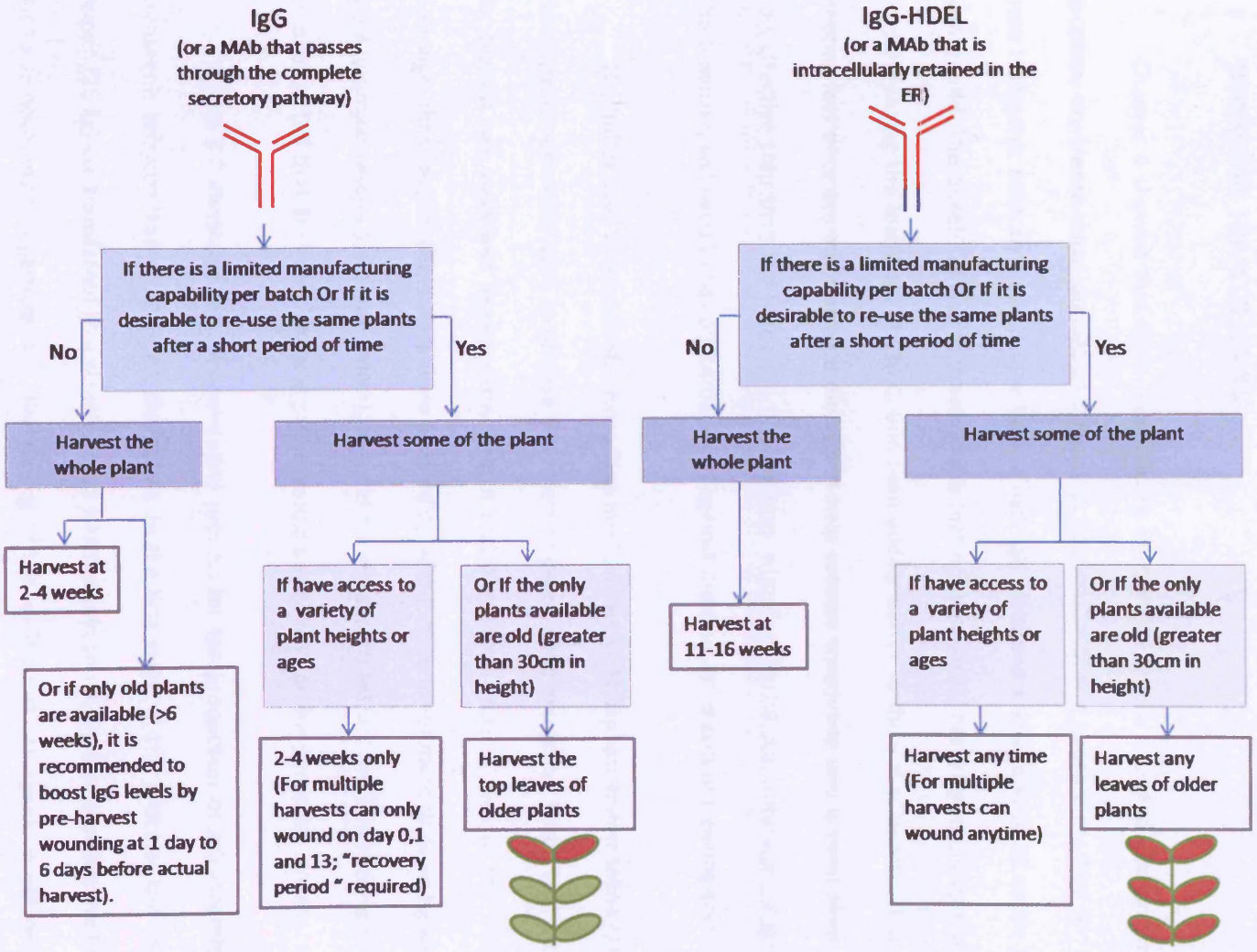

Figure 9.1: Recommended harvesting strategy for IgG (secreted form) or IgG-HDEL (intracellularly retained in the endoplasmic reticulum)

9.3. PROCESS MODEL DESCRIPTION

9.3.1. PROCESS OVERVIEW FOR ANTIBODY PRODUCTION OF IgG (SECRETED FORM) FROM TRANSGENIC TOBACCO LEAVES

Chapter 4 showed that for a recombinant murine IgG that is secreted and accumulated in the apoplast, dry freeze-thaw (defined in Chapter 2, Section 2.4.5) is a suitable method for IgG extraction from transgenic tobacco leaves, since both a high IgG yield and a low release of native plant proteins were found. The benefit of this to processing is that no mechanical breakage technique is required, and simply freezing the leaf discs at -20^{o}C, and then adding buffer to thaw is sufficient. It is expected that freezing leaf discs pre-addition to buffer could help process scheduling and is most likely to be a more cost-effective step than the utilisation of an energy intensive mechanical breakage (or grinding) device. This however, will need to be counterbalanced against the associated cost of freezing and storage.

The buffer used to analyse this extraction method was 1X Phosphate buffer saline (1X PBS) at pH 7. However, experiments done to analyse the effect of pH on MAb extraction found that the optimum pH for highest IgG yield and lowest extraction of native tobacco proteins was in the range of pH 5-6. Although, these experiments were done by grinding in buffer, an experiment done using wet freeze-thaw yielded similar results (data not shown), as it did for grinding to extract the other forms of the MAb. It is thus, expected that dry freeze-thaw at pH 5-6 would be optimal for this particular system.

Figure 9.2 illustrates the recommended process for the production of IgG (secreted form) from transgenic tobacco leaves based on the above. In the first stage of the process, the harvested whole leaves (25 kg) are transferred to a cleaning step which would simply involve blowing the leaves with cool air to remove any soil particles etc. The rinsing or the addition of detergents is not recommended as some antibody loss may occur in this way. The leaves are shredded pre-extraction, for example via industrial tobacco shredding or cutting equipment (US patent 3659620, 3946954). The shredded leaves are then sent through weighing tanks to control the feed rate to the process. (Note there is a surge tank

between the shredder and the weighing tanks to account for the fact that the shredder can only shred a certain amount of leaf material at any one time). However, the whole process of whole leaf harvest to weighing should be optimised to make this as fast as possible to limit any MAb loss, which may occur due to handling fresh wet tissue.

Shredded leaf tissue are then mixed with 450L of extraction buffer in the dry freeze-thaw equipment (maintaining the leaf mass to buffer ratio of the small-scale experiments described in Chapter 2). It is recommended that this is done in a 500L tank of the novel CryoFin^{TM} system (Wilkins *et al.*, 2001).

This CryoFin^{TM} system (Figure 9.3) was especially designed for bioprocessing for the storage of frozen solutions at large scale, for cryopreservation. This system permits controlled, reproducible freezing of solutions by encouraging dendritic ice formation. Dendritic ice crystals grow as 'fingers' from the ice mass into the unfrozen solution, engulfing solutes and thereby resulting in a more homogeneous distribution of solutes within the ice mass (Wilkins *et al.*, 2001). This is in contrast to fast or slow freezing regimes, in which ice crystals form a flat front, leading to non-uniform distribution of solutes. This system then allows the thawing process to be done in a relatively fast and reproducible manner, under non-invasive, sterile and low-turbulence mixing. This mixing quickens thawing by promoting heat transfer, resulting in a higher melting rate. These novel freeze-thaw systems have been used in production processes for approved therapeutic products by key biologics manufacturers in the US and Europe (Wilkins *et al.*, 2001). Pre-optimisation of this process unit step is also possible since it is operable at a range of temperatures and times. In fact, it is likely that as the scale of production is far greater than in our small-scale experiments the required freezing and thawing time will be significantly extended.

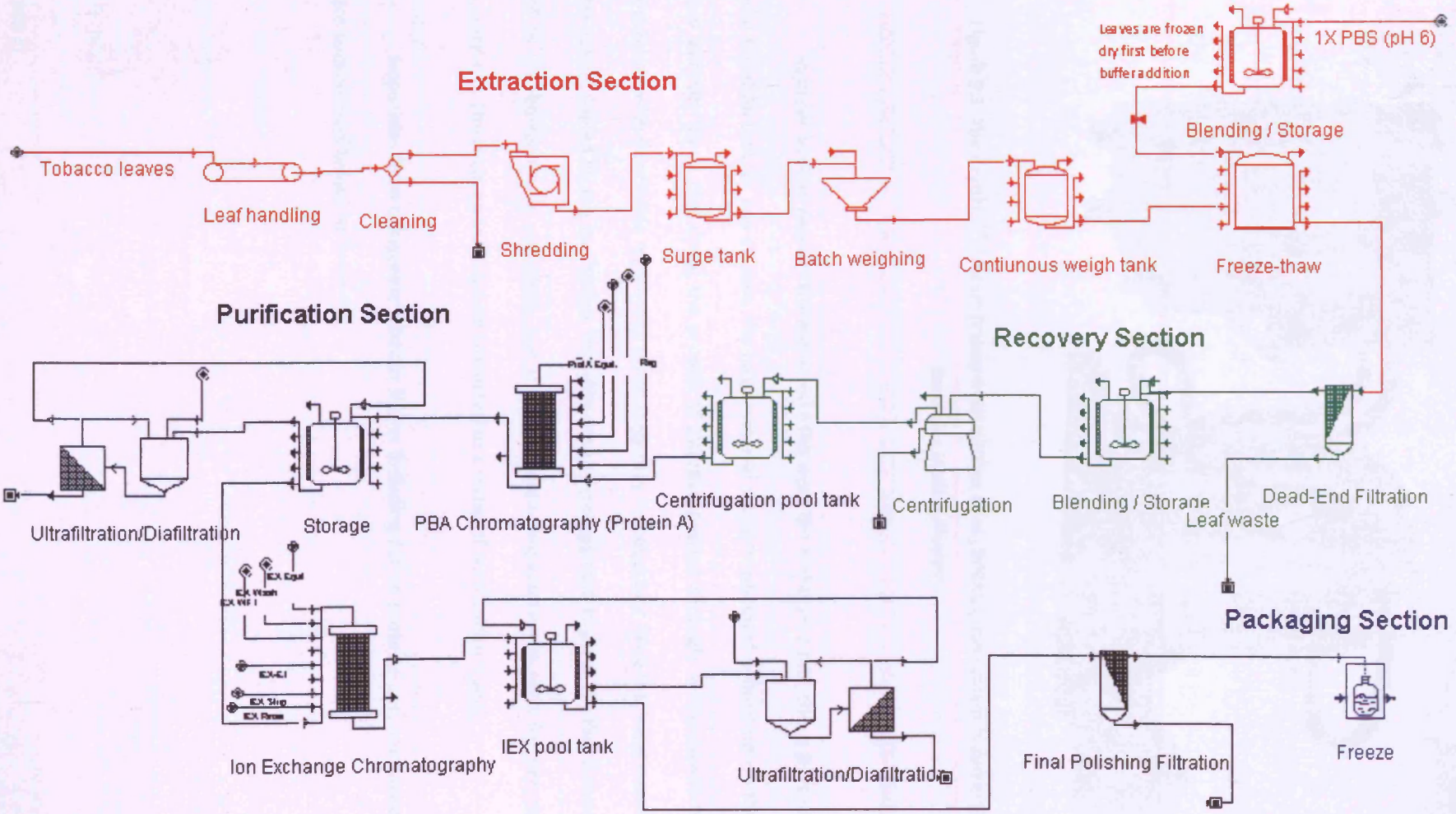

Figure 9.2: A process flowchart for IgG (secreted form) production from transgenic tobacco leaves

Figure 9.3: The CryoFin™ system (taken from Wilkins *et al.*, 2001). (This system is currently provided by Sartorius Stedim Biotech.

In order to then recover the extracted MAb from the leaf-buffer mix, this is passed through a dead end filtration unit. In this system, the large wet leaf sections will quickly build up on the filter, with the low viscosity liquid containing the protein of interest, passing through. A few passes through this unit operation with disposable membrane technology may be necessary since the initial membrane is likely to be quickly fouled by the leaf tissue. Post-filtration, a storage tank is used for the duration that filtration of all leaf-buffer mix is complete, and the MAb containing solution is then further clarified though a centrifuge. The recoved MAb is then subjected to a series of purification stages.

Impurities from transgenic tobacco leaves including native proteins and non-protein contaminants are summarised below, in Table 9.1.

Component	% Dry weight
Water	80-90 (% wet weight)
Sugars	25-28
Cellulose	35-40
Lignin	4-5
Protein (soluble)	7-10
Alkaloids	1-2
Chlorophyll	1-0.8
Polyphenols	1-2
Phenols	200-350 ppb (not a %)

Table 9.1: Selected component composition of green tissue of tobacco. (Adapted from Mulesky *et al.*, 2004).

The first step in the purification would be a Protein A affinity chromatography. This expensive but most efficient step, is commonly used in the current monoclonal antibody production industry. This stage is expected to give a product purity of 95%. In the following stage of ultrafiltration, residual phenolics are removed in the filtrate, and the product concentrated. This step is used to concentrate and to perform low-level purification of the protein solution. The molecular weight cut-off of the membrane is pre-chosen to retain the product whilst allowing impurities such as low molecular weight solutes, such as phenolics to filter through the membrane.

This is then followed by ion exchange chromatography to increase the MAb's purity to 99.9%, by binding the impurities, and allowing the product to flow through. This intermediate purification step separates proteins with differences in charge to give a very high resolution separation with a high loading capacity. The separation is based on the reversible interaction between a charged protein and an oppositely charged chromatographic medium. The next step in the recommended process is another ultrafiltration step to further concentrate and purify the product, potentially maintaining a purity level of 99.9%. Following extraction and dead-end filtration, this process is very similar to processes used to produce MAbs from mammalian cell culture. The main difference in the downstream process is the lack of several intermediate polishing filters and virus inactivation stages used in mammalian cell culture to remove these risks.

Implementation and validation of virus removal currently remains an economic challenge to the mammalian cell culture industry. (The regulatory requirement of mammalian cell-derived products is to prove a final level of less than one virus particle per million doses (van Reis and Zydney, 2001). However, there are no comparable viruses in transgenic tobacco plants, and at present it is thought that viruses are incapable of propagation in humans (Quemada, 2002). For transgenic plants used for food purposes, the environmental protection agency (EPA) granted waivers from the requirement of detailed toxicity data. These waivers were given on the basis of a long history of the entire plant virus particles in foods being consumed in mammals, in the absence of any deleterious effects to human health. The EPA accept that virus-infected plants are currently part of both the human and domestic animal food supply, and that plant viruses have never been shown to be toxic to humans or other vertebrates. However, appropriate measures will have to be taken to eliminate any possible fungal toxins or pesticides from the original tobacco plants (Russell, 1999), which is why a final polishing filter step has been included before the product is ready for formulation. (Pesticides are often removed by microfiltration or ultrafiltration operated in dead end mode in water purification treatments, Laîné *et al.*, (2000)).

Depending on the usage to which the product is put, the purity required may be as high as 99.9%, alternatively if only a 95% purity level is required, it may be possible to remove 1 or 2 of the final purification stages, for a product that is only 95% pure, thus lowering capital cost, and increasing overall yield per batch.

9.3.2. PROCESS OVERVIEW FOR ANTIBODY PRODUCTION OF MEMBRANE-BOUND IgG FROM TRANSGENIC TOBACCO LEAVES

For the membrane-bound IgG, Chapter 4 showed that grinding in buffer that included a non-ionic detergent was necessary to extract the monoclonal antibody (MAb). Triton X-100 was the detergent used in these studies, and its optimal concentration was found to be 0.1% (v/v). Thus, the recommended process for the production of this form of the MAb from transgenic tobacco leaves (Figure 9.4) differed from that for the secreted form of IgG in that Triton X-100 is included, and a milling step replaces the freeze-thaw process, based on the assumption that milling will be a suitable mimic of the breakage mechanism of grinding. For this, it is suggested that the Fitzmill Comminutor (www.fitzmill.com) is used. This equipment was chosen from a list of suitable leaf breakage devices (Appendix E), since there are small-scale and large scale equivalents that are commercially available, where the latter is also able to meet stringent Good Manufacturing Practice (GMP) requirements, and is easy to clean. This has been used at small-scale for the production of Hepatitis B vaccine from transgenic tobacco (Valdés *et al.*, 2003). An additional advantage of this particular milling device, is that leaf material may not need to be pre-shredded before processing, thus potentially minimising product loss by reducing loss of leaf tissue caused by shredding. An important consideration when deciding on the solid-liquid working volume of the device is that leaf material itself contains a large volume of water, increasing the total volume slightly. Chapter 4 indicated that this can be done at room temperature, but a temperature control mechanism would be required since mechanically stirred equipment is likely to increase temperature of the mixture during operation.

An important consideration for the use of plant material is the high volumes of solid waste that will have to be treated using rigorous waste disposal procedures to prevent contamination.

Another addition to this process, in comparison to that for the secreted form of the MAb, is the addition of an additional chromatography step to remove Triton X-100. This commonly used detergent at large scale can be easily removed by ion exchange chromatography. In particular, the polymeric

adsorbent, XAD-4 is recommended since many studies have shown that it is efficient in removing Triton X-100 (Saitoh *et al.*, 2004; Kee *et al.*, 2008). This step is added prior to Protein A affinity chromatography because it is important to remove any major contaminants very early on in the process, and also to reduce the process fluid's viscosity by removal of the viscous detergent, thereby increasing the efficiency of subsequent purification steps.

The detergent involved in the extraction step would result in the simultaneous release of the phospholipid membrane and lipids that in turn would compartmentalize various sections of a cell, releasing other intracellular contaminants (Maire *et al.*, 2000). This is visible by the increasing green colour of the solution indicating the extra release of chlorophyll with increasing detergent concentration. Although this is an added burden on the subsequent downstream processing steps, it is believed that the remaining purification steps would be sufficient in producing a product of the highest purity.

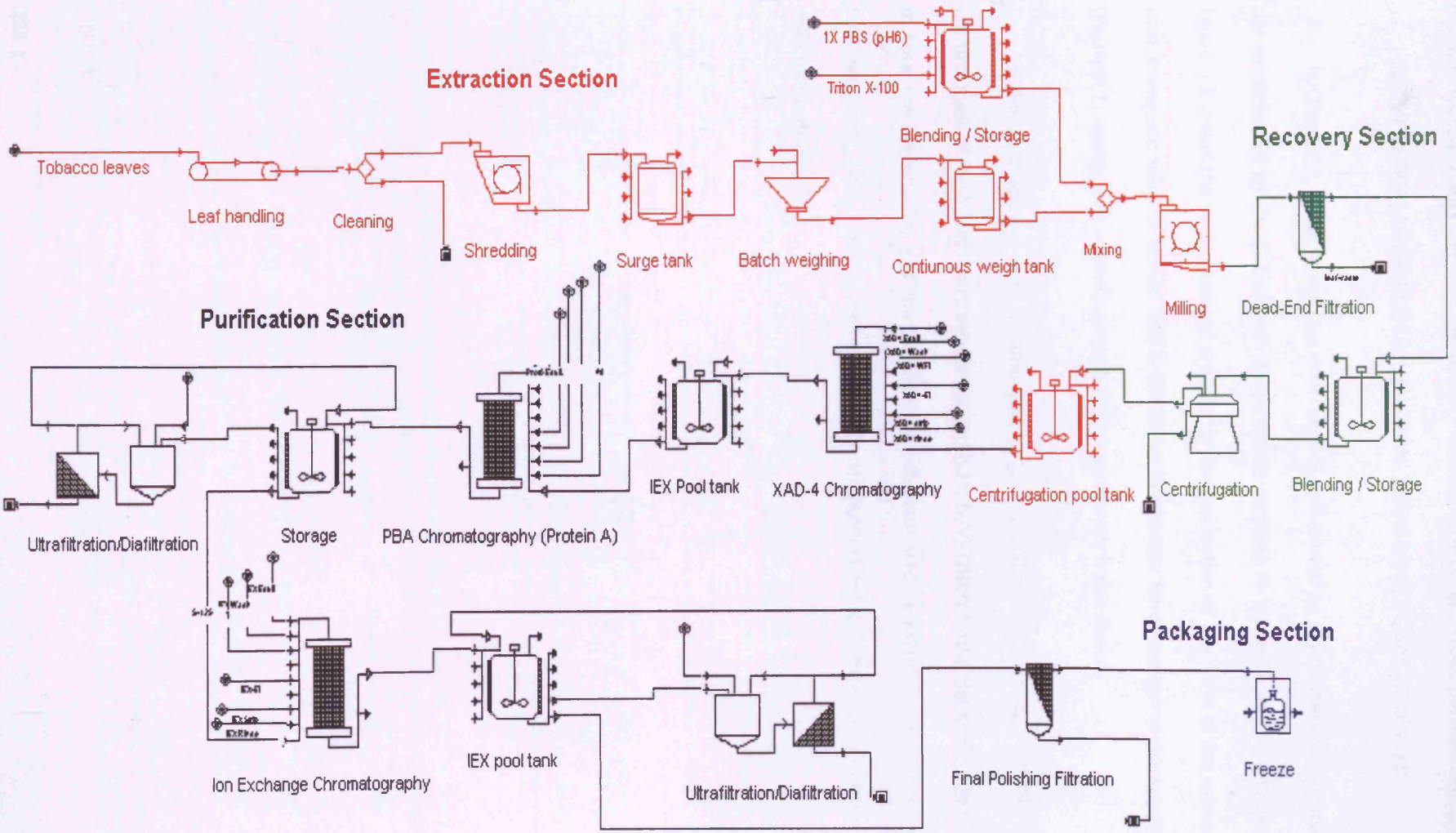

Figure 9.4: A process flowchart for membrane-bound IgG production from transgenic tobacco.

9.3.3. PROCESS OVERVIEW FOR ANTIBODY PRODUCTION OF IgG-HDEL (INTRACELLULARLY RETAINED IN THE ENDOPLASMIC RETICULUM) FROM TRANSGENIC TOBACCO LEAVES

In Chapter 4, it was found that dry-freeze-thaw followed by grinding was an optimal technique for the extraction of IgG-HDEL that was intracellularly retained in the endoplasmic reticulum of leaf cells. Figure 9.5 shows the recommended process for the production of this form of the monoclonal antibody from transgenic tobacco leaves. This is similar to the process for extraction of the secreted form of IgG (Figure 9.2), except that a grinding step is included after dry freeze-thaw.

Although Chapter 4 demonstrated that for IgG-HDEL like mIgG, there was a 2-fold increase in MAb per unit mass of fresh leaf tissue between 0 and 0.1% (v/v) Triton X-100, the purification burden in terms of total soluble protein, and the additional purification step required, is likely negate the increased upstream yield. Thus, because, unlike for mIgG, detergent is not a necessity it has been eliminated from our process design.

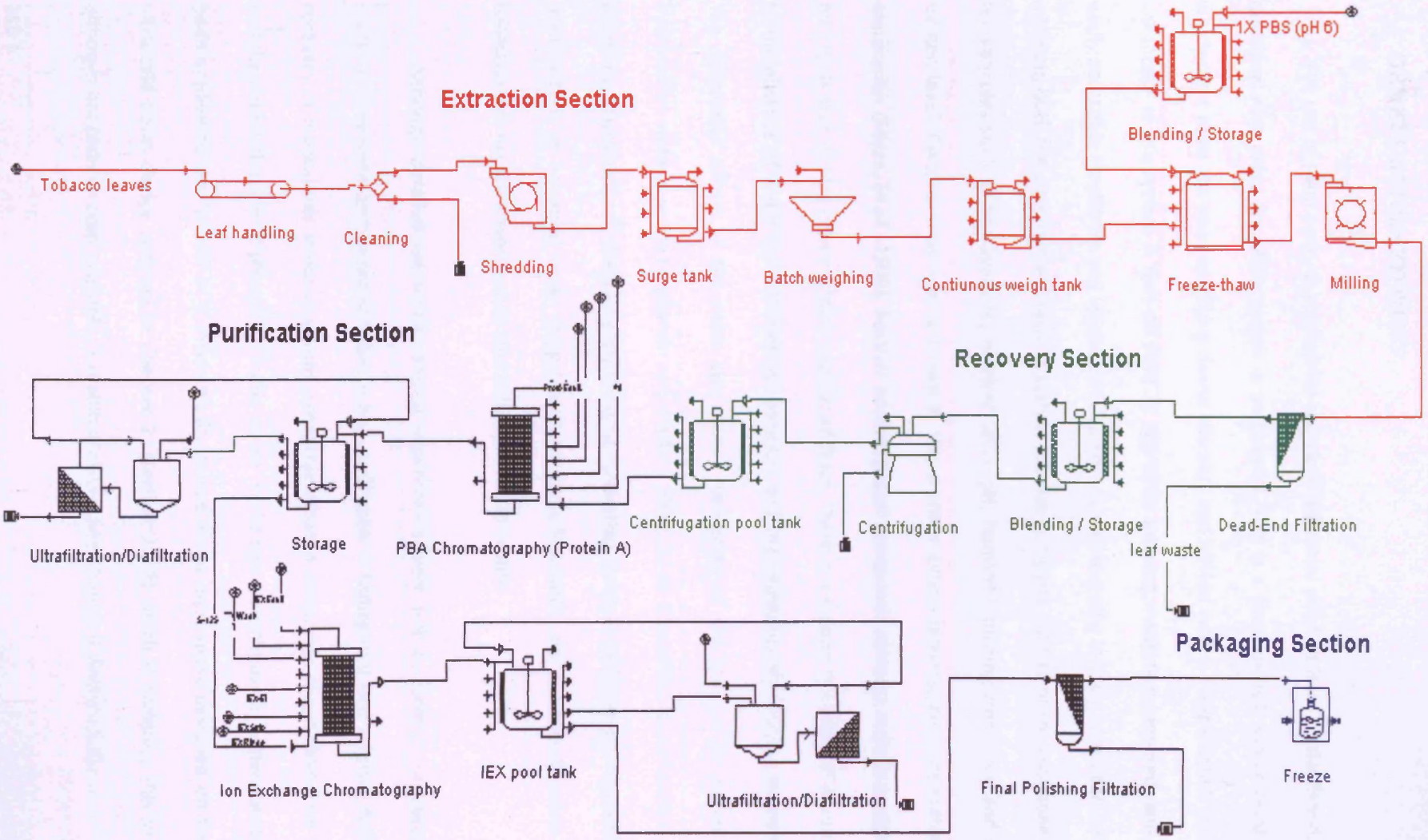

Figure 9.5: A process flowchart for IgG-HDEL production from transgenic tobacco.

9.3.4. PROCESS OVERVIEW FOR ANTIBODY PRODUCTION OF IgG (SECRETED FORM) FROM TRANSGENIC TOBACCO ROOTS

The use of plant roots as a potential source of industrial product is well-established. For example, medicinal root crops are often grown in aeroponics. This is a form of hydroponic plant cultivation in which plant roots are suspended in a closed chamber and misted with a complete nutrient solution. The advantage of this system is that no solid or aggregate growing medium is required, and the roots are easily accessible (Pagliarulo and Hayden, 2001). Thus, a cleaning step in the process can be eliminated. In addition, both the chamber and misting system provide complete control of the root zone environment, for variables such as temperature, nutrient level, pH, humidity, misting frequency and duration, and oxygen level. Consequently, plants grown in this manner often demonstrate accelerated growth and maturation (Mirza, *et al.*, 1998). Further advantages of aeroponics systems include a higher root yield, and roots that display greater uniformity. In addition, there is a greater potential of dense planting, due to the absence of water and nutrient competition, and the capability of recycling nutrients and water. The suspended nature of the roots also makes harvesting of the roots a far easier process than hydroponics systems or soil (Pagliarulo and Hayden, 2001). As an alternative to aeroponics, there is also a company, Phytomedics™ that currently focus on cultivating plants in hydroponics in greenhouses for the manufacture of botanical drugs (http://www.phytomedics.com/). As a result, the use of transgenic tobacco roots may be a worthwhile alternative production route.

Although detailed extraction ranging experiments were not performed on transgenic tobacco roots, as they were on transgenic tobacco leaves, Chapter 8 highlighted that a fitting technique for the recovery of monoclonal antibodies from transgenic tobacco roots, was to cut them into 1 cm sections, and then break them in 1X phosphate buffer saline (in the same fresh mass to buffer volume ratio, as had been applied to the leaves) in a mechanically stirred shear equipment designed on the basis of the ultrascale down device outlined in Chapter 2, (Section 2.7.2) which is scalable. This in-house device, although not commercially available, is readily scalable (See Chapter 8, Section 8.8).

The overall process design for the production of IgG (secreted form) from transgenic tobacco roots is therefore similar to that for the production of this form of the antibody from the leaves, however, the dry freeze-thaw step has been replaced with a mechanically stirred shear equipment.

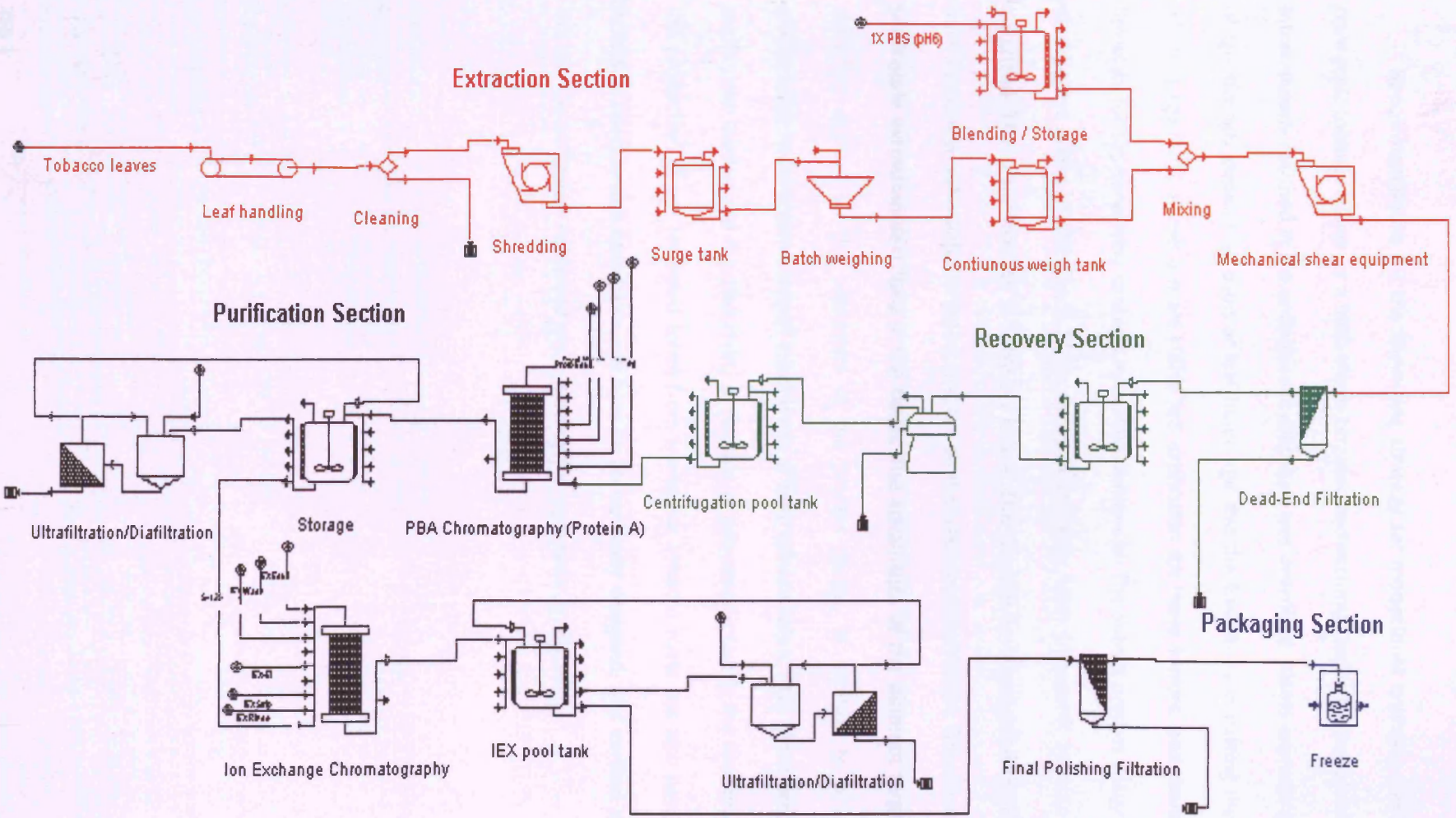

Figure 9.5: A process flowchart for IgG production from transgenic tobacco roots.

9.4. SUMMARY

Recommendations for the harvesting strategy for monoclonal antibody (MAb) production from transgenic tobacco leaves for a MAb that is targeted and accumulated in the apoplasm, and that which is intracellularly retained in the endoplasmic reticulum was described. Plants expressing the secreted form of IgG strongly depend on plant or leaf tissue age and the frequency of cutting the tissue for harvest, whereas IgG-HDEL shows a more stable IgG expression for these factors, and therefore offers greater flexibility for the harvesting strategy. Recommendations for the overall process design for the production of different forms of the Guy's 13 monoclonal antibody from transgenic tobacco leaves have been described. This is summarised in Table 9.2 below. This Chapter has highlighted the importance of initial immunoglobulin subcellular targeting strategy on the whole process design. The processes were based on small-scale extraction described in the thesis. The advantages of the different targeting strategies will therefore depend on the economics of the process design, in addition to other factors such as glycosylation requirements, overall initial levels of MAb accumulation, ease of extractability, the extent of purification burden and the desirability of peptide or polypeptide tags in the final product. A process for the production of IgG (secreted form) from transgenic tobacco roots has also been described. All the individual process unit operations will have to be optimally designed, and verified at pilot-scale, which can then be accurately optimised and scaled-up for large-scale production.

	Harvesting and Cleaning	Extraction	Separation	Detergent removal step	Purification	Final polishing filtration	Bulk fill and freeze
IgG (secreted form) from leaves	√	Dry freeze-thaw	Dead-end-filtration and centrifugation	X	1. Affinity (Protein A) 2. Ultrafiltration/Diafiltration 3. Ion exchange chromatography 4. Ultrafiltration/Diafiltration	√	√
mIgG (membrane-bound) from leaves	√	Grinding (i.e. milling) with detergent	Dead-end-filtration and centrifugation	Ion exchange chromatography	1. Affinity (Protein A) 2. Ultrafiltration/Diafiltration 3. Ion exchange chromatography 4. Ultrafiltration/Diafiltration	√	√
IgG-HDEL (retained in the endoplasmic reticulum from leaves	√	Dry freeze-thaw the grind (i.e. milling)	Dead-end-filtration and centrifugation	X	1. Affinity (Protein A) 2. Ultrafiltration/Diafiltration 3. Ion exchange chromatography 4. Ultrafiltration/Diafiltration	√	√
IgG (secreted form) from roots	√	Mechanically stirred shear equipment (based on small-scale model)	Dead-end-filtration and centrifugation	X	1. Affinity (Protein A) 2. Ultrafiltration/Diafiltration 3. Ion exchange chromatography 4. Ultrafiltration/Diafiltration	√	√

Table 9.2: Summary of the recommended process for the production of a monoclonal antibody that is targeted to three different subcellular locations in the leaves transgenic tobacco plants, and for IgG production from the roots.

Chapter 10: Conclusions and Future work

10.1 MAIN CONCLUSIONS

This thesis has explored the use of transgenic tobacco plants for the production of monoclonal antibodies (MAbs). Despite the often stated advantage of lower upstream processing costs due to high upstream scalability of plants (Whitelam et al., 1993), and many reported successes on optimising expression and the functionality of the expressed protein, there is currently limited information on the downstream processing options to allow for a thorough economic appraisal. This is particularly important as downstream processing often represents a high processing cost (Kusnadi et al., 1997). Furthermore, until now, there have been no detailed studies comparing the extractability of either recombinant or native proteins that were targeted to different cellular locations in transgenic plants.

The research set out to investigate methods for the initial extraction of recombinant IgG antibodies from transgenic tobacco leaves. Three different subcellular targeting strategies for Guy's 13 (IgG) antibodies that act against Streptococcus mutans (the main agent of tooth decay in the mouth) were explored, in order to determine the parameters for optimal extraction with respect to antibody targeting to the apoplasm, plasma membrane or endoplasmic reticulum. Seven small-scale techniques for physical extraction were compared for each transgenic line, with the view to establishing the most suitable potential method for scale-up.

To carry out these studies both IgG (secreted form) and membrane-bound IgG (mIgG) were already available. A third line of transgenic plants expressing the same monoclonal antibody targeted to the endoplasmic reticulum membrane by the addition of the –HDEL tetrapeptide was successfully produced.

The functionality of the expressed IgG-HDEL in transgenic plants was demonstrated, followed by its retention in the endoplasmic reticulum.

In addition to the most commonly used techniques for extraction currently used in the laboratory such as grinding in buffer and grinding in liquid nitrogen, five other extraction techniques were investigated. Although these techniques demonstrated a degree of variability between them, they were statistically proven to be reproducible for this scale of investigation because the variability of multiple extractions from the same plant never reached statistical significance. This thesis demonstrated that for IgG that is secreted and accumulated in the apoplasm, dry freeze-thaw (the freezing of leaf discs at -20oC followed by room temperature thawing before buffer addition) is an appropriate technique for extraction of a high yield and a low release of native plant proteins from transgenic tobacco leaves with respect to the other techniques investigated. As well as lowering the downstream purification burden, the large-scale equipment involved in this step is likely to have a lower operating cost than a mechanical, energy-intensive grinding device. Another consideration however, was that although the passive (non-grinding) extraction techniques were effective at laboratory scale, the leaf samples used had a high cut surface to volume ratio, which would need to be considered when scaling up to large scale purification from whole plants, for example by the employment of one of the shredding devices already used in the tobacco industry.

Freeze-thawing leaf discs dry or wet (i.e. within buffer) and "passive elution" were new techniques which have not previously been discussed in the literature for this application. This is in contrast to prior literature that had reported that a high level of physical damage to leaf tissue was needed to release the maximum amount of recombinant protein (Menkhaus et al., 2004). However, in addition to increasing the operational cost of a large-scale equivalent of this equipment and increasing the purification burden, the complete disintegration of leaf tissue will generate a high degree of fibre that could foul chromatographic columns and filtration membranes. Thus, the ability to use gentle techniques such as dry freeze-thaw to

extract MAbs that are secreted into the apoplasm of the cell is likely to be welcomed by process engineers.

IgG-HDEL-expressing transgenic plants demonstrated an increase in IgG-HDEL yield with technique severity, indicating that harsher techniques such as dry-freeze-thaw followed by grinding were optimal. For mIgG-expressing transgenic plants, there was a marked difference in antibody yield between the less severe techniques (passive elution, dry freeze-thaw and wet freeze-thaw) and the harsher techniques which all involved grinding. Grinding in buffer was chosen as the optimal technique in this case, but a downside of this form of the MAb is that detergent was required, the optimal concentration of which was found to be 0.1% (v/v) for Triton X-100. Triton X-100 is a non-ionic detergent that acts by solubilising the plasma membrane, whilst the integrity of the protein is maintained. For IgG (secreted form), detergent concentration had no effect on absolute IgG yield. Although, 0.1% (v/v) Triton X-100 also led to an increase in IgG-HDEL yields, it was not a necessity as it was for the membrane-bound IgG. Downsides of the inclusion of detergent include an increase in the extraction of native proteins and the indicated release of chlorophyll (burdening the downstream process), the necessity to remove the detergent itself downstream after extraction, the cost of its initial inclusion, and waste considerations for its removal at the end of the process.

Grinding samples on ice or at room temperature was found to have no effect on IgG yield for all three MAbs. This indication of plant-derived IgG stability at room temperature is an obvious cost benefit at industrial scale. For all forms of the IgG, there was a wide variety of usable pHs (pH 5 to 7) with the exception of very low pHs of 3 and 4. Overall, this study has shown that the specific IgG target location in the tobacco leaf cell has an important impact on the determination of an optimal extraction procedure, which needs to be considered in developing production strategies.

This thesis also preliminarily addressed the issue of harvesting for the secreted form of IgG and the intracellularly retained IgG-HDEL which is one of the main issues that are often overlooked in related literature. Analysis of the data led to an interesting observation of the wound response in plants and the consequences for time-response IgG levels, but this response varied significantly for the same monoclonal antibody (MAb), targeted to two different subcellular compartments. For plants expressing the secreted form of IgG, there was a marked difference on the effect of mechanical wounding on subsequent IgG levels in young and old plants, with a negative effect (IgG reduction) on young growing plants and a positive effect (IgG boost) in older plants, 2, 4, or 6 days after first administration of the wound. (Young plants were able to recover from the detrimental effect of wounding on IgG levels after 2 weeks). The difference in the plant's reaction to wounding according to its age was explained by the growth differentiation balance theory. Intracellularly retained IgG located in the endoplasmic reticulum, however, was not significantly affected by wounding at any age. For secreted IgG expressing plants, IgG was found to be age dependent with the highest amount of IgG per unit mass found in young plants (2-4 weeks old) and in young leaves of old plants (at the top of the plant), with a very significant reduction in older tissue (at the bottom of the plant) and old plants (15-18 weeks old), most likely due to senescence and its associated increase in detrimental apoplasm-residing proteases. IgG-HDEL-expressing plants, in which the MAb is retained in the endoplasmic reticulum, however, had a much more stable IgG level with tissue or overall plant age. In large-scale terms, IgG-HDEL-expressing plants may therefore be more favourable as the avoidance of any mechanical damage when the plants are at a young age pre-harvesting, is not so critical.

Roots were also examined as a possible source of the MAb. A new approach was described that allowed the determination of the magnitude of force required to break single plant roots. These experiments were performed on roots expressing IgG (secreted form). Although this antibody can be secreted into the medium in a hydroponic system, the rate of secretion is slow and a large medium

requirement is likely. It was found that it was possible to separate the roots into four developmental root stages, as identified by their colour. The novel micromanipulation technique involved pulling single tobacco roots in buffer to breakage, in order to determine their peak force for breakage. A characteristic uniform step-wise increase in the force up to a peak force for breakage was observed. The peak force for breakage (101 $\pm$ 7mN), mean work done (97 $\pm$ 6 μJ), and nominal stress representing tensile strength (2400 $\pm$ 200 kPa) were the same for the four root development stages. However, there was a slight but significant increase in the peak force for breakage from the youngest white roots to the oldest dark red-brown roots, and we speculated that this was due to increasing lignin deposition with age (as shown by Phloroglucinol staining). There were no significant differences between fresh root mass, original root length, and mean root diameter for any of the root categories, displaying their uniformity, which would be beneficial for bioprocessing. There was also no significant difference in the amount of antibody expressed in any of these roots. These data showed that it is possible to characterise the force requirements for root breakage.

Encouragingly, similar levels of IgG were found when equivalent fresh masses of leaf discs and 1 cm root sections (from the same plants) were sheared in this mechanically stirred shear device demonstrating that roots offer a potential alternative to leaves for MAb production. The next stage was then to see if it was possible to relate the mechanical properties of single roots characterised by micromanipulation to their behaviour in a small-scale, scalable mechanically stirred shear device. Experimental data was used together with non-specific mathematical models from literature, to develop a mathematical model of breakage that occurred in the mechanically stirred shear device. It was concluded that root breakage in this system was most likely due to root-impeller collisions. In addition, the maximum strain energy theory of failure of an elastic material under this mode of stress was used to establish a relationship between the stable length of the root debris and some of the physical parameters influencing it. The experimental data suggested that root breakage was approximately a first-order kinetic

process. The analysis provided a means of studying the efficiency of fragmentation and provided the basis for further studies of size distribution changes accompanying root size minimisation. An estimation of the relative root tensile strength of transgenic tobacco roots by experimental data and theoretical equations (macromanipulation) gave an estimated tensile strength of 2100 kPa $\pm$ 600 kPa thus, comparing well with the tensile strength measured by micromanipulation. Thus, it appeared that measurements of root tensile strength by micromanipulation would be a valid means of finding the minimum energy required for breaking roots in a mechanical shear device. It is important to note, however, that these results are consistent for this particular set-up e.g. biomaterial type, impeller speed, impeller/vessel type etc., and a change in any of these parameters may affect the similarity of values of root tensile strength derived at micro- and macro- scales.

Finally, a framework for the overall process design for the production of three different forms of the same monoclonal antibody (targeted to different subcellular compartments) from transgenic tobacco leaves was described. A potential process design for the production of IgG (secreted form) from transgenic tobacco roots was also depicted. Although largely based on processes for monoclonal antibody production from mammalian cell cultures, there was no need for virus inactivation or several virus filtration steps in the process. Ultrafiltration was included to remove plant specific phenolics, and it was thought necessary to include a dead-end filtration step prior to centrifugation to ensure clarification of the process liquid from the fibrous plant tissue. The inclusion of the non-ionic detergent, Triton X-100 for extraction of the membrane-bound IgG necessitated the addition of an additional ion exchange step for its subsequent removal.

This research has highlighted the importance of initial immunoglobulin subcellular targeting strategy on the whole process design. Overall, IgG-HDEL appeared to be present in a greater absolute yield than IgG in transgenic plants. However, the choice between the different targeting strategies will therefore inevitably depend on the economics of the process design in addition to other factors such as

the preference of secretion over intracellular retention (greenhouse vs. contained field), glycosylation requirements in terms of FDA regulations and the effectiveness of the glycosylated antibodies during immunisation, overall initial levels of MAb accumulation, total extractable yield of MAb from plants, the simplicity and scalability of the extraction method, the extent of purification burden after extraction on the downstream process, and the desirability of peptide or polypeptide tags in the final product.

10.2 NOVEL CONTRIBUTIONS MADE TO THE FIELD BY THIS THESIS

Novel contributions made to the field by this thesis include:

- The construction of Guy's 13-HDEL in transgenic *Nicotiana tabacum* plants.
- The identification of the optimal extraction technique and buffer composition at small-scale for 3 versions of the same monoclonal antibody targeted to different subcellular compartments in transgenic tobacco plants.
- The discovery of the optimal location of harvest of leaves within a plant and optimal harvest time in terms of overall plant age for both a secreted form and intracellularly retained version of a monoclonal antibody.
- The investigation of the feasibility of physical extraction from roots of whole transgenic tobacco plants for the production of monoclonal antibody.
- The development of a novel micromanipulation technique for the measurement of the force required to break single plant roots. (Although this was done for tobacco, this would be applicable to any fine roots from any plant).
- The characterisation of the mechanical properties single transgenic tobacco roots in terms of force, work done and tensile strength.

- A model that is able to relate the mechanical characteristics of single transgenic tobacco roots established by micromanipulation to the mechanical breakage of multiples of these roots in buffer, in a mechanically stirred shear device (macromanipulation).
- A proposal of the downstream process for the production of monoclonal antibodies that are targeted to different subcellular compartments from transgenic tobacco plants that is based upon identified optimal harvesting and extraction methods.

10.3 RECOMMENDATIONS FOR FUTURE WORK

Research ideas that ensue from the work in this thesis include the following:

- Pilot scale or large scale experiments to mimic our "dry freeze-thaw" experiments using a system such as CryoFin^{TM} under controlled freezing and thawing conditions to confirm our results of a high IgG (secreted form) and a low co-extraction of native protein.
- An extension of our harvesting experiments in the field or large-scale greenhouse trials would be useful.
- It would be interesting to try to establish whether during micromanipulation, individual roots were being broken within cells or via the middle lamella (between cells).
- Further work is required to determine whether the mathematical model developed in Chapter 8 is a generic method that will work for ranges of values of all critical input operating parameters and vessel geometries.
- Scale-up studies of the laboratory scale mechanically stirred shear device is required to confirm its suitability at large scale for transgenic tobacco leaf or root breakage for monoclonal antibody extraction.

- All the individual downstream process unit operations will have to be optimally designed, with experimentation using laboratory scale ultra-scale down mimics of each unit operation, followed by pilot-scale equivalents, which can then be accurately optimised and scaled-up for large-scale production.

References

Akerstrom B, Bjorck L. 1989. Protein L: An immunoglobulin light chain-binding bacterial protein. J. Biol. Chem. 264: 19740-19746.

Allen M, Allen E, Friese C. 1989. Responses of the non-mycotrophic plant *Salosa kali* to invasion by vesicular-arbuscular mycorrhizal fungi. New Phytol 111:45-49.

Amanullah A, Blair R, Nienow AW, and Thomas CR. 1998. Effects of agitation intensity on mycelia morphology and protein production in chemostat cultures of recombinant Aspergillus oryzae. Biotech Bioeng. 62(4): 434-446.

Asenjo JA, Turner RE, Mistry SL and Kaul A. 1994. Separation and purification of recombinant proteins from *Escherichia coli* with aqueous two-phase systems. J. Chromatogr. A. 668: 129–137.

Austin S, Bingham ET, Koegel RG, Mathews DE, Shahan MN, Straub RJ, Burgess RR. 1994. An overview of a feasibility study for the production of industrial enzymes in transgenic alfalfa. Ann. NY. Acad. Sci. 721: 234-244.

Ayazi Shamlou, PA, Makagiansar HY, Ison AP, Lilly MD and Thomas CR. 1994. Turbulent Breakage of Filamentous Microorganisms in Submerged Culture in Mechanically Stirred Bioreactors, Chem. Eng. Sci. 49: 2621-2631.

Azzoni AR, Farinas CS and Miranda EA. 2005. Transgenic corn seed for recombinant protein production: relevant aspects on the aqueous extraction of native components. J. Sci. Food Agric. 85: 609–614.

Azzoni AR, Kusnadi AR, Miranda EA and Nikolov ZL. 2002. Recombinant aprotinin produced in transgenic corn seed: extraction and purification studies. Biotech. Bioeng. 80: 268–276.

Baenziger JU and Fiete D. 1979. Structural determinants of Concanavalin A specificity for oligosaccharides. J. Biol. Chem. 254: 2400–2407.

Bai Y and Nikolov ZL. 2001. Effect of processing on the recovery of recombinant β-glucuronidase (rGUS) from transgenic canola. Biotechnol. Prog. 17:168–174.

Bai Y, Glatz CE. 2003a. Bioprocess considerations for expanded bed chromatography of crude canola extract using STREAMLINE expanded bed anion exchange. Biotechnol. Bioeng. 81: 855-864.

Bakker H, Bardor M, Molthoff J W, Gomord V, Elbers I, Stevens LH, Jordi W, Lommen A, Faye L, Lerouge P, and Bosch D. 2001. Galactose-extended glycans of antibodies produced by transgenic plants. Proc. Natl. Acad. Sci. U. S. A. 98: 2899–2904.

Balasubramaniam D, Wilkinson C, Van Cott K and Zhang C. 2003. Tobacco protein separation by aqueous two-phase extraction. J. Chromatogr. 989: 119–129.

Baldwin IT, Zhang ZP, Diab N, Ohnmeiss TE, McCloud ES, Lynds GY, Schmelz EA. 1997. Quantification, correlations and manipulations of wound-induced changes in jasmonic acid and nicotine in Nicotiana sylvestris. Planta. 201: 397–404.

Bardor M, Faveeuw C, Fitchette A-C, Gilbert D, Galas L, Trottein F, Faye L, and Lerouge P. 2003. Immunoreactivity in mammals of two typical plant glyco-epitopes, core α(1,3)-fucose and core xylose. Glycobiology. 13: 427-434.

Benvenuto E, Ordas RJ, Tavazza R, Ancora G, Biocca S, Cattaneo A, Galeffi P. 1991. Phytoantibodies: a general vector for the expression of immunoglobulin domains in transgenic plants. Plant Mol. Biol. 17: 865–874.

Bhairi SM, and Mohan C. 2007. Detergents: A guide to the properties and uses of detergents in biology and biochemistry. Calbiochem®CB0068-2007 INTL Detergents Booklet (www.calbiochem.com)

Birch JR, Racher AJ. 2006 Antibody production. Advanced Drug Delivery Reviews. 58: 671-685.

Bjorck L, 1988. Protein L: A novel bacterial cell wall protein with affinity for Ig L chains. J. Immunol. 140: 1194-1197.

Blaszczyk A, Sirko L, Hawkesford MJ and Sirko A. 2002. Biochemical analysis of transgenic tobacco lines producing bacterial serine acetyltransferase. Plant Sci. 162: 589–597.

Blixt O, Allin K, Pereira L, Datta A, and Paulson JC. 2002. Efficient chemoenzymatic synthesis of O-linked sialyl oligosaccharides. J. Am. Chem. Soc. 124, 5739–5746.

Borisjuk N, Borisjuk L, Logendra S, Petersen F, Gleba Y, Raskin I. 1999. Production of recombinant proteins in plant root exudates. Nat Biotechnol 17: 466–469.

Boulding N, Yim SSS, Keshavarz-Moore E, Ayazi Shamlou P and Berry M. 2002. Ultra scale-down to predict filtering centrifugation of secreted antibody fragments from fungal broth. Biotech. Bioeng. 79: 381–388.

Boychyn M, Doyle W, Bulmer M, More J, Hoare M. 2000. Laboratory Scaledown of protein purification processes involving fractional precipitation and centrifugal recovery. Biotech Bioeng. 69(1): 1-10.

Buchanan-Wollston V. 1997. The molecular biology of leaf senescence. J. Exp. Bot. 48: 181-199.

Buis B., Wever PC, Koomen GC, van Acker BA, Groothoff JW, Krediet RT and Arisz L. 1997. Clearance ratios of amylase isoenzymes and IgG subclasses: do they reflect glomerular charge selectivity? Nephron. 75: 444–450.

Burgess T, St J HARDY GE, McComb JA, Colquhoun I. 1999. Effects of hypoxia on root morphology and lesion development in Eucalyptus *marginata* infected with *Phytophthora cinnamomi.* Plant Pathol 48 (6): 786-796.

Cabanes-Macheteau M, Fitchette-Laine A-C, Loutelier-Bourhis C, Lange C, Vine ND, Ma J K-C, Lerouge P and Faye L. (1999) N-glycoslation of a mouse IgG expressed in transgenic tobacco plants. Glycobiology. 9: 365–372.

Chargelegue D, Vine ND, van Dolleweerd CJ, Drake PMW and Ma JK-C. 2000. A murine monoclonal antibody produced in transgenic plants with plant-specific glycans is not immunogenic in mice. Transgenic Res. 9: 187–194.

Chein R, Chung JN. 1988. Simulation of particle dispersion in a two-dimensional mixing layer. AIChE J. 34(6): 946-954.

Chen Z, Ricigliano JW, Klessig DF. 1993. Purification and characterization of a soluble sacylic acid-binding protein from tobacco. Proc. Natl. Acad. Sci. USA. 90: 9533-9537.

Cheryan M. 1980 Phytic acid interactions in food systems. Crit. Rev. Food Sci. Nutr. 13: 297–335

Chong DKX and Langridge WHR. 2000. Expression of full-length bioactive antimicrobial human lactoferrin in potato plants. Transgenic Research. 9:71-78.

Christensen AH and Quail PH. 1996. Ubiquitin promoter-based vectors for high-level expression of selectable and/or screenable marker genes in monocotyledonous plants. Transgenic Res. 5: 213–218.

Christou P. 1996. Transformation Technology. Trends in Plant Sciences. 1:423-431.

Coleman L, Mahler S. 2003. Purification of Fab fragments from a monoclonal antibody papain digest by Gradiflow electrophoresis. Protein Expression and Purification. 32: 246-251.

Comas LH, Eissenstat DM, Lakso AN. 2000. Assessing root death and root system dynamics in a study of grape canopy pruning. New Phytol. 147: 171-178.

Conrad U and Fiedler U. 1998. Compartment-specific accumulation of recombinant immunoglobulins in plant cells: an essential tool for antibody production and immunomodulation of physiological functions and pathogen activity. Plant Mol. Biol. 38: 101–109.

Cramer C.L. Boothe JG, Oishi KK. 1999. Transgenic plants for therapeutic proteins: linking upstream and downstream technologies. Curr. Top. Microbiol. Immunol. 240: 95–118.

Daniell H, Khan M, Allison L. 2002. Milestones in chloroplast genetic engineering: an environmentally friendly era in biotechnology. Trends Plant Sci. 7: 84-91.

Dawson RF, Solt ML. 1959. Estimated contributions of root and shoot to the nicotine content of the tobacco plant. Plant Physiol 656-661.

Dawson RF, Solt ML. 1959. Estimated contributions of root and shoot to the nicotine content of the tobacco plant. Plant Physiol 656-661.

De Neve M, De Loose M, Jacobs A, Van Houdt H, Kaluza B, Weidle U, Depicker A. 1993. Assembly of an antibody and its derived antibody fragment in Nicotiana and Arabidopsis. Transgenic Res. 2: 227–237.

De Wald DB, Sadka A, Mullet JE. 1994. Sucrose modulation of soybean VSP gene expression is inhibited by auxin. Plant Physiol. 104: 439–444.

Delichatsios MA. 1980. Particle coagulation in steady turbulent flows: application to smoke aging. J. Colloid Interface Sci. 78, 163-174.

Delichatsios MA and Probstein RF. 1976. The effect of coalescence on the average drop size in liquid–liquid dispersions, Industrial Engineering Chemistry Fundamentals. 14: 134-138.

Denecke J, De Rycke R. and Botterman J. 1992. Plant and mammalian sorting signals for protein retention in the endoplasmic reticulum contain a conserved epitope. EMBO J. 11: 2345–2355.

Desai U, Sur G, Daunert S, Babbit TR. and Li Q. 2002. Expression and affinity purification of recombinant proteins from plants. Prot. Expression Purif. 25: 195–202.

Drake PMW, Chargelegue DM, Vine ND, van Dolleweerd CJ, Obregon P, Ma J K-C. 2003. Rhizosecretion of a monoclonal antibody protein complex from transgenic tobacco roots. Plant Mol. Biol. 52: 233-241.

Dunn R. 1979. Effect of *Xiphinema americanum* and *Rhizoctonia solani* on browning of apple roots. Fungicide and Nematicide Test. 35:214.

Evangelista RL, Kusnadi AR, Howard JA and Nikolov ZL 1998. Process and economic evaluation of the extraction and recombinant b-glucuronidase from transgenic corn. Biotechnol. Prog. 14: 607–614.

Evans TW, Sarofim AF and Margolis G. 1974. Models of secondary nucleation attributable to crystal-crystalliser and crystal-crystal collisions. AIChE J. 20 (15): 959-966.

Farid SS. 2007. Process economics of industrial monoclonal antibody manufacture. J. Chromatogr. B. 848:8-18.

Fiedler U, Phillips J, Artsaenko O, Conrad U. 1997. Optimization of scFv antibody production in transgenic plants. Immunotechnology. 3: 205–216.

Fischer R and Emans N. 2000. Molecular farming of pharmaceutical proteins. Transgenic Res 9: 279-299.

Fischer, R. Vaquero C, Sack M, Drossard J, Emans N and Commandeur U. 1999. Towards molecular farming in the future: transient protein expression in plants. Biotechnol. Appl. Biochem. 30: 113–116.

Fitter A. 1996. Characteristics and Functions of Root systems. In: Waisel Y, Eshel A, Kafkafi U. Plant roots, the hidden half. Second ed., rev. and expanded. New York: Marcel Decker, Inc. p 1-17.

Flatman S, Alam I, Gerard J and Mussa N. 2007. Process analytics for purification of monoclonal antibodies. Journal of Chromatogr. B. 848: 79-87.

Frigerio L, Vine N.D., Pedrazzini, E., Hein, M.B, Wang F, Ma JK and Vitale A. 2000. Assembly, secretion, and vacuolar delivery of a hybrid immunoglobulin in plants. Plant Physiol. 123: 1483–1494.

Fry SC. 2004. Primary cell wall metabolism: tracking the careers of wall polymers in living plant cells. New Phytologist 161 (3): 641 – 675.

Garger SJ, Holtz RB, McCulloch MJ and Turpen TH. 2000. Process for isolating and purifying viruses, soluble proteins, and peptides from plant sources. US Patent 6,033,895.

Gazaryan IG, Lagrimini LM. 1996. Purification and unusual kinetic properties of a tobacco anionic peroxidase. Phytochemistry. 41 (4): 1029-1034.

Giddings G. 2001. Transgenic plants as protein factories. Curr. Opin. Biotechnol. 12: 450–454.

Gilissen L JW, van Staveren MJ, Hakkert JC, and Smulders MJM. 1996. Competence for regeneration during tobacco internodal development. Plant Physiol. 11 1 : 1243-1 250.

Gill NK. Appleton M. Baganz F., Lye G. 2008. Quantification of power consumption and oxygen transfer characteristics of a stirred miniature bioreactor for predictive fermentation scale-up. 100 (6): 1144 – 1155.

Glatz CE, Hoare M, Landa-Vertiz J. 1986. The formation and growth of protein precipitates in a continuous stirred-tank reactor. AIChE J. 32: 1196-1204.

Gleba, Y., Klimyuk, V. and Marillonnet, S. 2007. Viral vectors for the expression of proteins in plants. Curr. Opin. Biotechnol. 18: 134–141.

Goldstein G, Drake DR, Melcher P, Giambelluca TW, Heraux J. 1996. Photosynthetic gas exchange and temperature-induced damage in seedlings of the tropical alpine species argyroxiphium sand wicense. Oecologia. 106: 298-307.

Gomord V, Denmat LA, Fitchette-Laine AC, Satiat-Jeunemaitre B, Hawes C and Faye L. 1997. The C-terminal HDEL sequence is sufficient for retention of secretory proteins in the endoplasmic reticulum (ER) but promotes vacuolar targeting of proteins that escape the ER. Plant J. 11: 313–325.

Gomord V, Sourrouille C, Fitchette A-C, Bardor M, Pagny S, Lerouge P and Faye L. 2004. Production and glycosylation of plant-made pharmaceuticals: the antibodies as a challenge. Plant Biotechnol. J. 2, 83–100.

Gore MG, Ferris WF, Popplewell AG, Scawen M and Atkinson T. 1992. pH-sensitive interactions between IgG and a mutated IgG-binding protein based upon two B domains of Protein A from Staphylococcus aureus. Protein Eng. 5: 577–582.

Gray PP, Dunnill P and Lilly MD. 1973. The clarification of mechanically disrupted yeast suspensions by rotary vacuum precoat filtration. Biotech. Bioeng. 15: 309-320.

Green TR and Ryan CA. 1972. Wound-induced proteinase inhibitor in plant leaves – possible defense mechanism against insects. Science. 175: 776-777.

Hassan S, Liu W, Ma JK-C, Thomas CR, Keshavarz-Moore E. 2008. Characterization of mechanical properties of transgenic tobacco roots expressing a recombinant monoclonal antibody against tooth decay. Biotech Bioeng. 100, (4): 803-809.

Hassan S, van Dolleweerd CJ, Ioakeimidis F, Keshavarz-Moore E, Ma JK-C. 2008b. Considerations for extraction of monoclonal antibodies targeted to different subcellular compartments in transgenic tobacco plants. Plant Biotech. J. 6: 733–748.

He Y, Takahashi K and Nomura T. 1995. Particle-impeller impact for a six-bladed 45° pitched turbine in an agitated vessel. J Chem Eng Jpn. 28(6): 786-789.

Headon DR, Walsh G. 1994. The industrial production of enzymes. Biotechnol. Adv. 12: 635-646.

Hearle DC, Aguilera-Soriano G, Titchener-Hooker N J, Wiksell E. 1994. Quantifying the fouling effects of a biological process stream on chromatographic supports. Proc. IChemE Res.Event: 174-176.

Hein MB, Tang Y, McLeod DA, Janda KD., Hiatt A. 1991. Evaluation of immunoglobulins from plant cells. Biotechnol Prog 7: 455-461.

Helenius A. and Aebi M. 2004. Roles of N-linked glycans in the endoplasmic reticulum. Annu. Rev. Biochem. 73, 1019–1049.

Henderson IR and Dean C. 2004. Control of Arabidopsis flowering: the chill before the bloom. Development 131 (16): 3829-3838.

Hendrick RL, Pregitzer KS. 1992. The demography of fine roots in a northern hardwood forest. Ecology 73:1094–1104.

Hepworth DG, Vincent JFV, Schuch W. 1998. Using Viscoelastic Properties of the Woody Tissue from Tobacco Plants (*Nicotiana tabacum*) to Comment on the Molecular Structure of Cell Walls. Ann Bot 81: 729-734.

Herms DA, Mattson WJ. 1992. The Dilemma of Plants: To Grow or Defend. The Quarterly Review of Biology. 67(3) 283-335.

Hetherington P J, Follows M, Dunnill P, Lilly MD. 1971. Release of protein from Bakers' yeast (Saccharomyces cerevisiae) by disruption in an industrial homogeniser. Trans. Inst. Chem. Eng. 49: 142-148.

Hiatt AC, Cafferkey R, Bowdish K. 1989. Production of antibodies in transgenic plants. Nature. 342: 76-78.

Hibino T, Shibata D, Ito T, Higuchi T, Pollet B, Lapierre C. 1994. Chemical properties of lignin from Aralia cordata. Phytochemistry 37: 445-448.

Hoekema A, Hirsch PR, Hooykaas PJJ and Schilperoort, RA. 1983. A binary plant vector strategy based on separation of vir- and T-region of the Agrobacterium tumefaciens Ti-plasmid. Nature, 303, 179–180.

Holler C and Zhang C. 2008. Purification of an acidic recombinant protein from transgenic tobacco. Biotechnol. Bioeng. 99, 902–909.

Holler C, Vaughan D and Zhang C. 2007. Polyethyleneimine precipitation versus anion exchange chromatography in fractionating recombinant beta-glucuronidase from transgenic tobacco extract. J. Chromatogr. A, 1142: 98–105.

Hood EE, Woodard SL and Horn ME. 2002. Monoclonal antibody manufacturing in transgenic plants — myths and realities. Curr. Opin. Biotechnol. 13: 630–635.

Hood EE, Witcher D R, Maddock S, Meyer T, Baszczynski C , Bailey M, Flynn P , Register J, Marshal l L, Bond D, Kulisek E, Kusnadi A , Evangelista R, Nikolov Z, Wooge C , Mehigh RJ , Hernan R, Kappel WK , Ritland D, Li C P and Howard JA. 1997. Commercial production of avidin from transgenic maize: characterization of transformant, production, processing, extraction and purification. Mol. Breed. 3: 291–306.

Horowitz B, Wiebe ME, Lippin A and Stryker MH. 1985. Inactivation of viruses in labile blood derivatives. Transfusion, 25, 516–522.

Horsch RB, Fry JE, Hoffman NL, Wallroth M, Eichholtz DZ, Rogers SG and Fraley RT. 1985. A simple and general method for transferring genes into plants. Science. 227: 1229–1231.

Humphrey JAC. 1990. Fundamentals of fluid motion in erosion by solid particle impact. Int J Heat Fluid Flow. 11(13): 170-195.

Hutchings IM, MacMillan NH and Rickerby DG. 1981. Further studies of the oblique impact of a hard sphere against a ductile solid. Int J Mech Sci. 23(11): 639-646.

Hutchings IM, Winter RE and Field JE. 1976. Solid particle erosion of metals: the removal of surface material by spherical projectiles. Proc R Soc Lond A348: 379-392.

Hutchings IM. 1987. Wear by particulates. Chem Eng Sci. 42(4): 869-878.

Imanishi S, Hashizume K, Kojima H, Ichihara A, Nakamura K. 1998a. An mRNA of tobacco cell, which is rapidly inducible by methyl jasmonate in the presence of cycloheximide, codes for a putative glycosyltransferase. Plant and Cell Physiology 39: 202–211.

Imanishi S, Hashizume K, Nakakjta M, Kojima H, Matsubayashi Y, Hashimoto T, Sakagami Y, Yamada Y, Nakamura K. 1998b. Differential induction by methyl jasmonate of genes encoding ornithine decarboxylase and other enzymes involved in nicotine biosynthesis in tobacco cell cultures. Plant Molecular Biology 38: 1101–1111.

Izawa T, Takahashi Y and Yano M. 2003. Comparative biology comes into bloom: genomic and genetic comparison of flowering pathways in rice and Arabidopsis. Curr. Opin. Plant Biol. 6, 113-120.

James DC and Dinnis DM. 2005. Engineering mammalian cell factories for improved recombinant monoclonal antibody production: lessons from nature? Biotech Bioeng. 91(2): 180 - 189.

Jensen RA. 1985. The shikimate/arogenate pathway: link between carbohydrate metabolism and secondary metabolism. Physiol. Plant. 66: 164-168.

Jervis L and Pierpoint WS. 1989. Purification technologies for plant-proteins. J. Biotechnol. 11, 161–198.

Jones WR, Ting-Beall HP, Lee GM, Kelley SS, Hochmuth RM, Guilak F (1999) Alterations in the Young's modulus and volumetric properties of chondrocytes isolated from normal and osteoarthritic human cartilage. J. Biomechanics 32: 119–127.

Jüsten P, Paul GC, Nienow AW, and Thomas CR. 1996. Dependence of mycelial morphology on impeller type and agitation intensity. Biotech Bioeng. 52: 672-684.

Jüsten P, Paul GC, Nienow AW, and Thomas CR. 1998a. A mathematical model for agitation-induced fragmentation of Penicillium chrysogenum. Bioprocess Eng. 18: 7-16.

Jüsten P, Paul GC, Nienow AW, and Thomas CR. 1998b. Dependence of Penicillium chrysogenum growth, morphology, vacuolation, and productivity in fed-batch fermentations on impeller type and agitation intensity. Biotech. Bioeng. 59 (6): 762-775.

Kapila J, De Rycke R, Van Montagu M, and Angenon G. 1997. An agrobacterium-mediated transient gene expression system for intact leaves. Plant Sci. 122: 101–108.

Kapusta J, Modelska A, Figlerowicz M, Pniewski T, Letellier M, Lisowa O, Yusibov V, Koprowski H, Plucienniczak A and Legocki AB. 1999. A plant derived edible vaccine against hepatitis B virus. The FASEB Jour. 13, 1796-1799.

Karaivazoglou NA, Papakosta DK, Sfaciotakis EM and Koutroubas SD. 2004. Ethylene biosynthesis, ripening and senescence behavior of tobacco (*Nicotiana tabacum* L) leaves New directions for a diverse planet: Proceedings of the 4th International Crop Science Congress Brisbane, Australia, 26 Sep – 1 Oct 2004, ISBN 1 920842 20 9, wwwcropscienceorgau.

Kay E, Vogel MT, Bertolla F, Nalin R, and Pascal Simonet. 2002. In situ transfer of antibiotic resistance genes from transgenic (transplastomic) tobacco plants to bacteria Appl Environ Microbiol. 68: 3345–3351.

Kay R, Chan A, Daly M and McPherson J. 1987. Duplication of CaMV-35S promoter sequences creates a strong enhancer for plant genes. Science. 236: 1299–1302.

Kee GS, Pujar NS, and Titchener-Hooker NJ. 2008. Study of Detergent-Mediated Liberation of Hepatitis B Virus-like Particles from S cerevisiae Homogenate: Identifying a Framework for the Design of Future-Generation Lipoprotein Vaccine Processes Biotechnol Prog: 24, 623-631

Kee KC and Rielly CD. 2004. Measurement of particle impact frequencies and velocities on impeller blades in a mixing tank Trans IChemE, Chem Eng Res Des 82(A9): 1237-1249

Keshavarz-Moore E, Hoare M, Dunnill P. 1987. Biochemical engineering aspects of cell disruption, pp 62-79 In: M S Venal and M J Hudson (eds), Separations for biotechnology Ellis Horwood,

Khoudi H, Laberge S, Ferullo J-M, Bazin R, Darveau A, Castonguay Y, Allard G, Lemieux R and Vézina L-P.I. 1999 Production of a diagnostic monoclonal antibody in perennial alfalfa plants Biotechnol Bioeng 64, 135–143

Kipke K. 1980. Erosion Verschleiss non Ruhroanen Chem-Ing-Tech 52: 658-659

Ko K, Wei X, Crooks PA and Koprowski H. 2004. Elimination of alkaloids from plant-derived human monoclonal antibody J Immunol Methods 286 (1-2): 79-85

Komarnytsky S, Borisjuk NV, Borisjuk LG, Alam MZ, Raskin I (2000) Production of recombinant proteins in tobacco guttation fluid Plant Physiol 124: 927–934.

Komartynytsky S, Borisjuk N, Yakoby N, Garvey A, and Raskin I. 2006. Cosecretion of Protease Inhibitor Stabilizes Antibodies Produced by Plant Roots Plant Physiology: 141: 1185–1193.

Kostandini G, Mills BF, and Norton GW. 2006. The Potential Impact of Tobacco Biopharming: The Case of Human Serum Albumin. American Journal of Agricultural Economics. 88(3):671-679.

Krishnan R, McDonald KA, Dandekar AM, Jackman AP, Falk B. 2002. Expression of recombinant trichosanthin, a ribosome inactivating protein, in transgenic tobacco. J Biotechnol. 97:69-88.

Kusnadi AR, Evangelista RL, Hood EE, Howard JA and Nikolov ZL. 1998a. Processing of transgenic corn seed and its effect on the recovery of recombinant β-glucuronidase Biotech. Bioeng: 60, 44–52.

Laîné J -M, Vial D and Moulart P. 2000. Status after 10 years of operation — overview of UF technology today 131: 17-25.

Laitone JA. 1979. Aerodynamic effects in the erosion process. Wear. 56: 239-246

Larrick JW, Yu L, Naftzger C, Jaiswal S and Wycoff K. 2001. Production of secretory IgA antibodies in plants Biomol Eng 18, 87–94.

le Maire M, Champeil P, Moller JV. 2000. Interaction of membrane proteins and lipids with solubilizing detergents. Biochim. Biophys. Acta. 1508: 86–111.

Lee TS, Turner MK and Lye GJ. 2002. Mechanical stability of immobilized biocatalysts (CLECs) in dilute agitated suspensions Biotechnol Prog 18, 43–50.

Li ZJ, Shukla V, Wenger K, Fordyce A, Pedersen AG, Marten M. 2002. Estimation of hyphal tensile strength in production-scale Aspergillus oryzae fungal fermentations Biotech Bioeng 77 (6): 601-613

Liljeroth E. 1995. Comparisons of early root cortical senescence between barley cultivars, *Triticum* species and other cereals New Phytol 130: 495-501

Ma J K-C and Lehner T. 1990. Prevention of colonisation of *Streptococcus mutans* by topical application of monoclonal antibodies in human subjects Archs oral Bid Vol 35, Suppl,p p II5S-122S

Ma J K-C, Drake PMW and Christou P. 2003. The production of recombinant pharmaceutical proteins in plants Nature Rev Genet. 4: 794-805

Ma JK -C, Barros E, Bock R, Christou P, Dale PJ, Dix PJ, Fischer R, Irwin J, Mahoney R, Pezzotti M, Schillberg S, Sparrow P, Stoger E, and Twyman RM. 2005. Molecular farming for new drugs and vaccines: Current perspectives on the production of pharmaceuticals in transgenic plants EMBO Rep 6(7): 593–599.

Ma JK-C, Hiatt A, Hein MB, Vine N, Wang F, Stabila P, van Dolleweerd C, Mostov K and Lehner T. 1995. Generation and assembly of secretory antibodies in plants Science, 268, 716–719.

Ma JK-C, Lehner T, Stabila P, Fux CI, Hiatt A. 1994. Assembly of monoclonal antibodies with IgG1 and IgA heavy chain domains in transgenic tobacco plants. Eur J Immunol. 24: 131-138.

Ma, JK-C, Hikmat BY, Wycoff K, Vine ND, Chargelegue D, Yu L, Hein MB and Lehner T. 1998. Characterization of a recombinant plant monoclonal secretory antibody and preventive immunotherapy in humans. Nature Med. 4: 601–606.

Mae T, Makino M, Ohira K. 1983. Changes in the amounts of ribulose biphosphate carboxylase synthesized and degraded during the life span of rice leaf (*Oryza sativa* L) *Plant cell Physiol* 24: 1079-1086.

Maire ML, Champeil P and Møller JV. 2000. Interaction of membrane proteins and lipids with solubilizing detergents. Biochim. Biophys. Acta. 1508: 86–111.

Male D. 2004. Antigen recognition In: Immunology- An illustrated guide 4th edition Elsevier Science Limited. pp. 26-33.

Masclaux C, Valadier M, Brugière N, Morot-Gaudry J, Hirel B. 2000. Characterization of the sink/source transition in tobacco (*Nicotiana tabacum* L) shoots in relation to nitrogen management and leaf senescence Planta 211: 510–518.

Mason HS, Lam DMK and Arntzen CJ. 1992. Expression of hepatitis B surface antigen in transgenic plants Proc Natl Acad Sci USA. 89: 11745–11 749.

Matile P. 1992. Chloroplast senescence In Baker NR, Thomas H (eds) Crop photosynthesis: Spatial and temporal determinants Elsevier, Amsterdam, pp 413-440

Mazur P. 1984. Freezing of living cells: Mechanisms and implications Am J Physiol 143:C125–C142.

McCrady R, Comerford N. 1998. Morphological and anatomical relationships of loblolly pine fine roots Trees 12: 431-437.

McGarvey PB, Hammond J, Dienelt MM, Hooper DC, Fu ZF, Dietzschold B, Koprowski H and Michaels FH. 1995. Expression of the rabies virus glycoprotein in transgenic tomatoes Bio Technol 13: 1484-1487.

McKenzie BE and Peterson CA. 1995. Root browning in Pinus banksiana Lamb and Eucalyptus pilularis Sm 1 Anatomy and permeability of the white and tannin zones. Botanica Acta. 108:127–137.

McKey D. 1974. Adaptive Patterns in Alkaloid Physiology *Amer Nat*, 108 (961): 305-320.

Meadhra RO, Kramer HJM and van Rosmalen GM. 1996. Model for secondary nucleation in a suspension crystalliser AIChE J 42(4): 973-982.

Mejare M, Lilius G, Bulow L. 1998. Evalulation of genetically attached histidine affinity tails for purification of lactate dehydrogenase from transgenic tobacco. Plant Sci. 134: 103-114.

Menkhaus TJ and Glatz CE. 2004a. Compatibility of column inlet and adsorbent designs for processing of corn endosperm extracts by packed bed and expanded bed adsorption Biotech Bioeng. 20: 1001–1014.

Menkhaus TJ, Bai Y, Zhang C, Nikolov ZL, Glatz CE. 2004. Considerations for the recovery of recombinant proteins from plants. Biotechnol. Prog. 20: 1001-1014.

Miele L. 1997. Plants as bioreactors for biopharmaceuticals: regulatory considerations. TIBTECH. 15: 45-50.

Milburn PT, Dunnill P. 1994. The Release of Virus-like Particles from Recombinat Saccharomyces cerevisiae: Effect of Freezing and Thawing on Homogenisation and Bead Milling. Biotech. Bioeng. 44: 736-744.

Mirza M, Younus M, Hoyano Y, and Currie R. 1998. Greenhouse production of Echinacea and other medicinal plants Paper presented at Opportunities and Profits II: Special Crops into the 21st Century Nov 1-3, Edmonton, AB, Canada.

Moloney MM and Boothe J, van Rooijen G. 2003. Oil bodies and associated proteins as affinity matrices, US 6,509,453. SemBioSys Genetics Inc.

Montgomery DC. 2005. Experiments with random factors. In: Design and Analysis of Experiments. 6th edition. John Wiley and Sons. Inc. Pp. 492-495.

Moo-Young M, Blanch HW. 1981. Design of biochemical reactors Mass transfer criteria for simple and complex systems Adv Biochem Eng 19:1–69.

Mulesky M, Oishi KK, Williams D. 2004. The primary development model for producing human recombinant proteins in tobacco is based on green tissue (leaf) biomass processing In: Chloroplasts: Transforming Biopharmaceutical Manufacturing Biopharm International, www.biopharminternational.com

Narendranathan TJ and Dunnill P. 1982. The effect of shear on globular proteins during ultrafiltration; studies of alcohol. 24(9): 2103- 2107.

Neal G, Christie J, Keshavarz-Moore E and Shamlou PA. 2003. Ultra scale-down approach for the prediction of full-scale recovery of ovine polyclonal immunoglobulins used in the manufacture of snake venom-specific Fab fragment Biotechnol Bioeng 81,149–157.

Newcombe C, Newcombe AR. 2007. Antibody production: Polyclonal-derived biotherapeutics. Journal of Chromatography B: Analytical Technologies in the Biomedical and Life Sciences. 848 (1): 2-7.

Nielsen J, Krabben P. 1995. hyphal growth and fragmentation of Penicillium chrysogenum in submerged cultures. Biotechnol Bioeng 46: 588-598

Nienow AW. 1976. The effect of agitation and scale-up on crystal growth rates and on secondary nucleation Trans IChemE, Chem Eng Res Des. 54: 205-207.

Nilson BHK, Solomon A, Bjork L, Akerstrom B. 1992. Protein L from Peptostreptococcus magnus binds to the κ light chain variable domain. J. boil. Chem.. 267: 2234-2239.

Noodén LD, Guiamét JJ, John I. 1997. Senescence mechanism. Physiol Plant. 101: 746-753.

Nuttall J, Vine N, Hadlington JL, Drake P, Frigerio L and Ma JK-C. 2002. ER–resident chaperone interactions with recombinant antibodies in transgenic plants Eur J Biochem 269, 6042–6051.

Ohnmeiss TE, McCloud E, Lynds G, Baldwin IT. 1997. Within-plant relationships among wounding, jasmonic acid, and nicotine: implications for defense in Nicotiana sylvestris. New Phyto.l 137:441–452.

Ouzineb K, Lord C, Lesauze N, Graillat C, Tanguy PA, McKenna T. 2006. Homogenisation devices for the production of miniemulsions Chem Eng Sci. 61: 2994-3000.

Owen, PR. 1969. Pneumatic transport. J Fluid Mech. 39: 407–432.

Padidam M. 2003. Chemically regulated gene expression in plants. Curr. Opin. Plant Biol. 6:, 169–177.

Pagliarulo CL and Hayden AL. 2001. Potential for Greenhouse Aeroponic Cultivation of Medicinal Root Crops Proceedings of the 30th National Agricultural Plastics Congress, San Diego, CA, American Society for Plasticulture, February 23 – 26, 2002 pps 47-53 Paper # P-125933-09-01.

Park, J-I Grant, CM, Attfield PV, Dawes IW. 1997. The Freeze-thaw Stress Response of the Yeast Sacchromyces cerevisiae is growth phase specific and is controlled by nutritional state via the RAS-Cyclic AMP Signal Transduction Pathway. Applied and Envirnomental Microbiology. 63: 3818-3824.

Pavlou AK, Belsey MJ. 2005. The therapeutic antibodies market to 2008, Eur J Pharm Biopharm. 59: 389– 396.

Persidis A. 1999. Agricultural biotechnology .Nat Biotechnology. 17:612-614

Petra ten Hoopen. 2002. Immunomodulation of jasmonate functions; In: Dissertation; Mathematisch-Naturwissenschaftlich-Technischen Fakultät der Martin-Luther-Universität Halle-Wittenberg Fachbereich Pharmazie pg 6.

Petrides DP, Koulouris A, Lagonikos PT. 2002b. The role of process simulation in pharmaceutical process development and product commercialisation. Pharmaceutical Engineering 22 (1): 1-8.

Piquemal J, Lapierre C, Myton K, O'Connell A, Schuch W, Grima-Pettenati J, Boudet A-M. 1998. Down-regulation of Cinnamoyl-CoA Reductase induces significant changes of lignin profiles in transgenic tobacco plants. Plant J 13(1): 71-83.

Piquemal J, Lapierre C, Myton K, O'Connell A, Schuch W, Grima-Pettenati J, Boudet A-M. 1998. Down-regulation of Cinnamoyl-CoA Reductase induces significant changes of lignin profiles in transgenic tobacco plants. Plant J 13(1): 71-83.

Plasterk RHA and Ketting RF. 2000. The silence of the genes. Curr. Opin. Genet. Dev. 10: 562–567.

Platzer B, Noll G. 1983. Moglichkeiten zur analytischen Beschreibung der turbulenten Stromung in unbewehrten und teilbewehrten Ruhrkesseln mit radialfordernden Riihrern. Chem Tech. 35: 235-239

Ploss R and Mersmann, A. 1989. A new model for the effect of stirring intensity on the rate of secondary mucleation Chem Eng Tech 12: 137-146

Poethig RS. 1990. Phase change and the regulation of shoot morphogenesis in plants Science 250: 923-930.

Pulatov AA, Turakhozhaev MT and Shakirov TT. 1978. The precipitation of isolated cotton-plant protein Chem Nat. Compound, 14, 93–94.

Quemada H. 2002. Virus resistant crop In: Genetically modified crops: Assessing Safety. pp 219-235.

Ramos-Vara JA. 2005. Technical aspects of immunohistochemistry. Vet Pathol. 42:405–426.

Rasband WS and Bright DS. 1995. NIH Image A public domain image processing program for the Macintosh Microbeam. Anal4: 137-149.

Reichert JC, Rosensweig CJ, Faden LB, Dewitz MC. 2005. Monoclonal antibody successes in the clinic, Nat Biotechnol. 23: 1073– 1078.

Richards D and Considine JA. 1981. Suberization and browning of grapevine roots In: Brouwer R, editor Structure and Function of Plant Roots London: Dr W Junk p 111–115.

Rickerby DG and MacMillan NH. 1980 On the oblique impact of a rigid sphere against a rigid-plastic solid. Int J Mech Sci. 22: 491-494.

Righetti M, Romano GP. 2004. Particle-fluid interactions in a plane near-wall turbulent flow. J Fluid Mech. 505: 93–121.

Ritter and Ladyman. 1995. (Eds.). Production of recombinant antibody fragments. In: Monoclonal antibodies – Production, engineering and clinical application. Cambridge University Press. pp. 154-162.

Rogers SG, Klee HJ, Horsch RB and Fraley RT. 1987. Improved vectors for plant transformation: expression cassette vectors and new selectable markers. Methods Enzymol. 153: 253–277.

Rouf SA, Douglas PL, Moo-Young M, Scharer JM. 2001. Computer simulation for large scale bioprocess design, Biochemical Engineering Journal. 8: 229-234.

Russell DA. 1999. Feasibility of antibody production in plants for human therapeutic use. Curr Topics Microbiol. 240:119–38.

Sadik OA and Wallace GG. 1993. Pulse damperometric detection of proteins using antibody containing conducting polymers. Analytica Chimica Acta. 279(2) 209-212.

Saitoh T, Hattori N, Hiraide M. 2004. Protein separation with surfactant-coated polystyrene involving Cibacron Blue 3GA-conjugated Triton X-100. Journal of Chromatography A. 1028: 149–153.

Schillberg S, Emans N and Fischer R. 2002. Antibody molecular farming in plants and plant cells. Phytochem Rev. 1: 45–54.

Schilmiller AL, Howe GA.2005. Systemic signalling in the wound response. Curr Opin Plant Biol. 8: 369-377.

Schouten A, Roosien J, van Engelen FA, de Jong GAM, Borst-Vrenssen AWM, Zilverentant JF, Bosch D, Stiekema WJ, Gommers FJ, Schots A and Bakker J. 1996. The C-terminal KDEL sequence increases the expression level of a single-chain antibody designed to be targeted to both the cytosol and the secretory pathway in transgenic tobacco. Plant Mol. Biol. 30: 781–93.

Schreiber L .1996. Chemical composition of casparian strips isolated from *Clivia miniata* Regroots: evidence for lignin. Planta. 199: 596-601.

Schurr U. 1997. Growth Physiology and measurement of growth In: Behnke H –D, Lüttge U, Esser K, Kadereit JW, Runge M Eds Progress in botany Berlin: Springer Verlag. 59: 355-373.

Shattock, R. and Solomon, S. (2004) Microbicides – aids to safer sex. Lancet, 363, 1002–1003.

Shewry PR and Fido RJ. 1996. Protein extraction from plant tissues In: *Methods in Molecular Biology* (Doonan, S, ed), pp 23–29 Totawa, NJ: Humana Press.

Shi Q, Li C and Zhang F. 2006. Nicotine synthesis in *Nicotiana tabacum* L induced by mechanical wounding is regulated by auxin J Exp Bot, 57 (11): 2899–2907.

Shukla AA, Hubbard B, Tressel T, Guhan S, Low D. 2007. Downstream processing of monoclonal antibodies-Application of platform approaches Journal of Chromatogr B. 848: 28-39.

Simmons LC, Reilly D, Klimowski L, Raju TS, Meng G, Sims P, Hong K, Shields RL, Damico LA, Rancatore P, Yansura DG. 2002. Expression of full-length immunoglobulins in *Escherichia coli*: rapid and efficient production of aglycosylated antibodies. Journal of Immunological Methods. 263 133– 147.

Simpson GG and Dean C. 2002. *Arabidopsis*, the Rosetta stone of flowering time? Science. 296: 285-289.

Sivars U, Abramson J, Iwata S and Tjerneld F. 2000. Affinity partitioning of a poly(histidine)-tagged integral membrane protein, cytochrome bo3 ubiquinol oxidase, in a detergent-polymer aqueous two-phase system containing metal-chelating polymer. J. Chromatogr. B. 743: 307-316.

Smart CM. 1994. Gene expression during leaf senescence New Phytol 126: 419-448.

Smith JJ, Lilly MD. 1990. The effect of agitation on the morphology and penicillin production of Penicillium chrysogenum. Biotech Bioeng. 35: 1011-1023.

Smith PG. 2007. Particle size distribution. In: Applications of Fluidization to Food Processing. Blackwell Publishing. pp. 22-26.

Smith, R. and Lehner, T. 1989. Characterisation of monoclonal antibodies to common protein epitopes on the cell surface of *Streptococcus mutans* and Streptococcus sobrinus. Oral Microbiol. Immunol. 4: 153–158.

Sparrow PAC, Irwin JA, Dale PJ, Twyman RM and Ma JK-C. 2007. Pharma-Planta: Road testing the developing regulatory guidelines for plant-made pharmaceuticals. Transgenic Res. 16: 147–161.

Speer EO. 1987. A method of retaining phloroglucinol proof lignin. Stain Technol 62: 279-280.

Spök A, Twyman RM, Fischer R, Ma JKC, Sparrow PAC. 2008. Evolution of a regulatory framework for pharmaceuticals derived from genetically modified plants. Trends Biotechnol. 26(9): 506-17.

Sriraman R, Bardor M, Sack M, Vaquero C, Faye L, Fischer R, Finnern R, and Lerouge P. 2004. Recombinant antihCG antibodies retained in the endoplasmic reticulum of transformed plants lack core-xylose and core-α(1,3)-fucose residues. Plant Biotechnol. J. 2: 279–287.

Steudle E, Peterson CA. 1998. How does water get through roots? J Exp Bot. 49:775–788.

Stewart CW and Crowe CT. 1993. Bubble dispersion in free shear layers Int J Multiphase Flow 19: 501–507.

Stoger E, Ma JK-C, Fischer R, and Christou P.2005. Sowing the seeds of success: pharmaceutical proteins from plants Curr Opin Biotechnol 16: 167-173.

Stoger E, Sack M, Perrin Y, Vaquero C, Torres E, Twyman RM, Christou P, Fischer R. 2002. Practical considerations for pharmaceutical antibody production in different crop systems. Mol Breeding. 9: 149-158.

Stoger, E, Sack M, Fischer R, Christou P. 2002. Plantibodies: applications, advantages and bottlenecks Curr Opin Biotechnol 13, 161–166.

Stoger, E, Vaquero C, Torres E, Sack M, Nicholson L, Drossard J, Williams S, Keen D, Perrin Y, Christou P, Fischer R. 2000. Cereal crops as viable production and storage systems for pharmaceutical scFv antibodies Plant Mol Biol 42, 583–590.

Stoll A and Dieterkutzbach H. 2000. Guidance of a Forage Harvester with GPS Precision Agriculture. 2: 281-291.

Storey KB and Storey JM. 2005. Freeze tolerance In: Extremophiles (Gerday, C and Glansdorff, N, eds) Encyclopedia of Life Support Systems (EOLSS), Developed under the Auspices.

Synoweic P, Jones AG and Ayazi-Shamlou P. 1993. Crystal breakup in dilute turbulently agitated suspensions Chem Eng Sci. 48 (20): 3485-3495.

Takabe K, Fujita M, Harada H, Saiki H. 1986. Lignification process in Cryptomeria (Cryptomeria japonica D Don) tracheid: electron microscopic observation of lignin skeleton of differentiating xylem Research Bulletins of the College Experiment Forests Hokkaido University. 43: 783–788.

Takahashi, K, Gidoh, Y, Yokota, T and Nomura, T. 1992. Particle-impeller impact in an agitated vessel equipped with a Rushton turbine. J Chem Eng Jpn. 25: 73-77.

Tang, BL, Wong, SH, Low, SH and Hong, W. 1992. Retention of a type I1 surface membrane protein in the endoplasmic reticulum by the Lys-Asp-Glu-Leu sequence. J Biol Chem. 267: 7072–7076.

Tatyana K, Daniela P, Atanas A, Dimitar D. 2002. Freezing tolerant tobacco, transformed to accumulate osmoprotectants. Plant science. 163 (1): 157-164.

Terashima N, Fukushima K, Takabe K. 1986. Heterogeneity in formation of lignin. Holzforschung. 40: 101-105.

Thomas CR, Nienow AW and Dunnill P. 1979. Action of shear on enzymes: studies with alcohol dehydrogenase Biotechnol Bioeng 21, 2263–2278.

Thomas CR, Zhang Z, Cowen C. 2000. Micromanipulation Measurements of Biological Materials. Biotechnol Lett. 22: 531-537.

Thomas H, Stoddart JL. 1980. Leaf senescence. Annu Rev. Plant Physiol 31:83-111.

Tomos D. 2000. The plant cell pressure probe. Biotechnol. Lett. 22:437–442.

Torikaiu K, Uwano Y, Nakamori T, Tarora W and Takahashi H. 2005. Study on tobacco components involved in the pyrolytic generation of selected smoke constituents. Food Chem Toxicol. 43, 559–568.

Twyman R M, Stoger E, Schillberg S, Christou P, Fischer. 2003. Molecular farming in plants: host systems and expression technology. Trends Biotechnol. 21: 570-578.

Tyagi AK. 2001. Plant genes and their expression. Curr Sci. 80: 161–169.

Vain, P, Finer KM, Engler DE, Pratt RC, Finer JJ. 1996. Intron-mediated enhancement of gene expression in maize (Zea mays L) and bluegrass (Poa pratensis L). Plant Cell Rep. 15: 489–494.

Valdés R, Gómez L, Padilla S, Brito J, Reyes B, Álvarez T, Mendoza O, Herrera O, Ferro W, Pujol M, Leal V, Linares M, Hevia Y, García C, Milá L, García O, Sánchez R, Acosta A, Geada D, Paez R, Vega JL and Borroto C 2003 Large-scale purification of an antibody directed against hepatitis B surface antigen from transgenic tobacco plants Biochem Biophys Res Commun 308: 94–100

van der Heijden AEDM, van der Eerden JP, and van Rosmalen,GM. 1994. The secondary nucleation rate: a physical model Chem Eng Sci 49(18): 3101-3113.

van Dolleweerd CJ, Chargelegue D, Ma J K-C. 2003. Characterization of the Conformational Epitope of Guy's 13, a Monoclonal Antibody That Prevents *Streptococcus mutans* Colonization in Humans. Infect Immun. 71: 754-765.

van Reis R, and Zydney A. 2001. Review: Membrane separations in biotechnology *Current opinion in Biotechnology* 12(2): 208-211.

van Suijdam JC, Metz B. 1981a. Influence of engineering variables upon the morphology of filamentous molds. Biotechnol Bioeng. XXIII: 111-148.

Vaquero C, Sack M, Schuster F, Finnern R, Drossard J, Schumann D, Reimann A, Fischer R. 2002. A carcinoembryonic antigen-specific diabody produced in tobacco. FASEB J. 16: 408–410.

Varga EG, Titchener-Hooker NJ, Dunnill P. 1998. Use of scale-down methods to rapidly apply natural yeast homogenisation models to a recombinant strain. Bioprocess Engineering. 19: 373-380.

Verch T, Yusibov V and Koprowski H. 1998. Expression and assembly of a full-length monoclonal antibody in plants using a plant virus vector J Immunol Methods. 220: 69–75.

Vermeer AWP and Norde W. 2000. The thermal stability of immunoglobulin: unfolding and aggregation of a multi-domain protein. Biophys J. 78: 394–404.

Vine DV, Drake P, Hiatt A and MaJK-C. 2001. Assembly and plasma membrane targeting of recombinant immunoglobulin chains in plants with a murine immunoglobulin transmembrane sequence. Plant Mol Biol. 45: 159–167.

Virkar PD, Narendranathan TJ, Hoare M and Dunnill P. 1981. Studies of the effects of shear on globular proteins Extension to high shear fields and to pumps. Biotech Bioeng. 23: 425–429.

Walter A, Schurr U. 1999. The modular character of growth in *Nicotiana tabacum* plants under steady-state nutrition. J Exp Bot. 50(336): 1169-1177.

Wang Z, Burch WH, Mou P, Jones RH, Mitchell RJ 1995. Accuracy of visible and ultraviolet light for estimating live root proportions with minirhizotrons. Ecology. 76:2330–2334.

Watt GM, Lund J, Levens M, Kolli VSK, Jefferis R and Boons G-J. 2003. Site-specific glycosylation of an aglycosylated human IgG1-Fc antibody protein generates neoglycoproteins with enhanced function Chem Biol 10, 807–814.

Weetman R. 1994. Development of an erosion resistant mixing impeller for large scale solid suspension application with CFD comparisons. ICHEME Symp Ser. 136: 49-56.

Weetman RJ. 1996. Simulation helps quadruple mixer life on abrasive conditions. Chem Technol. 3(1): 1-5.

Wells CE, Eissenstat DM. 2001. Marked differences in survivorship among apple roots of different diameters. Ecology. 82:882–892.

Wells CE, Eissenstat DM. 2003. Beyond the roots of young seedlings: The Influence of age and order on fine root physiology. J Plant Growth Regul. 21: 324-334.

Wells CE, Glenn DM, Eissenstat DM. 2002. Changes in the risk of fine-root mortality with age: A case study in peach, *Prunus Persica* (Rosaceae). Am J Bot. 89(1): 79–87.

Whitelam GC, Cockburn B, Gandecha AR, Owen MRL. 1993. Heterologous protein production in transgenic plants. Biotechnol Genet Eng Rev. 11: 1–29.

Whitelam GC. 1995. The production of recombinant proteins in plants. J. Sci. Food Agric. 68: 1-9.

Whitty EB. 2006. Basic Cultural Practices for Peanuts. University of Florida IFAS Extension. pp. 7. http://edis.ifas.ufl .edu/AA258.

Wilkins J, Sesin D, Wisniewski R. 2001. Large-Scale Cryopreservation of Biotherapeutic Products. Innov Pharm Technol. 1(8): 174–180.

Wilson IBH and Altmann F. 1998. Concanavalin A binding and endoglycosidase D resistance of β1,2-xylosylated and α1,3-fucosylated plant and insect oligosaccharides. Glycoconjugate Journal. 15(2): 203-206(4).

Winder R. 2005. Cell culture changes gear. Chem Ind. 18–20.

Witcher, D, Hood EE, Petersen D, Bailey M, Bond D, Kusnadi A, Evangelista R, Nikolov Z, Wooge C, Mehigh R, Kappel W, Register J, Howard JA. 1998. Commercial production of b-glucuronidase (GUS): a model system for the production of proteins in plants. Mol Breed 4: 301–312.

Wongsamuth R, Doran P M. 1997. Production of monoclonal antibodies by tobacco hairy roots. Biotechnol Bioeng.;54 (5):401-15.

Wurm FM. 2004. Production of recombinant protein therapeutics in cultivated mammalian cells. Nat Biotechnol. 22(11): 1393-8.

Wycoff KL. 2004. Secretory IgA Antibodies from Plants. Current Pharmaceutical Design. 11(19): 2429-2437.

Xu L and Diosady LL. 2002. Removal of phenolic compounds in the production of high-quality canola protein isolates. Food Res Int. 35: 23–30.

Yamawaki-Kataoka Y, Nakai S, Miyata T and Honjo T. 1982. Nucleotide sequences of gene segments encoding membrane domains of immunoglobulin gamma chains. Proc. Natl. Acad. Sci. USA. 79: 2623–2627.

Yildirim S, Fuentes RG, Evangelista R and Nikolov ZL. 2002. Fractionation of transgenic corn for recovery of recombinant enzymes. J Am Oil Chem Soc. 79: 809–814.

Zeitlin, L Olmsted SS, Moench TR, Co MS, Martinell BJ,Paradkar VM, Russell DR, Queen C, Cone RA, and Whaley KJ. 1998. A humanized monoclonal antibody produced in transgenic plants for immunoprotection of the vagina against genital herpes. Nat Biotechnol. 16: 1361–1364.

Zhang C, Love RT, Jilka JM and Glatz CE. 2001. Genetic engineering strategies for purification of recombinant proteins from canola by anion chromatography: an example of β-glucuronidase. Biotechnol Prog 17, 161–167.

Zhang CM, Glatz CE. 1999. Process engineering strategy for recombinant protein recovery from canola by cation exchange chromatography. Biotechnol. Prog. 15: 12-18.

Zhong GY, Peterson D, Delaney DE, Bailey M, Wicher DR, Register JC, Bond D, Li CP, Marshall L, Kulisek E, Ritland D, Meyer T, Hood EE and Howard JA. 1999. Commercial production of aprotinin in transgenic maize seeds. Mol Breed. 5: 345–356.

www.millipore.com/immunodetection/id3/antibodiestutorial

www.medicago.com

www.prodigene.com

www.kbpllc.com

www.sembiosys.com

www.meristem-therapeutics.com

www.planetbiotechnology.com

www.solvay.com

www.phytomedics.com

http://rsb.info.nih.gov/nih-image

www.fitzmill.com

www.calbiochem.com

Appendix A

SEQUENCING RESULTS

```
########################################
# Program:  water
# Rundate:  Wed Mar 02 11:11:30 2005
# Align_format: srspair
# Report_file: /ebi/extserv/old-work/water-20050302-11111295397098.output
########################################

#=======================================
#
# Alignment of
                                    SH01_08
                    Guy's13-HDEL cloned in pBluescriptIISK+
# Matrix: EDNAFULL
# Gap_penalty: 10.0
# Extend_penalty: 0.5
#
# Length: 742
# Identity:     701/742 (94.5%)
# Similarity:   706/742 (95.1%)
# Gaps:           8/742 ( 1.1%)
# Score: 3377.0
#
#
#=======================================

SH01_08             1 GGGT-CCGGGCCCCCCCTCGAGCCAGGTGCAACTGCAGCAGTCAGGACCT     49
                      |||| |||||||||||||||||||||||::|:|||||||:||||:||||||
Guy's13-HDEL      652 GGGTACCGGGCCCCCCCTCGAGccaggtsmarctgcagsagtcwggacct    701

SH01_08            50 GACCTGGTGAAACCTGGGGCCTCAGTGAAGATATCCTGCAAGGCTTCTGG     99
                      ||||||||||||||||||||||||||||||||||||||||||||||||||||
Guy's13-HDEL      702 gacctggtgaaacctggggcctcagtgaagatatcctgcaaggcttctgg    751

SH01_08           100 ATACACATTCACTGACTACAACATACACTGGGTGAAGCAGAGCCGTGGAA     149
                      ||||||||||||||||||||||||||||||||||||||||||||||||||||
Guy's13-HDEL      752 atacacattcactgactacaacatacactgggtgaagcagagccgtggaa    801

SH01_08           150 AGAGCCTTGAGTGGATTGGATATATTTATCCTTACAATGGTAATACTTAC     199
                      ||||||||||||||||||||||||||||||||||||||||||||||||||||
Guy's13-HDEL      802 agagccttgagtggattggatatatttatccttacaatggtaatacttac    851

SH01_08           200 TACAACCAGAAGTTCAAGAACAAGGCCACATTGACTGTAGACAATTCCTC     249
                      ||||||||||||||||||||||||||||||||||||||||||||||||||||
Guy's13-HDEL      852 tacaaccagaagttcaagaacaaggccacattgactgtagacaattcctc    901

SH01_08           250 CACCTCAGCCTACATGGAGCTCCGCAGCCTGACATCTGAGGACTCTGCAG     299
                      ||||||||||||||||||||||||||||||||||||||||||||||||||||
Guy's13-HDEL      902 cacctcagcctacatggagctccgcagcctgacatctgaggactctgcag    951

SH01_08           300 TCTATTACTGTGCAACCTACTTTGACTACTGGGGCCAAGGCACCACTCTC     349
                      ||||||||||||||||||||||||||||||||||||||||||||||||||||
Guy's13-HDEL      952 tctattactgtgcaacctactttgactactggggccaaggcaccactctc   1001

SH01_08           350 ACAGTCTCCTCAGCCAAAACGACACCCCCATCTGTTTATCCACTGGCCCC     399
                      ||||||||||||||||||||||||||||||||||.|||||||||||||||
Guy's13-HDEL     1002 acagtctcctcagccaaaacgacaccccatctgtctatccactggcccc   1051

SH01_08           400 TGGATCTGCTGCCCAAACTAACTCCATGGTGACCCTGGGATGCCTGGTCA     449
                      ||||||||||||||||||||||||||||||||||||||||||||||||||||
Guy's13-HDEL     1052 tggatctgctgcccaaactaactccatggtgaccctgggatgcctggtca   1101
```


SH01_08 450 AGGGCTATTTCCCTGAGCCAGTGACAGTGACCTGGAACTCTGGATCCCTG 499
Guy's13-HDEL 1102 agggctatttccctgagccagtgacagtgacctggaactctggatccctg 1151
SH01_08 500 TCCAGCGGTGTGCACACCTTCCCAGCTGTCCTGCAGTCTGACGTCTACAC 549
Guy's13-HDEL 1152 tccagcggtgtgcacaccttcccagctgtcctgcagtctgacgtctacac 1201
SH01_08 550 TCTGAGCAGCTCAGTGACTGTCCCCTCCAGCACCTGGCCCAGCGAGACCG 599
Guy's13-HDEL 1202 tctgagcagctcagtgactgtccctccagcacctggcccagcgagaccg 1251
SH01_08 600 TCACCTGCAAGGTNGCCCACCCGGCCAGCAGCACCAAGGNGNAAANAAAA 649
Guy's13-HDEL 1252 tcacctgcaacgttgcccacccggccagcagcaccaaggtggacaagaaa 1301
SH01_08 650 ATTGTGCCCAGGGANTGNGGTNGTAANCCNTGGCATATNTACAGGTCCC 699
Guy's13-HDEL 1302 attgtgcccagggattgt-ggttgtaagcctt-gcatatgtaca-gtccc 1348
SH01_08 700 NNAAAAANAAACNGGGNT-TNNATNTTNCCCCCAAANNCCAA 740
Guy's13-HDEL 1349 agaagtatcatctg---tcttcatcttccccccaaagcccaa 1387

```
########################################
# Program:  water
# Rundate:  Wed Mar 02 11:16:24 2005
# Align_format: srspair
# Report_file: /ebi/extserv/old-work/water-20050302-11161967038278.output
########################################

#=======================================
#
# Alignment of:
                                    SH02_10
                Reverse of Guy'13-HDEL cloned in pBluescriptIISK+
# Matrix: EBLOSUM62
# Gap_penalty: 10.0
# Extend_penalty: 0.5
#
# Length: 744
# Identity:     701/744 (94.2%)
# Similarity:   701/744 (94.2%)
# Gaps:          20/744 ( 2.7%)
# Score: 4099.5
#
#
#=======================================

SH02_10             1 GGAGCTC--CCGCGGTGGCGGCCGCTCTAGAACTAGTGGATCCCCCGGGC     48
                      ||||||| ||||||||||||||||||||||||||||||||||||||||||
reverse          2201 GGAGCTCCACCGCGGTGGCGGCCGCTCTAGAACTAGTGGATCCCCCGGGC   2250

SH02_10            49 TGCAGGAATTCTTAAAGTTCATCATGCTTCCCAGGAGAGTGGGAGAGGCT     98
                      ||||||||||||||||||||||||||||||||||||||||||||||||||||
reverse          2251 TGCAGGAATTCTTAAAGTTCATCATGCTTCCCAGGAGAGTGGGAGAGGCT   2300

SH02_10            99 CTTCTCAGTATGGTGGTTGTGCAGGCCCTCATGTAACACAGAGCAGGTGA    148
                      ||||||||||||||||||||||||||||||||||||||||||||||||||||
reverse          2301 CTTCTCAGTATGGTGGTTGTGCAGGCCCTCATGTAACACAGAGCAGGTGA   2350

SH02_10           149 AAGTATTTCCTGCCTCCCAGTTGCTCTTCTGCACATTGAGCTTGCTGTAG    198
                      ||||||||||||||||||||||||||||||||||||||||||||||||||||
reverse          2351 AAGTATTTCCTGCCTCCCAGTTGCTCTTCTGCACATTGAGCTTGCTGTAG   2400

SH02_10           199 ACGAAGTAAGAGCCATCTGTGTCCATGATGGGCTGAGTGTTCTTGTAGTT    248
                      ||||||||||||||||||||||||||||||||||||||||||||||||||||
reverse          2401 ACGAAGTAAGAGCCATCTGTGTCCATGATGGGCTGAGTGTTCTTGTAGTT   2450

SH02_10           249 CTCCGCTGGCTGCCCATTCCACTGCCACTCCACAGTAATGTCTTCAGGGA    298
                      ||||||||||||||||||||||||||||||||||||||||||||||||||||
reverse          2451 CTCCGCTGGCTGCCCATTCCACTGCCACTCCACAGTAATGTCTTCAGGGA   2500

SH02_10           299 AGAAGTCTGTTATCATGCAGGTCAGACTGACTTTATCCTTGGCCATCTGC    348
                      ||||||||||||||||||||||||||||||||||||||||||||||||||||
reverse          2501 AGAAGTCTGTTATCATGCAGGTCAGACTGACTTTATCCTTGGCCATCTGC   2550

SH02_10           349 TCCTTGGGAGGTGGAATGGTGTACACCTGTGGAGCCTTCGGTCTGCCTTT    398
                      ||||||||||||||||||||||||||||||||||||||||||||||||||||
reverse          2551 TCCTTGGGAGGTGGAATGGTGTACACCTGTGGAGCCTTCGGTCTGCCTTT   2600

SH02_10           399 GGTTTTGGAGATGGTTTTCTCGATGGGGGCAGGGAAAGCTGCACTGTTGA    448
                      ||||||||||||||||||||||||||||||||||||||||||||||||||||
reverse          2601 GGTTTTGGAGATGGTTTTCTCGATGGGGGCAGGGAAAGCTGCACTGTTGA   2650

SH02_10           449 CCCTGCATTTGAACTCCTTGCCATTGAGCCAGTCCTGGTGCATGATGGGA    498
                      ||||||||||||||||||||||||||||||||||||||||||||||||||||
```


reverse 2651 CCCTGCATTTGAACTCCTTGCCATTGAGCCAGTCCTGGTGCATGATGGGA 2700
SH02_10 499 AGTTCACTGACTGAGCGGAGAGTGCTGTTGAGCTGCTCCTCCCGGGGTTG 548
reverse 2701 AGTTCACTGACTGAGCGGAAAGTGCTGTTGAGCTGCTCCTCCCGGGGTTG 2750
SH02_10 549 CGTCTGANCTGTGTGCACCTCCACATCATCTACAAACCAGCTGAACTGGA 598
reverse 2751 CGTCTGAGCTGTGTGCACCTCCACATCATCTACAAACCAGCTGAACTGGA 2800
SH02_10 599 CCTCNGGNATCATCCTTGCTGANGTCTACCACAAACACACGTGANCNTTA 648
reverse 2801 CCTC-GGGATCATCCTTGCTGATGTCTACCAC-AACACACGTGA-CCTTA 2847
SH02_10 649 GNAGTCAAAAATAATGGGTGANCCAAATCCCTTGGGNCTTTTGGGGGGGG 698
reverse 2848 GGAGTC-AGAGTAAT-GGTGAGCACAT--CCTTGGG-CTTT---GGGGGG 2889
SH02_10 699 AAAANTGAAAAACCGAATGAAAACTTTTNGGGGAANTGTAANAA 742
reverse 2890 AAGA-TGAAGA--CAGATG-ATACTTCT---GGGACTGTACATA 2926

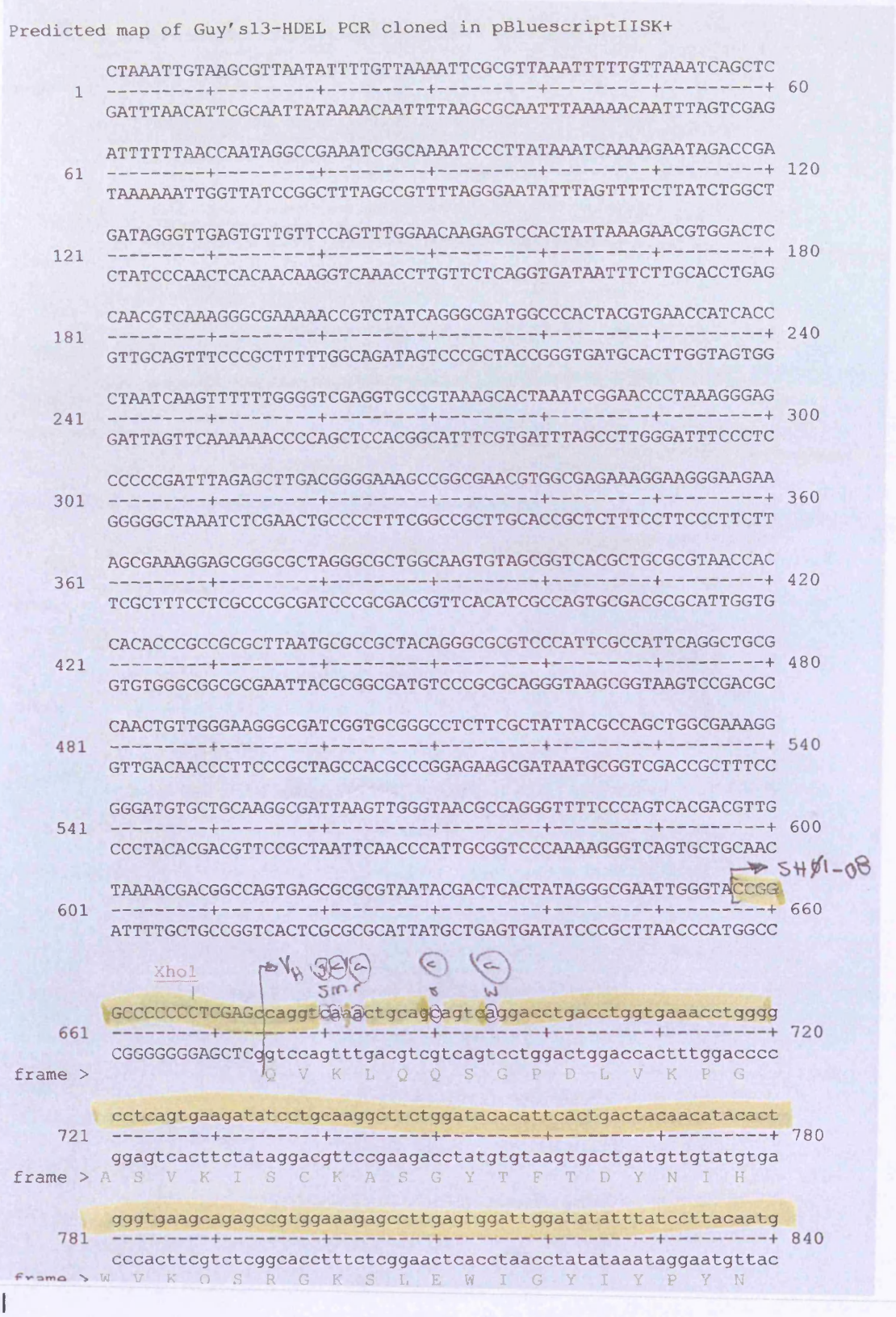
Predicted map of Guy's13-HDEL PCR cloned in pBluescriptIISK+
CTAAATTGTAAGCGTTAATATTTTGTTAAAATTCGCGTTAAATTTTTGTTAAATCAGCTC
GATTTAACATTCGCAATTATAAAACAATTTTAAGCGCAATTTAAAAACAATTTAGTCGAG
ATTTTTTAACCAATAGGCCGAAATCGGCAAAATCCCTTATAAATCAAAAGAATAGACCGA
TAAAAAATTGGTTATCCGGCTTTAGCCGTTTTAGGGAATATTTAGTTTTCTTATCTGGCT
GATAGGGTTGAGTGTTGTTCCAGTTTGGAACAAGAGTCCACTATTAAAGAACGTGGACTC
CTATCCCAACTCACAACAAGGTCAAACCTTGTTCTCAGGTGATAATTTCTTGCACCTGAG
CAACGTCAAAGGGCGAAAAACCGTCTATCAGGGCGATGGCCCACTACGTGAACCATCACC
GTTGCAGTTTCCCGCTTTTTGGCAGATAGTCCCGCTACCGGGTGATGCACTTGGTAGTGG
CTAATCAAGTTTTTTGGGGTCGAGGTGCCGTAAAGCACTAAATCGGAACCCTAAAGGGAG
GATTAGTTCAAAAAACCCCAGCTCCACGGCATTTCGTGATTTAGCCTTGGGATTTCCCTC
CCCCCGATTTAGAGCTTGACGGGGAAAGCCGGCGAACGTGGCGAGAAAGGAAGGGAAGAA
GGGGGCTAAATCTCGAACTGCCCCTTTCGGCCGCTTGCACCGCTCTTTCCTTCCCTTCTT
AGCGAAAGGAGCGGGCGCTAGGGCGCTGGCAAGTGTAGCGGTCACGCTGCGCGTAACCAC
TCGCTTTCCTCGCCCGCGATCCCGCGACCGTTCACATCGCCAGTGCGACGCGCATTGGTG
CACACCCGCCGCGCTTAATGCGCCGCTACAGGGCGCGTCCCATTCGCCATTCAGGCTGCG
GTGTGGGCGGCGCGAATTACGCGGCGATGTCCCGCGCAGGGTAAGCGGTAAGTCCGACGC
CAACTGTTGGGAAGGGCGATCGGTGCGGGCCTCTTCGCTATTACGCCAGCTGGCGAAAGG
GTTGACAACCCTTCCCGCTAGCCACGCCCGGAGAAGCGATAATGCGGTCGACCGCTTTCC
GGGATGTGCTGCAAGGCGATTAAGTTGGGTAACGCCAGGGTTTTCCCAGTCACGACGTTG
CCCTACACGACGTTCCGCTAATTCAACCCATTGCGGTCCCAAAAGGGTCAGTGCTGCAAC
SH01-08
TAAAACGACGGCCAGTGAGCGCGCGTAATACGACTCACTATAGGGCGAATTGGGTACCGG
ATTTTGCTGCCGGTCACTCGCGCGCATTATGCTGAGTGATATCCCGCTTAACCCATGGCC
XhoI
GCCCCCCCTCGAGccaggtcaaactgcagcagtcaggacctgacctggtgaaacctgggg
CGGGGGGGAGCTCggtccagtttgacgtcgtcagtcctggactggaccactttggacccc
frame > Q V K L Q Q S G P D L V K P G
cctcagtgaagatatcctgcaaggcttctggatacacattcactgactacaacatacact
ggagtcacttctataggacgttccgaagacctatgtgtaagtgactgatgttgtatgtga
frame > A S V K I S C K A S G Y T F T D Y N I H
gggtgaagcagagccgtggaaagagccttgagtggattggatatatttatccttacaatg
cccacttcgtctcggcacctttctcggaactcacctaacctatataaataggaatgttac
frame > W V K Q S R G K S L E W I G Y I Y P Y N

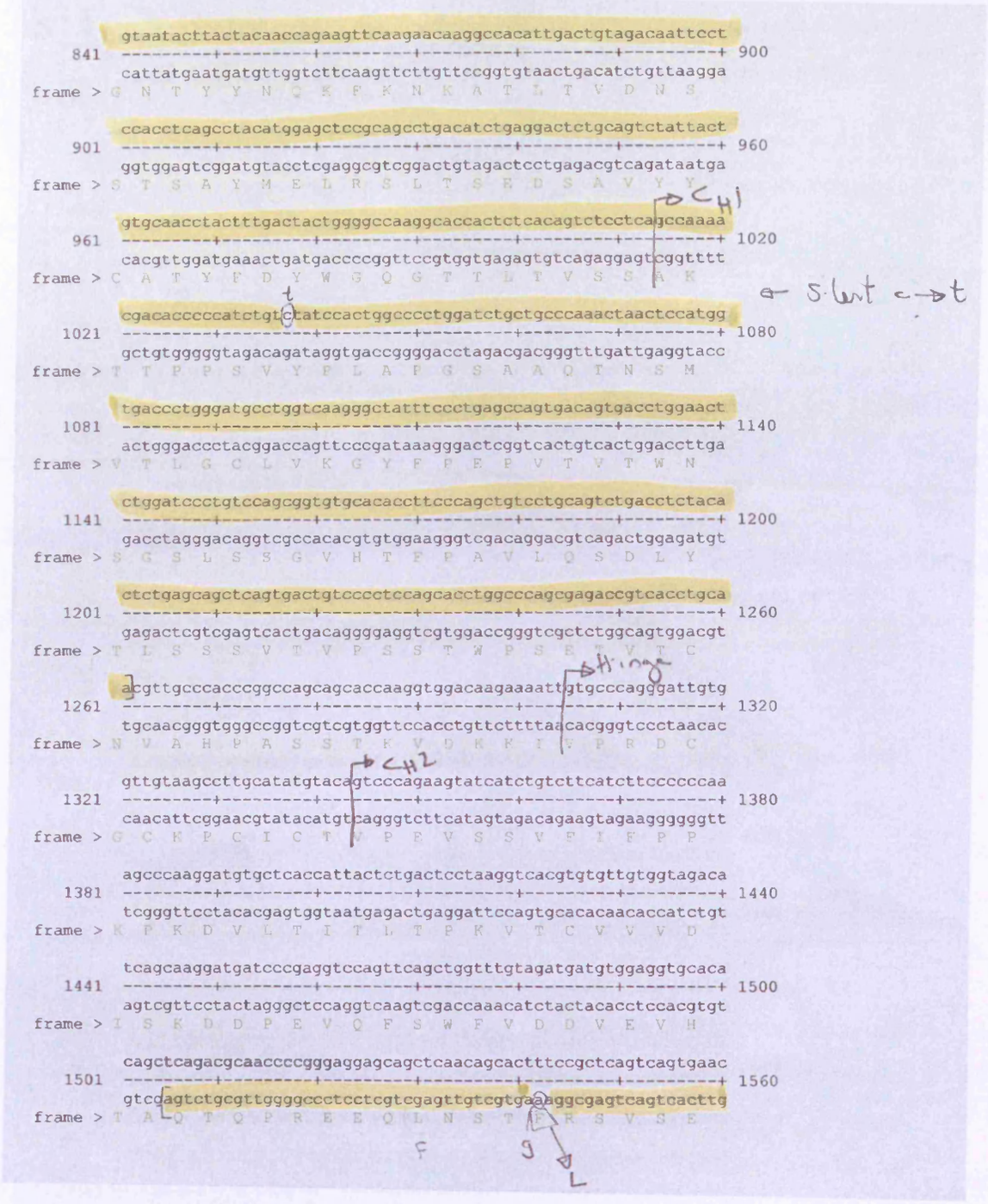
CH1
Silent c→t
Hinge
CH2
F
J
L

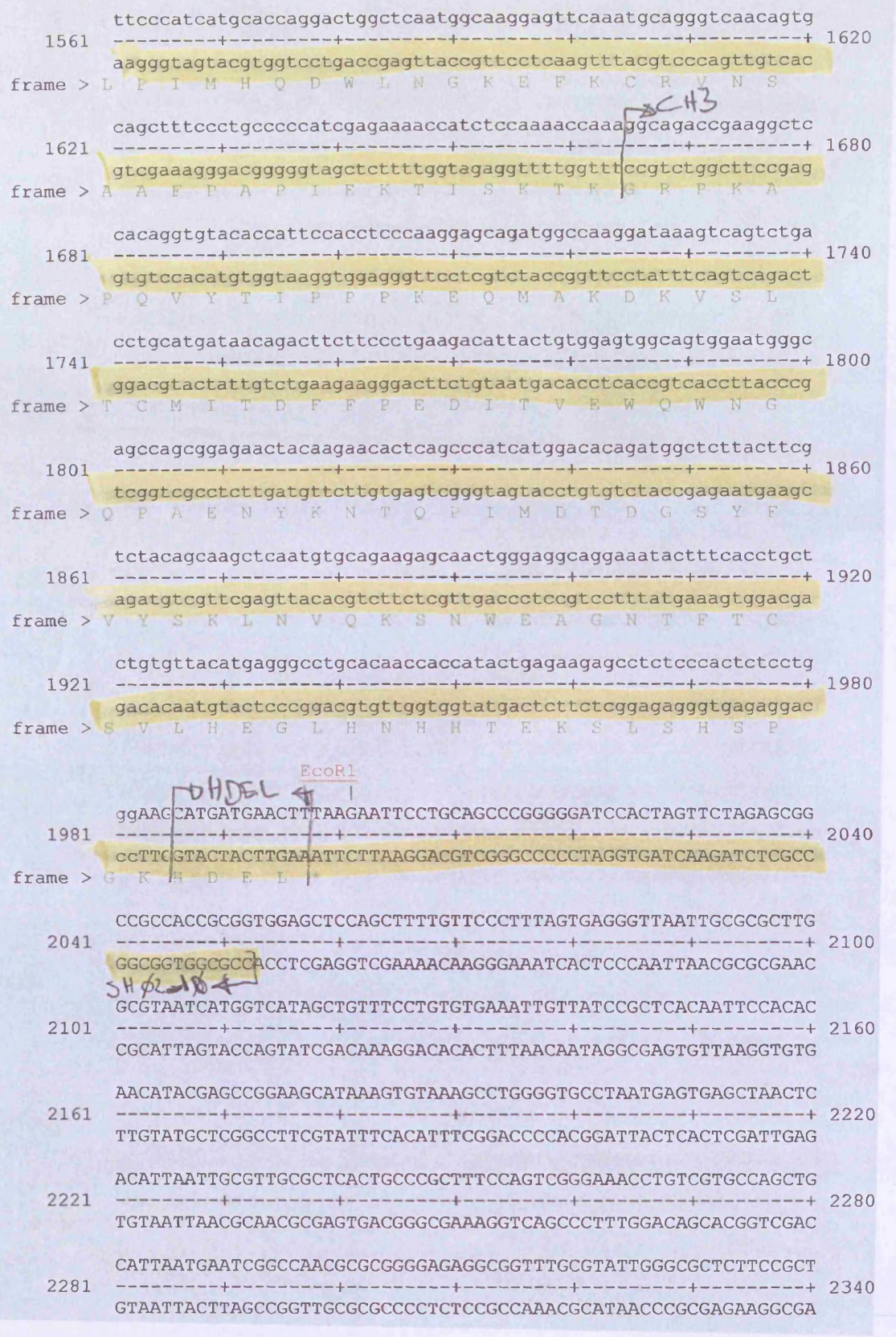
ttcccatcatgcaccaggactggctcaatggcaaggagttcaaatgcagggtcaacagtg
1561
1620
aagggtagtacgtggtcctgaccgagttaccgttcctcaagtttacgtcccagttgtcac
frame > L P I M H Q D W L N G K E F K C R V N S
CH3
cagctttccctgcccccatcgagaaaaccatctccaaaaccaaaggcagaccgaaggctc
1621
1680
gtcgaaagggacgggggtagctcttttggtagaggttttggtttccgtctggcttccgag
frame > A A F P A P I E K T I S K T K G R P K A
cacaggtgtacaccattccacctcccaaggagcagatggccaaggataaagtcagtctga
1681
1740
gtgtccacatgtggtaaggtggagggttcctcgtctaccggttcctatttcagtcagact
frame > P Q V Y T I P P P K E Q M A K D K V S L
cctgcatgataacagacttcttccctgaagacattactgtggagtggcagtggaatgggc
1741
1800
ggacgtactattgtctgaagaagggacttctgtaatgacacctcaccgtcaccttacccg
frame > T C M I T D F F P E D I T V E W Q W N G
agccagcggagaactacaagaacactcagcccatcatggacacagatggctcttacttcg
1801
1860
tcggtcgcctcttgatgttcttgtgagtcgggtagtacctgtgtctaccgagaatgaagc
frame > Q P A E N Y K N T Q P I M D T D G S Y F
tctacagcaagctcaatgtgcagaagagcaactgggaggcaggaaatactttcacctgct
1861
1920
agatgtcgttcgagttacacgtcttctcgttgaccctccgtcctttatgaaagtggacga
frame > V Y S K L N V Q K S N W E A G N T F T C
ctgtgttacatgagggcctgcacaaccaccatactgagaagagcctctcccactctcctg
1921
1980
gacacaatgtactcccggacgtgttggtggtatgactcttctcggagagggtgagaggac
frame > S V L H E G L H N H H T E K S L S H S P
EcoR1
DHDEL
ggAAGCATGATGAACTTTAAGAATTCCTGCAGCCCGGGGGATCCACTAGTTCTAGAGCGG
1981
2040
ccTTCGTACTACTTGAAATTCTTAAGGACGTCGGGCCCCCTAGGTGATCAAGATCTCGCC
frame > G K H D E L *
CCGCCACCGCGGTGGAGCTCCAGCTTTTGTTCCCTTTAGTGAGGGTTAATTGCGCGCTTG
2041
2100
GGCGGTGGCGCCACCTCGAGGTCGAAAACAAGGGAAATCACTCCCAATTAACGCGCGAAC
SH 62-18
GCGTAATCATGGTCATAGCTGTTTCCTGTGTGAAATTGTTATCCGCTCACAATTCCACAC
2101
2160
CGCATTAGTACCAGTATCGACAAAGGACACACTTTAACAATAGGCGAGTGTTAAGGTGTG
AACATACGAGCCGGAAGCATAAAGTGTAAAGCCTGGGGTGCCTAATGAGTGAGCTAACTC
2161
2220
TTGTATGCTCGGCCTTCGTATTTCACATTTCGGACCCCACGGATTACTCACTCGATTGAG
ACATTAATTGCGTTGCGCTCACTGCCCGCTTTCCAGTCGGGAAACCTGTCGTGCCAGCTG
2221
2280
TGTAATTAACGCAACGCGAGTGACGGGCGAAAGGTCAGCCCTTTGGACAGCACGGTCGAC
CATTAATGAATCGGCCAACGCGCGGGGAGAGGCGGTTTGCGTATTGGGCGCTCTTCCGCT
2281
2340
GTAATTACTTAGCCGGTTGCGCGCCCCTCTCCGCCAAACGCATAACCCGCGAGAAGGCGA

Appendix B

Optimisation of dilution factor for surface antigen I/Π and the positive control (Guy's 13 hybridoma) for the antigen-specific ELISA assay

Surface antigen I/Π had been directly purified from the *Streptococcus mutans* Guy's 13 strain (serotype c). This had previously been done as described in Russell *et al.*, (1980).

The aim of this experiment was to find the optimal dilution factor for the coating antibody and positive control (Guy's 13 murine hybridoma) for antigen-specific binding ELISA assays (outlined in section 2.4.1). Thus, the ELISA was performed as in 2.4.1 but with the initial coating step of SA I/Π done as described here, and the later test antibody-containing sample addition step of Guy's13 hybridoma only as described in this section. In order to obtain the optimal SA I/Π Guy's 13 hybridoma dilutions, ELISAs were set up in a grid format with increasing dilution factors (2-fold dilutions) of SA I/Π (105.1_{13}) across the 12 columns, and increasing concentrations (from 0.2 to 1.2 μg/ml with incremental increases of 0.2 μg/ml) of murine Guy's 13 hybridoma supernatant along the 8 rows on the same plate. As a negative control, the plates were alternatively coated with the non-specific SA I/Π fragment, 110.1, again with the same increasing dilution factors of SA I/Π (110.1) in the horizontal direction, and increasing dilutions of Guy's 13 hybridoma supernatant in the vertical direction. (This experiment was repeated twice). In addition, the dilution range of SA I/Π (105.1_{13}) was increased to 5-fold in subsequent repeat experiments on the basis of initial results.

Surface antigen I/Π assay optimisation results

Figure B.1 shows the raw results of an experiment to find the optimal dilution factor for surface antigen (SA) I/Π (105.1_{13}) and Guy's 13 hybridoma supernatant, where 2 fold-serial dilutions of the coating antigen where carried out, thus ranging from no dilution to a dilution factor of 1024. Similarly, Guy's 13 hybridoma concentrations were serially diluted 5-fold from a starting concentration of 0.68 μg/ml. From this figure it is evident that increasing the dilution factor of surface antigen I/Π to 1024 has

no significant effect on the response signal, (optical density measured at 450nm). Figure B.3 illustrates a negative control where the plates were coated with another fragment of the surface antigen, (110.1) which was non-specific for Guy's 13 hybridoma. The response signal is positive in this figure, but is less positive than that with SA I/Π 105.1_{13}, illustrating the background "noise" of this assay, under these SA I/Π and Guy's 13 hybridoma ranges.

A repeat of this experiment in Figure B.2 shows more of a clear difference between the response signal in SA I/Π (105.1_{13}) (Figure B.2) and SA I/Π(110.1) i.e. a non-specific control (Figure B.3). The result of this difference in the experiment shown in Figure B.1 and B.2 and that in Figure B.2, is due to a change in the blocking agent from 2.5% (w/v) Bovine serum albumin (BSA) to 5% (w/v) non-fat milk (indicated in the Materials and Methods section). This is thought to be due to the fact that non-fat dry milk contains many proteins and is thus able to block several plant proteins in the immunoassay whereas BSA is a single protein blocking agent. However, the response signal in Figure B.2 indicated that a wider explorative range of dilution factors for surface antigen I/Π was required, hence we repeated the experiment with dilution factors ranging from none to 4.9 X 10^7 in 5-fold serial dilutions (Figure B.4 and Figure B.5). As a result of Figures B.4 and B.5, a constant surface antigen dilution factor of 1 in 5000 was chosen, with serial dilution factors of Guy's 13 hybridoma.

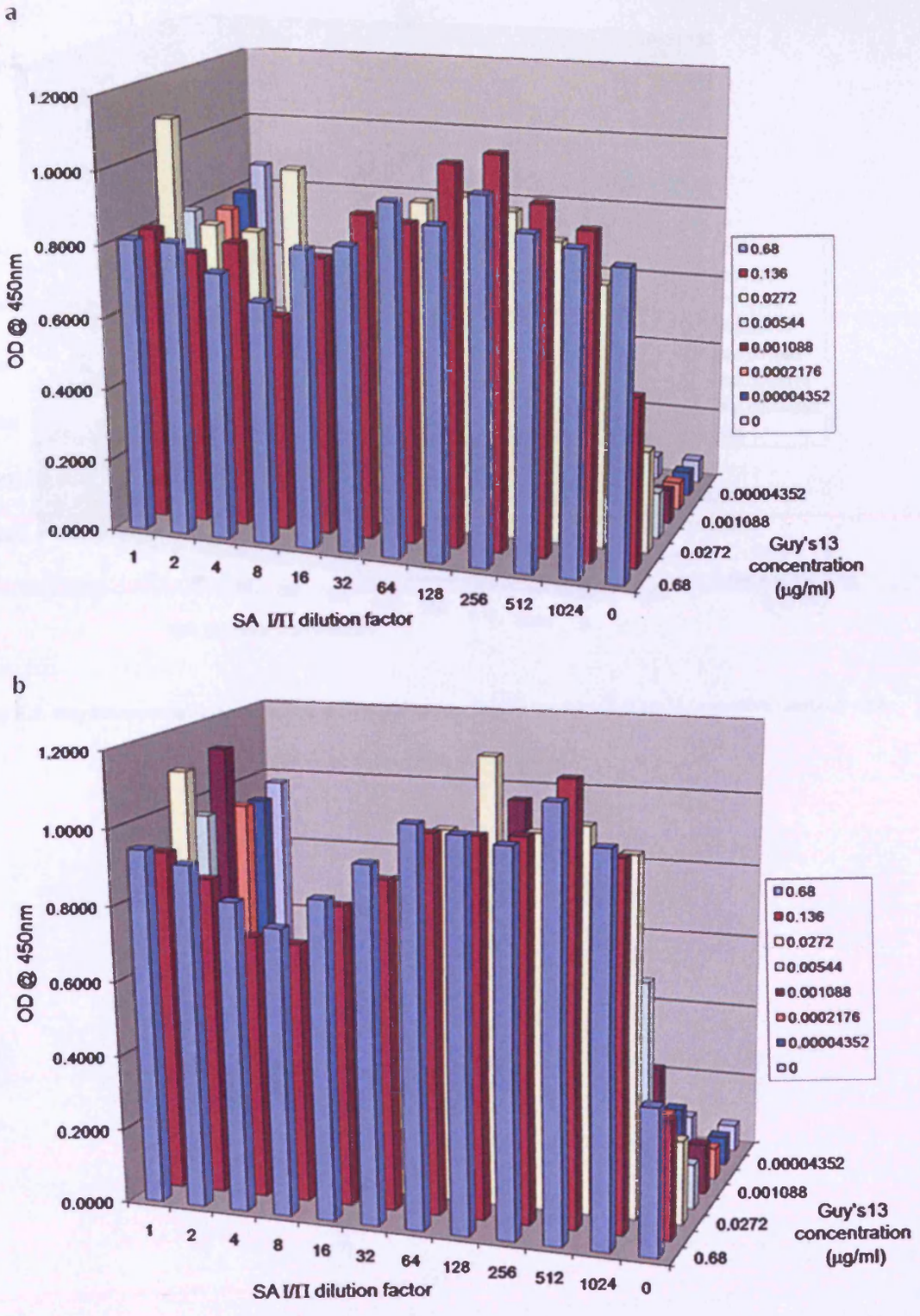

Figure B.1: Finding the optimal dilution factor for SA I/II (105.1_{13}) and Guy's 13 hybridoma supernatant. a and b represent different repeat experiments.

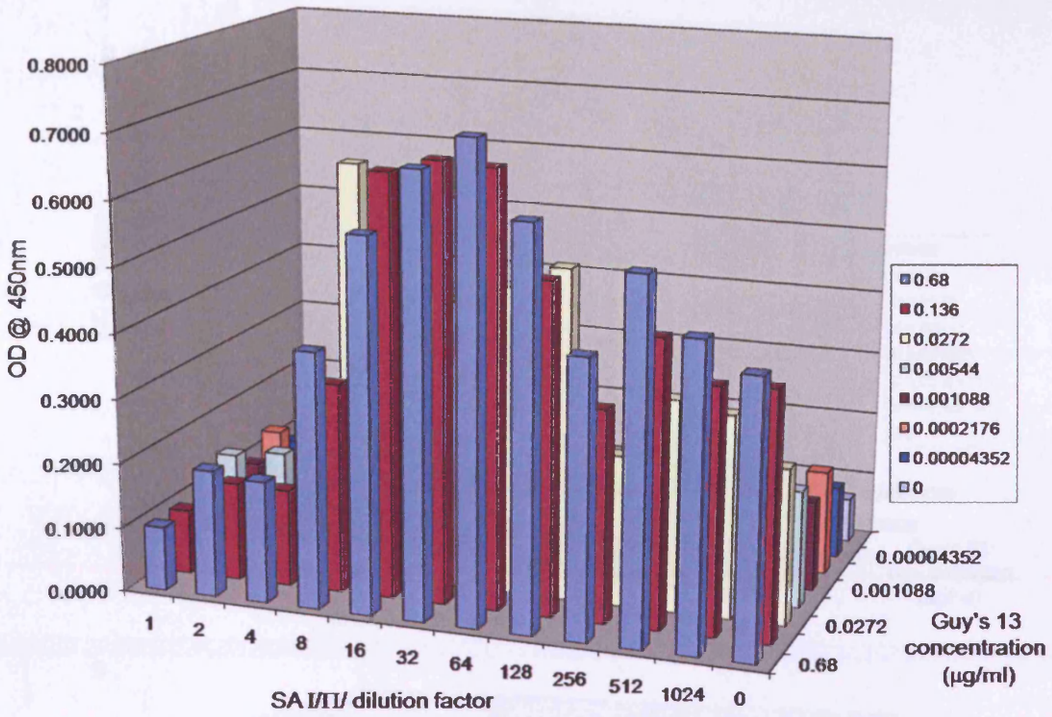

Figure B.2: Negative control: Finding the optimal dilution factor for SA I/II (110.1) (negative control) and Guy's 13 hybridoma supernatant.

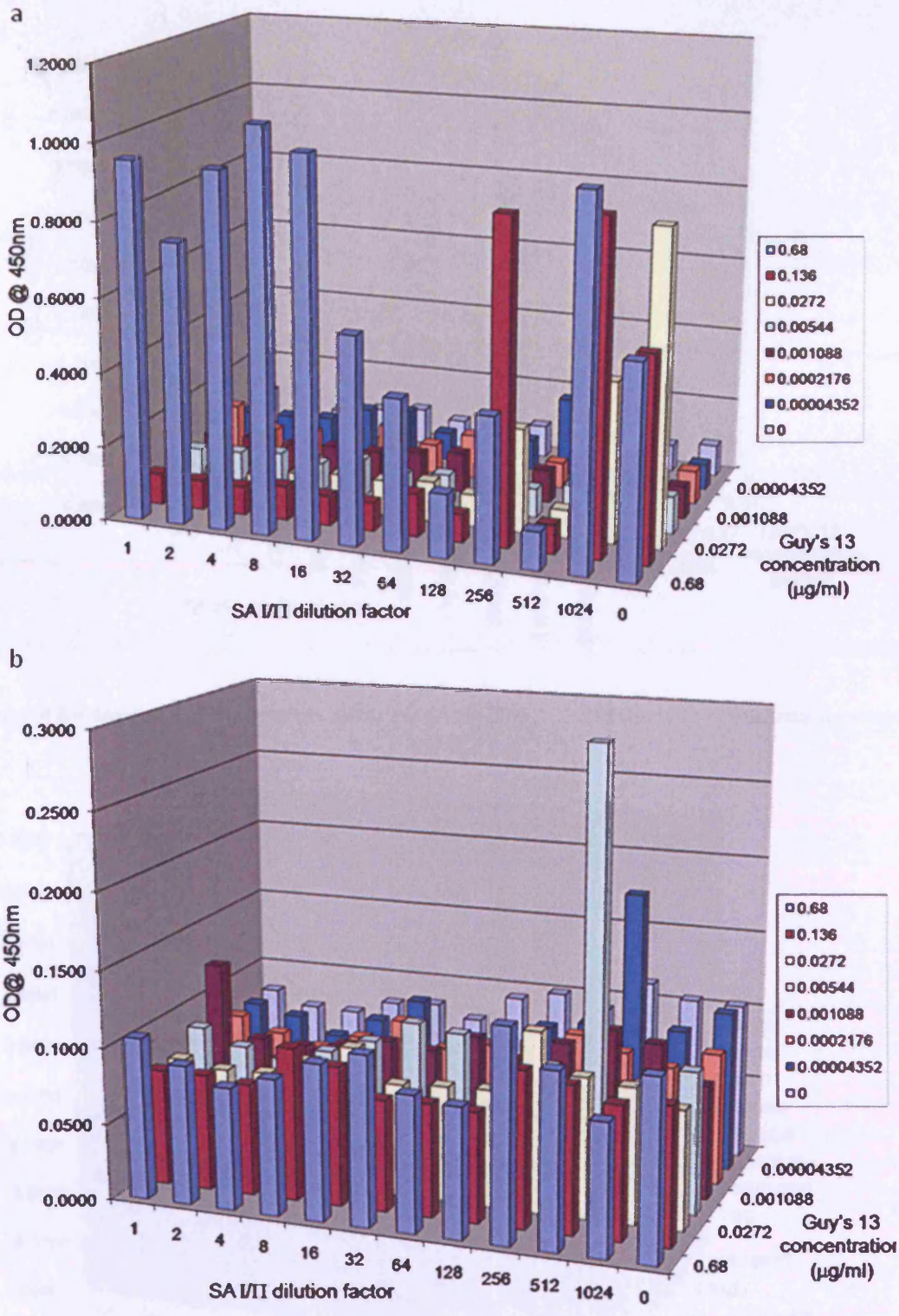

Figure B.3: a Finding the optimal dilution factor for SA I/II (105.1_{13}) and Guy's 13 hybridoma supernatant. b SA I/II (110.1) and Guy's 13 hybridoma supernatant.

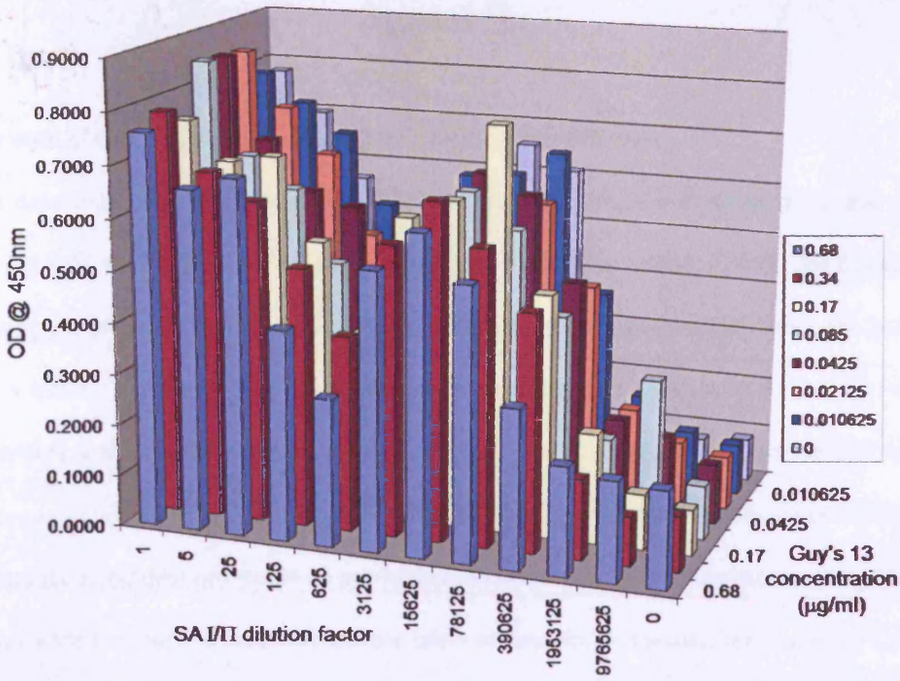

Figure B.4 Finding the optimal dilution factor for SA I/II (105.1_{13}) and Guy's 13 hybridoma supernatant.

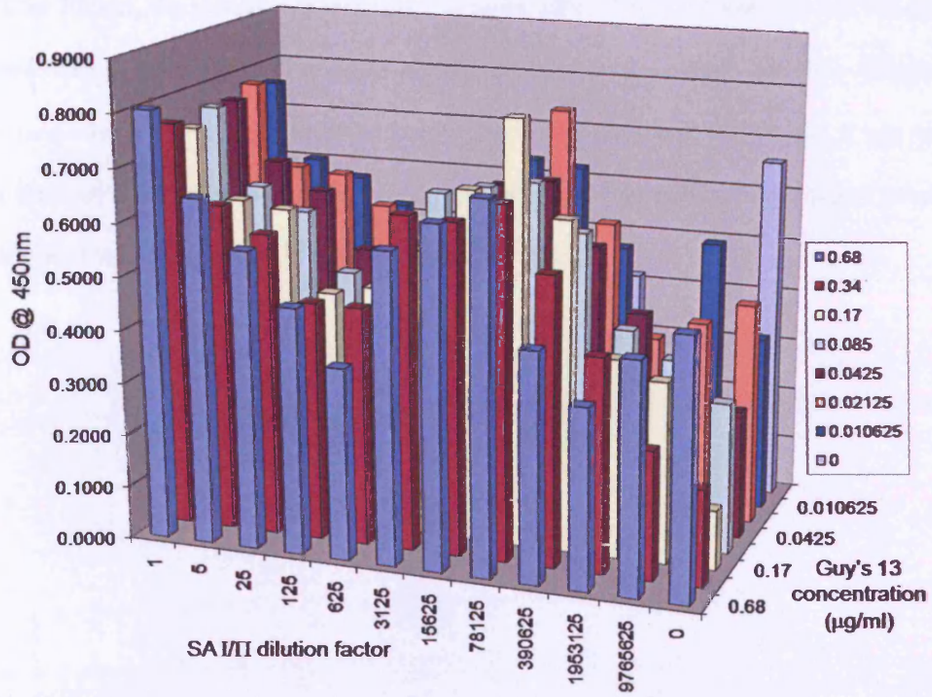

Figure B.5: Finding the optimal dilution factor for SA I/II (105.1_{13}) and Guy's 13 hybridoma supernatant.

Appendix C

Concentration of Guy's 13 hybridoma (positive control) determination

To determine the concentration of Guy's 13 supernatant, a microwell plate was coated and incubated at 37°C for 2 hours with sheep α-mouse IgG γ (1:1000 in 1XPBS, AU272, The Binding Site, UK). After rinsing the plate three times with distilled water, the plate was blocked with 2.5% (w/v) BSA in 1 XPBS for a further 2 hours at 37°C. The plate was then washed six times with 0.1% (v/v) Tween 20 (in distilled water), and duplicate samples of Guy's 13 supernatant (diluted 1:100), mouse IgG1 kappa at the known concentration of 10 μg/ml, and dilution buffer (DB, (1XPBS)). Since it was expected that Guy's 13 supernatant (at 1:100 dilution) would be at a higher initial concentration than the mouse IgG1 kappa, the former was added in fourfold titrations and the latter in twofold, and incubation was at 37°C for 2 hours. After washing 6 times in 0.1% (v/v) Tween 20 (dH_20), horseradish peroxidase conjugated sheep α-mouse IgG1 (1:1000 in 1XPBS, AP272, The Binding Site, UK) was added as a 1:1000 dilution. After incubation at 37°C for 2 hours, the plates were re-washed six times with 0.1% (v/v) Tween 20, and the substrate added as described in Section 2.4.1. The concentration of Guy's 13 supernatant was then determined from the standard curve of mouse IgG1 kappa of known concentration as described below. It was now possible to use this Guy's 13 supernatant stock as a positive control in subsequent antigen binding assays to determine the concentrations of unknown plant extracts.

Appendix D

Method of IgG yield quantification from ELISA raw results

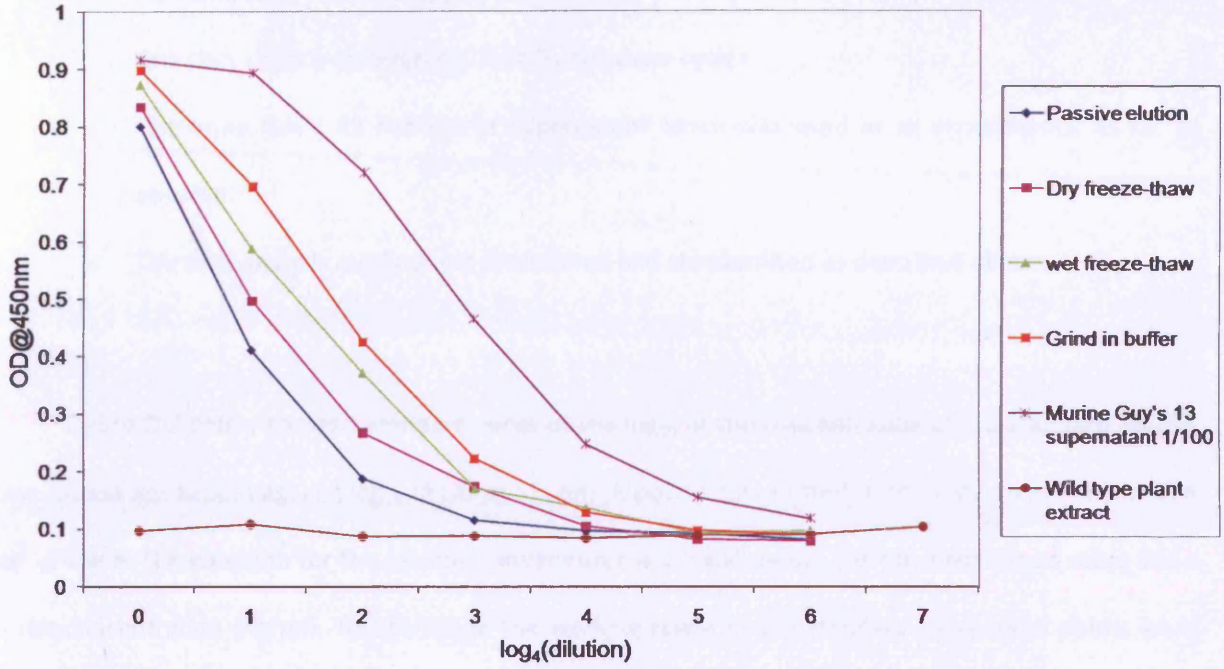

Figure D.1: Example graph- OD@450nm versus $\log_4$(dilution) results from single ELISA plate. Data is shown for comparing obtainable IgG yields by different extraction methods from a plant expressing IgG (secreted form).

Figure D.1 shows an example graph, comparing obtainable IgG yields by different extraction methods from a plant expressing IgG (secreted form). The type of ELISAs performed in all investigations within this research were Sandwich ELISAs which are known to be very reproducible in comparison to Competitive ELISAs. Steps undertaken to ensure reproducible results include the following:

- Original background optimisation experiments were performed to ensure that a good detection of sample (OD range typically 0.2-0.9 was achievable), and Guy's 13 hybridoma supernatant was diluted to 1 in 100 to ensure that this was within the working range. 7 serial dilutions across the wells (either 1in 4 for each dilution or 1 in 2, depending on the typical starting concentration of the IgG) was performed.

- The concentration values for each plate were all normalised with the first plate within the experiment, and with the original experiment.
- All samples were analysed as fresh samples (i.e. extracted then centrifuged), and the standard (Guy's 13 hybridoma supernatant) was stored in 1 ml aliquots at -20°C, to ensure that they did not undergo multiple freeze-thaw cycles.
- The same Guy's 13 hybridoma supernatant batch was used in all experiments, as far as possible.
- The data analysis method was established and standardised as described above.

Figure D.2 below shows a standard curve of the $\log_{10}$ of the concentration of the standard (in this case mouse IgG kappa) against $\log_{10}$ of OD at 450nm. A power curve fitted to the data points results in a straight line. The equation for the resulting linear curve is $y = a.x^b$ where y is the absorbance value and x is the concentration (ng/ml). To determine the working range of the standard curve, data points were omitted using the following guidelines:

- The correlation coefficient (R^2) had to be greater than 0.99. If R^2 was lower, points that obviously deviated from this line were excluded. (In fact data points that clearly deviated from this staright line even if R^2 is 0.99 was eliminated).
- Data points with absorbances less than 0.05 were not included in the working range.

In order to calculate the concentration of the each sample, the mean absorbance of duplicate titration samples was calculated. The concentration of the diluted samples was calculated using the equation for adjusted standard curves determined above. (Note that a standard and a wild type sample (background) were included in each ELISA plate, thus a separate standard curve could be generated for each plate). For these calculations, only sample dilutions that fell within the working range of the standard curve (in the linear region of the sigmoid) where included. The calculated sample concentration was then multiplied by the dilution factor to obtain the sample concentration in the original sample. The determined concentrations in each plate were then normalised with the first plate in the experiment, and

again with the first plate of a previous experiment, so that all concentrations could be compared on the same reference basis.

The final sample concentrations calculated in this way were subtracted from the wild type (background values) in order to obtain the "true" concentration value for each sample.

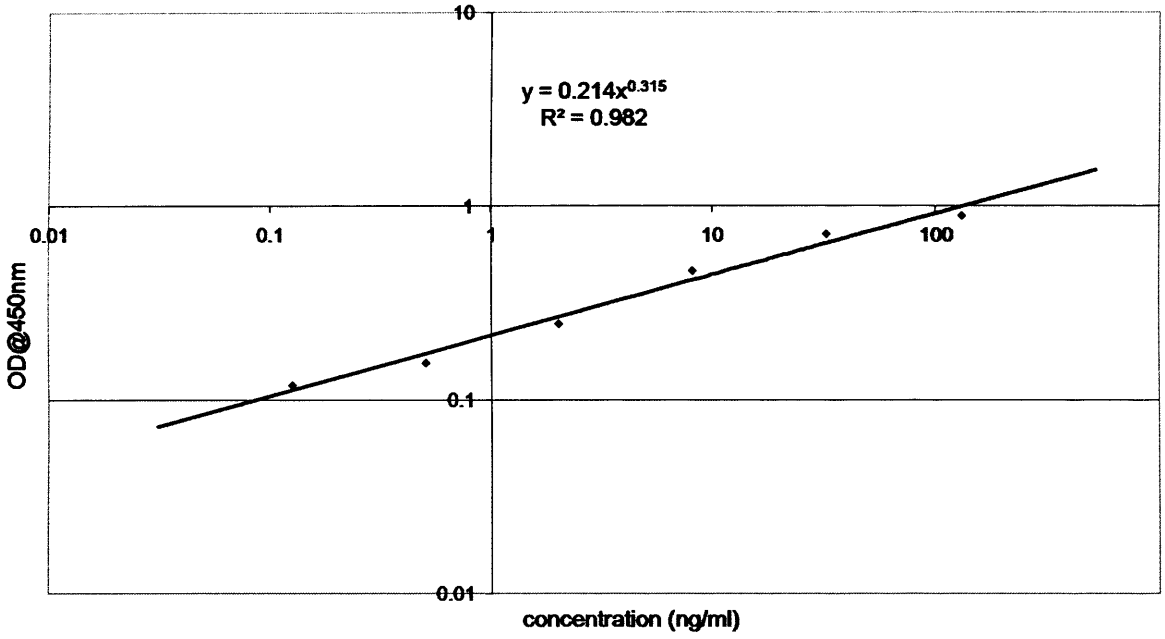

Figure D.2: Standard curve of OD@450nm versus concentration for Guy's 13 supernatant (positive control) that is also illustrated in Figure 2.2.

Appendix E

Processing techniques for release of products from plants

Commercially available mechnanical disruption techniques for protein extraction from the leaves and/or roots were identified from literature. These techniques were reported to be capable of breaking plant material into small particles in the presence of the appropriate extraction buffer. This would enable the monoclonal antibody (product) (along with the other plant proteins) to be released and captured in an aqueous environment, that would allow analytical analysis, protein recovery and further purification. The criteria for a suitable extraction technique may be identified as:

- Maximal release of functional monoclonal antibody with minimal release of proteases, alkaloids, and overall contaminants.
- The ability to process very small volumes of plant material.
- The capacity to change the settings of the device (e.g. speed and power input) in order to vary the degree of plant material disruption in accordance to usage, product location, product sensitivity to mechanical forces and the inevitable co-released proteases, and to cater for different strength plant materials (e.g. roots vs. leaves).
- Scalable device. The small-scale model should be used to design a larger scale mimic. This is dictated by its geometrical and operational features.

Tables E.1 (a and b) highlight some of the main techniques that were initially considered. However, the in-house shear device was opted for due to its many advantages of the other systems, as detailed in Table E.1 and in Chapter 8 above.

References: www.fitzmill.com; www. silverson.com;
http://home.twcny.rr.com/htihome/matrixmill.htm

Table E.1 Details of potential mechanical techniques for investigating extraction at small scale.

a Possible Extraction technique	Description	Picture	Minimum processing volume or mass	Maximum processing volume or mass for a large-scale equivalent	Advantages	Disadvantages
Silverson	- high shear rotor/stator laboratory mixer - multi-stage mixing/shearing action as materials are drawn through the specially designed perforated workhead.	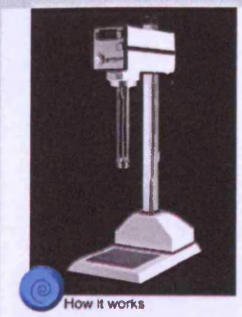	1mL	12 litres	- scalable - Workhead can be varied to achieve different particle sizes.	- Requires thorough cleaning of apparatus between samples! - Not currently used at large-scale in the pharmaceutical indutstry
Fitz Mill	- Size reduction unit - Process wet or dry products - Easy to disassemble and clean - Results can be applied to larger scale production units - Various rotors, screens and speeds available for ultimate size reduction flexibility - All product contact parts constructed of stainless steel - Compact design and minimal weight for ease of transport - Integral product containment system		5g	>10 litres (exact figure not found yet)	- Has been used for this purpose at lab scale before; (Vald'es *et al.*, 2003)	- Overall size of unit is large (takes up space on the lab bench) -Requires thorough cleaning of apparatus between samples.

b Possible Extraction technique	Description	Picture	Minimum processing volume or mass	Maximum processing volume or mass for a large-scale equivalent	Advantages	Disadvantages
Bead Mill (UCL)	- Continuously operating media mill with a horizontal grinding container for dispersion and finest wet grinding - Grinding action by glass/borosilicate/glass beads.	-	-	-	- Scalable. - Can operate in continuous mode at large scale.	- Need to separate beads from plant cell material. - Difficult to clean in comparison to other techniques. - Currently used at large-scale in the pharmaceutical industry
Matrix Mill	- For medium and large scale DNA extraction for PCR - Processes samples in standard 96-well assay trays. - Operation further simplified with Pestle Magnet for pin loading - Extracts sufficient DNA for over 1000 PCR amplifications in minutes. - Compact 18" ´ 15" footprint.		-	-	- Extraction time greatly reduced (can process 96 samples at a time!) - Easy to use and clean. (Requires 1 cleaning cycle per assay).	- More difficult design for efficient scale-up of an equivalent system at large-scale.
Shear device (UCL)	- Scale-down rotating-disc shear device.	As shown in Chapter 2, Section 2.7.2	7ml cylindrical processing chamber with a central rotating disc (with a serrated edge)	Determined by design (currently no commercial equivalent)	- Scalable - Energy dissipation equations have been developed for a similar model (Boychyn *et al.*, 2000)	- Not yet known whether disruption forces will be sufficient to handle tough plant material, as has been designed for cells in an aqueous environment...may require adaptation. - Cleaning between samples.